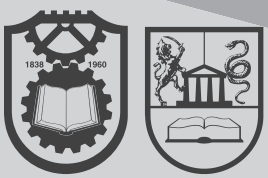

Faculty of Engineering
University of Kragujevac

IRMES
KRAGUJEVAC 2019

9th International Scientific Conference - IRMES 2019
Research and Development of Mechanical Elements and Systems

BOOK OF ABSTRACTS

05. – 07. SEPTEMBER 2019

Department for
Mechanical Constructions and Mechanization

UNIVERSITY OF KRAGUJEVAC

FACULTY OF ENGINEERING

DEPARTMENT OF MECHANICAL CONSTRUCTIONS AND MECHANIZATION

IRMES KRAGUJEVAC 2019

9TH INTERNATIONAL SCIENTIFIC CONFERENCE - IRMES 2019

RESEARCH AND DEVELOPMENT OF MECHANICAL ELEMENTS AND SYSTEMS

BOOK OF ABSTRACTS

Editor: Nenad Marjanović

5-7 September 2019, Kragujevac

Book of Abstracts for the 9th International Scientific Conference [on] Research and Development of Mechanical Elements and Systems, IRMES 2019

ISBN 978-86-6335-061-8

Editor:	Nenad Marjanović, Faculty of Engineering, University of Kragujevac
Editorial assistant:	Nenad Kostić, Faculty of Engineering, University of Kragujevac
Technical editor and graphic design:	Nenad Petrović, Faculty of Engineering, University of Kragujevac
Publisher:	Faculty of Engineering, University of Kragujevac, Department for Mechanical Constructions and Mechanization, Sestre Janjić 6, 34 000 Kragujevac, Serbia
For Publisher:	Vesna Ranković, Vice dean, Faculty of Engineering, University of Kragujevac
Printed by:	InterPrint, Jurija Gagarina 12, 34000 Kragujevac, Serbia
Circulation:	200 copies

DOWNLOAD PDF

The publication of this Proceedings was supported bz Ministry of Education, Science and Technological Development of the Republic of Serbia

FOREWORD

The 9th International Scientific Conference - IRMES 2019 - Research and Development of Mechanical Elements and Systems is organized by the Department for Mechanical Constructions and Mechanization of the Faculty of Engineering at the University of Kragujevac and the Association for Design, Elements and Constructions – ADEKO.

On the previous eight IRMES Conferences (the first in 1995, the last in 2017), around a thousand papers have been presented, and there were over a thousand participants from all over the world. A long and successful tradition is a stable basis for organizing this and future IRMES Conferences.

The mission of IRMES Conferences is to serve the global community by improving, spreading and applying new engineering knowledge, with the goal of being used as a source of the newest and most relevant information for mechanical engineers and experts in related fields – on a local, regional and global level.

Specific goals, themes and fields of the IRMES 2019 Conference are defined in cooperation with the ADEKO association, and in accordance with current topics and problems. Thematic units of the conference are: Mechanical Elements and Systems (modeling and simulation, loading and stress conditions, tribology, noise and vibrations, maintenance and monitoring, safety, quality, reliability), Power and Motion Transmission Systems (development of new concepts, modeling and simulations, noise and vibrations, testing, safety, quality, reliability), Product Development Process (technology transfer, creativity and innovations, development and design, Innovative product development, smart systems, industry 4.0, knowledge economy) and New Technologies and Materials (CAD/ CAM/ CAE technology, intelligent production systems, robotics and mechatronics, rapid prototyping, new materials).

We have ensured a wide international participation, in order to have as many high quality research papers as possible and in order to increase the significance and influence of IRMES Conferences on a global level. Of a total of over 180 submitted papers, authors of over 60% of the papers are from over 30 different foreign countries.

All submitted papers have undergone the process of international review, and of the submitted papers 140 were accepted which met the high set criteria. We would like to thank the reviewers on their hard work and dedication, which have increased the quality of the IRMES 2019 Conference.

This Book of Abstracts features extended abstracts of those papers, while the complete papers will be, according to authors' preferences be published through IOP Publishing Service in "IOP Conference Series: Materials Science and Engineering", or in one of six eminent journals.

Keynote lectures for the IRMES 2019 Conference will be held by prominent professors: Marco Ceccarelli - President of IFToMM, professor of Mechanics of Machines at the University of Rome Tor Vergata, Italy, Radoslav Martinović - retired professor at the University of Montenegro, Vojislav Miltenović - Chief of the Smart office 1 of the Innovation Center of the University in Nis (ICUN), and Milosav Ognjanović - professor emeritus at the University of Belgrade, Faculty of Mechanical Engineering. He is a full member of Academy for Engineering Sciences of Serbia – AESS and works for EDePro – Engine Design and Production.

Included in the IRMES 2019 Conference is also the Honorary Committee, which is made up of the most respected and experienced professors and researchers from the field of machine elements and design, with the goal of achieving continuity and a high quality of IRMES conferences to come.

Using good experiences from the previous IRMES 2017 conference, a student section will be organized again this year. Our goal is to spark interest in, and include, a large number of students, young and creative people, to work in the field of elements and design and to suggest new ideas and specific solutions, and to, through their participation in the conference, gain new experiences.

A large support for the organization of the Conference was provided by our sponsors. Aside from material help, it is important that a large number of companies understands and supports the importance of research and connecting results to practical application. We would like to thank or sponsors on their support.

The IRMES 2019 Conference will also include a number of other manifestations in order to ensure a high quality of exchanging knowledge and experiences, as well as a pleasant stay in Kragujevac in September of 2019.

We would like to thank all authors, committee members, reviewers, sponsors and others who have helped this Conference and attributed to its quality and importance.

To all participants we wish successful involvement in the IRMES 2019 Conference and a pleasant stay in Kragujevac.

Chairman of the Organizing Committee of IRMES 2019

Professor Nenad Marjanović, PhD

CONFERENCE CHAIR

Nenad Marjanović, *Serbia*

INTERNATIONAL SCIENTIFIC COMMITTEE

Ranko Antunović, *Bosnia and Hercegovina*
Saeid K. Azad, *Turkey*
Nicolae Bâlc, *Romania*
Milan Banić, *Serbia*
Mirko Blagojević, *Serbia*
Marian Borzan, *Romania*
Maja Čavić, *Serbia*
Marco Ceccarelli, *Italy*
Snežana Ćirić Kostić, *Serbia*
Nicolae-Florin Cofaru, *Romania*
Kalyan Deb, *USA*
Remzo Dedić, *Bosnia and Hercegovina*
Lubomir Dimitrov, *Bulgaria*
Mircea-Viorel Dragoi, *Romania*
Jožef Duhovnik, *Slovenia*
Dragan Đurđanović, *USA*
Alexandru Catalin Filip, *Romania*
Alfonso Fuentes-Aznar, *USA*
Pedro Javier Gamez-Montero, *Spain*
Fuad Hadžikadunić, *Bosnia and Herzegovina*
Safet Isić, *Bosnia and Herzegovina*
Lozica Ivanović, *Serbia*
Janko Jovanović, *Montenegro*
Janez Kramberger, *Slovenia*
Božidar Križan, *Croatia*
Siniša Kuzmanović, *Serbia*
Stanislaw Legutko, *Poland*
Vlado Lubarda, *USA*
Tamás Mankovits, *Hungary*
Dragan Marinković, *Germany*
Nenad Marjanović, *Serbia*
Biljana Marković, *Bosnia and Hercegovina*
Svetislav Marković, *Serbia*
Athanasios Mihailidis, *Greece*
Dragan Milčić, *Serbia*
Vojislav Miletnović, *Serbia*
Radivoje Mitrović, *Serbia*
Milosav Ognjanović, *Serbia*
Giorgio Olmi, *Italy*
Marko Popović, *Serbia*
Milan Rackov, *Serbia*
Ravipudi V. Rao, *India*
Mileta Ristivojević, *Serbia*
Božidar Rosić, *Serbia*
Ivan Samardžić, *Croatia*
József Sárosi, *Hungary*
Vimal Savsani, *India*
Vilmos Simon, *Hungary*
Dušan Stamenković, *Serbia*
Victor E. Starzhinsky, *Belarus*
Blaža Stojanović, *Serbia*
Jaroslaw Stryczek, *Poland*
Ghanshyam G. Tejani, *India*
Milan Tica, *Bosnia and Herzegovina*
Radoslav Tomović, *Montenegro*
Sanjin Troha, *Croatia*
Lucian Tudose, *Romania*
Miroslav Vereš, *Slovakia*
Reiner Vonderschmidt, *Germany*
Adisa Vučina, *Bosnia and Hercegovina*
Krešimir Vučković, *Craotia*
Manfred Zehn, *Germany*

IRMES PROGRAMME COMMITTEE

The IRMES Programme Committee is a constant body which decides on important matters for future IRMES conferences, such as: the organizer, time and place of conferences, themes, etc. The committee is made up of representatives from ADEKO member institutions and organizers of previous IRMES conferences.

Programme Committee Chairman:
Radivoje Mitrović
Programme Committee Secretary:
Žarko Mišković
Programme Committee Members:
Milosav Ognjanović
Vojislav Miltenović
Dragan Milčić
Milan Rackov
Nenad Marjanović
Radoslav Tomović
Milan Tica
Biljana Marković
Adisa Vučina

HONORARY COMMITTEE

The honorary committee for IRMES 2019 is made up of members which have through their work and/or authority contributed to the development of machine elements and systems, as well as creating and maintaining IRMES conferences. Honorary committee members are from the ranks of distinguished academic citizens and experts specializing in relevant fields to the conference theme. The idea behind forming the Honorary committee as a permanent IRMES conference body is to show much deserved respect and appreciation to deserving researchers, and to have them actively and formally be included in the organization and workings of IRMES conferences.

Honorary Committee Chairman:
Slobodan Tanasijević
Honorary Committee Secretary:
Lozica Ivanović
Honorary Committee members:
Radoš Bulatović
Vlastimir Đokić
Milomir Gašić
Danica Josifović
Svetislav Jovičić
Zvonimir Jugović
Siniša Kuzmanović
Vojislav Miltenović
Slobodan Navalušić
Ružica Nikolić
Milosav Ognjanović
Miroslav Vereš
Aleksandar Vulić

ORGANIZING COMMITTEE

Organizing Committee Chairman:

Nenad Marjanović

Organizing Committee Vice Chairmen:

Mirko Blagojević
Lozica Ivanović
Blaža Stojanović

Organizing Committee Secretary:

Nenad Kostić

Organizing Committee Members:

Zorica Đorđević
Dobrivoje Ćatić
Vesna Marjanović
Nenad Miloradović
Ivan Miletić
Rodoljub Vujanac
Saša Jovanović
Nenad Petrović
Miloš Matejić
Sandra Veličković
Slavica Miladinović

REVIEWERS

Adisa Vučina
Aleksandar Miltenović
Aleksandar Živković
Alexandru Filip
Ana Pavlović
Biljana Marković
Blaža Stojanović
Cristiano Fragassa
Dejan Jeremić
Dragan Marinković
Ileana Ioana Cofaru
Ivan Knežević
Ivan Miletić
Janko Jovanović
Jelena Živković
Jovanka Lukić
Krešimir Vučković
Livia Beju
Lozica Ivanović
Lucian Tudose
Maja Čavić
Marko Popović
Milan Banić
Milan Rackov
Miloš Matejić
Mircea-Viorel Dragoi
Mirko Blagojević
Nebojša Rašović
Nenad Petrović
Nicolae Florin Cofaru
Pedro Javier Gamez Montero
Radivoje Mitrović
Radoslav Tomović
Ranko Antunović
Remzo Dedić
Ružica Nikolić
Sandra Veličković
Saša Jovanović
Siniša Kuzmanović
Slavica Mačužić
Slavica Miladinovic
Snežana Ćirić-Kostić
Stanislaw Legutko
Vesna Marjanović
Žarko Mišković
Zorica Djordjević

CONTENTS:

PRODUCT DEVELOPMENT PROCESS (technology transfer, creativity and innovations, development and design, Innovative product development, smart systems, industry 4.0, knowledge economy)

RESEARCH AND DEVELOPMENT IN FIELD OF VECIHLES AND TRANSPORT

9th International Scientific Conference
Research and Development of Mechanical Elements and Systems
Kragujevac, Serbia, September 5-7 2019

- KEYNOTE LECTURE -

INNOVATIONS IN ROBOTICS WITH MECHANISM DESIGN

Marco Ceccarelli [1, 2]

[1] LARM2: laboratory of Robot Mechatronics, University of Rome Torvergata, Rome, Italy;
[2] Beijing Advanced Innovation Center for Intelligent Robots and Systems, Beijing Institute of Technology, Beijing, China, marco.ceccarelli@uniroma2.it

Key words: Robotics, Mechanism Design, Innovation.

SUMMARY

Challenges for Robotics can be considered from several viewpoints in technical, social, and financial ones as due to new designs and applications of robots. In this keynote paper new horizons in Robotics are discussed in terms of Innovation issues coming from Mechanism Design. The attention is focused on challenging aspects that are related to the mechanical structure of a robot system as a key design issue both for the robot structure and operation when considering assigned tasks either in substituting or helping human operators. The keynote speech presents aspects emphasizing the role of mechanism design in robot developments as based on the fact that the action of robots in performing their tasks, either in coordination or not with human operators, is of mechanical nature due to motion and force transmission goals of the operation. The challenges of mechanism design for robots is presented both in terms of technical solutions and community activity, since each of them depends, impacts, and generates each other. Examples of past and current solutions are presented to show how a mechanism design can be determinant for a robot design for novel successful achievements.

Today, Innovation is understood as a multidisciplinary activity to produce technological developments with practical implementations for benefits both of their producers and users for society improvements. In the last decades Science achievements have made possible new engineering developments (and vice versa!) in many fields with evolutions that have been faster than in the past.

Figure 1 summarizes the concept of innovation as produced and exploited by individual actors within a multidisciplinary frame of several different areas. The success of innovation requires that all these aspects will be properly developed and concur to the final implementation of an innovative product/idea in the usage by a large community or public. However, it is to note the innovation is strongly based on technical ideas/achievements, but its success is obtained thanks other non-technical factors.

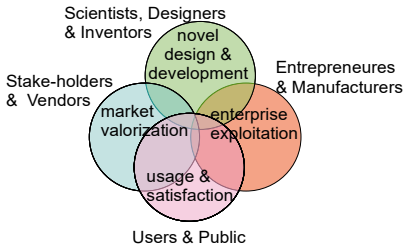

Figure 1. A scheme for actors and areas in Innovation activity

Robotics has shown Innovation challenges and potentialities since the early days and nowadays is well recognized the impact that any further achievement in Robotics can have on the society improvements both in production aspects and in diary life quality. Innovation in Robotics can be recognized in developments for Science knowledge and novel solutions both with robotic systems and their operations in new areas and public fruition at proper level of complexity and cost.

Mechanism design is an important step in design procedures for new robot systems when considering the mechanical nature of the structure and task to be achieved.

Figure 2 summarizes the main concepts and activities of the design process of robot systems with a central role of mechanism design also as related to the challenges in Innovation expectations from a perspective giving a key role to the mechanical design matching operation and design issues also from the multidisciplinary (mechatronics) robot fea-tures. Although the scheme gives a sequential order of the activities, the design process can be considered iterative or even with implications from one step to another.

Examples of Innovation in Robotics are reported to clarify the challenges and results as due to Mechanism Design for robots, both in new robot systems and community developments. Figure 3 shows examples of humanoid robots as based on mechanism design: in Figure 3 a) is the pioneer first humanoid Wabot-1 that was presented by prof. I. Kato at the first Romansy in 1973, and in Figure 3 b) is the LARMbot humanoid design in 2015 by the author's team as based on several parallel mechanisms.

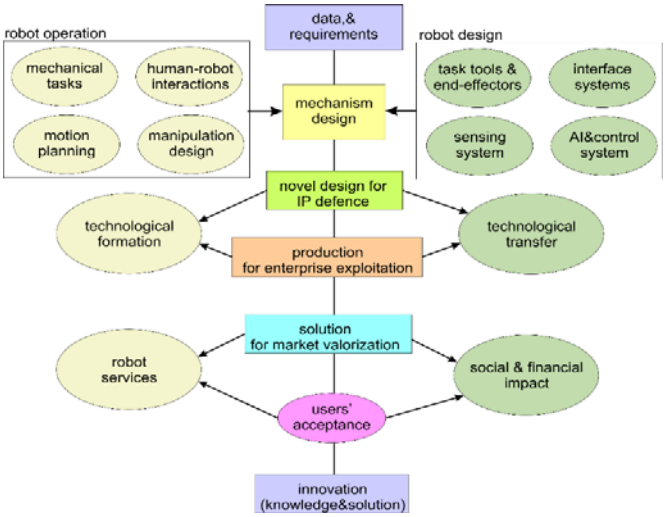

Figure 2. A scheme of the activity in Robotics challenge activity centered on Mechanism Design

An example of innovation from community viewpoints is the start of the Romansy conference series in 1973, Figure 4 a), as the first pioneering conference forum on Robotics and Figure 4b) shows the proceedings page of the MEDER con-ference series that is specifically started in 2009 on Mechanism Design for Robots.

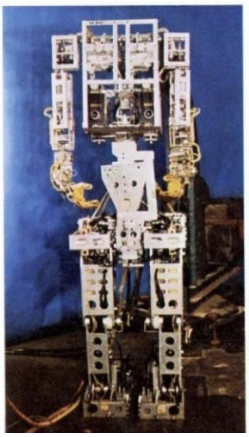

a)

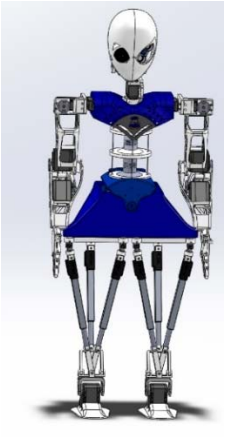

b)

Figure 3. Examples of mechanism design in humanoid robots: a) Wabot 1 humanoid in 197; b) LARM bot design in 2015

Innovations is produced by inventors coming from a community and producing new figures in the community. Significance of innovation is produced and supported by the corresponding community and particularly significant can be considered the history and role of IFToMM in Robotics and MMS at large. Significant examples of contributions of IFToMM with innovation contents can be summarized both in community aggregation and identification for new re-search subjects of large interest, new forums and publication frames, and new formation characters in research and profession. Specifically, in Robotics, the TC of Robotics and Mechatronics is the innovative community result that since the early days of IFToMM searches for new horizons in the field with main attention to mechanical implications of the mechatronic design and operation of robots. The Innovation in the TC is the TC itself with its peculiar character as per IFToMM vision stimulating promotion and new achievements not only with Romansy conference but also with many other conferences and activities that are organized on purpose or co-sponsored to support the mechanical engineering viewpoints within a multidisciplinary approach.

a)

b)

Figure 4. Title page of proceedings of: a) Romansy in 1973, [4]; b) MEDER in 2015, [7].

REFERENCES

Ceccarelli M., Innovation Challenges for Mechanism Design, Mechanism and Machine Theory, 125 (2018) 94–100.
Ceccarelli M., Figures and achievements in MMS as landmarks in history of MMS for inspiration of IFToMM activity. Mechanism and Machine Theory, 105, 2016, pp. 529-539.
Kobrinski I. et al (eds), First CISM-IFToMM ROMANSY (Udine 5-8 September 1973), Springer-Verlag Wien, 1974.
Ceccarelli M, Cafolla D, Russo M, Carbone G (2017) LARMBot Humanoid Design Towards a Prototype. MOJ int. Journal of Applied Bionics and Biomechanics 1 (2) 2017. DOI: 10.15406/mojabb.2017.01.00008
Bai S. and Ceccarelli M. (eds.), Recent Advances in Mechanism Design for Robotics, Mechanisms and Machine Science Vol. 33, Spring-er, Dordrecht, 2015.
Ceccarelli M., A short account of History of IFToMM and its role in MMS, Mechanism and Machine Theory, Vol. 89, 2015, pp.75-91

Marco Ceccarelli received his Ph.D. in Mechanical Engineering from La Sapienza University of Rome, Italy, in 1988. He is Professor of Mechanics of Machines at the University of Rome Tor Vergata, Italy, where he chairs LARM2: Laboratory of Robot Mechatronics.

His research interests cover subjects of robot design, mechanism kinematics, experimental mechanics with special attention to parallel kinematics machines, service robotic devices, mechanism design, and history of machines and mechanisms whose expertise is documented by several published papers in the fields of Robotics. He has been visiting professor in several universities in the world and since 2014 at Beijing Institute of Technology. He is ASME fellow. Professor Ceccarelli serves in several Journal editorial boards and conference scientific committees. He is editor of the Springer book series on Mechanism and Machine Science (MMS) and History of MMS. Professor Ceccarelli is the President of IFToMM, the International Federation for the Promotion of MMS. He has contributed to Romansy since 1986 and is in the Scientific Committee since 2004. He has started several IFToMM sponsored conferences including MEDER (Mechanism Design for Robotics) and MUSME (Multibody Systems and Mechatronics).

- KEYNOTE LECTURE -

THE LUCAS CHAIR IN CAMBRIDGE FROM NEWTON TO HAWKING

Radovan Martinović, retired *professor* [1,]

[1]University of Montenegro, Mechanical Engineering Faculty, bul. Džordža Vašingtona bb., Podgorica, Montenegro

SUMMARY

It was the fifth of October 1957 and our first lecture of Mechanics held by our well known Professor Danilo Rashkovich. Professor entered to the big amphitheatre 56 of the old building of Mechanical engineering faculty, followed by the group of assistants who always were charged by numerous lecturing devises. He started his impressive speech by the question:
Do you know who deserves to be glorified for the great historical achievement that today the Russian satellite is flying around the earth? The dead silence and Professor's answered The Russian Tcar Catarina the Second! She had brought the best mathematician in history of science Leonard Euler when he was only 27 years old and posted him position of professor at The University of Petersburg, and the chief of The Chair of Mechanics. Today just from that Chair THE FIRST MAN MADE DEVISE IS FLYING AROUND THE EART. Today is the glorious day of human being.

In the Hawking's' book "On the shoulders of giants" which has been published by Alnari, 2011, there are a lot details concerning the life and the scientific contributions of Nikola Copernic (1473 1543), Galileo Galilei (1564 - 1642), Johan Kepler (1571 - 1630), Issak Newton (1642- 1727), Albert Einstein (1879 - 1955). An other capital work in our language is "History of mathematics" written by our mathematician Miodrag Perovic, Crnogorska Akademija nauka I umjetnosti, Podgorica, Montenegro.

It is my great pleasure to start this presentation by reminding the audience to The Lucass Chair at The Trinity College, Cambridge. This much known Chair formed Henry Lucas 1663. And the first professor was Isaac Barrow. He will give the professorship to the young Isaac Newton when he was only 27. The strict rules of academic perfection were concerned to the work with students. Four hours belonged to the discussion with the students about lecturing astronomy, mathematics, mechanics etc. It was great honour to be a professor of this chair.

During the Plague of 1665- 1667 Newton went to Woolsthorp, Lincolnshire. This period is impotent by the result of his genius. He prepared there his most important work, Philosophiae Naturalis Principia Matematica which was first time published 1685. In this work he established mathematical ground of Keplers powers, the theory of universal gravitation, the concept of force expressed in three lows of motion.

Newtons' enormous contribution is to the theory and experimental works in optics. He investigated and made by own hands the first reflective telescope. That telescope was only 15 cm long. When it was shown to The king Karlo II he was so impressed and promoted Newton a member of the Society of the King (Academy of sciences) (1672).

From the book of Copernicus Keplers' works put a specific challenge to mechanics, Galilei's rules defined principles, definitely Huyges gave the first simplest methods for solving such problems. By such a way it looks to us when we study the history of science. But for the first time that was clear completely by Newton. The enormous potential to understand all that a genius mathematical potential enable Newton to solve the problem completely. This is an essential discovery of the low of general gravitation. But when he was asked does he know what the gravitation is, his answer was: I do not know. For me it is God. For us the fact that gravitation exists and that acts according to the given rules and that is convenient for explanation of the motion of planets and our sun. Just this Gods' phenomena was the subject of Hockings and Penrous research. They developed 1974 the mathematical description of the black holes. The black holes were seen by a Germen satellite at late seventies by discovering curious behaviour of the rays of light in the vicinity of their gravitation field. They published the very important article proving the validity of the general theory of relativity in this case.

Concluding this short glance to Principia we must emphasize that the new discoveries at the end of the 19th and the beginning of the 20th century, needed a lot of new discoveries out of Newtonian approaches.

At the conclusion let me to remind the audience to some technological achievement of celestial discovering or better to say, where and when we are living today after only halve of century from the flight of the first satellite. To leave the earth surface the speed that is needed is 11.2 km/s or 40.320 km/h. The speed on the earth needed to escape the Sun is 42.1 km/s or 151.600 km/h. Satellite New Horizon 2006 left the earth with the speed of 58.536 km/s. Now it flies by the speed of 14km/s. But the absolute champion is Pionier10 with the speed of 15.3 km/s. -Voyager 1 will leave Sun's system within 14.ooo to 28.000 years.

Radovan Martinović, PhD, retired professor. He graduated mechanical engineering at The Belgrade University. He got an MSc degree at the Liverpool polytechnic. He was visiting professor at Liverpool Polytechnic, visiting professor at the University of Gainesville, USA, Visiting professor at the University of Bary, Italy, Visiting scholar of the European Union at the University Karlsruhe, Germany for two years (1988- 1990). Retired in 2002.

9th International Scientific Conference
Research and Development of Mechanical Elements and Systems
Kragujevac, Serbia, September 5-7 2019

- KEYNOTE LECTURE -

DEVELOPMENT OF INNOVATIVE AND SMART PRODUCTS

Vojislav Miltenović[1], Nenad Marjanović[2]

[1]University of Niš, Innovation Centre – ICUN, Univerzitetski trg 2, 18000 Niš, Serbia
[2]University of Kragujevac, Faculty of Engineering, Sestre Janjić 6,
34000 Kragujevac, Serbia, nesam@kg.ac.rs

Abstract: In recent years, incredibly rapid changes have been taking place worldwide, largely due to the rapid development of science and technology, known as the Industry 4.0. At the heart of the Industry 4.0 are smart products and services. Smart technical products are also referred to as "cyber-physical systems" (CPS) and represent a combination of material and immaterial components, so besides reliable executing the work function, they also have the ability to digital networked and communicate with other products.
For this reason, one of the important tasks within the product development is the transformation of existing and new products into intelligent and digital networked products. Expectations are to come up to intelligent, autonomous fourth level systems.
Such trends make considerably more difficult and complex activities within the product development process, requiring teamwork of experts from various fields and the application of adequate methods and procedures for solving complex tasks and problems. This paper will present the situation in this area as opportunities and challenges expected in the future.

Key words: Industry 4.0, smart products, product development, innovations.

1. INTRODUCTION

Thanks to the rapid progress of information communication technologies (ICT) in recent years there have been major changes in the field of development, manufacture and exploitation of industrial products. The Internet has a major impact on industrial products, business processes and organization, so the term "Internet of Everything" has come to an end. It includes the Internet of Data, People, Services and Things.

Internet Things (Internet of Things) is a new kind of communication between intelligent devices. Practically, a parallel internet is created in which "things" communicate with each other, exchange information, manage each other, react and influence the environment in which they are without impacts of people.

This trend has led to Industry 4.0, which offers enormous potential for improvement and success not only for production but above all for product innovation. There is an efficient engineering of a new generation of smart products and services as well as their marketing using new business models. To succeed in exploiting this potential, industrial companies are faced with a major transformation process or radical change, where they have to overcome a multitude of challenges.

The focus of these changes is largely related to process models, methods, IT tools and information models in the development of smart products and services. The product and service development is the most important phase of the engineering, since in this phase the greatest innovation potential lies and the characteristics of future products are determined.

2. SMART PRODUCTS

We are seeing incredibly fast changes that are the result of the extremely rapid development of science and technology. They are recognized as the 4th Industrial Revolution. The first indications of 4 industrial revolutions appeared in 2001, so that for 10 years some countries formed working groups for defining national high technology strategies. For an adequate understanding of the trends Industry 4.0 is a necessary review of earlier events in this area. The review will be given primarily from the aspect of the product in certain periods.

It is estimated that the first industrial revolution began in 1784 using a steam-powered engine. So this period is characterized by switching from manual production to machine production with the use of steam-powered engines and water turbines (Fig.1). It was most used in agriculture, shipbuilding, textile industry and mining and contributed to the term “factory” became a little popular. So, key products are steam-powered engines and water turbines.

The beginnings of the second industrial revolution stem from 1850, but it is believed to have been in the period between 1870 and 2014. The greatest momentum of the second industrial revolution was gained by the beginning of the 20th century, primarily through the use of electricity, which enabled serial and mass production in the industry. It is characterized by significant innovations in chemistry, railroad development and mass production of steel. So the key products here are electrical energy.

The third industrial revolution was dated between 1950 and 1970 and carries the name of the information age. It is often referred to as the digital revolution because there have been changes from analog and mechanical systems to digital. The third revolution was a direct consequence of the great development of computers and information and communication technology.

The fourth industrial revolution is achieved in correlation between the existing traditional industries with Internet-based innovations in the field of information communication technologies (ICT). Innovations in these areas form the basis for "Internet of Everything" (IoX), where Data, People, Services and Things are networked with each other and can communicate with each other. IoX is the industry leader in Industry 4, whose core are smart products and services [1]. Smart products were created as a result of several stages of evolution through which conventional products have passed (Fig. 2).

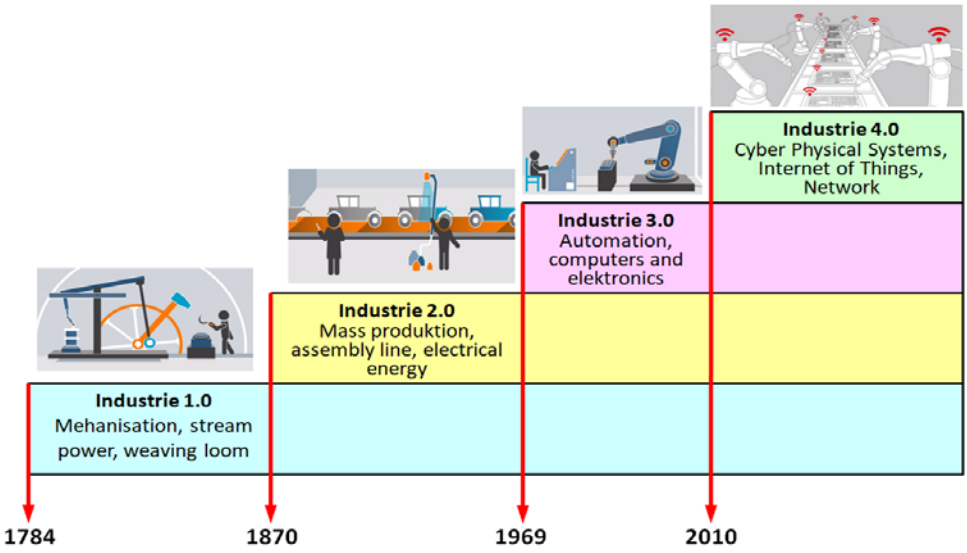

Figure 1. From Industry 1.0 to Industry 4.0 [2]

The basic structure of industrial products (BMS) is made up of mechanical components. In further evolutionary development, this structure was supplemented with electronic components and software, resulting in mechatronic products (MP). As a result of the development of miniature microprocessors and further software development, mechatronics products have been equipped with artificial intelligence, and intelligent mechatronics products (IMP) have emerged [3]. In the next evolutionary step, products are enhanced by the ability to communicate with other products and the Internet. These products are called "Cyber-Physical Systems" (CPS).

Smart products are "cyber-physical systems" that are supplemented by intelligent, Internet-based services, so-called smart services. With regard to their degree of complexity, smart products can be individual products, networked product systems or very complex, cross-sector product systems, so-called Systems of Systems.

Smart products combine both tangible and intangible components and can therefore be understood as smart product service systems (PSS). The key features of smart products are a high degree of (partial) autonomy, connectivity, personalization capability, and ease of use and centering [1].

According to their degree of intelligence smart products can be classified in four consecutive skill levels [6]:

- Smart products of the first level can monitor the condition of their operation as well as their environment by means of appropriately installed sensors and external data sources.
- Smart products of the second level can be controlled remotely via the embedded software or over the Internet platform, even outside the full self-monitoring. The products of this group also have a high degree of personalization.
- For smart products of third level of capability, the combination of above capabilities is enabled to continuously improve and optimize their work function, with the possibility to predict of potential product failures.
- The combination of all the mentioned abilities of the smart products leads to the fourth, highest skill level. Smart products in this category are autonomous products or systems with the ability to self-diagnose, improve or maintain themselves. Smart products of this group have a very high degree of personalization and can independently cooperate with other smart products of this skill level.

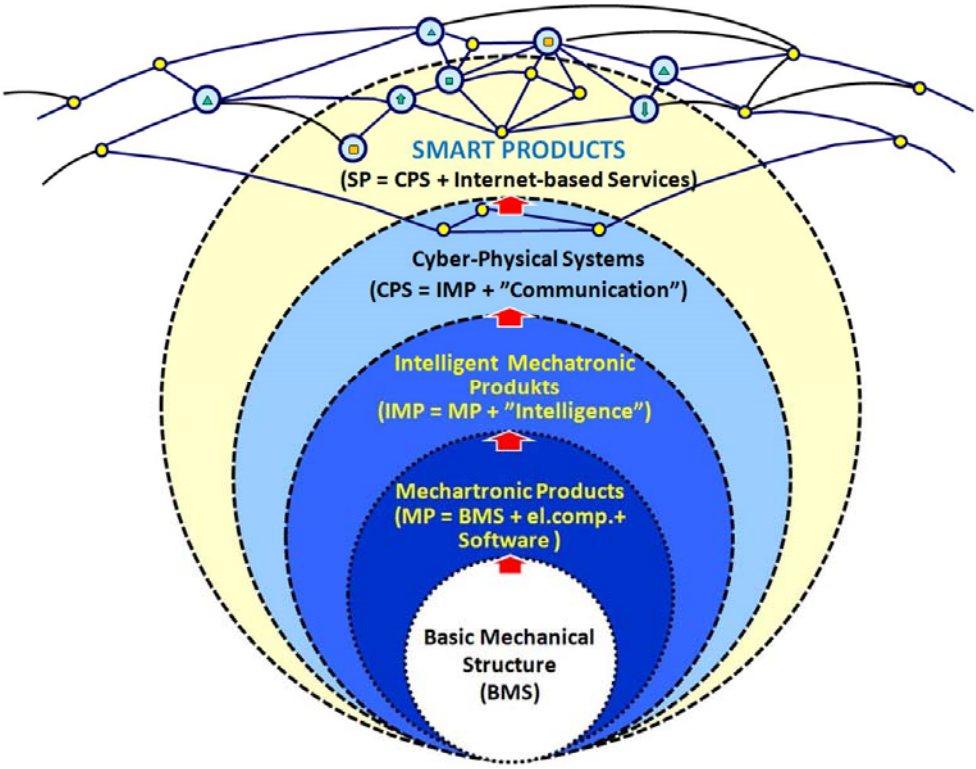

Figure 2. Evolution of stages from machine products (BMS) to smart products (SP) [3]

3. DEVELOPMENT OF INNOVATIVE SMART PRODUCTS

3.1 Design principles of smart products

According to the trends dictated by Industry 4 it is possible to identify the following principles of development and design of smart products [7]:

1. Interoperability: Objects, machines and people need to be able to communicate through the Internet of Things and the Internet of People. This is the most essential principle that truly makes a smart products.
2. Virtualization: CPSs must be able to simulate and create a virtual copy of the real world, i.e. they must be able to monitor objects in the environment.
3. Decentralization: Indicates the ability of CPSs to work independently. This should enable greater fulfillment of customer requirements and a more flexible environment for production.
4. Real-Time Capability: The smart factory must be able to collect real-time data, store and analyze it for making relevant decisions according to new findings. This contributes to the flexibility and the optimization of production.
5. Service-Orientation: The production must be oriented towards the customer. People and smart objects/ devices must be able to efficiently connect through the Internet of Services to create products based on the customer's specifications.
6. Modularity: Smart factories must be able to adapt quickly and smoothly to seasonal changes and market trends. This can best be achieved by applying a modular construction principle, where the modules form a functional and logical unit. Module manufacturers follow modern trends, so with an adequate selection of modules, they achieve multiple effects related to functionality, quality and economy.

3.2Product development process

The products are not created in one, big step, but in a larger number of small steps, whose content must be precisely defined. The resulting sequence of steps is called the "process", while the set of all steps of this process is called the "process of product creation". Therefore, it can be said that the process of product creation is a key process in the company, where ideas and innovations are identified, which leads to quality, innovative and commercially competitive products. In order to come from the idea to the finished product, it is necessary to successfully carry out a number of steps. In this respect, the structure of the product creation process plays a very important role.

During its life cycle, the product passes through different phases (Fig. 1). At the beginning of the life cycle is the process of product creation. The basis of product creation consists of methods and procedures, scientific research, innovations as well as the ideas and creativity of development engineers. The development of the product itself must be carried out systematically and in a clearly structured series of processes.

The process of product creation takes place in 3 phases (Fig. 1):

- Product planning;
- Product development;
- Product manufacturing.

In the product planning phase, intensive analysis of trends in technique and technology development, market demands, customer requirements, and product placement opportunities on the market are carried out. Data collection is continually and in real-time under constant analysis when making relevant decisions. This results in a precise definition of the product profile or the requirements that must be met during product creation. During the life cycle, products are constantly improving, enhancing and innovating. At this stage, it is necessary to co-ordinate the various expedition groups [8].

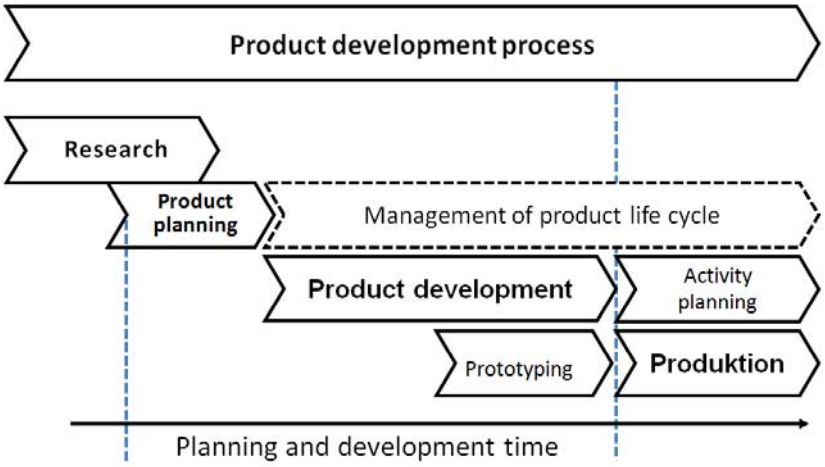

Figure 3. Phases of the product development process

3.3 Current product development model

Appropriate changes in technology, dictated by Industry 2 and Industrie 3, have defined theoretically and practically verified procedures of the process of product design and development. The greatest importance and the foreword had the guideline defined by the association of German engineers VDI (VDI-Richtlinie).

The guideline of VDI 2222 [9] issued in 1973 are primarily intended for the development of technical products as well as for education in the field of construction. The aim was to create design process of engineering on a scientific basis and to apply an adequate methods at various stages of the design process.

Guideline of VDI 2222 in 1993 were replaced by VDI 2221 - Methodology for developing and constructing technical systems and products (VDI-Richtlinie 2221, „Methodik zum Entwickeln und Konstruieren technischer Systeme und Produkte“ [10]). The purpose of these guideline is to provide a more efficient, methodical and systematic approach to the

development of technical systems. They were designed for machine, precision mechanics and process technology, and one of the main aspects is the integral data processing and CAD application.

The VDI guideline 2206 appeared in 2006 and represents a practice-oriented guideline for the systematic development of mechatronic products [11]. The aim of this guideline is to methodically support the interdisciplinary development of mechatronic systems.

There are 3 phases in this model:

1. *System design,*
2. *Domain-specific design,*
3. *System integration.*

1. System design

For the implementation of this phase it is necessary to have requirements, which is also the basis for the evaluation of the future product. The system design begins by abstracting the ideas described in the requirement list. Based on this, functional, effective and structural structures are created and evaluated. The result is a cross-disciplinary solution concept, also referred to as a principle solution, which is the basis of the domain-specific design. The concept is a result of the joint work of experts and development engineers in the field of machinery, electronics and information technology, mechanics, electronics and software engineers.

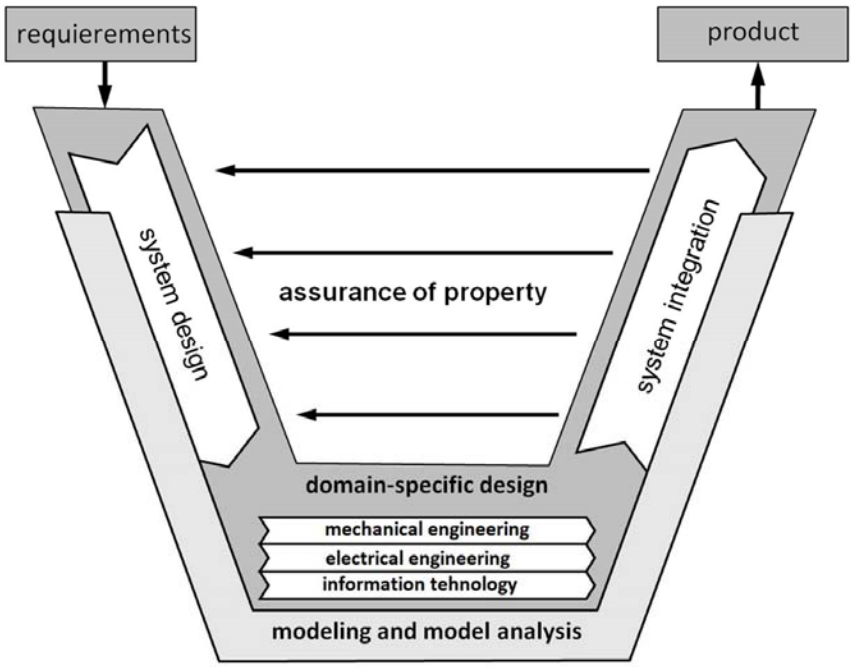

Figure 4.V-model according to VDI 2206

2. Domain-specific design

Based on the principle solution, the elements to be developed are distributed among the respective disciplines. Here the established methods and specification techniques of the different domains are to be used. In order to ensure the fulfilment of the product function at this stage, appropriate calculations and dimensioning of the elements and components of the system are performed.

3. System integration

At this stage, the integration of elements created in the individual disciplines, is done in order to form a higher level entity (future product).

System integration can be done in three different ways:

- Integration of distributed components: Components such as sensors and power actuators are connected to one another via signal and energy flows with the aid of communication systems, which of the energy flows via coupling and plug-in connectors.
- Modular integration: The overall system is made up of modules of defined functionality and standardized dimensions. The coupling takes place via unified interfaces such as for DIN plug and socket connection, standardized integral.
- Spatial integration: All components are spatially integrated and form a complex functional unit, for example integration of all elements of a drive system (controller, power actuator, motor, transfer element, operating element) into housing.

By compiling the appropriate models, the analysis and computational simulation of the partial function fulfilment as well as the global function of the integrated system are performed. Practical applications include physical, mathematical and numerical models.

Physical model is created from topological description. This representation is defined by system -adapted variables such as for example masses and lengths in case of mechanical systems or resistances and inductances in the case of electrical systems. Thus, the physical model describes the system properties in a domain specific form

Mathematical model forms the basis of the system's behavioural description. The physical properties of the physical model are formulated with the aid of mathematical descriptions.

Numerical model is then prepared in such a way that it can be algorithmically handled and subjected to a computer aided process, for example simulation.

As a rule, the phases described above are run through iteratively several times until the final end product is formed.

One of the key factors of successful V-model application is to ensure system property. It is therefore necessary that the concept of specific solutions and the fulfilment of the foreseeable requirements be continually verified during the design process.

3.4 Extension of the V-model for application to smart products

For a long time in the scientific and professional community, there is discussion about whether the V-model can be applied to smart products or should go for a new model. For now, the idea was that the V-model should be expanded and thus adapted to apply for the development and design of smart products. It is thought that research and supplementation of the V-model should be carried out in the following parts [1]:

- Approaches to extending the service domain
- Approaches for integrating agile methods into the V-model
- Integration of cooperative methods in the individual V-model phases
- Approaches to earlier property protection through rapid and virtual prototyping.

Smart product design is considered in the system design phase. The main focus in this part is on expansion of requirements engineering for the development of smart products, function definition and modelling as well as approaches to modelling the communication, interaction and behavioural skills of smart products. In this respect, appropriate research is needed in the field of methods, IT tools and information models.

The most important changes in the V-model are related to part of the domain-specific design. This section should be extended with service design and implementation. The most urgent research topic within the service domain is the simulation and validation of the integrated service components in smart products supported by methods, IT tools and information models. Priority was given to the need for research on IT tools for visualization and interaction with smart services. Methods for the intuitive modelling of product-related smart services were also identified as priority research needs.

However, also the parts related to mechanics, electrics/electronics (E/E), software should also be supplemented.

In the field of Mechanics design and implementation it is necessary to develop IT tools in the field of approaches to the design of smart human-product interaction, approaches to integrating multi-physics simulations into product modelling and design and also modelling approaches for products made of smart materials.

In the field of Electrics/electronics design and implementation it is necessary to develop IT tools in the field of approaches to virtual functional simulation and validation and also context-specific analysis and provision of usage data for existing product populations for product optimization.

The most urgent research topic in the part of software design and implementation are development of approaches for the design/implementation of the virtual twins. Concrete starting points are the unambiguous definition and delimitation of the virtual twin compared to activities with intersections. This includes, among other things, the determination of the necessary models (for example geometry models and behavioural models), the definition of interfaces (for example between digital island solutions) or the clarification of the task field of virtual twins (for example simulation or reconfiguration tasks).

Part of System integration also needs adequate adaptations. Smart products are extremely complex, making it difficult to prove safety and quality assurance. In this regard, there is an

urgent need to develop methods for testing and certifying smart products. One needs approaches that enable validation of smart products based on field data. The complexity of validation increases with the complexity of the product, which makes it impossible for the product developer to perform comprehensive validation without proper assistance systems. Priority should be given to the development of approaches for cross-discipline product protection and also hybrid validation approaches of real and virtual product components.

4. CONCLUSION

The development of smart products and services is a remarkable activity because it represents an important innovation and business potential of each country. According to the projection for the implementation of Industry 4, it is central activity.

Existing models of product development and design cannot be directly applied to the development of smart products, but they need to be expanded. For intelligent products, essential components are services, and in this sense, the existing V-model needs to be expanded with service design and implementation.

The above analysis shows the necessary expansion of the V-model and the following areas:

- Development of comprehensive methods for smart products
- System design of smart products
- Domain-specific design of components of smart products
- System integration, verification, validation of components of smart products
- Building IT infrastructures for smart products

One of the important activities is related to standardization in the field of engineering and smart product development.

REFERENCES

[1] Abramovici, M.:,Engineering smarter Produkte und Services Plattform Industrie 4.0 STUDIE. Deutsche Akademie der Technikwissenschaften. München, 2018.

[2] https://mensch-maschine-fortschritt.de/reportage/arbeit-4-0-im-zentrum-steht-der-mensch/

[3] CIRP Encyclopedia of Production Engineering. Int. Academy for Production Engineering, Laperrière, Luc, Reinhart, Gunther (Eds.) 2015.

[4] https://www.imk.engineering/industrie-4.0.html

[5] Miltenović, V., Đorđević, V.: Excellence, Relevance and Efficient Application of Research Results at University and Institutes from the Standpoint of Economy Developing. International Symposium MACHINE AND INDUSTRIAL DESIGN IN MECHANICAL ENGINEERING KOD 2018., Novi Sad, Serbia. IOP Conf. Series: Materials Science and Engineering 393 (2018) 012004 doi:10.1088/1757-899X/393/1/012004.

[6] Porter, M.E., Heppelmann, J.E.: How Smart, Connected Products Are Transforming Competition, 2014. URL: https://hbr.org/2014/11/how-smart-connected-products-are-transform¬ing-competition.

[7] https://www.cleverism.com/industry-4-0/
[8] Miltenović, V., Marković, B.: Third Mission of University - State, Challenges, Perspective. Proc of 4st Int.Con. ”Conference on Mechanical Engineering Technologies and Applications” COMET-a 2018, 2018, Jahorina. Plenary Session s. 18-36.
[9] VDI-Richtlinie 2222, „Konzipieren technischer Produkte“ VDI-Verlag, Düsseldorf, 1973.
[10] VDI-Richtlinie 2221, „Methodik zum Entwickeln und Konstruieren technischer Systeme und Produkte“, VDI Verlag, Düsseldorf, 1993.
[11] VDI-Richtlinie 2206, Entwicklungsmethodik für mechatronische Systeme. Beuth, Düsseldorf. 2006.

Prof. Vojislav Miltenović, **PhD**. Current position: Chief of the Smart office 1 of the Innovation Center of the University in Nis (ICUN). Previous position: Head of installation of Factory of plastic coated iron plates in metal industry “Lemind” Leskovac; Full Professor of Faculty of mechanical engineering, Niš; Visiting Professor of Fachhochschule Wilhelmshaven - FR Germany; Head of the Department for mechanical constructions, development and engineering; Visiting Professor of Faculty of mechanical engineering, East Sarajevo; President of Association for Design, Elements and Constructions. Member of IFToMM Technical Committee for Gearing and Transmissions. Academic qualifications: 1970, BS-Faculty of Mechanical Engineering; 1979, MS-Faculty of Mechanical Engineering; 1982, PhD-Faculty of Mechanical Engineering. Main areas of scientific research: machine elements, machine design, product design and development, innovations and innovative construction solutions, competence of development engineers. Research experience: Participant or manager of 20 scientific projects of national importance (in 9 projects participated in the capacity of researchers, in 11 in the capacity of project manager), and 36 expert projects; Coordinator 4 international projects; the author of 13 university books. Publications: Number of publications: about 170. Mentor: 5 doctoral and 11 magister thesis. Review: 28 books and 144 scientific and professional papers.

Prof. Nenad Marjanović, **PhD**. Full professor at the University of Kragujevac, Faculty of Engineering in Kragujevac, where he is the head of the Department for Mechanical Constructions and Mechanization.

Head of one and participant in the realization of 7 international projects of the national ministry. Author and co-author of 102 research papers, 4 textbooks, and one monograph. Member of 21 committees for evaluation and presentation of PhD theses. President of two Organizing Committees and member of 7 Program Committees of international conferences.

9th International Scientific Conference
Research and Development of Mechanical Elements and Systems
Kragujevac, Serbia, September 5-7 2019

- KEYNOTE LECTURE -

GEAR UNITS FOR EXTREME OPERATING CONDITIONS AND LOW WEIGHT
-INNOVATIVE DESIGN AND TESTING -

Milosav Ognjanović, *professor emeritus* [1, 2, 3]

[1] University of Belgrade, Faculty of Mechanical Engineering;
[2] Academy of Engineering Sciences of Serbia;
[3] EDePro – Engine Design and Production - Belgrade,
milosav.ognjanovic@gmail.com

Key words: Gear units, Engineering design, Laboratory testing, Turboshaft motor-reducer, Unmanned helicopter, Power transmission

SUMMARY

The basic message of the lecture is to support and encourage the innovative development of mechanical structures, which together with electronic, software and mental function executors represent the current direction of development of technical systems (TS). Actual trend of TS development implies hybridization and increase the level of existing TS, but also modernization and innovation of mechanical structures. New operating conditions require new functions and new properties that can satisfy new mechanical structures. In the field of gear trains, as example for presentation is chosen gearboxes and transmissions of unmanned helicopters, which we are developing in EdePro company. Especially for consideration is separated the reducer of a turbo-shaft engine with a free turbine for traction of this helicopter.

This motor-gearbox performs its function in extremely difficult operating conditions. In the first place, it is an extremely high rotational speed of 40,000 rpm, so that the peripheral speed of the gear teeth reaches values up to 100 m/s, and the teeth mesh frequency is deep in the supercritical frequency region. Another extremely disadvantageous condition is the close distance between the gear unit and the exhaust gas flow zone, whose temperature reaches 700^0C. The power to be transmitted is in the range of 80-160 kW, and can reach 200kW. Due to the need for high compactness and dynamic stability, a conceptual solution with three parallel branches whose axes are fixed was applied. To further reduce the dimensions and weight of this gearbox, several innovative solutions in structural details have been applied.

Some of these solutions are as follows. Grinding of dual gears on parallel axes is only possible if they are sufficiently spaced apart. This is in contradiction with the reduction of dimensions. A structural and technological solution was made according to which these gears are joined

after grinding so that they are jointed at a very close distance with identical teeth ratios for each of the coupled pairs. A number of possible consequences of such a merger have also been eliminated. Another innovative solution consists of a method of injecting oil into the gear teeth connections in order to maintain the oil film between the teeth. Without the oil film, the teeth scoring and high local temperatures occurred at extremely high speeds and loads. This is followed by a combined system of insulation and cooling of the gearbox, because in addition to the heat that develops inside the gearbox, intense heating also comes from the hot gas stream.

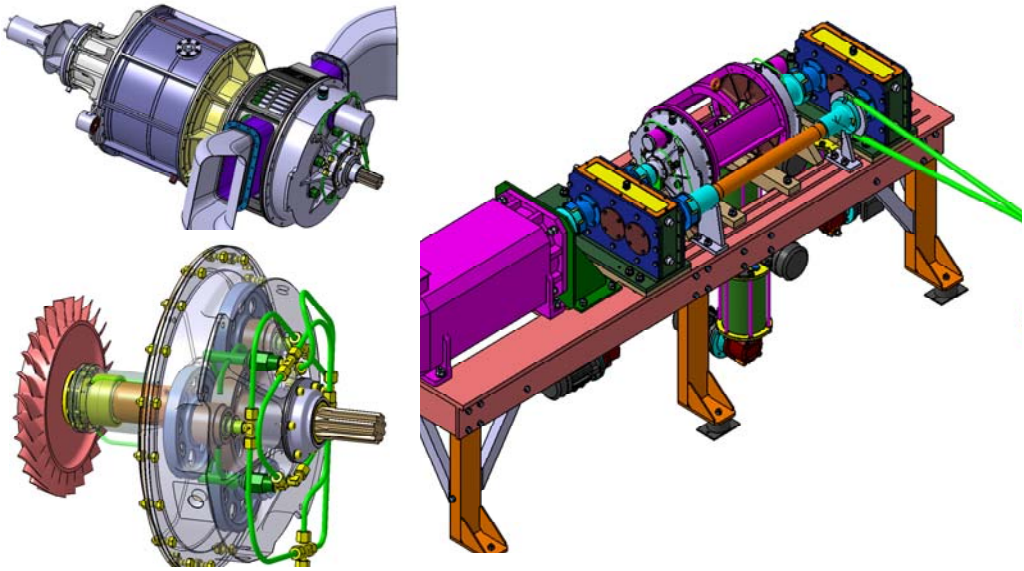

Figure 1. Turboshaft motor-reducer with test-stend

The performance of developed motor-reducer in extremely difficult operating conditions should be checked by laboratory testing. The laboratory installation shown in Figure 1 was developed for this purpose. The load is realized on the principle of power circulation. The rotational speed varies continuously up to 6,000 rpm while in the interconnect of the reducers tested is 40,000 rpm. Both tested gearboxes and both gearboxes for close the power flow are cooled by four separated oil cooling systems. The load and rotation speed are defined by the test installation. The vibrations of the tested gearboxes, the flow of oil and the temperature in several places, especially the oil temperature at the outlet and at the inlet of the tested gearbox, are measured. One of the important goals of this test is to determine the thermal balance and thermal state of the gearbox under steady-state of operating conditions. To determine performance, the test process takes until stationary operating and thermal conditions are achieved. In addition, testing is carried out to monitor the failure process and the time resource until possible malfunctions. Load and failure distribution in paralel branches of power transmission are wery important.

Acknowledgments. The development and testing of these gear units is realized in enterprise EDePro - Engine Design and Production - Belgrade.

Milosav Ognjanović, PhD is a professor emeritus at the University of Belgrade, Faculty of Mechanical Engineering. He is a full member of Academy for Engineering Sciences of Serbia – AESS and works for EDePro – Engine Design and Production.

His research interests are Design Science (Design Methods; Decision making, Modelling, Robust design, TRIZ), Machine Systems Dynamics (Vibration and Noise Generation in Machine Systems), Safety and Reliability (Fatigue, Teratology, Damage accumulation, Fracture, Reliability for Design), and Gear Transmission (Design, Vibration and Noise Generation, Fatigue and fracture, Reliability for design). He authored and coauthored 15 textbooks (2 of them "Machine elements" and "Innovative development of technical systems" are permanent university textbooks); 3 monographs; 5 chapters in international monographs as well as 39 journal articles and 155 conference articles. He has 120 technical contributions (projects, solutions, expertise and reports about experimental researches) and more than 250 hetero citations.

He was Editor-in-chief of two international journals, and member of editorial board of a few international journals. Organizer of a few national and international conferences and member of organizing and program committee of the set of international and national conferences. Member of Design Society, ESIS - The European Structural Integrity Society, Representative of Serbia in DANUBIA-ADRIA Society for Experimental Mechanics, BAPT-Balkan association for Power transmission. Coordinator of Tempus project for foundation of master studies for Design in mechanical engineering. Participation and carrier of work packet in FP-7 project. He also has visited and cooperated with more than 20 universities.

He teaches subjects on all study levels. Namely: Machine elements-1; Machine elements-2: Fundamentals of technical innovations (B.Sc Studies), Innovative design of technical systems; Methods in engineering design; Gearbox (gear transmission units) reliability (M.Sc Studies) and Structure testing methods; Product development in mechanical engineering; Reliability and dynamics of power transmission units; Engineering design methodology (Ph.D Studies). He is also a supervisor of 3 theses in the field of vibration and noise generation in gear transmission units and engines with internal combustion, 3 theses in the field of design methodology development, and 4 theses in the field of technical system conditions research and new approaches development.

MECHANICAL ELEMENTS AND SYSTEMS

modeling and simulation, loading and stress conditions, tribology, noise and vibrations, maintenance and monitoring, safety, quality, reliability

9th International Scientific Conference
Research and Development of Mechanical Elements and Systems
Kragujevac, Serbia, September5-7 2019

- PAPER BY INVITATION -

VIBROT - SOFTWARE FOR VIBRO-DIAGNOSTICS OF ROTATION MACHINE

R Tomović[1], D Bratić[1], M Mumović[1], V Vujošević [1], A Tomović[1]

[1]University of Montenegro, Mechanical Engineering Faculty, bul. Džordža Vašingtona bb., Podgorica, Montenegro, radoslav@ucg.ac.me

Key words: VIBROT, software for vibro diagnostics, rotation machine, rolling bearing, Fourier transform, Envelope analysis, Cepstrum analysis, Spectral Kurtosis

The aim of this paper is to present VIBROT - a complex software for diagnostics of rotary machines that was developed in the Laboratory for mechanical constructions at the Faculty of Mechanical Engineering in Podgorica. *Graphical User Interface* - GUI of the software is shown in Figure 1.

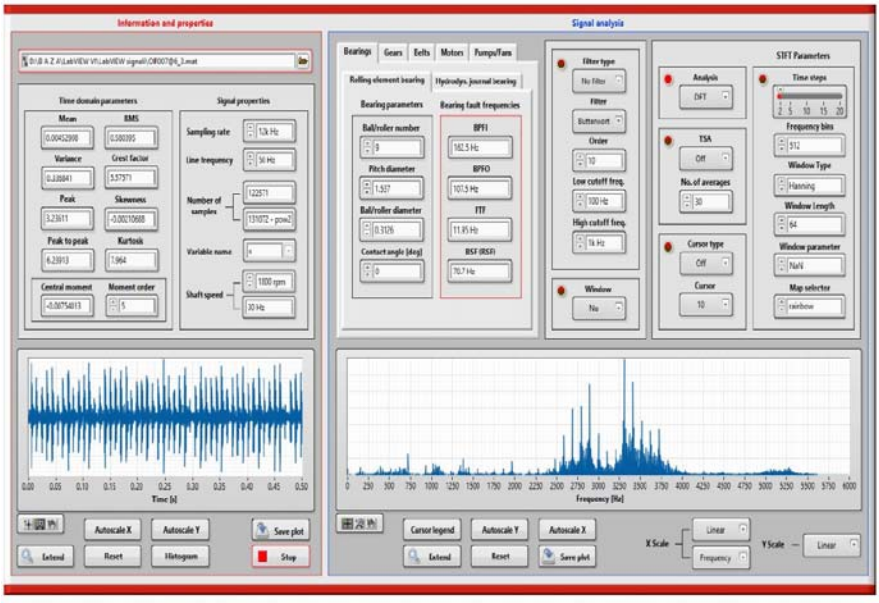

Figure 1. VBROT user graphical interface (VIBROT – GUI)

GUI software consists of two main panels:

• The left panel labelled with **Informations and properties** - also offers the possibility of a simple analysis of vibrations in the time domain and
• The right panel marked with **Signal analysis** - serves for more complex signal processing, using selected analytical methods.
Panel Information and properties allow you to enter the desired *.mat file, the frequency of discretization and other input parameters, and display the results of the analysis of the vibro diagnostics by graphics in the time domain and various statistical parameters such as kurtosis, crest factor, etc., and it provides simple vibro diagnostics analysis in the time domain. The second panel marked by Signal analysis allows for a more complex vibro diagnostics analysis, using more sophisticated analytical methods for signal processing. This part contains several cards to calculate the characteristic frequency of roller and slide bearings, gear and belt drives, as well as motors, pumps and fans. The input parameters of this part are the values of the structural parameters of the mentioned circuits (engine speed, number of teeth of the gear, number of balls in the roller bearing, etc.), and consequently, the corresponding characteristic frequencies are displayed at the exit. This panel offers the ability to filter signals using a variety of digital filters provided by the LabVIEW development environment. For the purposes of this software, Butterworth's, Chebyshev's, Inverse Chebyshev's, Elliptical and Bessel's low-pass and high-pass filters were used, as well as the frequency transient and steady-state filters. The Analysis type window inside the panel offers the ability to apply one of the following methods for signal processing: Discrete and Short-term Fourier transform, Envelope analysis, Cepstrum analysis, Spectral Kurtosis, Time synchronous signal averaging, etc.

To test the efficiency of the developed software, the analysis of the vibrations of real rolling bearings has been done in which the presence of certain irregularities or damages has already been undeniably determined. The bearings used in the test are artificially damaged and then assembled for the needs of certain experiments in progress research. A rolling ball bearing 6205 was used for testing. On one of the balls of the bearings the artificially made damage of the elliptical shape is about 2.5x3.5 mm made by grinding. Time-varying measurement results are processed in the VIBROT software, using the envelope frequency analysis and are shown in Figure 2. The obtained results indicate that using the developed software it is possible to perform an efficient diagnostic of the condition of the roller bearings.

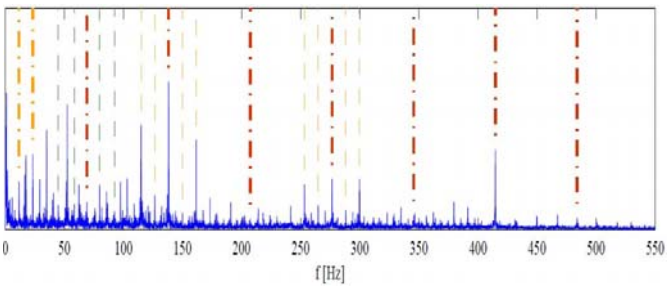

Figure 2. Spectrum envelope signal.

STUDY OF OPERATING TEMPERATURE OF SPUR GEARS UNDER MIXED LUBRICATION CONDITIONS

J D Jovanović[1], R B Bulatović[1]

[1]University of Montenegro, Faculty of Mechanical Engineering, Džordža Vašngtona bb, 81000 Podgorica, Montenegro, janko@ucg.ac.me

Key words: spur gears, mixed lubrication, operating temperature, CVFEM.

Continuous operation of gear transmissions running under mixed lubrication, generates a high temperature rise within tooth contacts and heats up the gear surface, which can cause surface failure, such as hot scoring, wear, surface pitting, micropitting and thermal cracking. For these reasons the surface temperature holds the critical information about the gear condition. Proper choice of gear geometry may reduce the friction and operating temperature of the gear, preventing surface defects in order to increase its reliability. Previous studies of the frictional heating of the gears are mainly in the field of numerical modeling and experimental measurements. Developed numerical models were used to investigate the influence of gear geometry and other influential parameters on the distribution of operating temperature along the pressure line of meshed gears. The influence of face width, outside diameter and pitch diameter presented by K.L.Wang and H.S.Cheng in 1981, as well as, influence of face width and module presented by H.Long et all in 2003 on the distribution of operating temperature of the gear were investigated by these models. The result of these investigations are insufficient for complete understanding of the gear geometry influence to distribution of its operational temperature. Therefore, this investigation deals with a sensitivity analysis of operating temperature to changes of spur gear geometry over a range of applied load and rotational speed in order to achieve deeper insight into influence of gear geometry to distribution of its operating temperature under mixed lubrication conditions. Control volume finite element model presented by J.Jovanović and R.Bulatović in 2017, using three-noded triangular elements, has been employed to investigate spur gear frictional heating over a range of gear dimensions.

Model boundary conditions are in accordance with proposal of H.Long et all from 2003. The coefficient of friction in full film lubrication and boundary lubrication, as well as, the film thickness are determined in accordance with proposal of J.O.Echavarri et all from 2016 and 2017. The heat flux on the contact area of the pinion and gear generated by frictional sliding

are determined in accordance with the proposal of H.Long et all from 2003. Heat transfer coefficient is determined in accordance with proposal of A.Dewinter and J.Blok from 1974.

Basic dimensions of investigated spur gear set are as follows: z_1=15, z_2=16 and face width b=4.755 mm. Both gears are made of 665M17 (EN-34) steel with the following basic mechanical and thermal properties: modulus of elasticity E=185.42 GPa, Poisson's ratio ν=0.3, thermal conductivity K=41.8 W/m·K, thermal difusivity χ=1.077·10^{-5} m^2/s , specific heat c=493 J/kg·K. This gear set is case-hardened and ground to a surface finish of σ_1=σ_2=0.6 μm. Synthetic oil poly-alfa-olefine PAO-6, with following properties at bath temperature T_b=80°C, is used as lubricant in gearbox: ρ_l=0.83 kg/dm^3 temperature-viscosity coefficient β=0.033 K^{-1}, n=0.81, shear modulus G=0.1 MPa, thermal conductivity K_l=0.15 W/m·K, specific heat c_l=2200 J/ kg·K. Lubricant viscosity at ambient pressure and piezoviscous coefficient: η_o=25 m·Pa·s and α=11.5 GPa^{-1} at T=40°C, η_o=12.57 m·Pa·s and α=10.1 GPa^{-1} at T=60°C, η_o=7.36 m·Pa·s and α=9.0 GPa^{-1} at T=80°C, η_o=4.78 m·Pa·s and α=8.2 GPa^{-1} at T=100°C.

In order to investigate an influence of gear geometry on the distribution of its operating temeperature a serie of gear models is generated with variation of module, pressure angle and coefficient of profile shift. Dimension ranges of interest for this research are m=(3÷8) mm, α_p =(20÷28)°, x_1=(-0.4÷0.2). Geometries of the pinion tooth with different values of module, pressure angle and coefficient of profile shift and corresponding triangular finite element meshes are generated. Finite element mesh of each model involved not more than 1000 nodes. Some of determined CVFEM temperature distribution over the pinion tooth for torque T=73 Nm and number of revolutions n=10000 rpm are illustrated in a following figure.

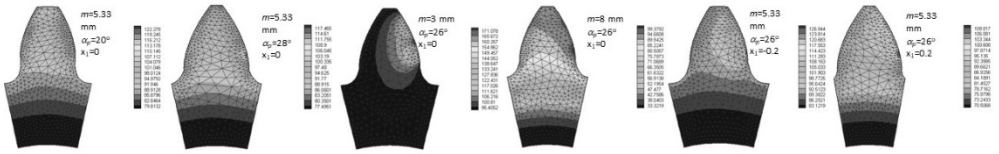

Figure 1. Distribution of pinion temperature

As shown in figure 1, increase of pressure angle from 20° to 28° influences on reduction of gear maximum temperature up to 4%, increase of module from 3 mm to 8 mm significantly influences on reduction of gear maximum temperature up to 42%, increase of coefficient of profile shift from -0.2 to 0.2 significantly influences on reduction of gear maximum temperature up to 14%.

The CVFEM models with different combinations of gear geometric dimensions are established for evaluating the influences of gear geometry on tooth temperature variations. According to this models the zone of highest operational temperature of gear is its meshing flank. There are two temperature peaks along meshing flank one below and another above the pitch circle. The maximum gear temperature for each investigated case is at the peak below the pitch circle. Regarding gear dimensions, distribution of the gear tooth temperature is quite sensitive to changes of its module and coefficient of profile shift and insensitive to changes of its pressure angle.

IRMES KRAGUJEVAC 2019

9th International Scientific Conference
Research and Development of Mechanical Elements and Systems
Kragujevac, Serbia, September5-7 2019

EFFECTS OF STRUCTURAL OPTIMIZATION ON PRACTICAL ROOF TRUSS CONSTRUCTION

Nenad Petrović[1], Nenad Kostić[1] Nenad Marjanović[1], Jelena Živković[1], Ileana Ioana Cofaru[2]

[1]University of Kragujevac, Faculty of Engineering, Sestre Janjić 6, 34000 Kragujevac, Serbia, npetrovic@kg.ac.rs
[2]University "Lucian Blaga" of Sibiu, Department of Industrial Machines and Equipment, Emil Cioran 4, Sibiu, Romania

Key words: truss, structural optimization, buckling, discrete variables, surface area.

In the search for more economical design solutions engineers today rely on optimization processes to find concepts which might not otherwise be logical or would require numerous iterations of analytical calculations. For practical applications complexity of the optimization process is increased significantly with multiple aspects of the construction being optimized and with every constraint which is added to avoid unusable solutions. The minimal weight optimization is generally approached through optimizing either sizing, shape, topology, or one of their combinations. The constraints used in this research are maximal allowed stress, maximal allowed displacement and dynamic constraints for buckling.

In this paper a typical roof truss (Figure 1) for a 20m wide warehouse was optimized for sizing, shape and their simultaneous combination in four separate topological layout cases (Figures 1-4). An original software was developed which also outputs calculated total outer surface area of the optimal truss designs. As surface protections plays a big part in the overall cost of constructing a roof truss, up to a quarter of the total cost in fact, this aspect of the optimal design concepts is compared to show whether a minimal weight design provides savings in other aspects of the construction as well.
The roof truss is loaded in the top nodes with point loads of F=17.652kN which represent a maximal load from snow. For this example S235JRG2 steel is used with a Young modulus of 210 000MPa and a density of 7.85g/cm^3. Constraints for the problem are a compression and tension strass limit of 180MPa for all bars, a maximal allowed displacement of ±0.036m for all nodes, and dynamic constraints for Euler buckling for all bars in every iteration. Moments of inertia for the 40 possible profiles were taken from various vendor's catalogues.

Figure 1. Bar layout of topological case 1.

Figure 2. Bar layout of topological case 2.

Figure 3. Bar layout of topological case 3.

Figure 4. Bar layout of topological case 4.

Figure 5 shows the differences in optimal weight for all four topological layout cases for both sizing and sizing shape combination. Overall outer surface areas of optimal model's bars are shown in Figure 6 for all cases and optimization aspects.

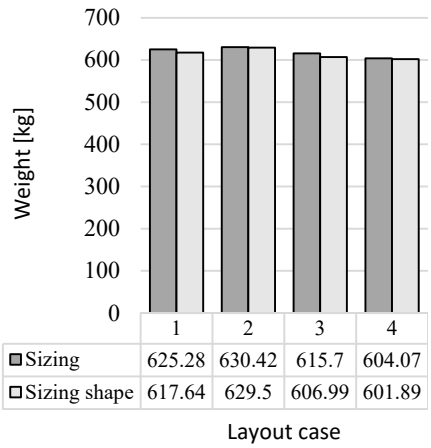

Figure 7. Difference in optimal weight according to topological layout case and optimization type.

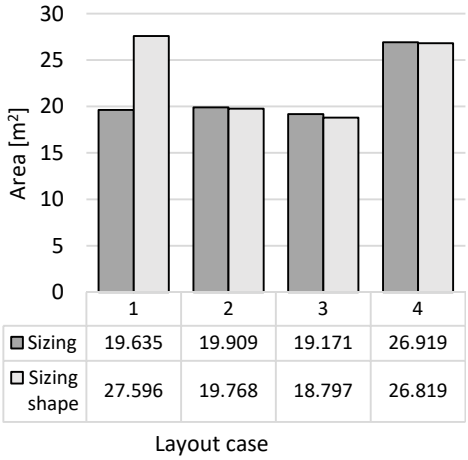

Figure 8. Difference in overall outer surface area according to topological layout case and optimization type.

It can be concluded that while the minimal weight design for trusses using a combined approach of sizing, shape and topology optimization gives the best results in terms of weight, it might not be the case when looking at the effects it has on other aspects of a construction which contribute to the overall cost in a meaningful part.

Acknowledgments. This paper is a result of the TR32036 project, which is an investigation of the Technological Development of the Republic of Serbia. The project is titled "Development of software for solving the coupled multi-physical problems". We would like to thank to the Ministry of Education, Science and Technological Development of the Republic of Serbia for their financial support during this investigation.

9th International Scientific Conference
Research and Development of Mechanical Elements and Systems
Kragujevac, Serbia, September5-7 2019

EFFECT OF FRICTION ON NOMINAL STRESS RESULTS IN A SINGLE TOOTH BENDING FATIGUE TEST

Mislav Vukić[1], Ivan Čular[1], Robert Mašović[1]

[1]University of Zagreb, Faculty of Mechanical Engineering and Naval Architecture, Ivana Lučića 5, 10000 Zagreb, Croatia

Key words: Spur gear, single tooth bending fatigue test, finite element method, friction, tooth root stress

One of the main reasons for gear failure is bending fatigue, which occurs due to cyclic stresses at the tooth root region. Bending fatigue can cause crack initiation which, in turn, may propagate and result in catastrophic tooth breakage. Single tooth bending fatigue tests are frequently employed to generate statistically significant fatigue data at relatively low price. Hence, they are often employed as screening tests for bending fatigue behavior of actual running gear pair. Since relatively small alteration of nominal tooth root stress values can produce significant change in bending fatigue lives, it is important to adequately consider the effect of friction and test fixture deformation when conducting single tooth bending fatigue tests. In this paper, numerical investigation of tooth flank friction effect on spur gear load capacity during single tooth bending fatigue test is carried out. Two different test fixtures are considered.

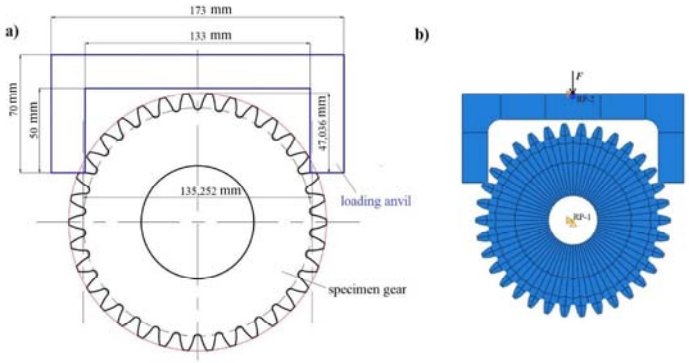

Figure 1. First test fixture: (a) geometric model and (b) numerical model with boundary conditions and loading point.

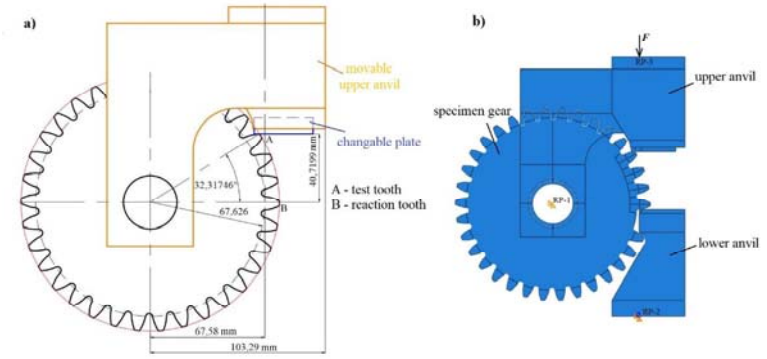

Figure 2. Second test fixture: (a) geometric model and (b) numerical model with boundary conditions and loading point.

Linear elastic finite element analysis is carried out to obtain nominal tooth root stresses. In addition to various friction coefficients, the effect of rigidity of the test fixture has also been considered. The results show that friction at gear tooth flank as well as fixture deformation can affect nominal tooth root stress results.

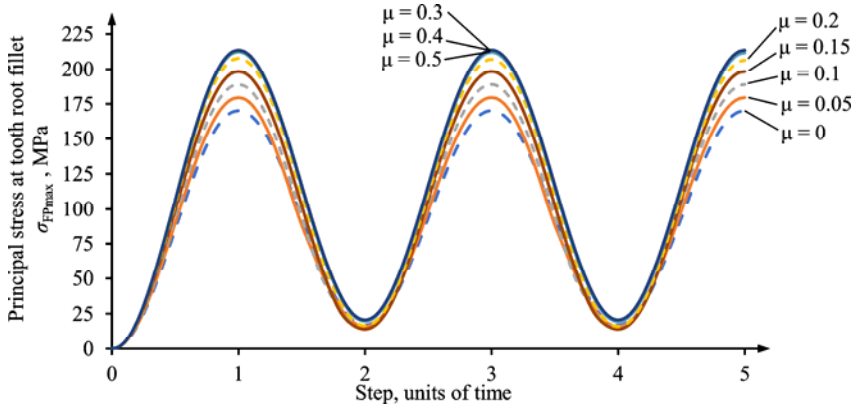

Figure 3. Principal stress-time history for the tooth root fillet and elastic behaviour of the loading anvil.

The results were compared with the initial predictions of stress behavior for various friction and rigidity conditions and were found to be in a good agreement. In this investigation, it was found that friction can impact nominal tooth root stress results, which can influence bending fatigue life of a gear. Since STBF tests are often used as screening tests for actual bending fatigue behavior of the gear, friction coefficient should be determined before the test and properly compensated for; or reduced to minimum for the most accurate results.

9th International Scientific Conference
Research and Development of Mechanical Elements and Systems
Kragujevac, Serbia, September5-7 2019

DETERMINATION OF THE PARASITIC FORCES THAT OCCUR AS A CONSEQUENCE OF THE MOVEMENT OF THE ROLLER OVER THE MINIATURE PROFILED GUIDE

V Kočović[1], S Kostić [2], S Vasiljević[2], Ž Santoši[3], A Košarac [4]

[1]University of Kragujevac, Faculty of Engineering, Sestre Janjić 6, 34000 Kragujevac, Serbia, vladimir.kocovic@kg.ac.rs
[2]Technical College of Applied Studies in Kragujevac, Kosovska 8, 34000 Kragujevac, Serbia, sonja25yu@yahoo.com
[3]University of Novi Sad, Faculty of Technical Sciences, Trg Dositeja Obradovića 6, 21101 Novi Sad, Serbia, zeljkos@uns.ac.rs
[4]University of East Sarajevo, Faculty of Mechanical Engineering, Vuka Karadžića 30, Sarajevo, Bosnia and Herzegovina, akosarac@gmail.com

Key words: frictional force, energy losses, roller, profiled guide

In order to achieve a greater efficiency degree of electrical, mechanical or other assemblies that work by consuming any form of energy, the frictional force that occurs between all moving elements of the system should be minimized. Nowadays, a lot of standard sliding and rolling pairs have been developed, which provide linear movement. Since manufacturers of these elements do not prescribe coefficient of friction when moving movable rollers on a fixed rail, it is often necessary to know the resistance to motion of these elements due to the correct selection of the drive system, and therefore it is necessary to determine them. In this paper, the resistance to motion of roller through the miniature profile guide 15 mm in width and 10 mm in height was tested.

When two solid bodies are in contact, there is a frictional force between them. Thus we distinguish two types of friction coefficient: the static friction coefficient - represents the friction that opposes the onset of relative motion and the kinetic coefficient of friction - is a friction that opposes the continuation of relative motion when motion has begun. The static friction coefficient increases with increasing surface roughness parameters, while low coefficient friction is associated with smooth surfaces.

In this paper authors will show an experiment of a single contact pair, rollers and miniature profiled guides, where the values of friction and friction coefficient will be obtained.

The principle of coefficient of friction measurement over an inclined plane, figure 1, is based on the use of a gravitational force. The static coefficient of friction, as is known, is the ratio of the frictional force and the force perpendicular to the surface of the contact, where the

equilibrium condition for inclined plane is given by the expression $F_\mu > m \cdot g \cdot \sin\alpha$. For the limit of sliding friction, equality applies:

$$\mu = \frac{F_\mu}{N} = \frac{m \cdot g \cdot \sin\alpha}{m \cdot g \cdot \cos\alpha} = tg\alpha$$

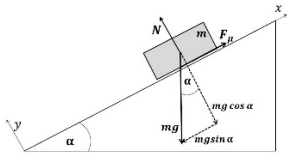

Figure 1. Equilibrium condition of the body on an inclined plane

Experimental examination was carried out on a specially designed tribometer, figure 2, to determine the static coefficient of friction according to an inclined plane principle. The contact pair, in this case, the profiled guide and the roller turn to one side until the moment of starting the roller move through the profiled guide. This is the moment when the driving force has reached the value of the resistive frictional force. By measuring this angle, the coefficient of friction of this contact pair is determined. Given the stochastic nature of the friction coefficient, the measurement was repeated 200 times to obtain as realistic friction coefficient as possible by statistical analysis of results. All the experimental results are divided into 10 classes to form the Gaussian distribution, figure 3, and the angle, as realistic as possible, at which the roller is moved by the profiled rail.

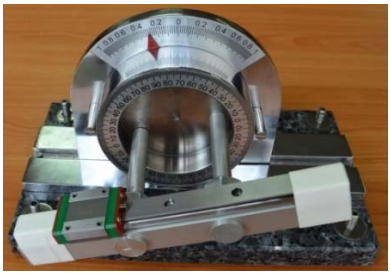

Figure 2. A device for testing the static coefficient of friction of the roller on an inclined plane

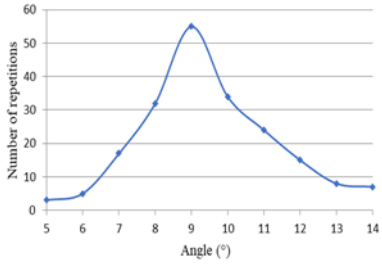

Figure 3. Gaussian distribution of experimental results

By analysing the experimental results it can be seen that statistically observed the highest probability that the angle value that makes the roller motion per profiled guide is 9° and that probability is 27.5%. By knowing this angle and the mass of the roller it is possible to calculate the frictional force of roller per profiled guide.

$$F_\mu = m \cdot g \cdot \sin\alpha = 0{,}059(kg) \cdot 9{,}81(m/s^2) \cdot \sin 9^\circ = 0{,}0905(N)$$

From the equation above it is seen that the frictional force of this contact pair is small, but it should certainly not be forgotten in the construction of the small power drive unit where it can occupy a large relative part. To this end, the knowledge of all the parasitic forces that must exist in any kind of movement is crucial to the proper design of the driving system.

Acknowledgments. This work was funded by the Ministry of Science and Technological Development of Republic of Serbia, Grant TR-35021, Title: Razvoj triboloških mikro/nano dvokomponentnih i hibridnih samopodmazujućih kompozita.

9th International Scientific Conference
Research and Development of Mechanical Elements and Systems
Kragujevac, Serbia, September5-7 2019

MACRO-ROUGHNESS HEIGHT DETERMINATION OF TEETH SURFACES OBTAINED BY GEAR GENERATING METHOD

Dmitry Babichev[1], Denis Babichev[2], Sergey Lebedev[1]

[1] Industrial University of Tyumen, Institute of Transport, Melnikayte Street 72, 625039 Tyumen, Russia, babichevdt@rambler.ru
[2]Sibur Holding, ZapSibNeftekhim LLC, East Industrial District, Block 1, No. 6, Building 30, 626150 Tobolsk, Russia, babichevda@tobolsk.sibur.ru

Key words: gear machining, macro-roughness, teeth surfaces.

The article describes three types of gear teeth surfaces (Fig. 1-3): smooth (Fig. 3 – envelope), striped (Fig. 1 – with combs) and scaled (Fig. 2 – with pyramids and combs connecting the pyramids). Scaled surfaces are generally composed of parallelogram (upper image in fig. 2) or hexagonal (lower image in fig. 2) pits. Pit central points touch calculated tooth surface.

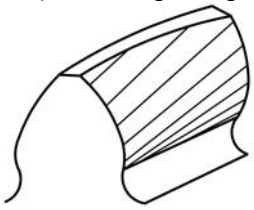

Figure 1. Stripped tooth surface

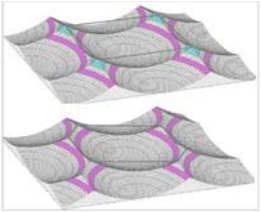

Figure 2. Scaled teeth surfaces

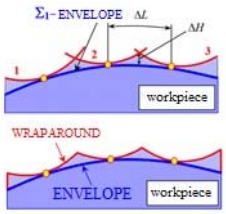

Figure 3. Envelope and wraparound

Determining the heights difference – Δ*H* in fig. 3 – for particular machining types is considered a quite challenging task. Typically to complete the task the envelope and points on the intersection line of complex adjacent pits or stripes surfaces should be found. . The paper uses kinematic method for determining surfaces and lines produced by generating process. The method is different from all known in the classical theory of gearing methods.

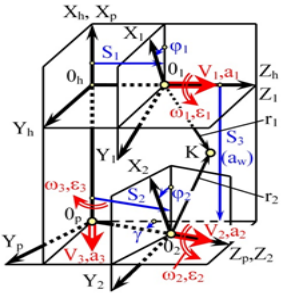

Figure 4. Generalized meshing

Method is based on «velocity of penetration» V_N (proposed by V.A. Shyshkov) and «acceleration of penetration» a_N (D.T. Babichev) conceptions. The paper provides calculation formulae for determining V_N and a_N. for generalized meshing (fig. 4).

The determination formulae of "Combs" height ΔH above an envelope surface in case of one-parametric generation:

$$\Delta H = -0{,}125 \cdot a_N \cdot \Delta t^2 \qquad (1)$$

where a_N – *generating tool* penetration acceleration, calculated at a contact point of an instrument (its CTIS) with machining surface; Δt – period of time between two moments of adjacent stripes cutting determined according to one of the formulae:

$$\Delta t = \frac{2 \cdot \pi}{\omega_0 \cdot z_0 \cdot k_X} = \frac{2 \cdot \pi}{\omega_1 \cdot z_1 \cdot k_X} = \frac{2 \cdot \pi}{\omega_0 \cdot z_0 \cdot k_Z} \qquad (2)$$

where ω_0, ω_1 – angular tool and workpiece velocities respectively wherein acceleration of penetration a_N is calculated; z_0, z_1 – shaping cutter and workpiece teeth number respectively; k_X – number of shaping cutter or rack-type tool strokes per one teeth machining; k_Z – involute gear cutter chip grooves number or toolheads cutters number.

Height ΔH in case of two-parametric generation:

$$\Delta H_{MAX} = -0{,}125 \cdot (a_{NV} \cdot \Delta t_V{}^2 + a_{NS} \cdot \Delta t_S{}^2) \qquad (3)$$

where a_{NV}, a_{NS}, a_N – generation and feed acceleration of penetration respectively.

Parameters ;Δt_v and ;Δt_S are determined according to the formulae:

$$\Delta t_V = \frac{60}{n_0 \cdot z_{0k}} \quad ; \quad \Delta t_S = \frac{60}{n_1 \cdot z_0} \qquad (4)$$

where z_0,z_{0k} –number of cutters and cutter chip grooves respectively.

Pits can be parallelogram or hexagonal in shape. For hexagonal pits obtained by a two-motions (generating and feeding) gear machining method it was analytically determined and computationally proven in [3] that: *all the six vertices heights are equal and comprise 75-100% o f* Δ_{MAX} *calculated according to the formula* (1).

For all pit types the following formula for pyramids height ΔH – i.e., maximum faceting height – determination was obtained:

$$K_Z = 1 - \frac{k_{HL}}{1 + k_H} \cdot (2 - k_{HL}) \qquad \Delta H = K_Z \cdot \Delta H_{MAX} \qquad (5)$$

where ΔH_{MAX} is calculated according to the formula (1), and

$$k_H = \frac{\Delta_1}{\Delta_2} = \frac{a_{NV} \cdot \Delta t_V^2}{a_{NS} \cdot \Delta t_S^2}; \qquad k_{HL} = k_H \cdot k_L \cdot (1 - k_L) \qquad (6)$$

Figures are given on how the shape of the pits and the height of the pyramids change with a two-parametric generation. Diagrams are given that show how the heights of the pyramids depend on the parameters of tooth processing. After calculating pits and pyramids sizes and shapes it was estimated how the macro-roughness height Δ can decrease depending on generation parameters. The ratio of macro-roughness height Δ to maximum macro-roughness height Δ_MAX cannot be less than 0.75 which is the significant result of the macro-roughness height analytical research.

Conclusion: methodology for determining a height of macro-roughness is developed and described, which does not require determining the cutting surfaces themselves.

Acknowledgments. This work was supported by grant (project № 9.6355.2017/БЧ) of government order of Ministry of education and science of Russia Federation for the period 2017–2019 in Tyumen Industrial University.

9th International Scientific Conference
Research and Development of Mechanical Elements and Systems
Kragujevac, Serbia, September5-7 2019

DELAMINATION ASSESSMENT OF COMPOSITE CURVED ANGLES USING SIMPLIFIED FEA MODELS BUILD-UP BY 2-D LAYERED SHELL ELEMENTS

Marius Nicolae Baba[1]

[1]Transilvania University of Braşov, Department of Mechanical Engineering, B-dul Eroilor no. 29, 500036 Braşov, Romania

Key words: delamination, folding-unfolding, composite curved angles, shell forces.

The use of fiber-reinforced composite laminates across a variety of industrial fields is becoming increasingly common due to their weight saving potential with respect to conventional metallic materials. When curved composite laminates are subjected to outward bending by unfolding, due to the combined effects of bending, axial and shear forces acting in plane of curvature the inner layers experience tension generating circumferential tensile stresses, whereas the outer layers undergo circumferential compression stresses. Otherwise, folding by inward bending generate compression of inner layers while tensile the outers. In addition, the radial stresses developed due to the internal bending moment tend to separate the interfaces while the shear stresses caused by the out-of-plane force components tend to shear apart the layers.
For design purposes, an efficient procedure to accurately predict the stress state across the thickness of a specific composite laminate requires the calculation of interlaminar through-the-thickness stresses as well as the shear stress components at the interfaces. These so-called out-of-plane stresses are the key parameters in failure analysis of curved composite laminates, particularly when their radius of curvature approaches the stacking thickness.
Based on the finite element analysis results obtained through the use of conventional layered shell elements, the aim of this paper is to propose a simplified post processing approach that enable to predict the interlaminar stress components originated across the thickness of symmetrically balanced curved composite laminates, under the combined action of axial forces, shear forces and bending moments applied in curvature plane. A benchmark analysis to provide a critical comparison between a reference model constructed based on 3-D layered solid elements and a simplified model build-up by 2-D layered shell elements is considered.
A detail view of curvature area for the layered shell finite element model is presented in Figure 1. In this regard it has to be mention that both for the simplified model as well as for the reference model, the loading is virtually represented by two unit forces (F_1 = -1kN; F_2 = 1kN) and a unit couple (M_3 = 1kNm), applied on the free side of the angle in the curvature

plane, with respect to the global reference coordinate system. As shown in Figure 1, the clamped boundary conditions at the bolt holes as well as the unit loads are applied by means of RBE2 elements.

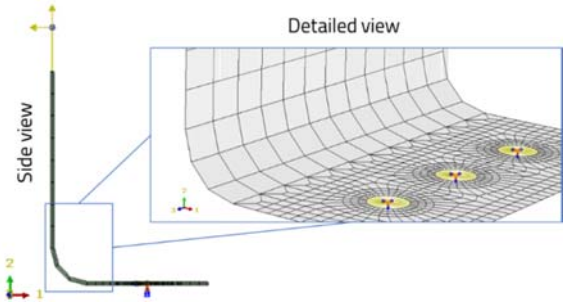

Figure 1. The simplified FE model of layered shell elements

The force and moment fluxes were extracted at both ends of the curved region. The local coordinate systems are defined for both angle sides so that their positive directions determine opening the angle. Figure 2 shows the selection of elements and the orientations of the local coordinate systems used for extraction of fluxes at the beginning and the end of curvature region.

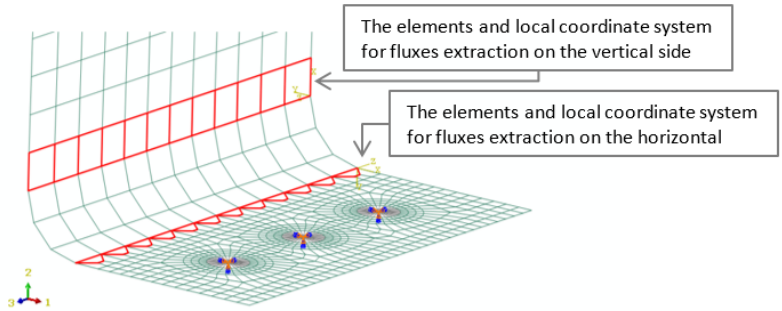

Figure 2. The elements selection and the local coordinate systems

The proposed simplified approach is based on a two dimensional analysis of the composite laminate angle, and it is assumed that the properties, the boundary conditions as well as the applied loads are constant along the width. The base assumption of this approach is that the solution of the elastic problem is constant in the transversal direction. Plane strain assumption is generally valid for wide composite laminate angles, when the transversal length is large compared with the other dimensions.

The comparative critical analysis of the finite element results obtained by means of using layered solid elements with respect to the results computed based on processing the shell forces and shell moments extracted at the baseline of curvature region, show that the proposed simplified approach provides conservative results.

Further extension is required to account for in-plane circumferential tensile/compression stresses and the use of an appropriate failure criterion.

9th International Scientific Conference
Research and Development of Mechanical Elements and Systems
Kragujevac, Serbia, September5-7 2019

REDESIGN OF THE BUCKET OF BUCKET CHAIN EXCAVATOR ERS1000/20 USING OF MODULAR DESIGN APPROACH

M Popović[1], I Milićević[1], G Marković[2], S Dragićević[1], M Marjanović[1]

[1]University of Kragujevac, Faculty of Technical Sciences,
Svetog Save 65, 32000 Čačak, Serbia, marko.popovic@ftn.kg.ac.rs
[2]University of Kragujevac, Faculty of Mechanical and Civil Engineering,
Dositejeva 19, 36000 Kraljevo, Serbia

Key words: bucket wheel and chain excavators, cutting teeth, design, FEM, cutting force

This paper presents an approach to facilitating the design of cutting teeth for bucket chain excavators. The approach combines the theoretical load model and the laboratory determination of the static load capacity of the bucket tooth. Designing cutting teeth for bucket chain excavators involves making decisions based on incomplete data, since assumptions regarding the characteristics of rock materials, the unpredictability of the digging process, the imperfection of the cutting tooth material, etc. are unsuitable in terms of measurement, qualification and documentation. With respect to this uncertainty, the designer must use an idealised computational model with clear boundary conditions describing the process of rock breakage by cutting teeth. The key to success in the light of these three seemingly uncontrolled circumstances is to use scientific uncertainty qualification. This means that the basic settings of digging-related problems and understanding of the necessary assumptions, along with a proper stress analysis of the bucket teeth for different load and boundary conditions, can facilitate making fundamental engineering decisions based on incomplete data.
This paper presents the Evans two-dimensional model for performing bucket tooth load calculations. The Evans model is a simple model of rock breakage i.e. cutting element loading. This model can be used in bucket chain excavators for the simple calculation of external loads acting on the cutting teeth during the digging operation. The main idea is to use this model for performing load calculations for different operating conditions of the excavator in order to obtain starting data to be used in preliminary calculations for cutting tooth design. For calculation of the cutting force Fc (horizontal component) and the penetration force Fp (vertical component) we used following equations:

$$F_c = F_{RH} = 2 \cdot \sigma_z \cdot h \cdot \frac{sin(\beta_E + \delta)}{1 - sin(\beta_E + \delta)} \cdot \frac{sin\theta}{sin(\theta - \alpha)} \cdot cos\alpha \cdot w$$

$$F_p = F_{RV} = 2 \cdot \sigma_z \cdot h \cdot \frac{sin(\beta_E + \delta)}{1 - sin(\beta_E + \delta)} \cdot \frac{sin\theta}{sin(\theta - \alpha)} \cdot sin\alpha \cdot w$$

In addition to these data, the design process would also employ data obtained from the laboratory testing of the maximum static load capacity of existing cutting teeth. Laboratory test data would also be used for the verification of the computational model and implementation of the finite element method. The established model for the maximum loading of existing cutting teeth would be used for the analysis of future similar designs as well as for the optimisation of new cutting tooth designs. In following Figure 1., are given the main model of loads of the cutting teeth (*Evans model*), and virtual and laboratory model for analysis of maximum static load capacity.

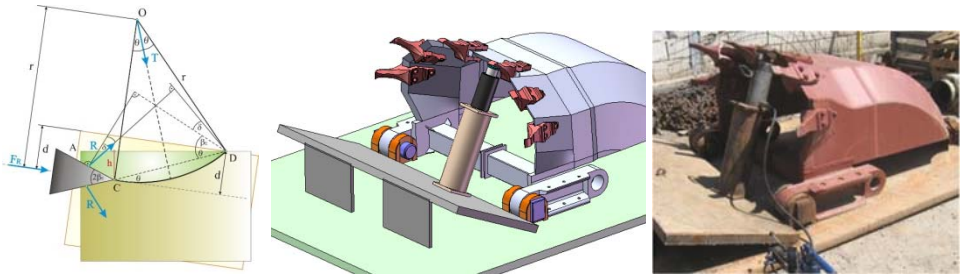

Figure 1. Evans model of load of the cutting teeth - approximation of cutting by a tooth on excavators; Virtual prototype; Laboratory testing for maximum bucket tooth load and

The advantage of the approach presented in this paper is that it reduces the time required to develop and test the cutting teeth of bucket chain excavators. This is of particular importance given the need for uniform optimised cutting tooth designs. Virtual prototyping allows the fabrication of a physical prototype at the very end of the process i.e. after the correction of most of the errors and after optimisation of the cutting tooth design. The simplified mechanical model provides a rough approximation to the excavating process, while substantially departing from the inclusion of all impact factors associated with the total load value. In particular, load values obtained by direct measurement (e.g. using strain gauges) on the cutting tooth during the excavation operation contribute to the design of more appropriate, more accurate simulation models. However, in general, there is no comprehensive solution to the problem due to a range of non-measurable effects (such as determination of the exact load direction, number of surfaces on cutting teeth across which loads are transferred, characteristics of the scooped rock material, dynamic effects etc.). The design of cutting teeth for bucket chain excavators is mostly based on empirical knowledge. Therefore, the authors believe that, towards a systemic approach to cutting teeth engineering, the approach presented in this paper is the optimal solution among all possible solutions entailing either simplification of the load defining process or inclusion of as many parameters affecting bucket tooth load as possible.

Acknowledgments. The project Ref. No. TR35037: “Development of a new bucket design for continuous excavators with the aim of integrating modular cutting elements” is financially supported by the Ministry of Science of the Republic of Serbia. The authors would like to acknowledge this contribution.

9th International Scientific Conference
Research and Development of Mechanical Elements and Systems
Kragujevac, Serbia, September5-7 2019

CALCULATION OF A MANHOLE HATCH ON A TANK

S Dizdar[1], R Tomovic[2]

[1]BerDiz Consulting AB, Andra Långgatan 48, 41327 Gothenburg, Sweden, samir.dizdar@berdiz.se
[2]University of Montenegro, Mechanical Engineering Faculty, Bul. Dzorda Vasingtona bb, 81000 Podgorica, Montenegro, radoslav@ac.me

Key words: manhole hatch, allowable stresses, elastic analysis, plastic analysis, preload.

A manhole hatch is mounted on a storage tank. There are several tanks of the same dimensions (20 [m] high and radius 10,2 [m]), but they have different thicknesses of the wall (9,6; 15; 20 and 25 [mm]). For inspection purposes, assembly of manhole hatch on all tanks is required. All tanks are filled with the water to the top (20 [m] high).
This article will prove that construction is done in such a way which guarantees that stresses in the material are below max. allowable value according to standard. EN-13445 is used for evaluation of the design and EN-10028 **Error! Reference source not found.**is used to retrieve material properties. Loads acting on the system are: hydrostatic pressure (0-2 [bar]), temperature (50 [°C]) and preload force (40 [kN/per bolt]). To get the right boundary conditions (for the sub-model) a shell model has been made on the whole tank and then hydrostatic pressure is applied. Pressure had 0 value at the top of the tank and 2 bar at the bottom of the tank (Figure 1). From this model, boundary conditions are taken and applied to a sub-mode (Figure 2).

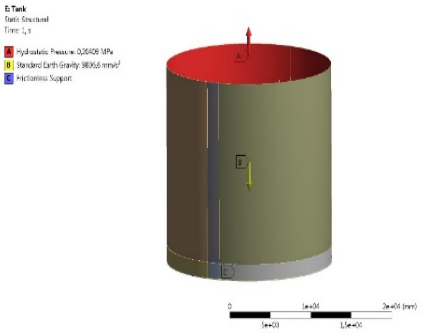

Figure 1. Boundary condition shell model

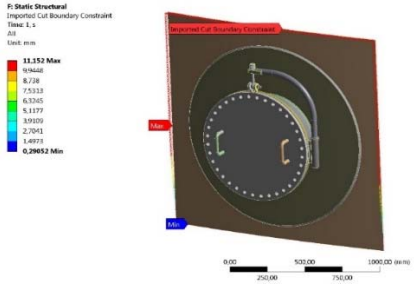

Figure 2. Boundary condition sub-model

Several different analyses have been carried out in order to finally qualify construction according to EN-13445 norm. In the first analysis, inner pressure 2 [bar] (0 bar at the top and 2 bar at the bottom of the tank) is applied to the shell model (whole tank) and then from the result retrieve boundary conditions to sub-model. As the next step, elastic analysis is performed with the sub-model that gave too high stresses in materials. The next step is a plastic analysis, where according to standard, plastic strain shouldn't exceed 5% if the design is approved. An analysis has been made with preloaded bolts to ensure that we don't get high stresses in the manhole hatch or bolts.

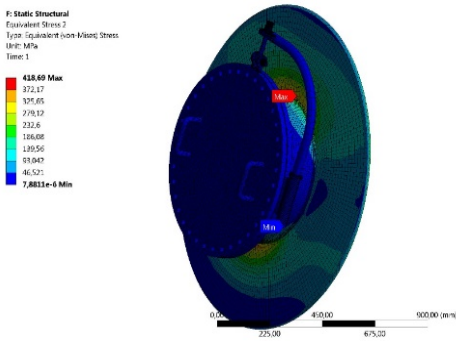

Figure 3. Equivalent (von-Mises) Stress.

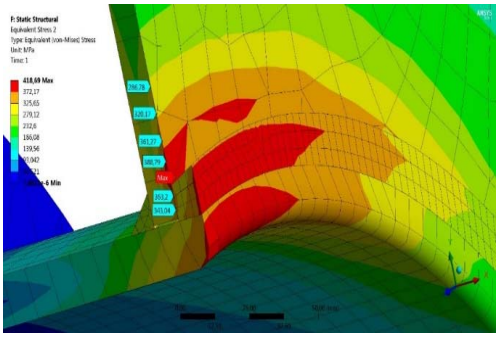

Figure 4. Equivalent (von-Mises) Stress.

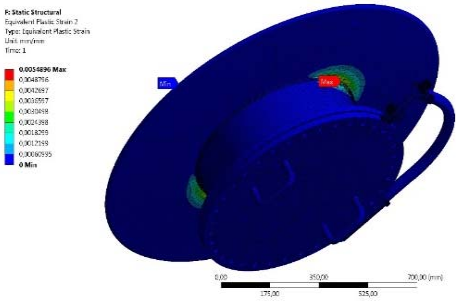

Figure 5. Equivalent Plastic Strain.

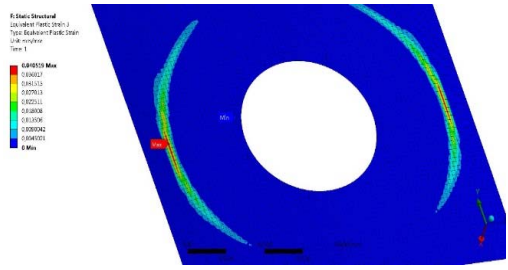

Figure 6. Equivalent Plastic Strain.

Elastic analysis shows that the stresses in the material is too high and design hasn't been approved. After the plastic analysis the design could be approved with restriction on preload force in the bolts 40 [kN]. Various analysis have been made with higher preload force but the stresses shows to be too high. The similar analyses have been made taking into consideration varying thicknesses of the wall. The results show that the greater thickness the smaller the deformations and the stresses.

Acknowledgments section immediately following the last numbered section of the paper.

9th International Scientific Conference
Research and Development of Mechanical Elements and Systems
Kragujevac, Serbia, September5-7 2019

THE APPLICATION OF THE BALLISTIC PENDULUM FOR THE BULLETS VELOCITY MEASUREMENTS

Jovana Milutinović[1], Nebojša Hristov[2], Damir Jerković[2], Svetlana Marković[2], Aleksandra Živković[1]

[1]University of Kragujevac, Faculty of Engineering, Sestre Janjić 6, 34000 Kragujevac, Serbia
[2]Military academy, University of Defence, Pavla Jurišica Šturma 33, 11000, Belgrade, Serbia

Key words: ballistic pendulum, muzzle velocity, optoelectronic encoder.

The accurate values of the initial velocity of bullets are significant for the quality and precision of small arms. The application of the simple measurement methods, during the tests of the weapon and ammunition, enables the determination of the velocity values from the group of shoots. The accuracy of bullet trajectory, appropriate trajectory correction parameters and terminal ballistics parameters are depended of the quality of initial conditions as initial velocity. The ballistic pendulum, as simple and old-design device, enhanced with optoelectronic encoder sensor and computer acquisition system, can be one of the good start-up device platform for measurement of velocity and observation of the terminal ballistics effects. The function principle of the considered device is based on the energy conservation. Initial data are mass of bullet, mass and dimension of pendulum, and result is velocity, according to the values of time and angle of pendulum. The output signals of measured angle in time are captured, and as required values for calculation the velocity on the microprocessor platform, for each shoot in the test group. The microprocessor platform saves measured and calculated values in memory and generates statistic report of results. The presented method can improve weapon and ammunition tests, by decreasing the time of measurement acquisition and increasing the quality and speed of results without errors. The method and system is simple and low-cost, and enables the design of small arms ammunition database of testing results.
There are two ways for the calculation of the velocity of the bullet. The first method (approximate method) assumes that the pendulum and bullet together act as a point mass located at their combined center of mass. This method does not take rotational inertia into account. It is somewhat quicker and easier than the second method, but not as accurate.
The second method (exact method) uses the actual rotational inertia of the pendulum in the calculations. The equations are slightly more complicated, and it is necessary to take more data in order to find the moment of inertia of the pendulum, but the results obtained are generally better. The projectile velocity calculation is more accurate using the exact method,

but the difference is minimal (less than 2 %). In this case, the approximate method was used for simpler calculation.

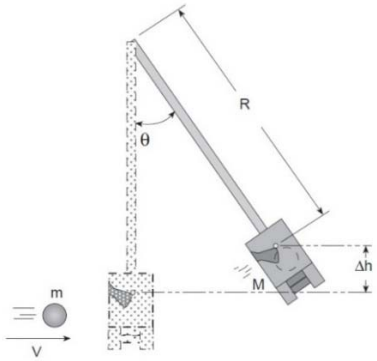

Figure 1. The motion of pendulum

Conceptual design for model is presented in the Figure 2. The system consists of the pendulum, the encoder and microprocessor platforms connected to the computer. The encoder registers the angle of movement after the collision of the projectile and the pendulum. The mass of pendulum and bullet are known in advance. The microprocessor calculate the output signal of the encoder with the corresponding mathematical model.

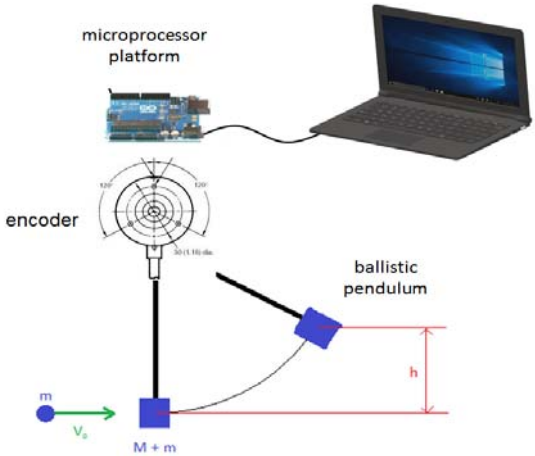

Figure 2. Principal scheme of system

For this system is used Arduino Uno microprocessor board platform with USB interface. The software is designed to record velocities of each single shoot, then process the statistical parameters of the shooting group (10 to 100 shoots). The calculation outputs are the mean of projectiles velocity, maximum and minimum velocity value, standard deviation and mean square deviation as statistical parameters. The software solution was made in the open Arduino code.

FAILURE DIAGNOSIS AND PROGNOSIS OF SLIDING BEARINGS

Ranko Antunović[1], Nikola Vučetić[1], Amir Halep[2]

[1]University of East Sarajevo, Faculty of Mechanical Engineering, Vuka Karadžića 30, 71123 East Sarajevo, Bosnia and Herzegovina, rankoantunovicmf@gmail.com, vuceticnikola@yahoo.com
[2]Cement Factory, Selima efendije Merdanovića 146, 72240 Kakanj, Bosnia and Herzegovina, Amir.Halep@heidelbergcement.com

Key words: failure diagnosis, fuzzy logic, sliding bearing, thermal analysis

Small problem in process oriented complex production system, as sliding bearing failure, can often cause long deadlocks during plant working, which results to huge financial costs in company business. Plain or sliding bearings are lubricated by the formation of a hydrodynamic film of lubricant, where the wedge formed lifts the shaft or journal off the bearing. Basic causes that cause damage and failure of sliding bearings include many aspects of construction, material selection, materials mistakes, production and processing, assembly, control, testing, storage, transportation, maintenance, unforeseen exposure to overload, direct mechanical or chemical damage during operation. Often, multiple causers contribute to the sliding bearing failure. Failures and damages caused by said groups of causers are manifested, most often, as wear, breakage and plastic deformation of the material.

Problems that occur in sliding bearings lead to high levels of vibration and noise. These problems mainly arise as a result of an inadequate gap in the bearing (oil gap) or the appearance of oil instability. An excessive gap in the bearing results in looseness and irregular lubrication. A sliding bearing with excessive grip, which is mainly caused by the wearing of white metal, causes a relatively small imbalance, a disturbance of centricity or the appearance of some other disturbing force that will cause mechanical looseness, Figure 1.

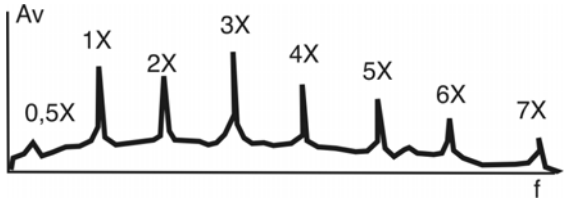

Figure 1. Spectral view when there is an excessive gap in the sliding bearing

Oil instability is manifested in the appearance of oil vortex and oil whip. The oil vortex occurs as a result of the orbital motion of the rotor and occurs at a frequency that is proportional to the rotation frequency and amounts usually 0.4 to 0.5 from the main frequency, Figure 2.

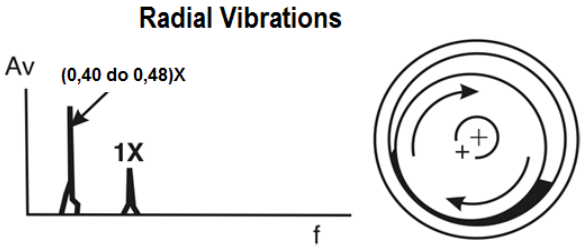

Figure 2. Spectral display due to oil instability

In machines that operate above the first critical speed, the oil vortex usually passes into an oil whip which frequency is equal to the frequency in the formation of the same.

In order to reliably determine the condition and prediction of sliding bearing failure, it is necessary to observe and analyze simultaneously several parameters of the condition. One such method is based on the fuzzy logic and enables the diagnostics of the state of the element and determining the urgency of the need for intervention on the machine element. Thus, by applying the disjunctive probabilistic fuzzy operator, a vibration-thermal indicator of malfunction of the sliding bearings (defect factor DFJB) can be defined which contains information about both the temperature and the vibration of the bearing defined as:

$$DFJB = (x(q) + w(v)) - x(q) \times w(v)$$

By applying the defined vibration-thermal indicator of the defects of sliding bearings (factors of malfunction), the procedure for diagnosing sliding bearings is considerably simplified, because the two most important technical indicators (temperature, vibrations) are integrated intelligently into a single technical indicator of malfunction. This is particularly important when it comes to complex systems with a large number of measurement points where there is often an overload of operators. Vibration-thermal malfunction indicator (fault factor) DFJB contains processed temperature information and bearing vibration, but in some applications, other than temperature and vibration, other parameters such as, for example, the thickness of the oil bearing film or the strength of the ultrasonic bearing, etc., which in some cases would increase the level of reliability of the method shown for the prediction of the sliding bearing failure.

9th International Scientific Conference
Research and Development of Mechanical Elements and Systems
Kragujevac, Serbia, September5-7 2019

RESEARCH ON DESIGNING A MULTILOOP PLANAR LINKAGE

Badoiu Dorin[1], Toma Georgeta[1]

[1]Petroleum-Gas University of Ploiesti, Faculty of Mechanical and Electrical Engineering, 39 Bucuresti Blvd., 100680 Ploiesti, Romania, ime@upg-ploiesti.ro

Key words: planar linkage, modeling and simulation, optimal design.

The design of linkages is a complex process that aims at establishing an optimal functional constructive solution that fulfils the conditions imposed by the task to be accomplished. Many times in such a process it starts from a certain structural configuration of the linkage and the dimensions of the component elements are determined by solving a problem of estimating the extreme values of a function that expresses certain characteristic parameters. From a mathematical point of view, this implies calculating the minimum or maximum value of this function in the presence of certain constraints expressing the conditions imposed by the functioning of the mechanism. In the paper is presented the way of determining the dimensions of the elements of a planar linkage (figure 1), when imposing certain conditions regarding the movement of the component piston 7, aiming at obtaining a mechanism whose total mass is minimal. The mechanism consists of three independent contours: 0-1-2-3-0, 0-1-2-4-5-0 and 0-5-6-7-0. The kinematics of the mechanism has been studied by projecting the vector circuits corresponding to the independent contours on the axes of the (Oxy) coordinate system. Using Maple programming environment a computer program that simulates the kinematics of the analyzed mechanism has been developed. The initial dimensions of the component elements have the following values: OA=0.15m; AB=1.05m; CD=0.5m; DF=0.5m; FG=0.8m; AC=$f_2 \cdot$AB, where f_2=0.2 and DE=$f_{51} \cdot$DF, where f_{51}=0.5. The coordinates of point *E* are: x_E=0.55m and y_E=0.35m and the *y* coordinate of point *G* is y_G=0.5m. The angular speed of the driving crank 1 is considered to have the value of 15 rad/s. The elements 1, 2, 4, 5 and 6 (figure 1) are made of steel bars with circular section having the following radii: r_1=0.04m; r_2=0.025m; r_4=0.04m; r_5=0.03m and r_6=0.025m. The mass of the piston *3* is 5kg and the mass of the piston 7 is also 5kg. We analyzed several cases in which it has been imposed the value of the stroke of the piston 7 and the values of the crank angle ϕ_1 for which the speed of the piston 7 is null, provided the total mass of the mechanism be minimal. In the paper have been presented some simulation results in the case when it was sought to determine the lengths of the bar-shaped components such that the piston *7* have zero velocity for the positions of the mechanism corresponding to the crank angle

ϕ_1=30° and ϕ_1=230° and its stroke be equal to 0.3 m, provided that the total mass of the linkage be minimal.

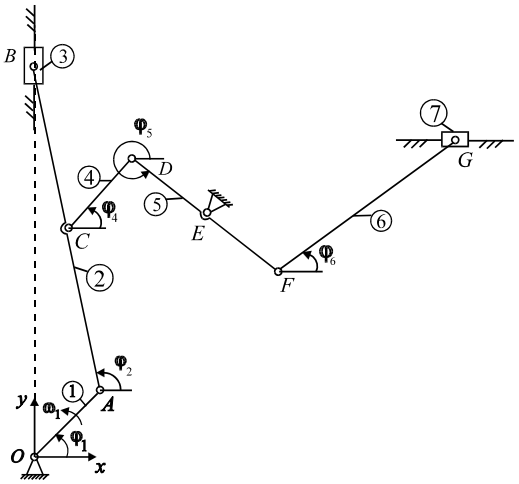

Figure 1. Planar mechanism

In this scope has been used the NLPSolve function included in the Optimization Package of Maple. The NLPSolve function solves problems involving the minimization or maximization of a continuous real nonlinear objective function possibly subject to constraints. The NLPSolve command uses various methods implemented in a built-in library and the solvers are iterative in nature and require an initial point. In this case, the **Sequential Quadratic Programming method has been used and the iterative calculus has been started with the initial values of the lengths of the component elements.** The NLPSolve function interrupts the calculation when one of the constraints is not fulfilled or complex numbers appear during the calculations. When solution of the problem is not identified after the calculations, a message appears specifying that no improved point could be found. To avoid the occurrence of complex numbers during computations, the variation of the lengths of the component elements, less the length of the element 4, was considered to be between 0.98 and 1.04 of the values corresponding to the previous step of the iterative process. For the length of the element 4 it was considered that its value may vary between 0.98 and 1.3 of the value corresponding to the previous step. After five iterations the program displayed the message that no improved point could be found. The values obtained for the lengths of the component elements are: OA=0.138m; AB=0.968m; CD=0.595m; DF=0.461m; FG=0.738m; AC=f_2·AB, where f_2=0.228 and DE=f_{51}·DF, where f_{51}=0.475. For the coordinates of point *E* have been obtained the following values: x_E=0.511m and y_E=0.346m and for the *y* coordinate of point *G* has been obtained the value: y_G=0.463m. The total mass of the mechanism is 75.568 kg.

Obviously, the way of realizing the synthesis of the analyzed linkage can be used in the case of any other planar linkage with different configuration. However, particular attention must be paid to choosing the intervals of variation of the values of the lengths of the component elements, as well as to the choice of the initial values of these lengths on each iteration.

9th International Scientific Conference
Research and Development of Mechanical Elements and Systems
Kragujevac, Serbia, September5-7 2019

TESTING STABILITY AND MANAGEABLENESS OF OSCILLATORY TRANSPORTING PLATFORM DURING THE SIEVING OF WET EARTH MASS

Goran Mihajlović[1], Milutin Živković[1]

[1] Higher Technical School of Mechanical Engineering, Radoja Krstića 19, 37240 Trstenik, Serbia, goran.vtms@gmail.com

Key words: oscillatory platform, wet earth mass, sieving, stability, manageableness

It is known a fact that the humidity of the earth mass (*w*) expressed in *%* is one of the most influential factors from which depends its transportation and sieving through the grille (sieve) of oscillatory platform. The best working effects are achieved during operation with dry and soft earth mass without the presence of solid pieces, because this mass will be sieving completely. However, the experience acquired from the exploitation has shown that problems in the work of oscillatory platforms appear after heavy rains, ie when the soil moisture (*w*) is greatly increased. Then the effect of transportation and sieving is the weakest, due to sticking moist earth for grille of the platform. In some extreme cases, occurred a complete disabling work of the platform. Therefore, the authors of this paper performed a complex theoretical and practical research and modeling in order to test how the platform works in extremely difficult working conditions after abundant and prolonged rains.

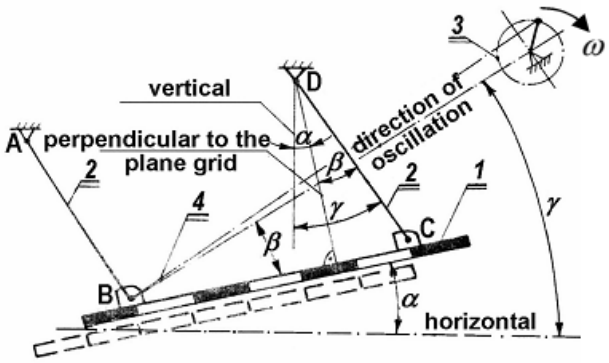

Figure 1. Stylized scheme of oscillatory transporting platform (1-platform; 2-suspension; 3-excenter; 4-driving lever; α, β, γ-influential angles of the platform; A, B, C, D-supporting points of the platform)

The paper presents the results of testing the stability and manageableness of the oscillatory transporting platform during the sieving of wet earth mass. All relevant results were obtained on the basis of a dynamic analysis of the mentioned processes, based on the mathematical model which is given by following equation:

$$T_V \frac{dy(t)}{dt} + (1 - K_\tau) y(t) = K_P \cdot x(t - \tau)$$

The individual sizes in previous equation have the following meanings:

T_V – temporal (inertial) constant of the system E-P-WP (environment-platform-working parameters);

K_P – coefficient (factor) amplification of the system E-P-WP;

K_τ=[0...1]– coefficient of delay depending on the delay time τ;

τ – time delay of the output-response signal of the system E-P-WP with respect to the input-excitation signal.

The transmissional function of the system E-P-WP has the following form:

$$G(p) = \frac{K_P}{T_V \cdot p + 1 - K_\tau} e^{-\tau p}$$

$e^{-\tau p}$ – delay operator the output signal relative to the input signal (due to the sticking of wet earth mass for grid platforms).

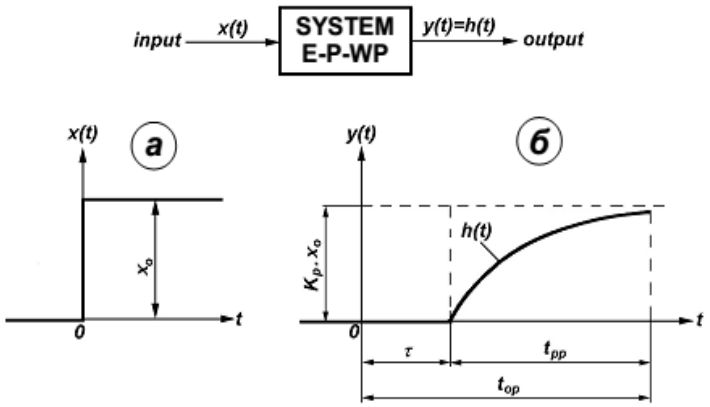

Figure 2. The response of oscillatory transporting platform during the sieving of wet earth mass due to disorder that is caused by jumping causal function (t_{pp} - length of the transition process; t_{op} - response time of the platform)

Based on the performed dynamic analysis of the E-P-WP system, the authors of the paper concluded that the system under study is always a STABLE SYSTEM, and also a system with SATISFACTORY MANAGEABLENESS, provided it exists sufficient RESERVE OF STABILITY (R_S) of oscillatory transporting platform during the sieving of wet earth mass:

$$R_S = \frac{\sqrt{(1 - K_\tau)^2 + T_V^2 \cdot \omega_0^2}}{K_P \cdot e^{\left(\frac{1 - K_\tau}{T_V}\right)\tau}}$$

If a greater the reserve of stability of platform R_S, insofar there is less possibility that during resonance and at frequencies that are close to the resonant ($\omega \approx \omega_0$) that may occur to disruption of the process of separation and sieving of wet earth mass.

SIMULATION OF EJECTOR FOR VACUUM GENERATION

Llorenc Macia[1], Robert Castilla[1], Pedro Javier Gamez[1]

[1] Universitat Politecnica de Catalunya, Faculty of Fluid Mechanics, CarrerColom 11, 08222 Terrassa, Catalunya, Spain

Key words: supersonic nozzle, vacuum ejector, CFD, OpenFOAM, simulation

Supersonic ejectors are used in a wide range of applications such as compression of refrigerants in cooling systems, pumping of volatile fluids, or vacuum generation. The objective of the present paper is to simulate, in an OpenFOAM environment with an open access implicit density-based solver, the physics of supersonic vacuum ejector, and to compare the results with experimental measurements. For a supersonic compressible flow, density based models are the favorite because of its capacity of capture discontinuities created by the shock waves. Other authors have developed before an implicit solver for the OpenFOAM toolbox, yet the solver HiSA has been used in the present work.
For the sake of simplicity a 2D axisymmetric mesh made by hexahedral cells has been created. Steady solutions have been obtained, with prescribed total pressure in primary and secondary inlets. Experimental results have been obtained with flow rate measured with Flange orifice according to ISO 5167. Vacuum levels have been measured with a vacuum sensor and they are done by means of a butterfly valve placed in the entrance of the Vessel. Figure 1 shows that the agreement is good between the experimental results and the simulation ones, although simulation tends to slightly overestimate flow rate for large values of vacuum level. Figure 1 shows the numerical simulations overestimate the flow rate, about 10%, at the same vacuum pressure for small vacuum level of Ps = 0,28 up to Ps = 1(large values of pressure in vacuum level) while underestimate the flow rate, about less than 5%, in the low values of vacuum pressure, at Ps =0,21 up to Ps = 0,2.

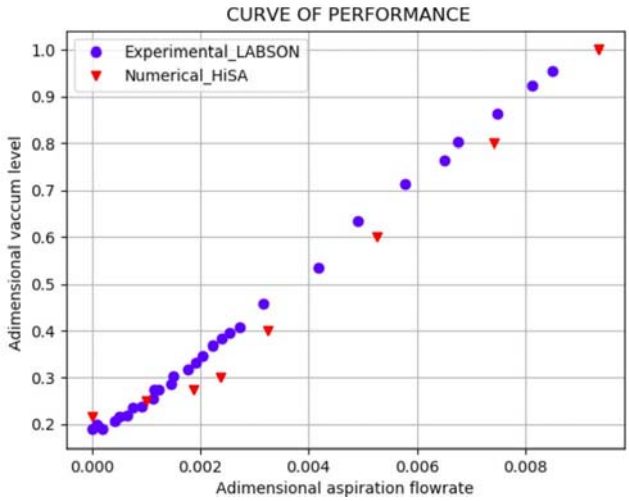

Figure 1: Experimental results vs HiSA results

Experimentally the secondary flow is zero at Ps=0,2 whereas the numerical simulation shows secondary flow at Ps=0,217 as shown in the Figure 2. Two regimes are encountered. In super critic regime the secondary is chocked and sonic flow is reached in the second nozzle, as shown in the Figure 2. In sub critic regime, the secondary flow is subsonic.

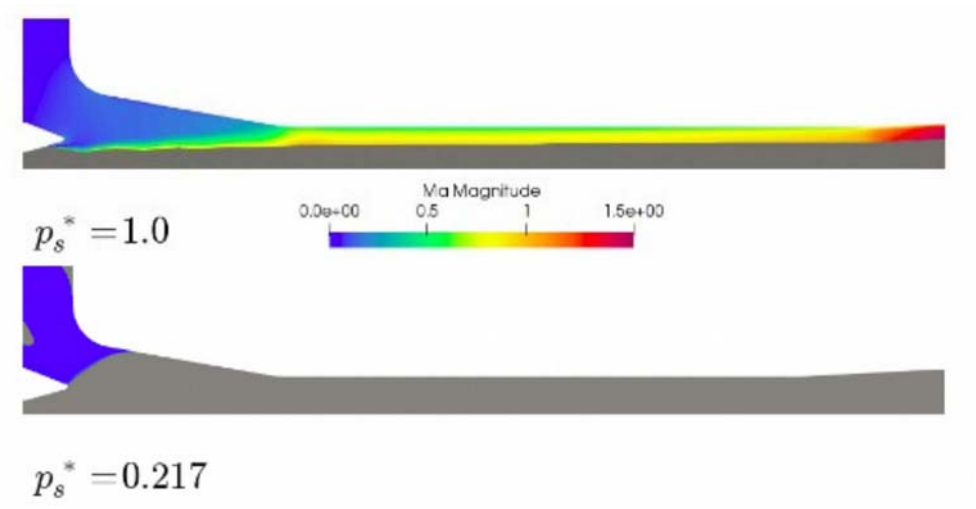

Figure 2. Ption of the figure 1

Acknowledgments. Support of Industrial Doctorate (2018 DI 025) from Generalitat de Catalunya is acknowledged.

9th International Scientific Conference
Research and Development of Mechanical Elements and Systems
Kragujevac, Serbia, September5-7 2019

RELIABILITY OF CYLINDRICAL TANK EXPOSED TO FIRE

Mirko Đelošević[1], Siniša Sremac[1], Goran Tepić[1]

[1]University of Novi Sad, Faculty of Technical Sciences,
Trg Dositeja Obradovića 6, 21101 Novi Sad, Serbia,
djelosevic.m@uns.ac.rs, sremacs@uns.ac.rs, gtepic@uns.ac.rs

Key words: reliability, stress analysis, fracture, explosion, cylindrical tank.

Explosion of process equipment is one of the most common causes of chemical accidents. Every rapid pressure build up in a confined space (thus a tank) causes an explosion. The root causes of rapid pressure increase within the process equipment can be due to evaporation of the liquid (BLEVE), overpressure (ME), combustion of gases, vapors and dust (CE) and uncontrolled chemical reactions (RR). Explosion of pressurized vessels is accompanied by the effects of fragmentation, blast wave and thermal radiation. The fragmentation effect is much more pronounced than the blast effect and thermal radiation (fireballs) and can manifest at distances over 1.2 *km*. The tank reliability assessment procedure is presented through a case study of the cylindrical storage tank for liquid petroleum gas (Fig. 1). The maximum stress of the tank with an ellipsoidal end cap is in cross-section B-B. The position of this cross-section is defined with x measured from the beginning of the cylinder ($x = \pi/4\lambda = 82$ *mm*). The operating pressure inside the storage tank of the LPG is from 16.4 to 16.9 *bar* (average 16.7 *bar*). Equivalent tank stress in accordance with the FEM model (ANSYS 15) is 150.2 *MPa*. This stress according to EN 13445-3 is 154.2 *MPa*. The equivalent stress according to shell theory is 163.7 MPa. The maximum deviation does not exceed 9%.

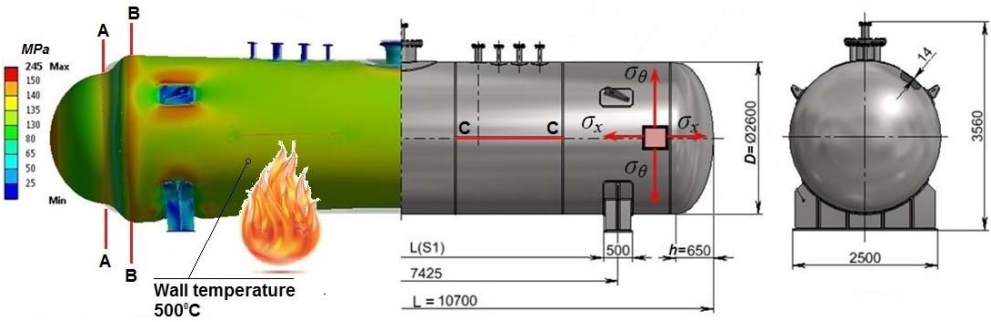

Figure 1. Dimensions and constructural type of tank with static structural analysis

The assessment of fracture lines and fragmentation patterns was performed on the basis of structural analysis and Monte Carlo simulation. The most likely fragmentation patterns due to the BLEVE effect are shown in Table 1. The mass of the empty tank is 12,300 *kg*.

Table 1. Characteristic forms of fragments due to tank explosion

One fragment	Two fragment	
Mass: 1350 *kg* Probability: 9.10% 	Mass: 820 *kg* and 480 *kg* Probability: 17.04% 	Mass: 1590 *kg* and 2050 *kg* Probability: 14.85% 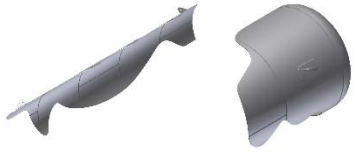
Mass: 2050 *kg* Probability: 10.00% 	Mass: 205 *kg* and 2050 *kg* Probability: 17.06% 	Mass: 1365 *kg* and 3545 *kg* Probability: 13.00% 

Assessment of tank reliability includes qualitative and quantitative analysis using Fault Tree Analysis – FTA. Maximum reliability values are achieved when the tank is not exposed to fire. The failure tree and the limit values of the tank reliability are given in Table 2. The minimum fragmentation probability corresponds to the thermal influence due to the BLEVE effect (the temperature of the tank wall is about 500^0C). Accident scenarios Sc1 and Sc2 include a fracture of the tank in at least two segments S1 and S2/S3. Accident scenarios Sc3, Sc4 and Sc5 include a fracture only in one of the segments S1, S2 and S3. The probability of tank failure is defined by $T = P(\text{Sc1}) + ... + P(\text{Sc5})$.

Table 2. Reliability of the tank relative to number of fragments

Fault of the tank	Reliability	Number of fragments					
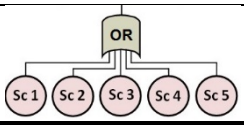	[%]	1	2	3	4	5	≥ 6
	Max	57.10	69.87	87.96	96.70	99.78	99.87
	Min	56.69	68.88	87.81	96.68	99.33	

The reliability assessment was carried out according to real exploitation conditions. A qualitative assessment of reliability can be made on the basis of available accidents. It was concluded that the thermal influence adversely affects the reliability of the tank. A larger number of generated fragments is a reflection of higher tank reliability. Preventive of the BLEVE effect implies the simultaneous increase in the reliability of the tank.

Acknowledgments. This work was funded by the Ministry of Education and Science of the Republic of Serbia under the project TR 36030.

9th International Scientific Conference
Research and Development of Mechanical Elements and Systems
Kragujevac, Serbia, September5-7 2019

ANALYSIS STATIC BEHAVIOUR OF BALL BEARINGS WITH TWO AND FOUR CONTACT POINTS

Aleksandar Živković[1], Miloš Knežev[1], Milan Zeljković[1], Mirjana Bojanić Šejat[1], Milivoje Mijušković[2], Slobodan Navalušić[1]

[1]University of Novi Sad, Faculty of Technical Sciences, Trg Dositeja Obradovića 6, 21000 Novi Sad, Serbia, acoz@uns.ac.rs,
[2]FKL D.O.O. Industijska zona bb, 21235 Temerin, Serbia, mile.mijuskovic@fkl-serbia.com

Key words: four point contact ball bearing, finite element method, ball bearing, static behaviour.

Today, more than ever, design engineers are challenged to simplify designs in order to reduce cost and weight. In many applications, a four point contact ball bearing saves space, because it can be seen as the combination of two single row angular contact ball bearings into one. Ball bearings with two contact point are suitable for high and very high speeds under radial and axial loads in both directions. Other hand, a **four point contact** ball bearing can stand under combination of moment loads, axial loads in both directions, in combination with radial loads up to a certain level, and provides a very tight axial shaft position tolerance. This paper presents compared analysis of ball bearings with two and four contact points from the standpoint of static behavior and their life, as well as load capacity. The modelling of static behavior of ball bearing consists of finite element (FE) model to describe the deformation and stress of the rings and balls. The loads used in this analysis are chosen in order that the maximum contact stress at the raceway remains 4200 MP according to EN ISO 76:2006. The maximum load capacity of the ball bearing has obtained when the most loaded ball reaches this stress value. The results show that the four points contact ball bearing have higher load capacity and less stress on the raceways

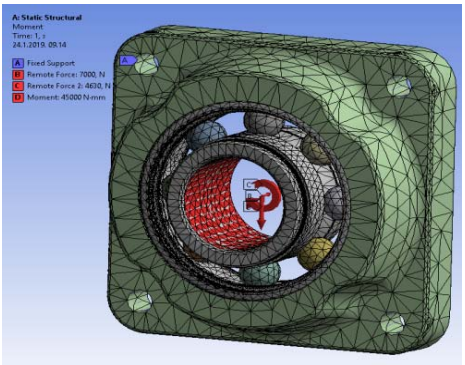

Figure 1 The mathematical model of the considered ball bearing with two contact point bearing LSFR 308

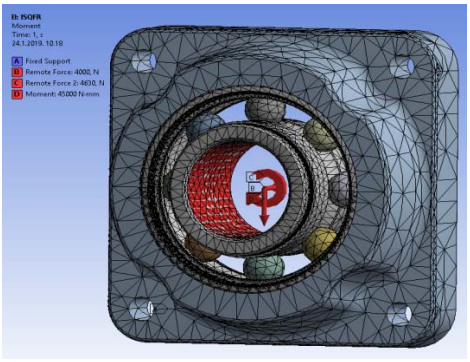

Figure 2 The mathematical model of the considered bearing with four contact point ball bearing LSQFR 308

The output results from ball bearing analysis as raceways deformation, contact loads, and stress are considered for each angular position of the ball. The ball bearings behavior simulations were done by the numerical method, whereby the displacement and the stress state of the assemblies were determined. The axial load is Fa = 7500 [N] which affects on the ball bearing, it is taken from the exploitation conditions, radial load due to the mass of the roller is Fr = 4630 [N], the load is displaced from the ball bearing axis for the size of the radial gap (clearance) in order to simulate noncoaxial ball bearing mounted on the roller. The torque M = 40 [Nm] comes also from exploitation condition.

Table 1. Load capacity and life, depending on ball bearing type

Ball bearing type	Dynamic capacity (KN)	Static capacity (KN)	Bearing life (h)
LSFR308	47.3	38	12456
LSQFR308	59.2	48.7	14576

Through the analysis of the considered ball bearings can be concluded that the LSQFR 308 has about 38 % less equivalent stress on the inner ring and about 32% on the outer ring. Also can be concluded that mentioned ball bearing has a more accurate stress distribution along the raceways. On the housing, the maximal equivalent stresses are the same for the both ball bearing variations. Basis on the previous assertion can be said that the LSQFR 308 will have about 25% longer lifetime than the LSFR 308.

Acknowledgments. In this paper some results of the project: "*Contemporary approaches to the development of special solutions related to bearing supports in mechanical engineering and medical prosthetics*" – TR 35025, carried out by the Faculty of Technical Sciences, University of Novi Sad, Serbia, are presented. The project is supported by Ministry of the education and science of the Republic of Serbia

9th International Scientific Conference
Research and Development of Mechanical Elements and Systems
Kragujevac, Serbia, September5-7 2019

CONTACT PRESSURE ANALYSIS OF SLEWING RINGS

Rudolf Skyba[1], Slavomír Hrček[1], Jan Šteininger[1], Maroš Majchrák[1]

[1]University of Žilina, Faculty of Mechanical Engineering, Univerzitná 8215/1, 010 26 Žilina, rudolf.skyba@fstroj.uniza.sk

Key words: bearing, contact, pressure, geometry, relations.

The well-known fact about large diameter slewing bearing is that they are primary designed for applications where large amount of axial load is transferred through thin-walled rolling rings to rolling elements. Research about the radial stiffness of the radial bearing was realized by Mullick and it was also based on John Harris's finite element method. For solving a nonlinear equation, the Newton Raphson's method has been used. For basic calculations of contact pressure, the Hertzian equations was used.

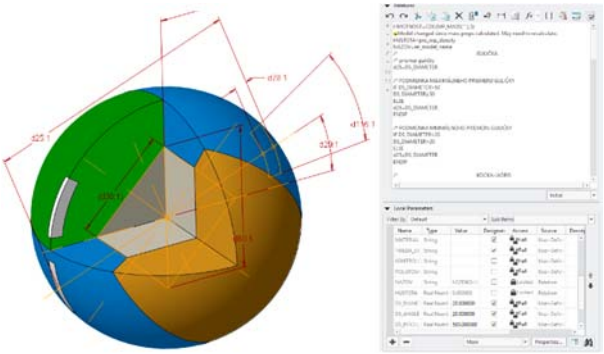

Figure 1. Parametric model with relations.

The main task of this paper is to select concrete type of bearing then create virtual 3D model parameterize it and then to modify this model by several parameters direct from the environment of Ansys workbench calculation program while the model is under the load. Methodology of solving this task includes selection of critical parameters for creation of the parametric bearing model. In this case we introduce two main parameters like ball diameter and contact angle. There are also minor parameters like bearing pitch diameter which has significant influence on the amount of used rolling elements. If we change number of rolling elements directly from Ansys then after we update model and value of elements will be increased, we lost defined boundary conditions of bearing. So we keep the same value of pitch diameter during all measurements.

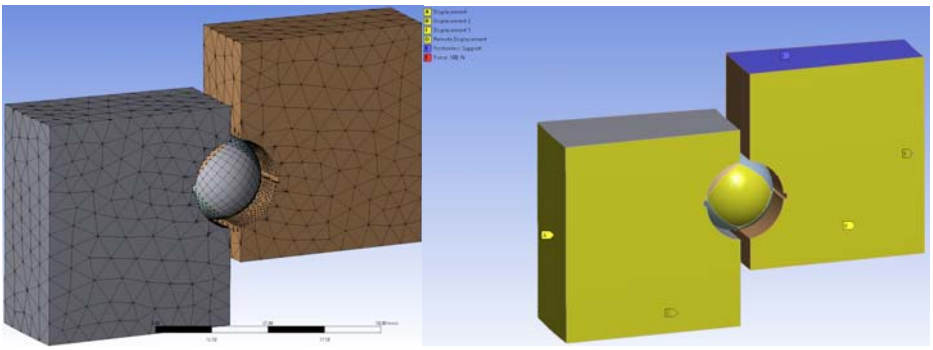

Figure 2. Mesh (left) and boundary conditions of the model (right).

A methodology based on finite element method has been developed to calculate accurately the value of ball forces around slewing bearing and its deformation.
This methodology can use the non-linear springs to simulate contact. It is necessary to use this method when stiffness of support structure is not uniform. In the end we need some calculations like calculation of semi-axis, contact pressures, and the depth at which the maximum tension is applied. If we have all of this we can move forward and based on many calculations of the deformations performed in the Ansys we can compare influence of ball diameter and contact angle. Based on analysis graphs were constructed.

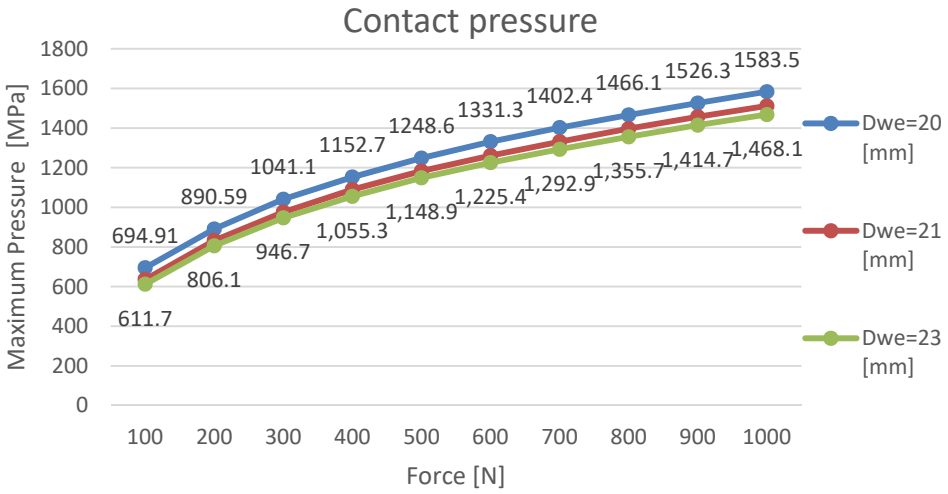

Figure 3. Graph of dependency between contact pressure and force.

Acknowledgments. This study was supported by Ministry of Education, Science, Research and Sport under the contract No. 1/0595/18 – Optimizing the internal geometry of roller bearings with line contact in order to increase their durability and reduce their structural weight. This study was supported by Slovak Research and Development Agency under the contract no. APVV-14-0508 – Development of new methods for the design of special large-size slewing rings.

9th International Scientific Conference
Research and Development of Mechanical Elements and Systems
Kragujevac, Serbia, September5-7 2019

USE OF INDENTION VELOCITY DERIVATIVE FOR ESTIMATION OF ENVELOPE POINTS WHEN THE WRAPAROUND POINTS ARE KNOWN METHOD

Sergey Lebedev[1], Denis Babichev[2], Dmitry Babichev[1]

[1] Industrial University of Tyumen, Institute of Transport, Melnikayte Street 72, 625039 Tyumen, Russia, babichevdt@rambler.ru
[2]Sibur Holding, ZapSibNeftekhim LLC, East Industrial District, Block 1, No. 6, Building 30, 626150 Tobolsk, Russia, babichevda@tobolsk.sibur.ru

Key words: gear machining, gear shaping, envelope surface.

Task definition. Earlier, we proposed a method a kinematic method of envelope points estimation when the wraparound points are known. The method is based on the usage of terms "indention velocity and acceleration", and as shown in Figure 1, it lets reduce the value of the calculated points deflection from theoretical envelope by 1 to 3 orders of magnitude.

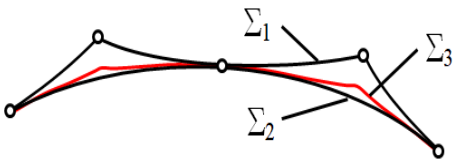

Figure 1. Types of surfaces: Σ_1 – wraparound; Σ_2 – envelope; Σ_3 – estimated using kinematic method

The kinematic method does not take account of higher order derivatives. It shall be noted that also earlier it was proposed to use high derivatives for analysis and synthesis of engagements. In such a way G.I. Shevelyova has developed the formal power series method D.T. Babichev wrote about utility value of indention velocity high derivatives, but up to now this idea has neither been implemented in methods, nor in calculations.

Research objective. To develop envelope points estimation method over wraparound points coordinates using indention acceleration derivative for calculations. And to assess accuracy of the kinematic method when third derivatives are used in it.

Derivative of indention acceleration:

$$\dot{a}_{BH} = \frac{da_{BH}}{dt} = \frac{d}{dt}(\mathbf{a}_{12} \cdot \mathbf{n} + \mathbf{V}_{12} \cdot \dot{\mathbf{n}}) = \mathbf{a}_{12} \cdot \mathbf{n} + 2 \cdot \mathbf{a}_{12} \cdot \dot{\mathbf{n}} + \mathbf{V}_{12} \cdot \ddot{\mathbf{n}}$$

where $\mathbf{V}_{12}$ –is relative velocity vector; $\mathbf{n}$ – unit normal vector to the surface, directed out of the generating element field; $\mathbf{a}_{12}$ – acceleration of the point situated on the generating surface Σ_1 and riding on it at a velocity "$-\mathbf{V}_{12}$"; $\dot{\mathbf{n}}$ – derivative of unit normal vector $\mathbf{n}$.

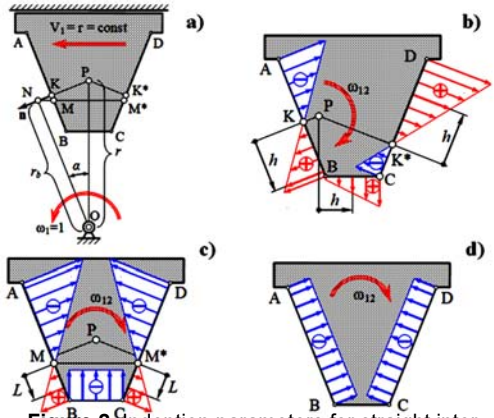

Figure 2. Indention parameters for straight intervals of a rack profile: a) engagement scheme; b) velocity V_{BH}; c) acceleration a_{BH}; d) its derivative $\dot{a}_{BH}$

For flat rack-and-gear drive where generating profile is a straight line, formula was deduced for calculation of derivative $\dot{a}_{BH}$ of indention acceleration a_{BH}:

$$\dot{a}_{BH} = \omega_{12}^3 \cdot r_b = \\ = -\omega_2^3 \cdot r_b = -r_b \qquad (2)$$

where r_b – base radius of the gear blank. Plots illustrate changes in: indention velocity V_{BH}, indention acceleration a_{BH} and its derivative $\dot{a}_{BH}$ along cutting edges in the rack gearing under consideration.

Principles of the kinematic method where indention acceleration derivative is used. Below is envelope points' estimation algorithm for the case of one-parameter envelope. The basis is formulas

$$\left.\begin{aligned} \Delta t &= \min\left\{ abs\left(\frac{-a_{BH} \pm \sqrt{a_{BH}^2 + 2 \cdot \dot{a}_{BH} \cdot V_{BH}}}{\dot{a}_{BH}} \right) \right\} \\ \delta &= abs\left(V_{BH} \cdot \Delta t + \frac{a_{BH} \cdot \Delta t^2}{2} - sign(V_{BH}) \cdot \frac{\dot{a}_{BH} \cdot \Delta t^3}{6} \right) \end{aligned}\right\} \qquad (3)$$

Evaluation of the method offered and accuracy estimation. Using software an involute spur gear forming process by counterpart rack has been simulated. Figure 3 shows the degree of accuracy improvement for two kinematic points calculation methods on the Σ3 (i.e. close to involute) compared to deflections of the wraparound jags (i.e. jagged curve tangent to involute). Two bottom curves are minimum and maximum accuracy. Two top curves are minimum and maximum accuracy, which is described above and includes use of derivative V_N и a_N.

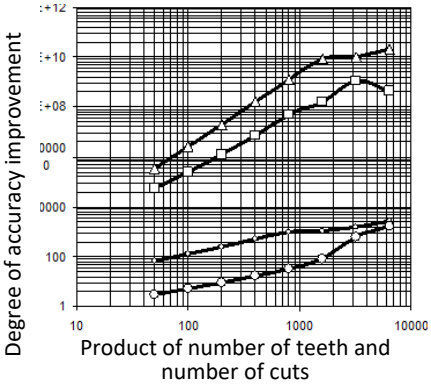

Figure 3. Comparative accuracy analysis of the two kinematic methods

Conclusion. Indention derivative was used in kinematic method of envelope points lumping given the wraparound points. Simple example demonstrated that in this case accuracy of kinematic calculation of coordinates under the same number of cuts increases by 3 to 6 orders of magnitude. It is assumed that in the general case use of the derivative $\ddot{a}_{BH}$ improves accuracy not by 3 to 6 orders of magnitude but only by 2 to 3 orders of magnitude, since it was involute to be considered as envelope and in case of its formation second derivative is $\ddot{a}_{BH}=0$. In other engagements, especially in space ones, forth derivative may be not zero, that would lead to calculation accuracy reduction.

Acknowledgments. This work was supported by grant (project № 9.6355.2017/БЧ) of government order of Ministry of education and science of Russia Federation for the period 2017–2019 in Tyumen Industrial University.

9th International Scientific Conference
Research and Development of Mechanical Elements and Systems
Kragujevac, Serbia, September5-7 2019

KINEMATIC METHOD OF ENVELOPE POINTS CALCULATION WHEN THE WRAPAROUND POINTS ARE KNOWN

Denis Babichev[1], Dmitry Babichev[2], Sergey Lebedev[2]

[1]Sibur Holding, ZapSibNeftekhim LLC, East Industrial District, Block 1, No. 6, Building 30, 626150 Tobolsk, Russia

[2]Industrial University of Tyumen, Institute of Transport, Melnikayte Street 72, 625039 Tyumen, Russia, lebedevsergey1995@gmail.com

Key words: gear machining, gear shaping, envelope surface.

Problem statement' Theory of surfaces formation by movable bodies distinguishes two types of formed surfaces: wraparound and envelope – see Figure 1. Wraparound Σ_1 is a discrete family connected set of the reference gear tool surfaces pieces; envelope Σ_2 is a surface tangent to all the elements of this discrete set. Envelope Σ_2 is normally a smooth surface; wraparound Σ_1 – is always a faceted surface (with jags). Wraparound Σ_1 is estimated by direct tracking of generating surface points situation Σ_0 relative to the blank. Majority of specialists dealing with computer simulation of forming processes prefer to estimate wraparound rather than envelope.

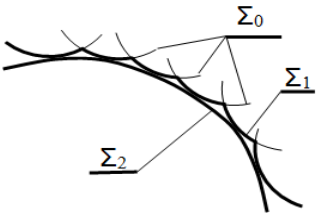

Figure 1 – Generating, wraparound, and envelope surfaces: Σ_0 – generating; Σ_1 – wraparound; Σ_2 – envelope

Work objective. To present a kinematic method of 'approach' of wraparound Σ_1 and envelope Σ_2, based on utilization of terms 'indention velocity V_N' and 'indention acceleration a_N '. Assess its accuracy, reliability and amount of calculations. Let us look upon indention velocity and acceleration, the basis of the method.

Indention velocity V_N, suggested by V.A. Shishkov – also known as velocity of mutual approach and separation – is a velocity of reference gear tool surface (RGTS) penetration into the blank volume. Indention velocity is estimated as projection of a vector of gear tool's movement velocity relative to machined element onto direction of a normal vector to the RGTS at this point:

$$V_N = \mathbf{V}_{12} \cdot \mathbf{n} = V_{12x} \cdot n_x + V_{12y} \cdot n_y + V_{12z} \cdot n_z \quad (1)$$

where $\mathbf{V}_{12}$ – relative velocity vector at the point on RGTS: $\mathbf{V}_{12} = \mathbf{V}_{tool} - \mathbf{V}_{blank}$; $\mathbf{n}$ – unit normal vector to RGTS at this point, always directed out of the gear tool body, e.g. out of grinding disc, but never inwards.

Indention acceleration a_N, suggested by D.T. Babichev, is acceleration at which generating element (normally surface) indents ('sinks in') into the volume of the other body to form a mating element (normally a surface as well). I.e. a_N indicates how fast indention velocity V_N varies with time at this particular point of the space where the formed element is situated Let's find a_N upon differentiation of V_N with respect to time t:

$$a_N = \frac{dV_N}{dt} = \frac{d}{dt}(\mathbf{V}_{12} \cdot \mathbf{n}) = \mathbf{a}_{12} \cdot \mathbf{n} + \mathbf{V}_{12} \cdot \dot{\mathbf{n}} \tag{2}$$

where $\mathbf{V}_{12}$ –is relative velocity vector; $\mathbf{n}$ – unit normal vector to the surface, directed out of the generating element field; $\mathbf{a}_{12}$ – acceleration of the point situated on the generating surface Σ_1 and riding on it at a velocity "$-\mathbf{V}_{12}$".

The article presents the calculation equations for all quantities included in the formulas (1) and (2). These equations are obtained for generalized engagement. Actually any specific transmission or generation may be refined in the systems of coordinates and motions of this gearing. Actually any specific transmission or generation may be refined in the systems of coordinates and motions of this gearing. For the principle of point estimation at the surface Σ_2 formed by one-parameter enveloping sees Figure 2.

Finding the envelope by our kinematic method at one parameter of the envelope:

$$\delta = -\frac{V_N^{\,2}}{2 \cdot a_N}; \qquad \Delta t = -\frac{V_N}{a_N} \tag{3}$$

$$\mathbf{N} = \mathbf{n}_1 + (\boldsymbol{\omega}_{12} \times \mathbf{n}_1) \cdot \Delta t; \quad N = \sqrt{N_x^2 + N_y^2 + N_z^2}; \quad \mathbf{n}^{(\Sigma 2)} = \frac{\mathbf{N}}{N}; \quad \delta_n = \delta \cdot (\mathbf{n} \cdot \mathbf{n}_1) \tag{4}$$

$$x_2^{(\Sigma 2)} = x_2 + \delta_n \cdot n_x^{(\Sigma 2)}, \quad y_2^{(\Sigma 2)} = y_2 + \delta_n \cdot n_y^{(\Sigma 2)}, \quad z_2^{(\Sigma 2)} = z_2 + \delta_n \cdot n_z^{(\Sigma 2)} \tag{5}$$

Each In order to assess accuracy of the method, the process of spur gear involute profile generation by rectilinear-face rack was studied. Such gearing was selected as a study object because for involute it is not difficult to deduce formulae for estimation of distances measured from theoretical envelope represented by the involute itself.

At the final stage, we investigated the effect of three parameters on the deviations from the involute of the points obtained by our kinematic method. See Fig. 3 for analysis results.

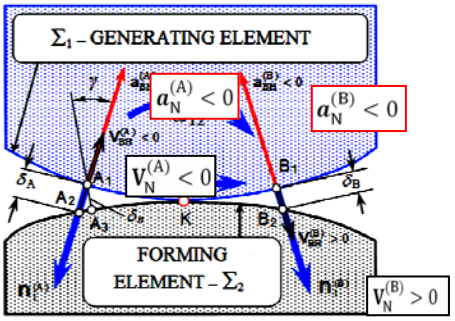

Figure 2 – Principle of estimation at the envelope surface Σ_2 points

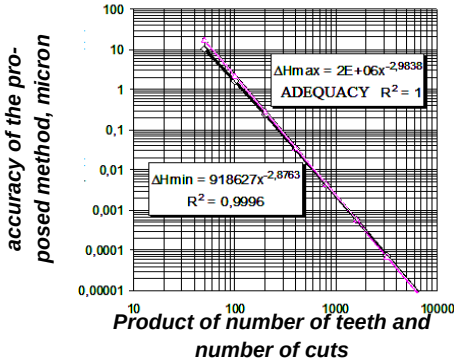

Figure 3 – Wraparound Σ_1 deflections from the involute Σ_2

Acknowledgments This work was supported by grant (project № 9.6355.2017/БЧ) of government order of Ministry of education and science of Russia Federation for the period 2017–2019 in Tyumen Industrial University.

IRMES KRAGUJEVAC 2019

9th International Scientific Conference
Research and Development of Mechanical Elements and Systems
Kragujevac, Serbia, September5-7 2019

MODELING LATERAL CRACK BREATHING IN A ROTOR USING FINITE ELEMENT METHOD

Vesna Marjanović[1], Nenad Kostić[1], Nenad Petrović[1], Nicolae Florin Cofaru[2]

[1]University of Kragujevac, Faculty of Engineering, Sestre Janjić 6,
34000 Kragujevac, Serbia, nkostic@kg.ac.rs
[2]University "Lucian Blaga" of Sibiu, Department of Industrial Machines and Equipment,
Emil Cioran 4, Sibiu, Romania

Key words: crack, cracked rotor, cracked rotor stiffness, finite element method, crack breathing.

Cracks in shafts and rotors of rotary machines are the most frequent and most dangerous due to the consequences which they can cause, but also because of the cost and difficulty of their timely discovery, and prevention of their initiation and spreading. The presence of a crack of certain characteristics causes a change in the rotors stiffness. When the rotor is deformed under the influence of its own weight, an unbalanced force or additional bending moment, the crack can be opened or closed. An opened crack causes asymmetric stiffness of the rotor in two mutually perpendicular directions, which leads to a nonlinearity in the dynamic behavior of the rotor. During rotation of the cracked rotor, the shape of the crack changes (completely opened, partially opened, completely closed) depending on the crack's and rotor's characteristics. Generally, during shaft rotation, the crack is constantly changing between these two extremes and it is said that the crack is breathing.

In this research DS CATIA software has been used for crack modeling. For modeling the part of the shaft with the crack the Sketcher Workbench for sketches, Part Workbench for making the parts, and Generative Structural Analysis for FEM analysis have been used, as well as Advanced Meshing tools for finer element mesh generating. Modeling and analyzing in the same software package gives numerous benefits, eliminates usually occurring errors from connecting models in different software and significantly saves time.

Figure 1 shows the shaft model and detail of the modeled crack. As an external load a continuously distributed force is placed along the volume. This type of load completely simulates real conditions because simulated inertial forces which act in all points of the continuum. Constraints do not allow for static equilibrium of the shaft model segment with the crack, because axial movement is enabled. As a result of this additional constraints have been added which prevent only axial movement of the bottom line of the crack. This

resembles real conditions (there are no causes for moving the top of the crack axially; the model allows all other degrees of freedom of all points of the crack).

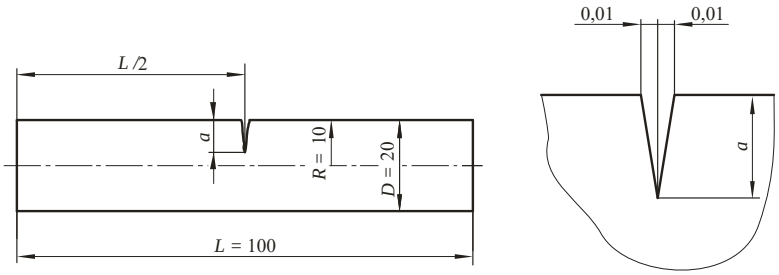

Figure 1. Cracked shaft model

The position of a neutral bending line is noticeable perpendicular to the direction of outer loading. It is also made clear that there is a concentration of stress at the crack tip, which is especially noticeable when the crack is opened.
When the crack is almost completely closed (shaft rotation angle of 170° or 190°), the areas of the opened crack are not noticeable. This is a result of a very small number of elements which are not in contact, not all of which are concentrated in one area, as well as due to the fact that the finial clearances between them are very small (maximal value of mm).
Based on results a diagram of crack breathing has been formed and shown in figure 2.

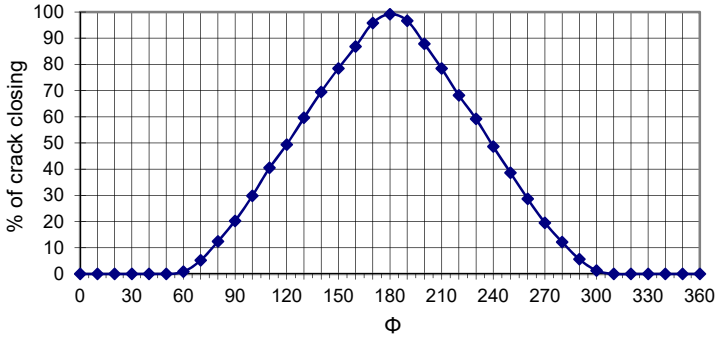

Figure 2. Crack breathing diagram during shaft rotation

FEA analysis gives usable results comparable with experimental results.

Acknowledgments. This paper is a result of the TR33015 project, which is an investigation of the Technological Development of the Republic of Serbia. We would like to thank to the Ministry of Education, Science and Technological Development of the Republic of Serbia for their financial support during this investigation.

9th International Scientific Conference
Research and Development of Mechanical Elements and Systems
Kragujevac, Serbia, September5-7 2019

STRESS ANALYSIS OF LIFTING TABLE USING FINITE ELEMENT METHOD

Nebojša Rašović[1], Adisa Vučina[1], Milenko Obad[1]

[1]University of Mostar, Faculty of Mechanical Engineering, Computing and Electrical Engineering, Matice hrvatske bb,
88000 Mostar, Bosnia and Herzegovina, nebojsa.rasovic@fsre.sum.ba

Key words: ANSYS, finite element method, topology optimization, lifting table.

Lifting table has been designed and developed through the concept of Learning Factory (LF) at the University of Mostar. The idea for lifting table design has come from the local industry needs for a lifting platform that should lift a man and/or load at a certain height. For safety reasons, design is checked under the loading using a method of finite element analysis. The paper predicts and explains methodology for structural analysis used in presented case study. Results of FEM analysis are basis for making ways and guidelines to optimize current design in order to get optimal parameters for weight, stability, capacity, mobility and layout of the lifting table. From the previous work, design of lifting platform has been realized through learning factory concept at Department of mechanical engineering University of Mostar. It is about mechanical lifting mechanism that is able to carry great loads by vertically hand moving. A need to use a lifting mechanism is very widespread across labs, workshops, departments etc. The goal of developed design is to lift some objects or man at a certain height in order to perform some operations. The required highest level of lifting was up to 550 mm. Stress and strain analysis for the entire structure of lifting table represents one of the main tasks in the phase of embodiment design. This is the most important step because calculation results need to confirm design correctness. Correctness of design implies capability to carry out full predictable load, easy mechanical handling, safe lifting and smooth motion of the mechanism. Because of very low working speed, it will be observed three characteristic positions of the lifting table mechanism: the highest, the lowest and middle position under acting of maximal load. The objective of this paper is to check the stress and strain for all three characteristic positions and on that basis make ways and guidelines to optimize current design. In accordance with previous mentioned, material selection has to be appropriate depending on component type and function it performs. The most of the components are made of structural steel (S275) like as two frames (upper and lower), four legs, longitudinally stiffener, transversely stiffener and lever. The four wheels are made of polyethylene. Slider and spindle screw nut are made of bronze, while spindle is made of stainless steel. Technical requirements will play main role in defining boundary

conditions of parametrized model of lifting table. The **Figure 1** shows workflow algorithm for structural analysis. Appropriate geometric mesh model that ensures low approximation errors and validity of obtained results has been created. This task can be done in few different derived mesh iterations in order to get congruence or confirmation of stress results (Table 1).

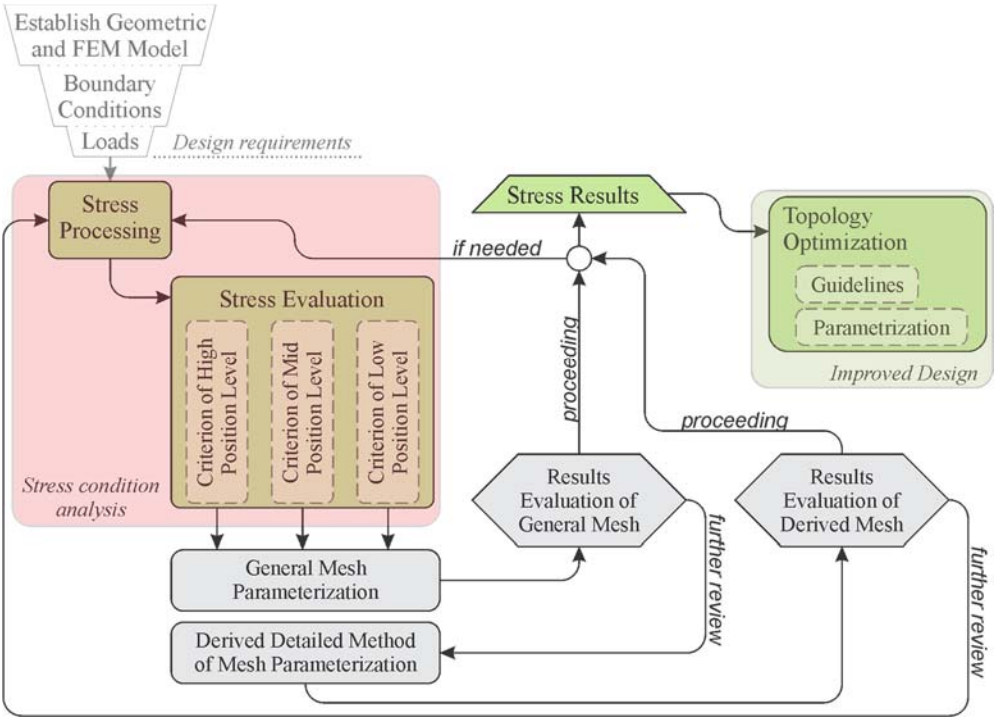

Figure 1. Workflow algorithm of stress analysis using FEM

Table 1. Mesh details for multiple iterations of structural analysis

Characteristics of Mesh	General Mesh(1)	Derived Detailed Mesh(2)	Derived Detailed Mesh(3)
Mesh Method	Automatic	Hex Dominant	Hex Dominant
Element Size [mm]	6	3	1
Size Function	Adaptive	Curvature	Proximity and Curvature
Mesh Quality	Medium	Fine	Fine
Transition Ratio	0,272	0,272	0,272

According to structural analysis (Table 1), three components had maximal stress values: lever (in high position), spindle (in middle position) and mounting bracket at welded joint (in low position). It can be noted that obtained results are compromise in numerical evaluation of multiple model parameters. Stress results obtained in this analysis will serve in creating guidelines for design improvement.

9th International Scientific Conference
Research and Development of Mechanical Elements and Systems
Kragujevac, Serbia, September5-7 2019

AUTOMATIC MEASUREMENT OF PRECISION AND ACCURACY FROM THE HIT PATTERN OF SMALL ARMS USING ELECTRONIC TARGET SYSTEM

Aleksandra B Živković [1], Nebojša P Hristov[2], Damir D Jerković[2], Bogdan S Bogdanović[3], Jovana M Milutinović[1]

[1]University of Kragujevac, Faculty of Engineering, Sestre Janjić 6, 34000 Kragujevac, Serbia
[2]Military academy, University of Defence, Pavla Jurišica Šturma 33, 11000, Belgrade, Serbia
[3]3Hexagon Metrology Serbia, Sestre Janjić 6, 34000 Kragujevac, Serbia

Key words: precision, accuracy, hit pattern, electronic target system.

The basic parameters of the combat training and weapon practicing are the determination of the accuracy and precision. The automatic systems for acquiring of the hit pattern are very expensive and inaccessible. Modern automatic systems are designed as non-material target system for accurate spatial positioning of the projectile trajectory in one or more planes. In the paper will be described the design of the non-material high-resolution target acquisition system developed on the optoelectronics IR (infra-red) sensors. The frame of the multiple IR sensors coupled with the microcomputer platform is the optical frame. The complete target acquisition system is consisted of the two frames for positioning in vertical and horizontal direction. Additionally, in the target system is incorporated the algorithm for the determination of the appropriate statistical values from the group of shots, as accuracy and precision parameters. The assembly hardware components are commercially accessible. The designed algorithm is applied through simple software code. The main aim of the developed target system is for the measurement of the small arms shooting. The presented target system is open for enhancement and can be used for different weapon system.
The determination of the accuracy and precision depends on the reliability of methods and equipment. The conventional experimental methods are consisted of the test fire from the small arms on the material target, on the proving test facilities. The test procedure is namely consisted of the required number of fire groups. The test group depends on the time that is required to fulfill the test conditions, and have to be less then several minutes. The determination of the precision begins from the measurement of the every hit. The group of hits is represented as hit pattern and can be visually described as „image of shots“ on the test target. The detection of the single hit begins with registration of the particular sensors in frame, that are mounted in two opposite directions – vertical and horizontal. Every hit is saved as data from specific sensors, as following information: number (i.e. position) of the sensors in vertical and horizontal direction of mounted frames, in specific time. Different hits

have different time tag. In the research, the precision parameters have to be evaluated from the relation of the specific hit to the average hit. The average hit is the point, specific center of the hit pattern, and doesn't represent any real hit.

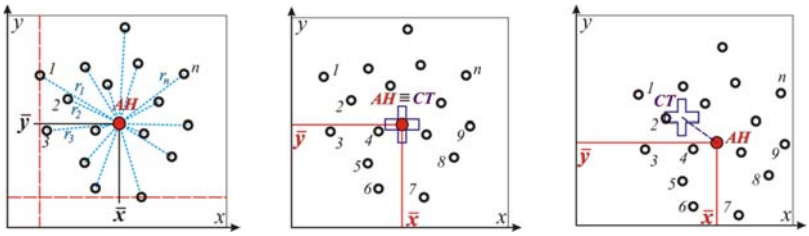

Figure 1. The hit pattern and precision parameters

The idea of the design of the device for automatic detection of the hits is based on the interruption of the established signal between transmitting sensor (IR diode) and receiving sensor (Phototransistor). The transmitter is IR sensor, source of the IR light, and the receiver is the detector of the transmitted light as phototransistor. The scheme of the conceptual design is presented in Figure 2.

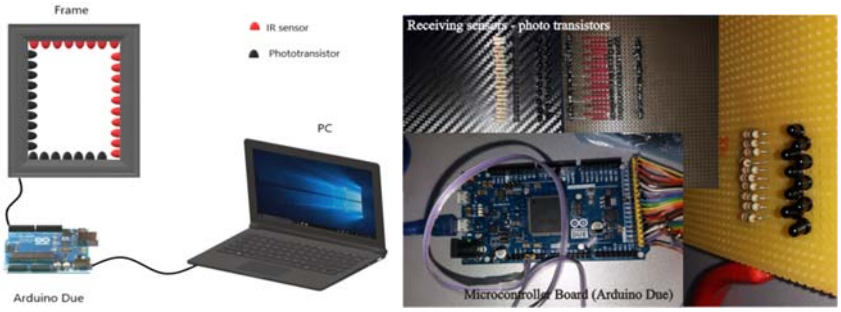

Figure 2. The design of start-up model of electronic target system

The purpose of the microcontroller board in the research is to provide the voltage supply to the IR diode, to detect the signals from phototransistors, provide the detected signal to PC and enables data processing. The graphic user interface of the Arduino Due enables communication with connected sensors and components. The software code is made for the research, in Arduino Environment, [4], for monitoring of the signal interruption between IR diode and phototransistor, according to the specific frame and position of the pair of transmitter and receiver. The interruption signal as information of the hit position in target plane is displayed to user and recorded.

The initial design of the system is made from available commercial electronic and IT components and custom made support mountings. The initial tests shows that designed system have improved performances in regard to the standard procedure with material test targets. Improved characteristics are the decreased time of test, automatic generation the results of the precision parameters, relatively simple and low-cost design and production, the possibility of perpetual usage.

9th International Scientific Conference
Research and Development of Mechanical Elements and Systems
Kragujevac, Serbia, September5-7 2019

PARAMETER OPTIMISATION AND FAILURE LOAD PREDICTION OF RESISTANCE SPOT WELDING OF ALUMINIUM ALLOY 57547

Biljana Markovic[1], Marijana Krajišnik[2], Aleksija Đurić[3]

[1]University of East Sarajevo, Faculty of Mechanical Engineering, Vuka Karadžoća 30, 71123 East Sarajevo, RS, B&H, biljana.markovic@ues.rs.ba, aleksija.djuric@ues.rs.ba
[2]Orao a.d. Bijeljina, Šabačkih đaka bb, 76300 Bijeljina, RS, B&H, marijanakrajisnik@gmail.com

Key words: wind effect, pressure calculation, mechanical and civil construction

Sunshade are used in different places and in different weather conditions, from high mountain areas with large amounts of snowfall, to sea beaches where tempest and storm can often do damage if the parasols are not adequately closed. As the sunshade has burdened by the wind (most cases), this paper presents the method of calculating the wind pressure on the sunshades, analogous to the method of calculating the influence of the wind on the roofs of building structures. The effect of the wind on a particular construction depends on the dimension of the structure and its position in the area. The description of the wind action is based on the adoption of the reference wind velocity (v_{ref}) defined based on meteorological measurements. Under special conditions - during weather conditions, the sunbathing is exposed to the wind effect and therefore the pressure of the wind (*Wi*) is operating on the surface of the dome, and the stated load is further transferred to the other elements of the sunshades, where they can break if they are not adequately designed. Figure 1 shows broken Collage 8x8 sunshade from the wind in Dubrovnik on August 13, 2017 (min daily temperature 21 ^{0}C, max daily temperature 30 ^{0}C, average wind speed 54 km/h, max hit the wind 84 km/h). In this paper, it has shown the calculation of wind pressure on the sunshade, just on the example given in the figure. The pressure of the wind on the outer surfaces w_e, as well as the wind pressure on the inner surfaces w_i, is calculated by the terms:

$$w_e = q_{ref} \cdot c_e(z_e) \cdot c_{pe} \quad (1)$$

$$w_i = q_{ref} \cdot c_e(z_i) \cdot c_{pi} \quad (2)$$

where are:

- $q_{ref} = \frac{1}{2} \cdot \rho \cdot v_{ref}^2$ - Medium pressure caused by an average wind speed
- $c_e(z_e), c_e(z_i)$- Coefficient of exposure, c_{pe}, c_{pi} - Coefficient of pressure

Figure 1. Deformation of sunshade Collage 8x8 – Dubrovnik 13.8.2017.

According to Figure 2a for the direction of wind 0^0, the four-stream roof of the dome of the sunshade is 19^0 and it has divided into eight surfaces, as shown in Figure 2b.

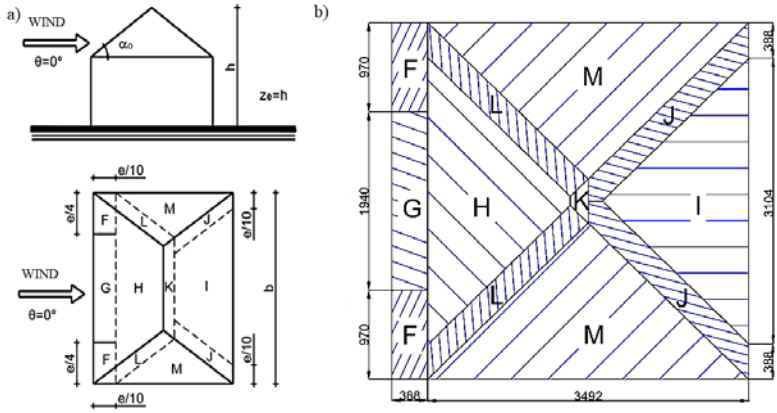

Figure 2. a) Division of quadruple roofs to surfaces; b) Figure 5. Division of the dome of sunshade to surfaces

The wind load has determined by algebraic addition of external and internal pressure:

$$w_1(F) = (-0{,}3975 + |-0{,}1064|) = -0{,}2911\frac{kN}{m^2} = -0{,}000291\frac{N}{mm^2}$$

$$w_1(G) = (-0{,}3192 + |-0{,}1064|) = -0{,}2128\frac{kN}{m^2} = -0{,}000212\frac{N}{mm^2}$$

$$w_1(H) = (-0{,}0581 + |-0{,}1064|) = 0{,}0483\frac{kN}{m^2} = 0{,}0000483\frac{N}{mm^2}$$

$$w_1(L) = (-0{,}4256 + |-0{,}1064|) = -0{,}3192\frac{kN}{m^2} = -0{,}000319\frac{N}{mm^2}$$

$$w_1(K) = (-0{,}34048 + |-0{,}1064|) = -0{,}23408\frac{kN}{m^2} = -0{,}000234\frac{N}{mm^2}$$

$$w_1(M) = (-0{,}1549 + |-0{,}1064|) = -0{,}0485\frac{kN}{m^2} = -0{,}0000485\frac{N}{mm^2}$$

$$w_1(J) = (-0{,}3021 + |-0{,}1064|) = -0{,}1957\frac{kN}{m^2} = -0{,}000195\frac{N}{mm^2}$$

$$w_1(I) = (-0{,}1007 + |-0{,}1064|) = 0{,}0057\frac{kN}{m^2} = 0{,}0000057\frac{N}{mm^2}$$

9th International Scientific Conference
Research and Development of Mechanical Elements and Systems
Kragujevac, Serbia, September5-7 2019

EXAMPLES OF KINEMATIC ANALYSIS OF COMPLEX MECHANISM USING MODERN SOFTWARE APPLICATIONS

Mustafa Imamović[1,2], Fuad Hadžikadunić[1], Amra Talić-Čikmiš[1], Armin Bošnjak[1]

[1]University of Zenica, Faculty of Mechanical Engineering, Fakultetska 1, 72000 Zenica, Bosnia and Herzegovina,
hfuad@mf.unze.ba, acikmis@mf.unze.ba, bosnjak.armin@gmail.com
[2]ArcelorMittal Zenica, Bulevar Kralja Tvrtka 17 , 72000 Zenica, Bosnia and Herzegovina,
mustafa.imamovic@arcelormittal.com

Key words: mechanisms, kinematic analysis, path, speed, acceleration, SolidWorks.

Analysis of planar or spatial mechanisms, as segments of real complex systems and machines in the domain of kinematics, kinetostatic, dynamic, functional and other aspects of analysis, can be done by analytical methods and by applying contemporary software applications. This paper shows an example of complex mechanism analysis using SolidWorks software, which provides a special module for quick analysis with a visual representation of characteristic data mechanism for different members position as a diagrammatic representation of certain parameters throughout the observed motion cycle. Such representations are very useful in designing mechanisms in the manner of analysis or synthesis. Analysis of characteristic points of moving members of the mechanism with the presentation of its path during the motion cycle, the analysis of velocity and acceleration vectors of members' moving points, forces on the members of the mechanism, definition of the moment or force on the drive member of the mechanism, the path of the executive member of the mechanism, the possibility of collision in the movement of the members of the mechanism, the geometry of the members of the mechanism based on the required path of the movement of the executive member of the mechanism, etc., are some of the possible areas of analysis. There are various software solutions that allow the creation and analysis of complex mechanisms, as well as very detailed analysis of all member movements in characteristic points, individual positions of the mechanism members, or for total movement cycles. Some of them are: SolidWorks, MechDesigner, SAM - the ultimate mechanism designer, Linkage, Pro/Engineer, etc. When applying software solutions, the basis of the overall analysis is to create a 2D or 3D model of all the components of the mechanism and connection of the component

kinematic links that limit the movement, or reduce the number of degrees of freedom of the mechanism.

Certainly, the creation of members of the mechanism in terms of geometric characteristics, the type of connection between them, and the assignment of driving characteristics to one of the members of the mechanism are features that have a crucial effect on the overall performance of the complete mechanism and its functionality. Benefits of using software packages, among others, include: visualization of the movement of the mechanism in the virtual environment with all the details, quick data processing and obtaining output data for various input parameter combinations, the ability to use output data for different applications, and the possibility of direct transfer to dynamic analysis. Figures 1a) to f) show some possible options.

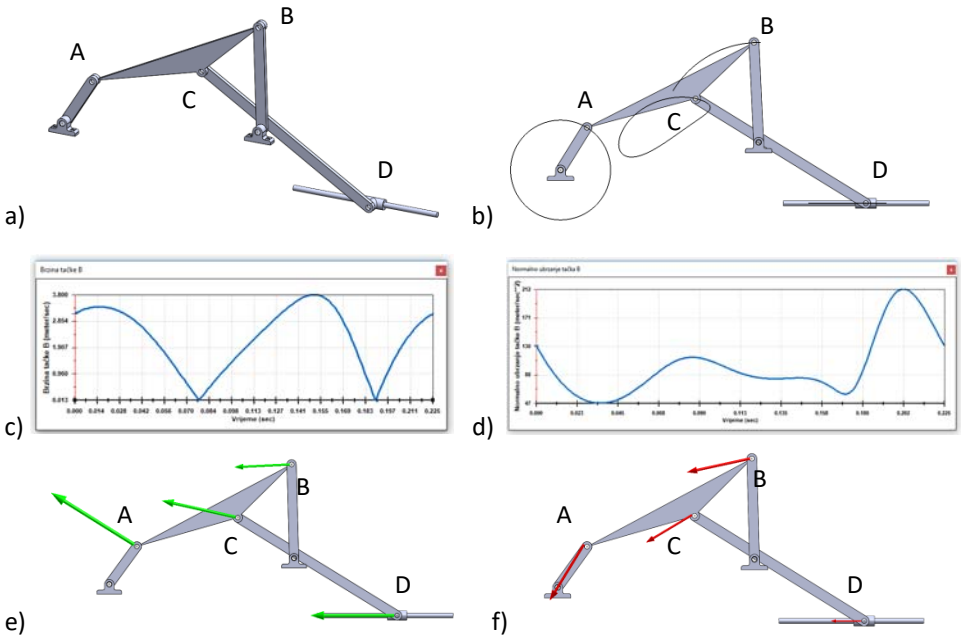

Figure 1. Planar mechanism and analysis displays: a) 3D model, b) display of trajectory of characteristic mechanism points using the 'Trace Path' option, c) B joint velocity, d) B joint normal component of acceleration, e) velocity vectors, f) acceleration vectors.

The most important of options are ‘path’ diagrams with respect to the motion requirements of the individual points of the mechanism, and the ‘speed and acceleration’ diagrams with special emphasis on the sudden changes in the speed values giving maximum acceleration, which are important for the dynamic mechanism stability. This reflects the scientific and practical application of the implemented software application methodology. In the case of analysis of mechanisms as parts of real devices or machines, such as: maximum mechanism member position, maximum speed or acceleration, motion point path, collision detection and real conduct of mechanism members motion, as well as creating an executive member of the mechanism according to the precisely defined motion curve for synthesis of mechanisms, etc. are just some essential segments that require a good understanding of vector calculation and application of software solutions.

IRMES KRAGUJEVAC 2019

9th International Scientific Conference
Research and Development of Mechanical Elements and Systems
Kragujevac, Serbia, September5-7 2019

THE RESEARCHES OF CARDAN SHAFTS / JOINTS DAMAGES IN THE EXPLOITATION

Aleksandar Ašonja[1], Eleonora Desnica[2]

[1]University Business Academy, Faculty of Economics and Engineering Management, Novi Sad, Serbia
[2]University of Novi Sad, Technical Faculty "Mihajlo Pupin", Zrenjanin, Serbia

Key words: cardan shafts, bearing assemblies**,** cross shaft the reliability, damages, the maintenance

The aim of the study was to explore the damages of double agricultural cardan shafts / joints in the exploitation. The most common reasons for failure are recorded on bearing assemblies and forks. On the basis of the conducted researches in order to increase the reliability of double agricultural cardan shafts, measures for the development of new and improvement of the existing technical solutions have been suggested in order to increase the reliability. At the end of the research, conclusions were drawn about the low reliability of double agricultural cardan shafts in exploitation conditions.
The subject of research in this paper is a double agricultural cardan shaft, size I. Investigations were carried out in the field in exploitation and laboratory conditions. For the purposes of the research it was used: visual assessment method, a method for quickly testing the current reliability of agricultural cardan shafts, the laboratory test table for testing the instantaneous reliability of cardan shafts (model: "ANA", type: 23-26-26-04).
Based on the research, it can be concluded that the highest probability of failure occurs with the joints and bearing assemblies on them. The most inefficient operation in the bearing assembly was recorded on needle bearings which, due to the increased radial clearance, could not make linear contact. In other words, the needle bearing reliability is the lowest. In the case of agricultural cardan shafts, the most common damage is the fork and the cardan joint bearings.
Damaged elements of bearing assemblies (crosses, needle bearings and cups) are the consequences of: improper lubrication (both at specified intervals and the use of inadequate lubricants), damaged seals, the use of inadequate materials in the elements of bearing assemblies, non-linear contact between the needle bearings of the crosspiece sleeves and cups, clogged lubrication channels, **Figure 1**, damaged lubricants.

Figure 1. The clogged central lubrication ducts on the cross shaft

The tests in laboratory conditions showed a technical malfunction according to the criterion of occurrence of temperature in the bearing assemblies. It is characteristic of most of the joints shown that they should have long been subjected to measures of technical maintenance, primarily lubrication and adequate storage, as well as overhaul measures.
A general finding that has been found to be significant for the mentioned tests of dual agricultural cardan shafts at an angle of rotation of 20^{o} joints is the discharge of lubricant from the bearing assembly space even for the smallest loads, **Figure 2**. With a minimum cardan shaft load of 36.15 Nm, lubricant leakage from the bearing assembly was made after 4 hours, and at more than 55.25 Nm, the leak occurred after 2 hours of the exploitation. At an angle of rotation of the twin cardan shafts of 20^{o}, even at minimum loads, lubricant leakage from the bearing assemblies on both joints was noticeable, which was due to the high level of vibration. Leakage of lubricant from the bearing assembly contributes to increased friction and wear, respectively, further increase of vibration and temperature, thus influencing the creation of radial, axial and circular clearance.

a) *b)* *v)*

Figure 2. Some examples of lubricant leakage from bearing assemblies during the exploitation

The reasons for the low reliability of double agricultural cardan shafts in exploitation conditions are to be found in the following statements: insufficient level of technical maintenance, primarily insufficient lubrication of the cardan joints every 8 hours, inability to constantly maintain equal angles on the input and output shaft, due to the very complex conditions (terrain configuration, machine turning, etc.) that prevail in agricultural production, inadequate use of telescopic shaft draw lengths is certainly a fact that influences the degradation factors of the elements in the bearing assembly of the cardan joint and it is not advisable to use dual cardan shafts at angles $\alpha_{12} \neq \alpha_{21}$, but in practice, this is primarily due to the terrain configuration.

9th International Scientific Conference
Research and Development of Mechanical Elements and Systems
Kragujevac, Serbia, September5-7 2019

THE RESPONSE OF A RANDOM VIBRATIONS OF NONLINEAR STRUCTURE UNDER WHITE-NOISE EXCITATIONS

Petre Stan[1], Marinică Stan[2]

[1]University of Pitești, Faculty of Mechanical Engineering and Technology, Romania, petre_stan_marian@yahoo.com
[2]University of Pitești, Faculty of Mechanical Engineering and Technology, Romania, stanmrn@yahoo.com

Key words: random vibration, linear equations, seismic response.

We present a method for estimating the power spectral density of the stationary response of oscillator with a nonlinear restoring force under external stochastic wide-band excitation. An equivalent linear system is derived, from which the power spectral density is deduced. A classical representation in seismic response analyzes it's that of a single or multi-degree-of-nonlinear oscillator subjected to earthquake ground motion at its support. An approximate method is presented for estimating the power spectral density of the response of multi-degree-of nonlinear random structure under white noise excitations. To illustrate the procedure of equivalent linearization theory, let us consider a three-story building. A three-story building is modeled by four identical columns of Young's modulus E and height h and two rigid floors of weight m. The damping can be approximated by an equivalent damping constant c_1 and c_2. The ground acceleration due to an earthquake is assumed to be a Gaussian white noise with a constant spectrumS_0. The method of the stochastic equivalent linearization is based on the idea that a nonlinear system may be replaced by a linear system by minimizing the mean square error of the two systems. The method will be briefly discussed in the following sections. The columns have cylinder sections of diameter D. Note that as the ground acceleration is assumed to be a Gaussian white noise of constant spectral density S'_0, the spectral density of the earthquake force that acts on the structure can be found to be$(0{,}5\ldots1{,}1)\ m^2 S'_0$. This can be readily seen from the definition of spectral density function which is the Fourier transform of the autocorrelation function. Considered a third story building with weight $m = 2 \cdot 10^5 kg$, by four identical columns of Young's modulus $E = 0{,}2 \cdot 10^{11} N/m^2$ and height $h = 2m$, with the diameter $d = 0{,}5m$, the damping factor

$\xi = 0{,}25$, with the nonlinear factor to control the type and degree of nonlinearity $\alpha = 20m^{-2}$, and $S'_0 = 0{,}52\frac{m^2}{s^3}$, which means that the power spectral density of excitation $S_F = m^2 S'_0 = 2{,}08 \cdot 10^{10} N^2 \cdot s$. Obtain $k = 29 \cdot 10^6 \frac{N}{m}$, $p = 12{,}04 s^{-1}$, $c = 1204 \cdot 10^3 \frac{N \cdot s}{m}$. For $\alpha = 20m^{-2}$, obtain $\sigma^2_{x_1} = 193{,}5 \cdot 10^{-5} m^2$, $\sigma^2_{x_2} = 201 \cdot 10^{-5} m^2$ $\sigma^2_{x_3} = 213 \cdot 10^{-5} m^2$. The values of k_{1e}, k_{2e} and k_{3e} is $k_{1e} = 31{,}57 \cdot 10^6 \frac{N}{m}$, $k_{2e} = 33{,}1 \cdot 10^6 \frac{N}{m}$, $k_{3e} = 33{,}1 \cdot 10^6 \frac{N}{m}$.

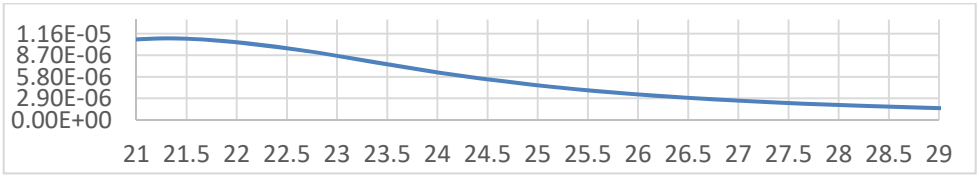

Figure 1. The power spectral density of the response $S_1(\omega)$ $[m^2 \cdot s]$ for the first structure in the freqency range (21,29) rad/sec.

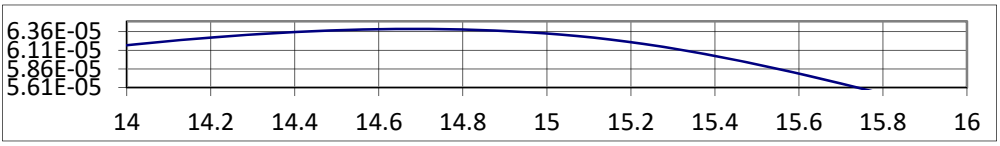

Figure 2. The power spectral density of the response $S_2(\omega)$ $[m^2 \cdot s]$ for the second structure in the freqency range (14,16) rad/sec.

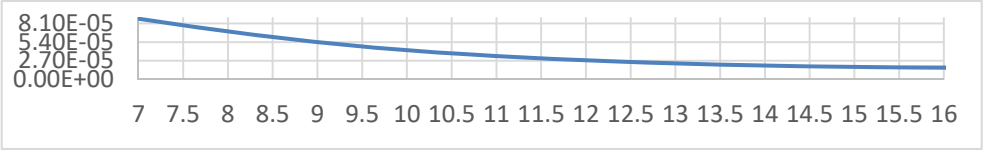

Figure 3. The power spectral density of the response $S_2(\omega)$ $[m^2 \cdot s]$ for the three structure in the frequency range (14, 16) rad/sec.

In the figures 1, 2 and 3, the power spectral density of the excitation is plotted for the different parameters. The graphs show how each floor of the structure is affected differently by the effect of seismic movement. By acting on the parameters in the calculation formulas, there is the advantage of taking preventive measures on the effect of seismic movement.

9th International Scientific Conference
Research and Development of Mechanical Elements and Systems
Kragujevac, Serbia, September5-7 2019

RESPONSE STATISTICS OF SINGLE DEGREE OF NONLINEAR RANDOM STRUCTURE WITH NONLINEAR DAMPING CHARACTERISTIC AND NONLINEAR ELASTIC CHARACTERISTIC UNDER WHITE-NOISE EXCITATIONS

Petre Stan[1], Marinică Stan[2]

[1]University of Pitești, Faculty of Mechanical Engineering and Technology, Romania, petre_stan_marian@yahoo.com
[1]University of Pitești, Faculty of Mechanical Engineering and Technology, Romania, stanmrn@yahoo.com

Key words: random vibrations, the spectral density of response, single-degree of freedom structure.

The paper investigates the applicability of the path integral solution method for calculating the response statistics of nonlinear dynamic systems whose equations of motion can be modelled by the use linearization differential equations. The present paper consists of discussion on dynamic response of structures under random load. They are random processes and commonly described by spectral density functions. Stiffness, damping and excitation are estimated from records of the stationary stochastic response. Assume that a single-degree of freedom structure is excited by a force which is a random process described by the spectral density. Nonlinear, dynamic systems subject to random excitations are frequently met in engineering practice. The source of randomness can vary from surface randomness in vehicle motion and environmental changes, such as earthquakes or wind exciting high rise buildings or wave motions at sea exciting of shore structures or ships, to electric or acoustic noise exciting mechanical structures. They are random processes and commonly described by spectral density functions. As a result, to obtain the standard deviation of the response, the velocity variance of the single-degree of freedom system the relative acceleration of this structure and the spectral density of the response. A single-story building is modeled by four identical columns of Young's modulus E and height h and a rigid floor of weight m. The damping can be approximated by an equivalent damping constant c. The ground acceleration due to an earthquake is assumed to be a Gaussian white noise with a constant spectrum S_0. The columns have cilinder sections of diameter D.

It starts from the equation of motion for this single-degree of freedom structure under earthquake excitation

$$\ddot{x}(t) + 2\xi pc[\dot{x}(t) + \varepsilon r_1 \dot{x}^3(t) + \varepsilon r_3 \dot{x}^5(t)] + p^2 x(t) + p^2 \alpha x^3(t) = w(t)$$

The method of the stochastic equivalent linearization is based on the idea that a nonlinear system may be replaced by a linear system by minimizing the mean square error of the two systems. Determination of solutions is done considering the following linear equation

$$\ddot{x}(t) + \beta_{ech}\dot{x}(t) + \gamma_{ech}x(t) = w(t).$$

Using an appropriate mathematical calculation obtain for the damping feature

$$\beta_{ech} = 2\xi_e p_e = \frac{E\{\dot{x}h\}}{E\{\dot{x}^2\}} = 2\xi p\left[1 + \varepsilon\left(r_1\frac{E\{\dot{x}^4\}}{E\{\dot{x}^2\}} + r_3\frac{E\{\dot{x}^6\}}{E\{\dot{x}^2\}}\right)\right] + p^2\frac{E\{\dot{x}x\}}{E\{\dot{x}^2\}} + \alpha p^2\frac{E\{\dot{x}x^3\}}{E\{\dot{x}^2\}}$$

and the elastic characteristic

$$\gamma_{ech} = \frac{E\{xh\}}{E\{x^2\}} = 2\xi p\left[\frac{E\{x\dot{x}\}}{E\{x^2\}} + \varepsilon\left(r_1\frac{E\{x\dot{x}^3\}}{E\{x^2\}} + r_3\frac{E\{x\dot{x}^5\}}{E\{x^2\}}\right)\right] + p^2\frac{E\{x^2\}}{E\{x^2\}} + \alpha p^2\frac{E\{x^4\}}{E\{x^2\}}$$

Using the transfer function obtain for the power spectral density of the response

$$S_x(\omega) = \frac{S_F(\omega)}{m^2\left[\left(\frac{E\{xh\}}{E\{x^2\}} - \omega^2\right)^2 + \omega^2\left(\frac{E\{\dot{x}h\}}{E\{\dot{x}^2\}}\right)^2\right]}.$$

In this example, for $S' = 0{,}52\, m^2/s^3, m = 2{,}2 \cdot 10^5 kg$, n=4 columns, $d = 0{,}5m$, $h{=}2m$, $E_b = 0{,}2 \cdot 10^{11} Pa$, $\xi = 0{,}25$, $\alpha = 7m^{-2}$, $k = 29 \cdot 10^6\ N/m$; $p = 12{,}04 s^{-1}$; $r_1 = 3 \cdot 10^2 s^2/m^2$, $r_3 = 12{,}142 \cdot 10^2 s^4/m^4$, $c = 1204 \cdot 10^3 \frac{N \cdot s}{m}$, $\varepsilon = 0{,}01$. The power spectral density for excitation is $S_F(\omega) = 2{,}08 \cdot 10^{10} N^2 \cdot s$. Obtain in this case for the displacement variance: $\sigma^2 = 105 \cdot 10^{-5} m^2$ and the coefficient p_e, $p_e^2 = p^2(1 + 15\alpha\sigma_x{}^2) = 15{,}21 s^{-2}$.

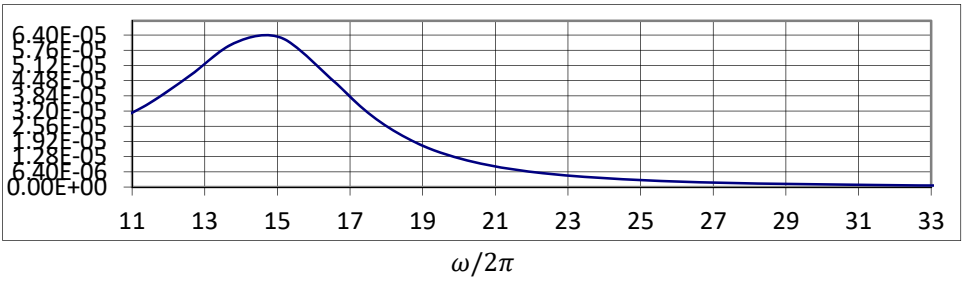

Figure.1. The power spectral density of response for $\alpha = 3m^{-4}$, in the freqency range (13, 33) rad/sec.

This suggests that the variance of absolute acceleration decreases as the damping increases when the damping ratio is smaller than$0{,}5$. The variance increases as the damping increases when the damping ratio is bigger than $0{,}5$.It can be seen that stiffening structure (increase stiffness) can reduce displacement but would result in the increase of absolute acceleration. A positive value of α represents a hardening system while a negative value represents a softening system behavior. On the other hand, increasing mass can reduce absolute acceleration but increase displacement.

9th International Scientific Conference
Research and Development of Mechanical Elements and Systems
Kragujevac, Serbia, September5-7 2019

GEARS OR ROTORS - THREE APPROACHES TO DESIGN OF WORKING UNITS OF HYDRAULIC MACHINES

J Stryczek[1], S Bednarczyk[1], E Codina[2], P J Gamez-Montero[2], L Ivanovic[3], M Matejic[3]

[1]Wroclaw University of Science and Technology, Wroclaw Fluid Power Research Group, 27 Wybrzeże Wyspiańskiego st., 50-370 Wrocław, Poland, jaroslaw.stryczek@pwr.edu.pl,slawomir.bednarczyk@pwr.wroc.pl
[2]Universitat Politecnica de Catalunya, IAFARG & LABSON - Dept. Fluid Mechanics, Campus Terrassa, Carrer de Colom, 11, 08222 Terrassa, Spain, esteban.codina@upc.edu pedro.javier.gamez@upc.edu,
[3]University of Kragujevac, Faculty of Engineering, Sestre Janjić 6, 34000 Kragujevac, Serbia, lozica@kg.ac.rs, mmatejic@kg.ac.rs

Key words: gerotor, trochoidal gear, pump design, hydraulic machines, plastic gears.

The gerotor pump has many advantages over other hydraulic pumps, such as high reliability, compactness, lower noise in running conditions etc. Considering the increasingly stringent regulations in the field of environmental protection, one of the main goals in the industrial applications of gerotors is to improve their design by using light materials and optimize their performance. This paper will give an overview of modern research that focuses on improving the performance of gerotor pumps. A joint publication of three university centers, namely of Wroclaw, Terrassa and Kragujevac, presents their original approaches to the problem of designing gerotor and orbital systems. All three approaches have been prepared in separate parts, but according to similar rules.
Wrocław Fluid Power Research Group assumes that gerotor and orbital systems should be treated as gear systems. Following that assumption, the scientists of the group has developed the knowledge of the fundamentals of designing and manufacturing of cycloidal gears and gear systems constituting gerotor and orbital systems. It is complex knowledge which includes geometry, kinematics, strength, hydraulics and cycloidal gears technology. For the description of those issues, an integrated system of technical parameters has been used, which is similar to the one applied for the classic involute gears. Using the characteristic parameters of the teeth and the mesh, a formula for calculating the delivery (absorption) q_{st} of gerotor machines is made:

$$\frac{q_{st}}{\pi bm} = \frac{1}{4}\left[(z_1 + 1 + \lambda - v)^2 - \frac{z_1}{z_1 + 1}(z_1 + 1 - v)^2 + z_1\lambda^2 \right],$$

where m is the module of the cycloidal gear, b is the tooth width, z_1 is the number of teeth of the internal gear ($z_2 - z_1 = 1$), λ is the tooth depth factor and v is the correction coefficient of the cycloidal profile.

The research group IAFARG & LABSON from Terrassa considers the gerotor pump as a hydraulic machine of which pumping action is carried out by means of a trochoidal-envelope toothed gear set. The research group unifies several approaches to characterize performance indexes either an existing gerotor pump or a new-born gerotor unit. These approaches mainly are dynamic simulation by using bond graph technique, computational fluid dynamics numerical simulation and experimental work. Their goal is to provide the design of a gerotor pump strikes a balance between volumetric efficiency, manufacturability and mechanical efficiency. GeroMAG concept as an innovative variable flow pump, sealed, compact and non shaft-drive with magnetic-driving outer rotor is obtained.

Contribution of the Kragujevac research group lays in the detailed analysis of the effects of the geometric parameters of the trochoidal gearing on the reduction of contact stresses performed using the analytical-numerical method and in the new possibilities it opens up for further studies. The condition for the existence of the maximum equivalent radius of the curvature dependent on coefficient $\lambda_c=1/\lambda$ and the external gear root radius parameter S_{fa} is derived, in the form of:

$$\frac{1}{\left(z_2\lambda_c+2-S_{fa}\right)^2}+\frac{\left(\frac{3}{z_2+1}\right)^3(z_2-1)\lambda_c\left[\left(\frac{3}{z_2+1}\right)^3(z_2-1)\left(\lambda_c^{\,2}-1\right)\right]^{-\frac{1}{2}}-1}{\left\{z_2\left[\left(\frac{3}{z_2+1}\right)^3(z_2-1)\left(\lambda_c^2-1\right)\right]^{\frac{1}{2}}-z_2\lambda_c-2+S_{fa}\right\}^2}=0 \quad .$$

All three research groups provide manufacturing and application review in the fluid power machines (Figure 1).

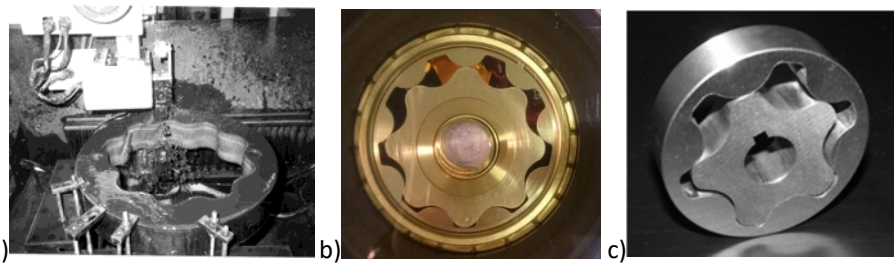

Figure 1. Designed and manufactured gerotors for hydraulic machines: a) Spark erosion machining of the internal hypocycloidal gear (Wrocław Fluid Power Research Group) b) GeroMAG prototype with an in house manufactured transparent polymer pump cover (IAFARG & LABSON research group) c) Optimal gear pair (research group from Kragujevac)

The developed mathematical models and the obtained results can be of use to the constructors of the gerotor pump and motors for choosing the best constructive solutions that reaches higher coefficient of efficiency.

Acknowledgments. This work was funded by the Ministry of Education and Science of the Republic of Serbia under the contracts TR35033 and TR33015.

9th International Scientific Conference
Research and Development of Mechanical Elements and Systems
Kragujevac, Serbia, September5-7 2019

DESIGN AND PERFORMANCE SIMULATION OF TORVEastro THREE-LINK ASTRONAUT ROBOT

Francesco Samani[1], Marco Ceccarelli[1]

[1]LARM2: Laboratory of Robot Mechatronics, University of Rome Tor Vergata, Rome, Italy,
francescosamani83@gmail.com

Key words: space robotics, service robots, robot design, performance evaluation.

In this article TORVEastro, a three-link astronaut robot, is presented with a conceptual design that is used also for a CAD design in performance simulations. This TORVEastro robot is designed for service applications in space stations. The TORVEastro space robot has a cylindrical body design with three legs, each of which is made up of two links and an end-effector. The symmetrical geometry of the legs makes them interchangeable thanks to the possibility of adopting a structure with multi-functional end-effectors. The conceptual design shows how one or two legs can be used for the most varied activities. The cylindrical body of the robot consists of curved surfaces and TORVEastro offers the possibility of facilitated movement in the outdoor space of orbital stations in order to be able to reach the localization objects. The service robot can move along, on the rods and handrails. In Figure 1 the conceptual design is shown with geometric and motion parameters.

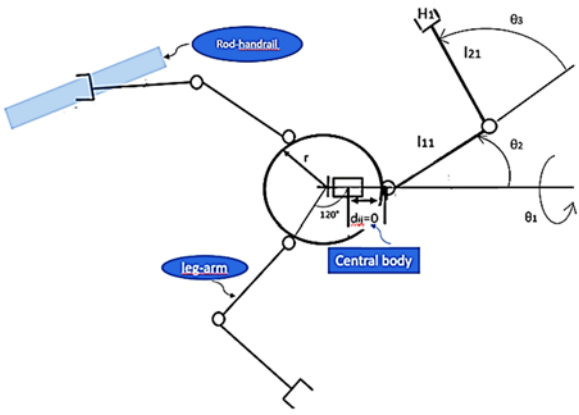

Figure 1. A conceptual design of TORVEastro

The proposed design of TORVEastro consists of a trunk and three legs. Control boards, sensors, battery and motors can be installed inside the cylindrical body (fig.2). The moment of inertia of the robot in the center of mass of the TORVEastro is: Px = 0.84 kg m2; Py = 1.1 kg m2; Pz = 1.7 kg m2. Calculations of the center of mass of the space robot have been performed in different configurations and the results show a proper dynamic capacity of TORVEastro. All electronic and sensitive parts can be repaired easily since the structure is easily accessible in each of its parts. The cylindrical body has a radius of 20 cm and a height of 15 cm. The max power of actuators is of 1 Watt, the max torque is of 1 N m, the number of actuators per end-effector is one, the number of the total actuators is twelve, the capacity of the battery is of 20 thou-sand mAh at the voltage is of 5V (valued consumption is of 0.2 J/sec, autonomy is 100 hours). The proposed TORVEastro configuration has the possibility to have symmetric three-link and the robot can be used with any posture that can be easily maintained because of a modular design with interchangeable parts. The end-effector can act either as a foot or as a gripper (fig. 1). Each link of the service robot consists of a 2.5-1 mm thick hollow cylinder with a circular cross-section arc of radius of 20 cm and an angular opening of 80 ° (fig.2).

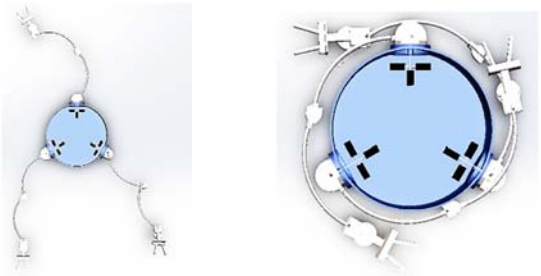

a) b)

Figure 2. A CAD model for mechanical design of TORVEastro in Fig. 1: a) full open configuration; b) full closed configuration.

Requirements and characteristics are discussed in the full paper with the aim to identify design problems and operation features. A study of feasibility is also discussed through performance evaluation by using kinematics and dynamics simulations whose results show the feasibility of TORVEastro robot operation and its peculiarities.

TORVEastro robot is proposed and simulated for service applications to help astronauts to do assembling and to do some other tasks like repairing and monitoring works outside space orbital stations.

The proposed conceptual kinematic design is obtained as a result from an analysis of operation problems and requirements in space. The robot design is composed of one central body and three legs/arms with the purpose to have robust, versatile, compact, and light design. Simulations have been used to characterize the mobility performance to give first indications for a feasible design of a first prototype. Future work is planned for experimental validation and performance testing.

9th International Scientific Conference
Research and Development of Mechanical Elements and Systems
Kragujevac, Serbia, September5-7 2019

TIGHTENS AS REQUIRED AND RESPONSIBLE ELEMENTS OF EQUIPMENT

Dusan Jesic[1], Pavel Kovac[2], Nenad Kulundžić[2], Dražen Sarjanovic[3]

[1]International Technology Management Academy, Novi Sad, Serbia
[2]University of Novi Sad, Faculty of Technical Sciences, Novi Sad, Serbia, pkovac@uns.ac.rs
[3]Sara-Mont. Doo, Belgrade, Serbia

Key words: design, shipbuilding, machine elements, equipment.

The tiles represent the Mechanical element, which is widely used in mechanical engineering, and orders its wide application in shipbuilding. These elements are standardized where they are specially standardized, dimensions and loads, as well as the technical conditions for design, delivery and marking. The work will show sections of the tent, as well as an example of labeling.

Tensile nuts-clips, used for adjustment) tightening) of wires and steel ropes or other parts like masts, pillars, wagon supports, etc. Ties are made of two screws and joint nuts. The screws with a different direction of slit thread engage in a common nut and thus pack or seal the parts. The tanks are standardized, the basic standard is JUS C. H4. 072 (Din 82004), since the tanks have the highest application in shipbuilding, it is also necessary to specify the ship standard SB 8696. A ship is a floating agent, moving by water using a kennel, sail or propeller, which is driven by a device or engine. It serves to carry passengers or cargo or some other special purpose. Our national Serbian standard is marked with the SRPS letter followed by the numerical standard mark. If the standard is homogenized with European standards then it is designated SRPSEN.

Figure 1 shows the housing (tensioning nut) with the necessary markings, the right and left thread of the tensioning nuts are visible.

The length of the tensioning nut (l6) is determined according to the thread length on the trunk of the connecting parts (l3) according to the thread standards in the tolerance field 7H, the class of construction C according to the standards JUS M.BO.221 and JUS M.BO.230.

Figure 2 shows the manufactured view of tension nut.

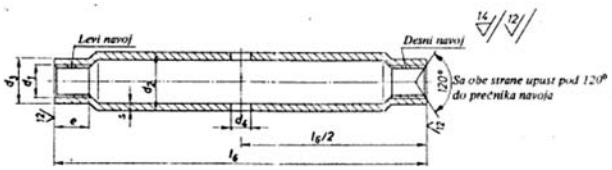

Figure 1. Tube-tightening screw nut

Figure 2. Manufactured View of tension nut

The tanks are very demanding responsible machine elements that have wide application

- Large and wide range of loads (4-320 KN) with safety factor 2.

When making, choose the most optimal production technology. It is obligatory to do a technological elaborate with a selection of the best order of technological operations

If standard or non-standard tension is required, it is necessary to approve basic and additional materials and to draw up a workshop drawing as well as drawings for the use of material for higher loads with a higher security factor. Perform all processing stages according to the specified standards and requirements of the contracting authority.

POWER AND MOTION TRANSMISSION SYSTEMS

development of new concepts, modeling and simulations, noise and vibrations, testing, safety, quality, reliability

9th International Scientific Conference
Research and Development of Mechanical Elements and Systems
Kragujevac, Serbia, September 5-7 2019

OPTIMAL DESIGN OF SELF-RETAINING FULL COMPLEMENT CYLINDRICAL ROLLER BEARINGS

C Ursache[1], A Barili[1,2], L Tudose[1,2], C Tudose[2]
[1]Technical University of Cluj-Napoca, Faculty of Machine Building, Bd. Muncii 103-105, 400641 Cluj-Napoca, Romania
[2] RKB Europe SA, Via Primo Agosto 1, 6828 Balerna, Switzerland

Key words: *c*ylindrical roller bearing, optimization, Particle Swarm Optimization, full complement, optimal design, self-retaining

The maximization of the bearing fatigue life can be obtained only by maximizing its basic dynamic load rating due to an optimal internal bearing geometry. To achieve this goal, in this paper, first it is described geometrically a self-retaining full complement cylindrical roller bearing, in order to obtain the necessary equations to permit the mathematical design of the optimization problem. The main innovation of this work is represented by the optimization of the internal bearing geometry of a self-retaining full complement roller bearing. Within the most important and related works, it's clear that the maximization of the bearing fatigue life, i.e. of the basic dynamic load rating, can be defined as the most common and diffused objective function in the optimal design of rolling bearings. Considering the full complement roller bearing geometry, it is not easy at all to find similar work in the field, especially for the assembling method of the bearing in discussion here, where the authors of this paper did not find anything in the open literature regarding the optimal design of the self-retaining full complement cylindrical roller bearings.
In

Figure 1 it is presented the bearing cross section perpendicular to the bearing axis. In this way, the objective function will not consider the roller length, which has nothing to do with the mounting procedure. As one can see, the rollers centers are staying on the bearing pitch circumference of diameter D_{pw} and δ is the space to insert the last roller. If the last roller is somehow mounted, δ is enough small that the all rollers support each other. But to mount the last roller the outer ring must be heated and the roller is inserted radially. Note that the outer ring has ribs on both sides and the rollers cannot be mounted from lateral.
In order to describe completely and unique the bearing geometry, it has been found that only two design variables are necessary being D_{we} (roller diameter) and F (inner ring raceway). With these, the objective function to be maximized is:

$$f(X) = \frac{C_r}{b_m (L_{we})^{\frac{7}{9}}} = f_c \, Z^{\frac{3}{4}} D_{we}{}^{\frac{29}{27}}$$

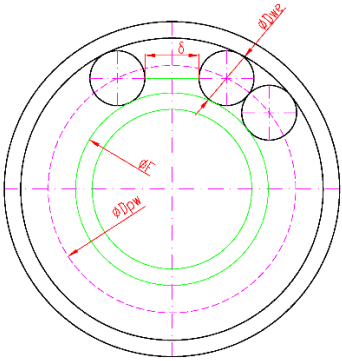

Figure 1. Optimized bearing scheme

Four constraints were applied to the optimization problem. The first one was developed considering the assembly method of the bearing, then that the last roller can be inserted only after heating of the outer ring and, the second one, once the last roller has been inserted and the bearing temperature is back to the environmental temperature, all the rolling elements must remain together and without falling (inner ring not inserted). The remaining constraints were conceived after studying many existing designs and to do not obtain unfeasible bearing designs.

To solve the presented optimization problem, it was used a Particle Swarm Optimization algorithm that, in literature, has been widely applied and proved to be a solid, simple and reliable optimization tool. After the initial population is randomly created, according with the designing variables range, the fitness of each particle is calculated and compared with the previous personal best position and with the global best position of all the particles. Once the new personals and global best position are obtained, the velocity of each particle is computed, and the new position of each particle can be defined. The algorithm is restarted till the chosen stopping criteria is met. The maximization of the objective function, the basic dynamic load rating, has been obtained by means of a basic PSO, but modified to implement the innovative set of constraints. The algorithm converged to a feasible solution and a set of optimal designing variables has been obtained.

Despite being a single objective optimization process with only 2 designing variables, the constraints handling of this problem was not easy to deal with. In fact, the only criticality found, it is related to the sensitivity of one of the mounting constraints. It has been demonstrated that a small variation (acceptable if considering a normal mechanical manufacturing process) of only one of the two components of the best individual has a great influence on the heating temperature of the outer ring. In conclusion, considering the mounting process and the self-retaining ability of the bearing geometry, the heating of the outer ring to fit the last roller also, lead to a feasible result in terms of internal geometry. The idea to embed this new type of constraint it can be considered solid and of extreme interest in many other cases.

Acknowledgments. The authors would like to thank the RKB Group, the Swiss bearing manufacturer, for the permission to publish these results and the RKB staff for their great interest and support during the development of this project.

IRMES KRAGUJEVAC 2019

9th International Scientific Conference
Research and Development of Mechanical Elements and Systems
Kragujevac, Serbia, September 5-7 2019

EXPERIMENTAL DETERMINATION OF PLASTIC GEAR DURABILITY

Gorazd Hlebanja[1], Matija Hriberšek[2] Miha Erjavec[2], Simon Kulovec[2]

[1]Podkrižnik d.o.o., Lesarska cesta 10, 3331 Nazarje, Slovenia
University of Novo mesto, FME, Na Loko 2, 8000 Novo mesto, Slovenia
[2]Podkrižnik d.o.o., Lesarska cesta 10, 3331 Nazarje, Slovenia

Key words: gear durability, plastic materials, gear shape, testing rig, S-gears.

Plastic gears became an important alternative in a broad spectrum of demanding applications, such as automotive, precision and medical equipment. Plastic gears have some advantages comparing to metal gears, e.g. lower weight and inertia, quieter operation, low manufacturing cost, corrosion resistance, vibration dampening. However, there are deficiencies, e.g. lower load, accuracy of moulded gears, thermal expansion and dimensional problems, thermal stability and moisture absorption. So, materials are improved by various fillers and new materials invented. Even very similar materials can have diverse characteristics.

Despite small testing rigs are quite effective for small gears, the new VDI Richtlinie, Blatt 4 requires some other gear sizes, so a new testing rig was manufactured. The basic idea is to produce tests, which can be directly compared to other research Tests in this paper were conducted entirely on the small devices with small involute gears. Raw parts were injected and gear cut subsequently. Despite net shape injected parts are preferred due to their price in mass production, cutting with professional hobs is necessary when gears of higher quality are required. A hob cutter for S-gears was already manufactured and tests are in plan later this year. S-gears are of interest due to lower frictional power comparing to E-gears.

Small gears (m = 1 mm, z1 = z2 = 20, b = 6 mm, with involute or S tooth flank shape) of varying material combinations were exposed to a constant torque and driving speed and run until failure. In this way Wöhler curves are obtained. Two series of tests were conducted: POM – PA66 and Steel C45 – PA66. POM and C45 gears were used as driving gears and PA66 as driven gear. Regarding PA66, four materials with different fillers (improved lubrication, thermal stability, improved load, etc.) were used.

Fig. 1 shows temperature time diagrams of POM/PA experiments. So, POM (Sabic's Lubricomp KA000M containing aramid fibres) was used for a driving gear and PA for driven gear. The best performance can be attributed to combinations Lubricomp KA000M (POM)/

Lubricomp RFP 36 (PA66) and Lubricomp KA000M/ Zytel 103 HSL NC010. Lubricomp performs slightly better at higher loads and Zytel with lower loads. So, one could expect better performance of Zytel gears with loads at fatigue strength level, which is due to stable mechanical properties of this material at increased temperatures.

Table 1 collects average contact spot temperatures in a stable region for mating POM/PA gears. Zytel 103 HSL NC010 develops the lowest temperatures in the stable range among all materials. Both other materials contain glass fibres and PTFE and it appears that the temperatures in these cases are higher. Regarding temperature range (heat development) and durability the basic, heat stabilized PA66, Zytel 103 HSL NC010, appears to be the most appropriate.

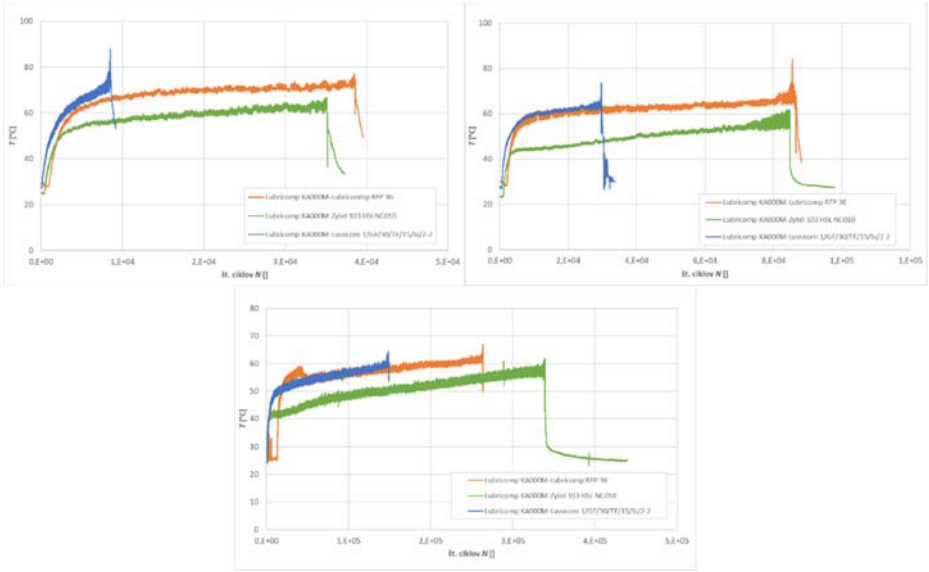

Colours: Zytel – green, Luvocom – blue, Lubricomp – orange)

Figure 1. Temperature rise during durability testing of material combinations POM – PA (n = 1400 min-1, Tok = 22°C) T = 1,5 Nm (top left), T = 1,3 Nm (top right), T = 1,1 Nm (bottom)

Table 1. Average spot temperatures in a stable range during testing (POM/PA)

Torque M [Nm]	**1,5**	**1,3**	**1,1**
Thermoplast	Average spot temperature T [oC]		
Lubricomp RFP 36	70	61	58
Zytel 103 HSl NC010	59	48	48
Luvocom 1/GF/30/TF/15/SI/2-2	66	62	55

Acknowledgments. The investment is co-financed by the Republic of Slovenia and the European Union under the European Regional Development Fund, no. SME 2/17-3/2017 and C3330-18-952014

EUROPEAN UNION
EUROPEAN REGIONAL DEVELOPMENT FUND

REPUBLIC OF SLOVENIA
MINISTRY OF ECONOMIC DEVELOPMENT AND TECHNOLOGY

IRMES KRAGUJEVAC 2019

9th International Scientific Conference
Research and Development of Mechanical Elements and Systems
Kragujevac, Serbia, September 5-7 2019

EXPERIMENTAL INVESTIGATION OF CONVEYOR IDLERS OPERATIONAL CHARACTERISTICS

Radivoje Mitrović[1], Žarko Mišković[1], Zoran Stamenić[1], Nataša Soldat[1], Nebojša Matić[1], Mileta Ristivojević[1], Aleksandar Dimić[1]

[1]University of Belgrade, Faculty of Mechanical Engineering, Kraljice Marije 16, 11120 Belgrade, Serbia, zmiskovic@mas.bg.ac.rs

Key words: conveyor idlers, experimental testing, belt conveyors.

The overall thermal power plants reliability and efficiency significantly depends on the efficiency of belt conveyor systems. Today's coal mining on open pit mine requires use of complex machinery with high productivity which allows continuous process of exploitation without unexpected malfunction with unplanned costs. For this reason, the tendency for daily analysis of existing and development of new, improved constructions of conveyor idlers (one of the most common reasons of bulk material conveyor transportation systems failures.) is present and growing. Conveyor idlers made by respectable worldwide manufacturers have up to three times longer service life than domestic. A prerequisite for improvement of reliability and efficiency of domestic conveyor idlers is introduction of performance testing methodologies in laboratory and exploitation conditions. Field tests take a very long time so they can't be fast enough to provide information for user to decide which of the offered products should be used in the actual transport system.

For the purpose of the quality and reliability inspection of conveyor idlers, a laboratory methodology for accelerated testing and comparison of conveyor idlers performance under the action of the radial load of constant intensity was developed. This methodology was used to provide qualitative comparison between different types of conveyor idlers – new and repaired, domestic and imported, conveyor idlers with different greases applied etc. According to this methodology, the basic parameters for determination of the conveyor idlers quality are: temperatures in idler's rolling bearings, deceleration during rotation stopping, rotational resistance, vibrations of idler's rolling bearings and noise. The procedure for determination of load capacity of conveyor idlers have been realized on the test rig SIV 300. Its basic look and operation principle are shown in Figure 1. Laboratory installation is designed for comparative testing of conveyor idlers (quality assessment), and for measuring changes of their operational characteristics over time (temperatures and vibrations). All tests have been performed under the action of radial load of different

intensity. Two pneumatic cylinders are used for radial force generation. They are controlled by system for data acquisition specifically developed for this purpose.

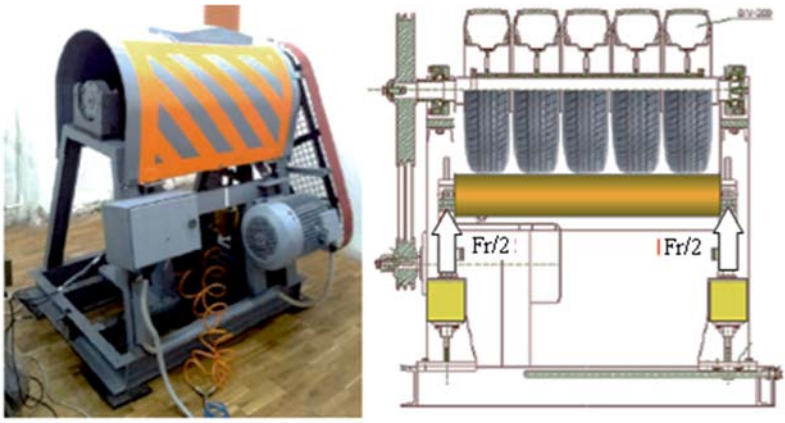

Figure 1. Test frame for performance testing of conveyor idlers

During the conveyor idlers experimental testing, all listed operational characteristics were recorded in time domain – using specific data acquisition system. The examples of obtained diagrams are presented in Figure 2.

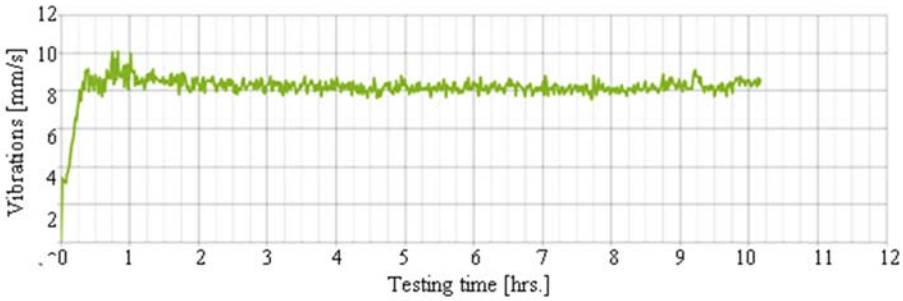

Figure 2. Example of obtained results for experimental testing of conveyor idlers vibrations

Implemented tests provide relevant information about the quality level of a large number of different types of conveyor idlers commonly used in open pit coal mines. The described conveyor idler testing methodology and equipment were developed in order to achieve potential increasement of conveyor idlers service life and reliability, reducing unnecessary and unplanned failures of belt conveyors as a system. Obtained results can also contribute to improvement of the quality as well as energy and financial loses reductions which are caused by conveyor idlers – both in belt conveyors and in the entire system of thermal power plants.

Acknowledgments. Results presented in this paper were realized within the Project TR35029 so authors would like to express their sincere gratitude to the Ministry of Education, Science and Technological Development of the Republic of Serbia, as well as to the company Thermal power plant and pit mines Kostolac (Serbia).

9th International Scientific Conference
Research and Development of Mechanical Elements and Systems
Kragujevac, Serbia, September 5-7 2019

RESEARCH OF WATER HYDRAULIC COMPONENTS AND SYSTEMS FROM ASPECTS OF QUALITY OF LIFE

Nenad Todić[1], Slobodan Savić[1], Saša Jovanović[1], Zorica Djordjević[1]

[1]University of Kragujevac, Faculty of Engineering, Sestre Janjić 6,
34000 Kragujevac, Serbia, ntodic@gmail.com

Key words: water, hydraulic, axial, piston, pump, experimental, research.

Modern water hydraulics is a unique field of science in which mathematical methods of describing processes and phenomena are in line with the results of experimental tests. The theory is confirmed and supplemented with experiments in order to create the basis for more exact and reliable research.

The most important component of the water hydraulic system is the pump. The modern development of water hydraulic pumps sets the standards in terms of the ever more stringent modes of operation of the pumps, and in terms of their quality and reliability. Special attention is paid to raising the level of technical performance through, improving the overall efficiency and energy savings, reducing the noise level as an important ecological factor, increasing the age of the devices in exploitation, correct structuring of the whole system in which the device works, optimization of the operating mode and management.

Axial Piston pump is one of the most frequently used hydraulic components in recent engineering technique (Figure 1).

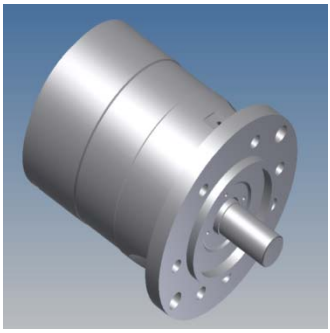

Figure 1. Axial piston pump of water hydraulic

The research and development challenges were to find engineering solutions to the specific problems in design and manufacturing of water hydraulic components and industrial systems suitable for using pure tap water as the pressure fluid. Current technological efforts for water hydraulics are far less than those for oil hydraulics. The experience gained from oil hydraulics is very important for future water hydraulics research.

Experimental research of piston axial pumps of water hydraulics carried out in the Research and Development Center RDC-PPT NAMENSKA. The tests were carried out on a test facility specially formulated for the examination of water hydraulic components. The basic component of the test installation is the test stand BAC 2063 (Figure 2).

Figure 2. Test stand BAC 2063

Energy efficiency of components and systems will be also very important aspect in the future. The consumption of energy during system use have to be minimized. The life cycle of the whole systems have to be considered. The situation at water hydraulic is different. Due the material requirements of components, the system building costs are higher than oil hydraulics at present. The use of water instead of oil is offering benefits, when considering energy consumption. The experiences of experimental research will provide good helps for design and development of water hydraulic axial piston pumps. Modern water hydraulic technology is still new and a lot of problems must be solved to make the technique more widely vailable for power transmission.

Acknowledgments. The research was supported by the Ministry of Education, Science and Technological Development of the Republic of Serbia, Grant III 42013.

9th International Scientific Conference
Research and Development of Mechanical Elements and Systems
Kragujevac, Serbia, September 5-7 2019

PLASTIC CUP STACKING MACHINE: PLANAR LINKAGE MECHANISM FOR GENERATION INTERMITTENT MOTION

Maja Čavić[1], Marko Penčić[1], Milan Rackov[1], Velibor Karanović[1], Marko Orošnjak[1]

[1]University of Novi Sad, Faculty of Technical Sciences, Trg Dositeja Obradovića 6, 21000 Novi Sad, Serbia, mpencic@uns.ac.rs

Key words: plastic cup stacking machine, planar linkage mechanism, intermittent motion, kinematic analysis, optimal synthesis.

Thermoforming is one of the oldest and most common industrial processes in which thermoplastic sheets or foils are processed by heating and pressure or vacuum into products of different dimensions and geometrics. Products obtained by thermoforming have the widest application in the food and pharmaceutical industries for the packaging of food and medicine, although there is considerable use in the automotive and construction industries for interior design with very complex geometries. The thermoforming process consists of three basic operations: foil manipulation, product forming and product manipulation whereby each operation is performed on a separate module of the thermoforming machine.

Plastic cup stacking machine presents the last module of thermoforming machine within which the formed products from the tool are accepted, transported and grouped for sorting and packaging. Modern plastic cup stacking machines contain sensitive electronics and numerous sensors – often quite fully robotic, to achieve high positioning accuracy and repeatability of movements, which is essential in order for the process to function. However, in addition to the high cost of automated and robotic systems, the main problem is that the control system is not always able to perform in time the process of stopping the panel within which are the formed products. This further implies the problem of sorting and packaging of formed products, which leads to a complete interruption of the process. For all of the above we have suggested a working mechanism for a thermoforming machine that has full mechanical control by which the driving motor is running at a constant speed at all times without the use of a frequency regulator and expensive electronics.

The paper presents kinematic analysis and optimal synthesis of a working mechanism consisting of a planar six-bar linkage mechanism with an oscillating slider for the generation of intermittent motion of the plastic cup stacking machine. Kinematic analysis defines the

kinematic parameters of the working mechanism – positions, angular velocities and angular acceleration. In addition, the extreme positions of the output link are defined, where output link represents the outer ring of the one-way clutch. The proposed mechanism contains a screw pair that allows the change and regulation of the machine's working step – the distance between the holes of the two adjacent panels is the working step of the machine. By changing panels with different openings, it is possible to manipulate products of different dimensions and shapes. This further implies a change in machines productivity without a motor regime change, which is also a benefit of the proposed solution.

Optimal synthesis increased the range of the machine's working step by 82%. In addition, the change law – step augmentation vs screw pair displacement, is linear in length up to 120 mm of screw displacement, while beyond that the dependence is nonlinear – therefore, linearity is only on the part of the range and in this zone the screw pair makes sense to apply. The proposed working mechanism is simple and reliable. It provides high positioning accuracy that allows high accuracy and repeatability of movements, which is essential for the proper functioning of the stacking process of formed products. It should be noted that the driving motor operates at a constant speed at all times without the use of expensive electronics – therefore, managing of the working mechanism and the change of the working step is completely mechanical so the malfunctions are minimized.

Further work will cover multi-criteria optimization with the aim of increasing the interval within which the change law is linear.

9th International Scientific Conference
Research and Development of Mechanical Elements and Systems
Kragujevac, Serbia, September 5-7 2019

ANALYSIS OF HARMONIC GEARBOX TOOTH CONTACT PRESSURE

Maros Majchrak[1], Robert Kohar[1], Michal Lukac[1], Rudolf Skyba[1]

[1]University of Žilina, Faculty of Mechanical Engineering, Department of Design and Mechanical Elements, Univerzitna 1, Žilina 010 26, Slovakia

Key words: harmonic gearbox, pressure in teeth gear, analysis, contact constrains, developing the mesh, mathematical calculation model

It is important to realize that harmonic gears (hereinafter referred to as "HG") were derived from traditional epicyclic gearing systems. In that case, a sun gear is the main input member and output speed and torque are obtained from planets that diverge from a central axis. HG is, in fact, a differential gear with a cylindrical gear pair in which gearing is achieved by elastic deformation of the flexible spline. This spline is characterized by its unique structure called a "Strain cam wave generator". The whole gear system is composed of four basic components, see Figure 1.

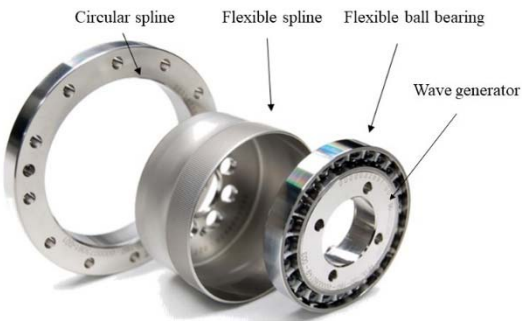

Figure 1. The basic components of a harmonic drive gear

Input torque is applied to a wave generator. This component is specific for its ellipse-shaped geometry. However, this ellipse is not regular — to secure clearance between the generating teeth of a circular spline and a flexible spline when rolling. The shape of the ellipse is flattened in line with the prescribed geometric function characteristc for stretching or flattening the shape. On this component, a flexible ball bearing is pressed and flexibly deformed according to the ellipse shape of the wave generator. When gearing this system, waves are generated, which is the basic driving component of this gear system.

HS are composed from some rigid and flexible parts through which the torque is transmitted thus generates the power. The contact pressure is specifically distributed in more teeth at the same time against conventional gearbox systems see Figure 2. Firstly, in this article the design description of dynamic calculation model of harmonic gearbox system in planar strain is analyzed. Ashwell as the definition of each contact constraints between rigid and flexible parts of these gear systems with respect of contact type „GLUE" and „TOUCHING". Last part of this article deals with force distribution analysis in teeth with respect of frictional forces in it. The graphical conclusions of this pressure on each tooth has been made. Focus of this article is mainly addressed on analysis of stress in gear teeth of harmonic gearbox systems. Ashwell as the research of special trajectory of rigid and flexible entity in solid circular spline of such gear system. It is the transmission of contact pressures that affects tooth wear and running accuracy.

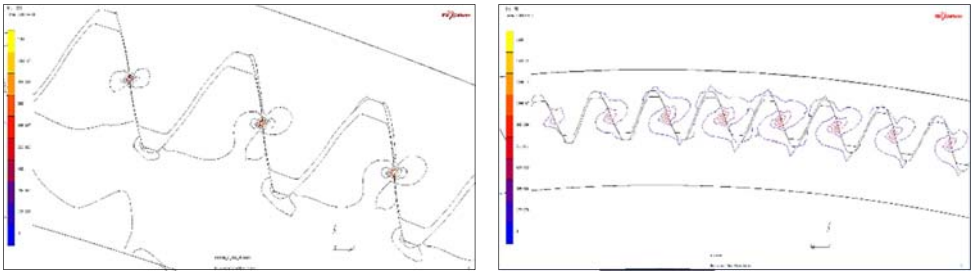

Figure 2. Details of the contact stress with regard

With this research, we explained the issue of harmonic gear systems and proposed the issue of their numerical solution, for 2D and 3D computational model. We also compared the characteristics of each model. This model was used as a basic model for the following research, which will be focused on optimizing design parameters for certain backslash. Our primary objective will be to optimize the parameters so that the backslash would be as small as possible. It is necessary to realise that these gear systems have been mostly used by industrial robots for very precise applications that require a really high rate of accuracy and rigidity.

Acknowledgments. This study was supported by Slovak Research and Development Agency under the contract no. APVV-18-0450 - Research of the influence design parameters of special transmissions with a high gear ratio with respect to kinematic properties.

iRMES KRAGUJEVAC 2019

9th International Scientific Conference
Research and Development of Mechanical Elements and Systems
Kragujevac, Serbia, September 5-7 2019

EXSPERIMENTAL DETERMINATION OF WORM GEARING EFFICIENCY

Aleksandar Skulić[1], Blaža Stojanović[1], Saša Radosavljević[1], Sandra Veličković[1]

[1]University of Kragujevac, Faculty of Engineering, Sestre Janjić 6, 34000 Kragujevac, Serbia, aleksandarskulic@gmail.com, blaza@kg.ac.rs

Key words: efficiency, power losses, worm gearing, materials, oil viscosity.

This paper deals with the analysis of impact of various factors on power loss and efficiency of worm gearing. Worm gearing power losses may vary in wide limits and that depends on the various influential factors such as: types of materials of meshed gears and the geometry of the worm pair, input rotational speed, type and the viscosity of lubricating oils, worm shape, loading, temperature etc.

Worm gearing are characterized by the line contact of teeth flanks which is followed by relatively high sliding friction between coupled elements and causes forming of a large amount of heat and power loss which is accompanied with low level of efficiency. The highest power losses in worm gearing appear in coupled worm and worm gear, in bearings, losess due to contact of oil and gears, in seals etc.

Worm gearing efficiency has a lower value in comparison with other types of gearboxes. In case of energy generating worm, overall efficiency is calculated by the equation:

$$\eta = \frac{P_2}{P_1} = \frac{P_2}{P_2 + P_G}$$

where are: P_1 - power on the worm; P_2 - power on the worm gear and P_G - overall power losses.

The values of efficiency were determined by the experimental methods on the specialized device AT200, whereby single-stage worm reducer constructed and made for that purpose was used. Mineral oils with different viscosity (ISOVG 220, ISOVG 460 and ISOVG 680) were used for the testing and their influence on the worm reducer efficiency was monitored. The values of the efficiency are determined with different input rotational speed whose values are 1500 min^{-1}, 2000 min^{-1} and 2500 min^{-1} and different loads, i.e. output torque. Changing the current intensity by the control unit causes the braking force on the magnetic brake to change also, therefore the value of the output torque is changed (load on the output shaft

of the reducer). Measurings were carried out for five levels of loads whereby the current intensity on the brake was in the interval 0.1 - 0.2 A with a step change 0.025 A. The results of the experimental testings are shown in figures 1 and 2.

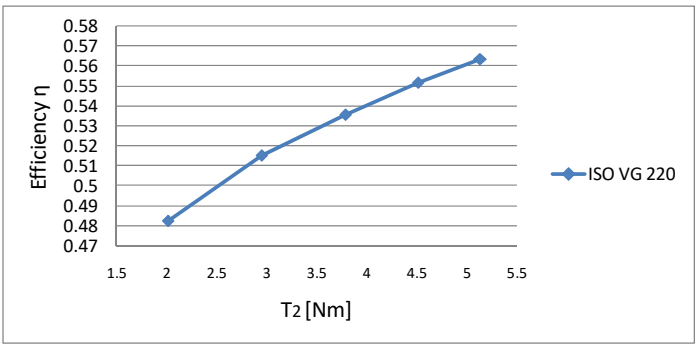

Figure 1. Overall worm reducer efficiency obtained by means of experiment for the input rotational speed n_1 = 1500 min^{-1} and different output torque values T_2 Nm.

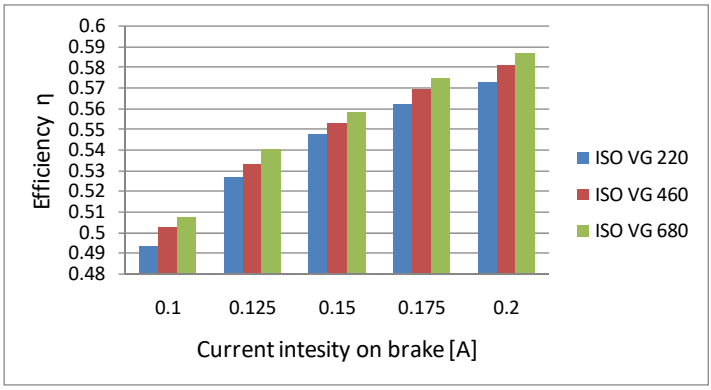

Figure 2. Values of efficiency for oils with different viscosity with input rotational speed n_1 = 2000 min^{-1}

Diagram of a dependency of the overall efficiency and output torque T_2 (figure 1) shows that higher values of efficiency were obtained with higher output torque i.e. loads. Likewise, higher values of efficiency were measured when using higher viscosity oils (figure 2) as well as with higher values of circumferential velocity. Using higher viscosity oils lead to lower power losses of worm gearing due to forming of oil film (that is thick enough) between the coupled flanks of the worm and worm gear, especially when the level of load and temperature are higher. On the other hand, with the increase of the circumferential velocity it is easier to form the oil film between the contact surfaces of gear teeth which creates conditions for total (hydrodynamical) lubrication, therefore the efficiency increases as well.

Acknowledgement. This paper presents the results obtained during research within the framework of the project TR 35021, supported by the Ministry of Education, Science and Technological Development of the Republic of Serbia.

9th International Scientific Conference
Research and Development of Mechanical Elements and Systems
Kragujevac, Serbia, September 5-7 2019

AN APPLICATION OF MULTICRITERIA OPTIMIZATION IN SELECTION OF THE TWO-SPEED TWO-CARRIER PLANETARY GEAR TRAINS

Sanjin Troha[1], Jelena Stefanović-Marinović[2], Branimir Rončević[3], Boban Anđelković[2], Miloš Milovančević[2], Kristina Marković[1]

[1]University of Rijeka, Faculty of Engineering, Vukovarska 58,
51000 Rijeka, Croatia, sanjin.troha@riteh.hr
[2]University of Niš, Faculty of Mechanical Engineering, Aleksandra Medvedeva 14,
18000 Niš, Serbia, jelenas@masfak.ni.ac.rs
[3]Vulkan Nova, Factory of Cranes & Ship Equipment, Rijeka, Croatia
broncev@yahoo.com

Key words: planetary gear trains, selection, multicriteria optimization, structure, important basic parameters.

This paper outlines the optimum selection procedure for a two-speed planetary gear train (PGT) with four external shafts based on two design and operational criteria: radial dimensions and efficiency. The paper outlines how to quickly determine the structure and important basic parameters of two-speed planetary gear trains that meet predefined transmission requirements. The relevance of the presented results is reflected in the fact that these transmissions offer significant advantages in systems which require speed change under load.

Compared to conventional gear trains, PGTs offer numerous benefits, and over the past several decades their use has proliferated significantly in a variety of branches in mechanical engineering. Multi-stage PGTs are built by linking one or two shafts between two different PGT stages from single-stage gear trains. A special multi-stage PGT type is a two-speed two-carrier PGT consisting of two coupling shafts and four external shafts. There are many important characteristics of this type of compound gear train, the most notable being the possibility of speed changes under load from the operator or control unit (machine tools, cranes, etc).

The main objective of this paper is to demonstrate the capabilities of the computer program *DVOBRZ* that has been developed for the purpose of analysis and optimization of two-speed PGTs. The basic part of the paper is the review of possible choice of the transmission for any defined application by using developed computer program. The choice between the computer obtained variants is then made by comparative analysis of the solutions.

Optimization is possible only if the desired transmission ratios are defined in both operating regimes, along with the torque and number of input shaft revolutions, as well as some other input data required by the computer program. The final selection of the transmission's kinematic structure and brake layout depends primarily on the main governing criterion chosen by the designer among a potentially large number of feasible solutions.

With the obtained data of ideal torque ratios t_{I} and t_{II}, transmission ratios i_{Br1} (effected by the activation of brake Br1) and i_{Br2} (effected by the activation of brake Br2), the teeth number of the ring gears z_{3I} and z_{3II}, as well as of the pitch diameters of the ring gears d_{3I} and d_{3II}, the program then determines the corresponding designation of the PGT and the required order of break engagements that produces the calculated transmission ratios.

The procedure is followed by a numerical example in which the optimal two-speed planetary gear train is selected, defined by the teeth number of the central gears, modules and transmission ratios. A numerical example demonstrates described principle, showing how conflicting criteria yield different solutions as optimality priorities change.

Based on the requirements and assumptions, the *DVOBRZ* program lists six possible two-speed PGT design structures as acceptable solutions, with the main parameters and kinematic capabilities. Since minimal radial dimensions are the main criterion in this example, the optimal solution is S16V2.

Power flow through the transmission by activating brake Br1and by activating brake Br2 is presented in the Fig.1

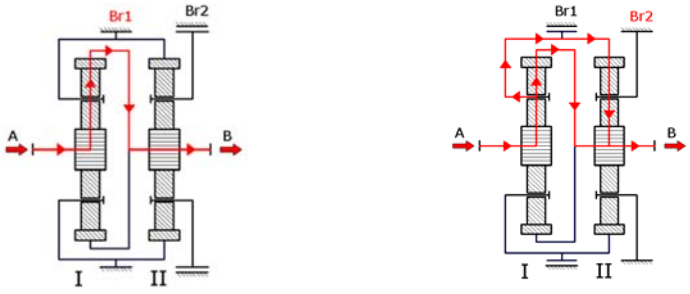

a) Brake Br1 activated

b) Brake Br2 activated

Figure 1. Power flow through the transmission

(A–input shaft; B–output shaft)

This example clearly outlines the procedure needed in the selection of a kinematic structure designed to operate optimally within a defined mechanical system. In the next step it is necessary to apply multicriteria optimization methods in order to define the PGT with design parameters.

9th International Scientific Conference
Research and Development of Mechanical Elements and Systems
Kragujevac, Serbia, September 5-7 2019

ANALYSIS OF THE INFLUENCE OF DIRECTION OF HELICAL TEETH IN THE UNIVERSAL HELICAL GEAR REDUCER ON SERVICE LIFE OF THE BEARINGS THAT SUPPORT THE REDUCER SHAFT

Milan Rackov[1], Siniša Kuzmanović[1], Ivan Knežević[1], Maja Čavić[1], Marko Penčić[1], Darko Stefanović[1], Mircea Viorel Dragoi[2]

[1] University of Novi Sad, Faculty of Technical Sciences, Trg Dositeja Obradovića 6, 21000 Novi Sad, Serbia, racmil@uns.ac.rs, kuzman@uns.ac.rs, ivanknezevic@uns.ac.rs, scomaja@uns.ac.rs, mpencic@uns.ac.rs, darkoste@uns.ac.rs
[2] Transilvania University of Brasov, Technological Engineering and Industrial Management Faculty, 1, University str., Brasov, Romania, dragoi.m@unitbv.ro

Key words: helical teeth direction, helical gear reducer, service life of the bearings.

The paper analyses the problems of the influence of direction of helical teeth in the universal helical gear reducer on service life of the bearings that support the reducer shaft, i.e. on the overall load carrying capacity of universal gear reducer. Directions of helical teeth for all gear units is adopted in that way that the overall axial force at the reducer shaft is lowest as possible, i.e. axial forces of a shaft are in counterbalance. It is a practice the same output gear pair is used within a helical gear reducer made in universal casing for two- and three-stage gear reducer. However, these gears are produced with different directions of helical teeth in order to obtain the lowest axial force on the fifth geared shaft. However, some gear reducer manufacturers, trying to simplify the production and reduce the number of manufactured components, produce the gears with the same helical teeth direction for both two- and three-stage gear reducers. In that way, they do not reduce the value of axial force on the fifth geared shaft in three-stage gear unit, but they make addition of axial forces that certainly affects the service life of the bearings and thus the overall load carrying capacity of the gearbox.

In the case of two-stage gear units, all the first gear pairs are kept the same as in single-stage gear unit because there are a large number of them. The direction of helical angles of the second gear pair (or the third gear pair, since the same gears are used in three-stage gear unit, just with opposite helical angle direction) is adopted in that way so the axial forces on the third (or fifth) geared shaft are in a reduction as much as possible.

In the case of three-stage gear units, the first gear pair is also kept the same as in single-stage gear unit, but the second and third gear pairs are adopted with such direction of gear

helical angle that the axial forces on the third and fifth geared shaft are in reduction at the shaft as much as possible (Fig.3).

In order to simplify the production and to reduce the number of necessary components, smaller manufacturers practice to use the third gear pair with only one direction of helical angle. In that case they could not provide the reduction of axial forces on the fifth geared shaft. Hence, the axial forces do not reverse each other on the fifth geared shaft of three-stage gear reducer. However, these forces are not large due to the small helical angle, but they are also not negligible due to the large torques on the fifth geared shaft. At the end, it is assumed that the sum of these axial forces will not be so large. The approval for such procedure is also reflected in the fact that the fifth geared shaft rotates significantly slower than the third geared shaft, which it certainly has more favourable impact on service life of the bearings.

Based on the carried out analysis, it follows that the adopted directions of helical teeth on the fifth geared shaft do not affect much the service life of bearings. Therefore, it is completely justified to manufacture only one output gear pair with only one helical teeth direction. First of all this procedure is justified for small manufacturers of gear reducers, but also some large manufacturers use this way of producing.

By producing the output gears with smaller value of helical angle, it is possible to reduce axial forces and to reduce the axial loading of the fifth geared shaft and the bearings, which means longer service life of the bearings. It is very important since the possible space in housing wall is very limited and it is not possible to mount stronger bearing (Table 1).

Table 1. Support forces and service life of the left bearing of the fifth geared shaft for both rotation directions and both helical teeth direction of the fifth gear

The way of loading	Forces in the left support and service life of ball bearing if helical angle is $\beta_{5/6}$ = 15°	Forces in the left support and service life of ball bearing if helical angle is $\beta_{5/6}$ = 10°
Right direction of rotation of output gear, where the axial forces have partially reduction	F_{rA} = 3694 N F_{aA} = 1547 N L_{hA} = 20200 h	F_{rA} = 3733 N F_{aA} = 848.6 N L_{hA} = 23700 h
Right direction of rotation of output gear, where the axial forces are summarized	F_{rA} = 3553.6 N F_{aA} = 2697.5 N L_{hA} = 10840 h	F_{rA} = 3642.3 N F_{aA} = 1999.1 N L_{hA} = 15200 h
Left direction of rotation of output gear, where the axial forces have partially reduction	F_{rA} = 4113.5 N F_{aA} = 1547 N L_{hA} = 17000 h	F_{rA} = 4228.5 N F_{aA} = 848.6 N L_{hA} = 16500 h
Left direction of rotation of output gear, where the axial forces are summarized	F_{rA} = 4426.2 N F_{aA} = 2697.5 N L_{hA} = 8130 h	F_{rA} = 4431.4 N F_{aA} = 1999.1 N L_{hA} = 11400 h

Acknowledgments. This paper is part of a research on project "Research and Development of a New Generation of Wind Generators of High Energy Efficiency" TR 35005, supported by the Ministry of Education and Science, Republic of Serbia.

9th International Scientific Conference
Research and Development of Mechanical Elements and Systems
Kragujevac, Serbia, September 5-7 2019

TRANSMISSION CHARACTERISTICS OF SIMPLE CYCLOID DRIVE WITH STEPPED PLANETS

Tihomir Mačkić[1], Milan Tica[1], Roland Šuba[2]

[1] University of Banja Luka, Faculty of Mechanical Engineering, Stepe Stepanovića 71, 78000 Banja Luka, Bosnia and Herzegovina, tihomir.mackic@mf.unibl.org
[2] Slovak University of Technology, Faculty of Materials Science and Technology in Trnava, J. Bottu 25, 917 01 Trnava, Slovakia, roland.suba@stuba.sk

Key words: cycloid drive, gear ratio, efficiency, self-locking.

In many industries, there is a need for using more compact and cheaper mechanical power transmissions. These targets are very difficult to achieve with conventional drive trains with fixed axes, so the need to replace these drive trains with suitable planetary drive trains is imposed. Very small dimensions of the gearbox and large transmission ratio can be achieved using planetary drive trains with cycloid gear. Simple cycloid drive is a type of high-sensitive gear train, by which it is possible to realize high transmission ratios in single-stage. Their advantage is also reflected in the compactness and simplicity of production, as well as achieving greater efficiency compared to conventional planetary drive train.

Single-stage cycloid drive or *simple cycloid drive* can be realized in two different ways:

- Adding a disc (*2*) with pins, this will accept the epicycle movement of the cycloid gear and transfer it to the shaft that coincides with the central axis (figure 1.a). This transfer method is used in today's cycloid reducers, and the disc (*2*) is called the output mechanism. There are the holes on the cylinder, which allow the transfer of the rotation movement from the cycloid gear to the mechanism;
- Adding another central ring gear (*2*) with the pins placed on the periphery, which meshes with the second cycloid gear (*2p*) (figure 1.b). The cycloid gears (*1p*) and (*2p*) are tightly connected in this case. In literature, such planets are called stepped planets.

In this paper, the basic equations for obtaining the transmission ratios, torque and efficiency of simple cycloid drive with stepped planets are shown. The dependence between basic transmission ratio and basic efficiency was also examined to find the optimum value of the transmission ratio and determine the point at which the self-locking occurs.

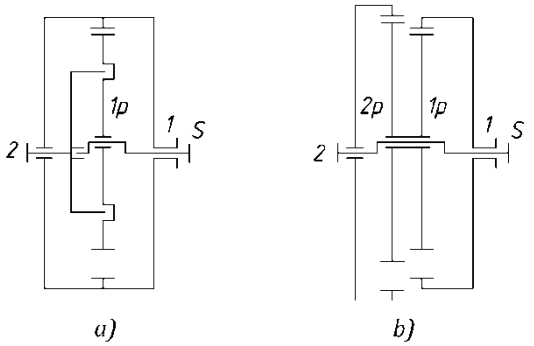

Figure 1. Simple cycloid drives

Basic transmission ratio of simple cycloid drive with stepped planets is:

$$i_o = i_{11p} i_{2p2} = \frac{n_1}{n_{1p}} \frac{n_{2p}}{n_2} = \frac{n_1}{n_2} = \frac{z_{1p}}{z_1} \frac{z_2}{z_{2p}} = \frac{z_2 (z_1 - 1)}{z_1 (z_2 - 1)}.$$

With the aid of the generalized Willis equation, it is possible to derive the equations for all transmission ratios of two-shaft cycloid drive with stepped gear. In figure 2, the function of the change of the transmission ratios i_{S1} and i_{S2} is shown.

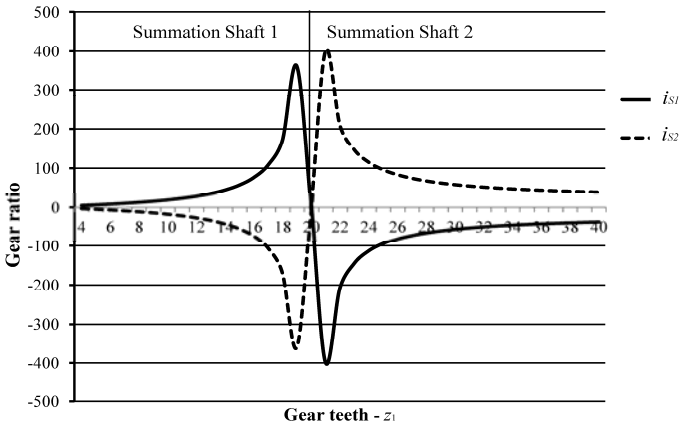

Figure 2. Change of transmission ratios i_{S1} and i_{S2}.

It is obvious that there is no need for gears with a larger number of teeth z_1 (when the shaft 2 becomes a summation shaft), since similar transmission ratios can be achieved in the first period, or when the shaft *1* is a summation shaft.

Theoretical analysis has shown that a simple cycloid drive with stepped gear can achieve very high transmission ratio, with great efficiency. In addition, the advantage of cyclo drive is reflected in the compactness and simplicity of production, as well as achieving greater efficiency compared to conventional planetary drive train. It is recommended to design these gearboxes with a smaller number of teeth, as this results in smaller dimensions of the gearbox while preserving a large transmission ratio.

IRMES KRAGUJEVAC 2019

9th International Scientific Conference
Research and Development of Mechanical Elements and Systems
Kragujevac, Serbia, September 5-7 2019

THE USE OF THE GAS FLOW MODEL TO IMPROVE THE DESIGN OF THE PISTON-RINGS-CYLINDER SYSTEM OF A DIESEL ENGINE

Grzegorz Koszalka

Lublin University of Technology, Faculty of Mechanical Engineering, Nadbystrzycka 38D, 20-618 Lublin, Poland, g.koszalka@pollub.pl

Key words: ring-pack modelling, blow-by, ring dynamics, engine development.

The piston-rings-cylinder system should ensure possibly small blow-by (gas leakage from the combustion chamber to the crankcase), low lubricating oil consumption and resistance to movement, and high durability. Generally, small clearances between the parts of the system favor the small blow-by. However, in such case the pressure in inter-ring spaces could be relatively high. When pressure in inter-ring spaces is higher than in the combustion chamber the gas flows in reverse direction – to the combustion chamber (such flow is called blow-back). Although the blow-back decreases blow-by it causes increased oil consumption and emissions of hydrocarbons and particulates. Higher pressure in inter-ring spaces could also force additional axial displacements of the rings in the grooves, which intensify the wear and affects the durability. Besides, additional ring displacements influence the gas and oil flows. The purpose of this work was to assess the possibility of reduction of the blow-back and axial displacements of the rings by modification of the selected dimensions of the compression rings and piston. An advanced mathematical model of the ring-pack developed by the author of this work was used for this assessment. This study was a part of a wider work aimed at reducing the emission of toxic components from the diesel engine produced by an independent manufacturer and used in delivery vehicles.

The influence of the following dimensions was examined: joint gaps of the top and second compression ring G1 and G2 and the diameters of the piston between the top and second ring D2u and D2d and below the second ring D3u (Figure 1). However, these dimensions could only be changed in the direction of increasing the clearances because the engine manufacturer did not allow the possibility of reducing the clearances for fear of seizing and damaging the engine (particularly, as it was also planned to increase the maximum power of the engine and hence the temperatures of the parts).

The results of the simulation showed that the top ring joint gap G1 should not be increased and the diameter of the shelf under this ring D2u should not be reduced because it leads to a very big increase in the blow-by and blow-back.

Increasing the second ring join gap G2 or reducing the diameter of the piston under this ring D3u leads to increased blow-by, but at the same time causes a large reduction in the blow-back. Increasing the diameter of the piston over the second ring D2d slightly reduces the blow-by and blow-back, however in combination with changes in other dimensions it can significantly affect the pressure in inter-ring spaces and axial displacement of the rings in the grooves.

As a result of the work, two solutions were proposed: the first one, which allows the complete elimination of the reverse gas flow from the inter-ring space towards the combustion chamber (in comparison to initial version, the second ring joint gap was increased from G2 = 0.35 mm to G2 = 0.6 mm, and piston dimensions were changed as follows: ΔD2d = –1.0 mm and ΔD3u = –1.0 mm). In this solution, the top ring moves axially in the groove once and the second and oil rings two times during one engine cycle. And the second solution (G2 = 0.45 mm, ΔD2d = -1.0 mm and ΔD3u = -1.0 mm), which ensures no displacement of the second ring and only two displacements of the oil ring (the top ring moves once in all examined versions), and a large reduction of blow-back – 3.5 times in relation to the initial version. In both cases, the benefits in blow-back come at the cost of increased blow-by, respectively by 65% and 40%. Pressures in inter-ring spaces for initial and two selected solutions are presented in Figure 1.

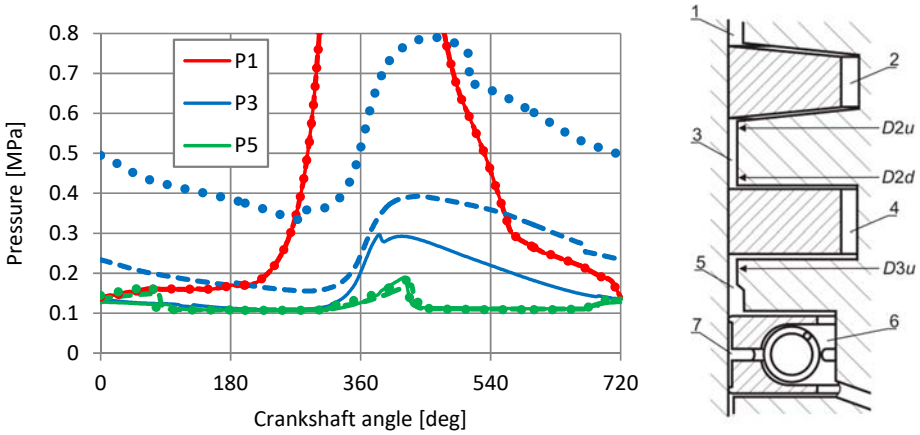

Figure 1. Pressure in inter-ring spaces for the initial dimensions (dotted line) and selected variants ensuring elimination of the blow-back (solid line) and preventing movements of the second ring (dashed line) and drawing of the engine ring pack on the right side

Summarizing, the application of the model allows to analyze the impact of many design variants on the operation of the ring-pack and to select one or more variants that will be manufactured and tested. This allows for a very large shortening and a huge reduction in the costs of an engine tests.

Acknowledgments. The research was financed in the framework of the project Lublin University of Technology – Regional Excellence Initiative, funded by the Polish Ministry of Science and Higher Education (contract no. 030/RID/2018/19).

iRMES KRAGUJEVAC 2019

9th International Scientific Conference
Research and Development of Mechanical Elements and Systems
Kragujevac, Serbia, September 5-7 2019

IMPACT OF A DRIVING BELT LENGTH ON A DEVICE NOISE

Peter Zvolensky[1], Milan Benko[2], Lukas Lestinsky[1], Jan Dungel[2]

[1]University of Zilina, Faculty of Mechanical Engineering, Univerzitna 1, 01026 Zilina, Slovakia, E-mail address: peter.zvolensky@fstroj.uniza.sk, lukas.lestinsky@fstroj.uniza.sk
[2]CEIT, a.s., Univerzitna 6A, 01008 Zilina, Slovakia, milan.benko@ceitgroup.eu, jan.dungel@ceitgroup.eu

Key words: planetary gearbox, gearbox design, gearbox measurement, gearbox noise

Transmission manufacturers are increasing requirements on their operating parameters (transmitted power, speed, operating temperature, noise ...). Change of these parameters can be achieved by design modifications. Although, it can positively influence required parameter, it may have negative effect on another. For this reason, it is necessary to design a universal testing system, so that transmission parameters can be modified and at the same time all required parameters can be tested immediately. When measuring gearbox noise, it is important to propose a way method how to bring the gearbox to the required speed.

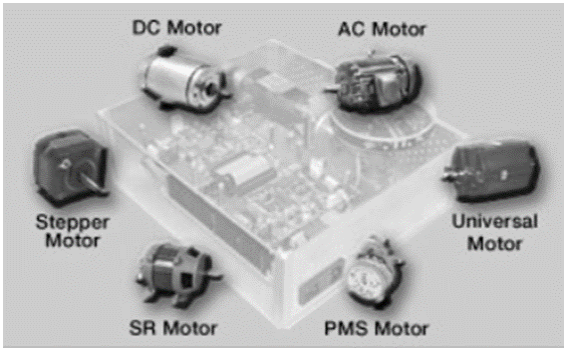

Figure 1. Classification of electric motors

The paper is dealing with design of high-rev planetary transmission and its overall noise. The transmission is able to reach high gear ratio, and provide very high revolutions per minute. These parameters can be achieved because of unconventionally mounted planet gears in two axles. Planet gears on the outside axle are in contact with ring gear and transfer torque to planet gears in the inner axle. Inner axle planet gears transfer torque to a sun gear. The paper defines an experiment of transmission design with possibility of changing number of

planetary gears. Number of planetary gears has an impact on overall noise of transmission. So it is possible to specify the transmission to fulfil of producer requirements. Aim for the experiment was to find trade-off between number of planetary gears, maximum torque, gear design and an impact on overall noise.

Further on, the paper presents test stand for the transmission. The test stand design allows definition of transmission structural units, without affecting noise of the transmission. Experiment also includes drive belt testing, and possibility of BLDC electric motor usage.

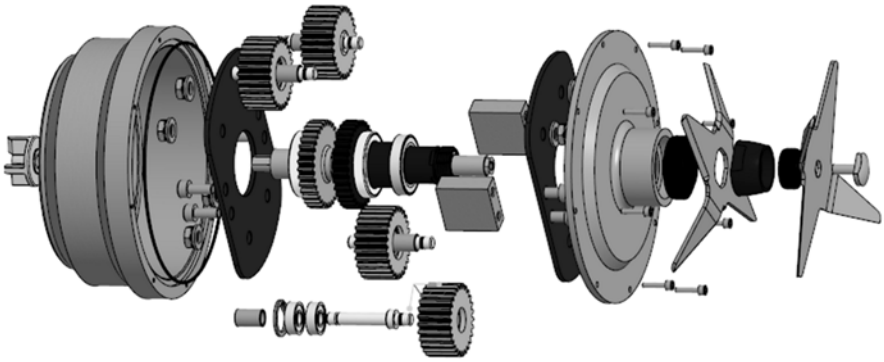

Figure 2. Components of measured gearbox

For the experiment it was necessary to design a test bench. The designed test bench consists of frame with a BLDC electric motor and the planetary transmission installed. Torque from the engine was delivered to the transmission via driving belt. Next, we were investigating the impact of the driving belt length on acoustic power level. Two lengths of the driving belt were used. We used two levels of rpms and the predefined place to measure acoustic power change.

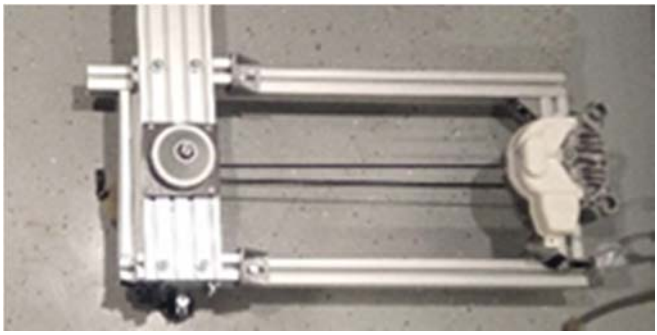

Figure 3. Test bench

Acknowledgments. This work was created by the implementation of the project “Low Cost Logistic System Based on Mobile Robotic Platforms for Industrial Use”, ITMS: 26220220205 supported by the Operational Programme Research and Development and by the European Fund for Regional Development.

9th International Scientific Conference
Research and Development of Mechanical Elements and Systems
Kragujevac, Serbia, September 5-7 2019

PRICE IMPACT ON ACOUSTIC COMFORT OF A WASHING MACHINE

Peter Zvolensky[1], Lukas Lestinsky[1], Jan Dungel[2]

[1]University of Zilina, Faculty of Mechanical Engineering, Univerzitna 1, 01026 Zilina, Slovakia, E-mail address: peter.zvolensky@fstroj.uniza.sk, lukas.lestinsky@fstroj.uniza.sk
[2]CEIT, a.s., Univerzitna 6A, 01008 Zilina, Slovakia, E-mail address: jan.dungel@ceitgroup.eu

Key words: washing machine, acoustic comfort, price, unbalance, maximum rpm, spin cycle

Acoustic comfort is becoming more important in the market with appliances. Customers require quiet appliances such as vacuum cleaners, washing machines or mixers. Many customers are willing to pay more for premium products. Customers that are not willing to pay more for appliances can choose models which are optimal or achieve minimum requirements. This comparison is focused on comparison of washing machines. Nowadays, many types of washing machines are available on the market. Customers can choose from many models, depending on their preferences. They can choose whetehr they prefer maximum rpms, noise reduction or vice versa. In most aspects, premium models should be better than regular, but often cheaper options can achieve also interesting parameters. The comparison is based on parameters that most of customers are focused on.

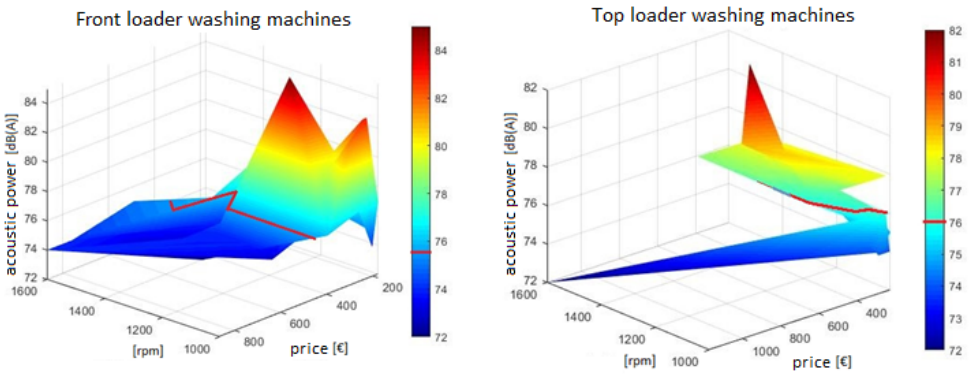

Figure 1. Washing machine comparison

The comparison includes 28 front loader and top loader washing machines. As one can see, the most expensive models can achieve the highest rpms and best-in-class acoustic comfort. But they are priced significantly above average range. Acoustic comfort optimum based on acoustic power during spin cycle (red lines) shows that half-priced washing machines can also achieve relatively good amount of noise reduction. In such a comparison, producers can choose price range of their products and customers can decide, if they are willing to pay for more premium products.

Of course, premium washing machines are better in more aspects than maximum rpm or acoustic comfort. Unbalance in washing machine tub has got significant impact on acoustic comfort. Premium washing machines are usually better with unbalance sorting out. The experiment was performed on front loader washing machine. In comparison of particular washing machines it was determined that with unbalance above 0.3 kg reduction of maximum rpm during spin cycle may occur. With reduction of maximum rpm, noise and load is also reduced. Even different models from the same producer have got different unbalance detection if different electric motor is used.

Table 1. Unbalance impact on maximum rpm

Maximum rpm	1440 rpm		
Load	0 kg	3 kg	6 kg
Unbalance 0kg	1360	1362	1360
Unbalance 0,3kg	1360	1362	1364
Unbalance 0,5kg	1050	1050	1364
Unbalance 0,8kg	820	820	1050
Unbalance 1kg	0	0	820

Price has got significant impact on acoustic comfort of washing machines. Premium washing machines are equipped with technology which can reduce noise during spin cycle. With unbalance detection and sorting, significant noise reduction can be achieved. Also, forces affecting components are smaller so longer life span can be achieved.

Acknowledgments. This work was created by the implementation of the project “Low Cost Logistic System Based on Mobile Robotic Platforms for Industrial Use”, ITMS: 26220220205 supported by the Operational Programme Research and Development and by the European Fund for Regional Development.

9th International Scientific Conference
Research and Development of Mechanical Elements and Systems
Kragujevac, Serbia, September 5-7 2019

DYNAMICS AND RIGIDITY OF SIMULATION CONTROL ON A 3-DOF MANIPULATOR

Serikbay Kosbolov[1], Gulnar Sadikova[1], Algazy Zhauyt[1], Saltanat Yussupova[1], Nurshat Uteliyeva[1, 3], Dana Maksut[4]

[1]Almaty University of Power Engineering and Telecommunications, Almaty 050013, Kazakhstan, kosbolov@mail.ru
[2]Kazakh Academy of Transport and Communications named after M. Tynyshpayev, Almaty 050012, Kazakhstan
[3]Al-Farabi Kazakh National University, Almaty 050040, Kazakhstan
[4]Nazarbayev Intellectual School, Almaty, Kazakhstan

Key words: dynamics, rigidity, simulation control, manipulators.

The problem of dynamic elastic four-link initial kinematic chain (IKC) of the load-bearing manipulator, which is the basis for various modifications are considered. Using the Lagrange operator for this system, equations of motion in matrix form are obtained. To determine the potential energy of an elastic four-link IKC manipulator, we use the formula for the elastic potential energy of a rectilinear homogeneous rod of length l. The cross-section of the rod is considered annular or circular. Solving the system of linear equations of motion on a computer using the ADAMS program, the results of the movement of links and cargo were obtained. Kinematics and dynamics are presented for a generic 3 DOFs Initial Kinematic Chain; with anthropometric data and the dynamics equations, simulations were performed to understand its behaviour.

Acknowledgement. We feel obliged to present our great thanks and gratitude to those who have kindly and patiently supported in our research.

PRODUCT DEVELOPMENT PROCESS

technology transfer, creativity and innovations, development and design, Innovative product development, smart systems, industry 4.0, knowledge economy

IRMES KRAGUJEVAC 2019

9th International Scientific Conference
Research and Development of Mechanical Elements and Systems
Kragujevac, Serbia, September 5-7 2019

CASE STUDY ON TOPOLOGY OPTIMIZED DESIGN FOR ADDITIVE MANUFACTURING

Abdulbasit M. Aliyi[1], Hirpa G. Lemu[2]

[1]Addis Ababa University of Science and Technology, Department of Mechanical Engineering, Addis Ababa, Ethiopia, obsinan1@yahoo.com
[2]University of Stavanger, Faculty of Science and Technology, N-4036 Stavanger, Norway, Hirpa.g.lemu@uis.no

Key words: additive manufacturing, layer manufacturing, lightweight design, optimized design, topology optimization.

Additive Manufacturing (AM), also known as rapid prototyping, rapid manufacturing, layer manufacturing and three-dimensional printing, represents one of the most promising aspects of manufacturing for highly complex geometries. In particular, AM is nowadays seen as provider of a wide range of possibilities to realize true design optimized manufacturing through topology optimization, which is an approach considered to be powerful in design. This is because it contributes to a design that can save energy, materials and time that are not economically achievable using other manufacturing processes. This paper explores the potentials of topology optimized design approach for AM in developing products that are lightweight, time efficient and capable of carrying loads. A case study has been conducted to demonstrate the steps involved in topology optimization and its benefits in terms of weight reduction.

Topology optimization provides the design freedom because it provides flexibility of design modifications and optimization at early stage of the design process, thus, creating a design concept in terms of a general material distribution as either solid or void. Its goal is to find the best use of material in load carrying so that an objective criterion (i.e., global stiffness, natural frequency and the like) is achieved subject to given constraints such as weight or volume reduction. In other words, the material distribution function serves as optimization parameter. However, there exists a series of remaining challenges to realize topology optimization including initiation of design parameterization that leads to physically optimal designs and making it effective and user friendly. Among these, the existing optimization algorithms are not yet fully capable to smooth the geometry that remains after optimization, which appears natural than a model defined by modelling functions. The challenge in design

parametrization is partly tackled due to the advances in finite element analysis (FEA) that enables generation of finite element meshes and definition of the meshed elements in design domain as design variables.

Topology optimization in design may be applied to two different types of structures; namely, continuum and discrete. While the former refers to optimized design of single objects like an engine block or a turbine blade, the latter is optimization of truss-like constructions composed of many members. The topology optimization algorithms solve design problems by applying boundary conditions, design responses and constraints to a design domain that involves all possible configurations of the design. Using finite element meshes, the optimization algorithms find the optimal distribution of material and voids in the given design space, depending on the loading and boundary conditions such that the resulting structure meets the prescribed performance targets.

In the conducted case study on an arbitrarily selected angle bracket, the processes involved in a topology optimized design approach are first identified. The process starts with developing a 3D CAD model and then design and non-design spaces are demarcated, where the former represents the part of the model that is subjected to topology optimization. Then, the topology optimization algorithm in ANSYS Workbench is “allowed” to remove materials from areas defined as the optimization design space, while the non-design space remains unchanged. All boundary conditions including loads and constraints are applied to the non-design space. The next step involves meshing and conducting finite element analysis, which provides stress and strain distributions. This distribution was used in the optimization procedure and materials were removed from areas that have insignificant contribution in load bearing.

The material removal normally leaves an irregular geometry that needs smoothing. Due to the lack of an effective smoothing algorithm, the optimized part is remodeled using approximate surface of the exterior boundaries of the optimized shape. This remodeled part was then subjected to FEA with the given design criteria so that the von Mises stress values for the load cases should not exceed the yield strength. For the considered triangular bracket, the final design satisfied the yielding condition with safety factor that varied from 1.067 to 50. The optimized design weighed only 1.188e-003 kg, compared to 4.378e-003 kg in the original design. As demonstrated by this case study, a 73% weight reduction implies a significant achievement in terms of products that require lightweight design such as in aircraft component design.

9th International Scientific Conference
Research and Development of Mechanical Elements and Systems
Kragujevac, Serbia, September 5-7 2019

TRENDS OF USING POLYMER COMPOSITE MATERIALS IN ADDITIVE MANUFACTURING

Yohannes Regassa[1], Hirpa G. Lemu[2], Belete Sirabizuh[1]

[1]Addis Ababa University of Science and Technology, Department of Mechanical Engineering, Addis Ababa, Ethiopia, yohannes.regassa@aastu.edu.et, belete.sirhabizu@aastu.edu.et
[2]University of Stavanger, Faculty of Science and Technology, N-4036 Stavanger, Norway, Hirpa.g.lemu@uis.no

Key words: additive manufacturing, additive fabrication, ceramic printing, composite materials, polymer composites, printing accuracy.

Additive manufacturing (AM) technology is nowadays one of the advanced manufacturing technologies used to convert 3D product data to physical objects without any special tooling. The emergence of the technology has made production of complex geometries having consumer demands and allows more customized products and services. Though the underlying technology was initially intended for rapid prototyping, the technology has recently getting wider attention in diverse industrial sectors. The forefront limitation of the technology is, however, the material types that can be used as input with regard to the required output product. Different material types that are commonly employed include polymers, metals, ceramics, and other compatible researched materials.

In this article, review and analysis of the opportunities and existing challenges for AM technology in processing polymer composites is presented. Due to the fact that the technology processes the input materials with no or very low wastes, the use of polymer composite materials leads to a no waste manufacturing system. Polymers are not only the first material types for layer by layer fabrication; they are also preferred as commonly used materials for the AM industry. This is primarily because of the diversity of polymer-based composites and the simplicity to adopt them to different AM processes. Polymer-based materials for AM are available as thermoplastic filaments, reactive monomers, resin or powder forms. Among others, the benefits of fabricating polymer composites using AM technology include the ability to customize complex geometries with high accuracy. However, their inferior mechanical properties have limited their application for load bearing structures. As a result, recent research and development has focused on reinforcement of

polymers with fibres and nano-materials, which may enhance the mechanical properties of the printed products to be used as load-bearing or functional components.

Ceramic based and concrete based composites are also candidate materials for additive fabrication. Ceramic based additive fabrication, in particular, provides tailor-designed materials with a high strength to weight ratio and facilitates creation of complex ceramic lattices for diverse applications. For instance, strong and versatile ceramic scaffolds with complex shapes can be used for tissue engineering purposes because biosensors can be easily embedded in medical devices or human organ. The main challenge of ceramic composites is the limited availability of the materials for additive fabrication using currently existing methods, relatively poor dimensional accuracy and quality. Similarly, concrete based additive fabrication has attracted the construction sector due to the possible mass-customization, building process automation without the need for formwork and the like. However, a poor research progress has been reported in this area due to limitations such as the suitability of the concrete type for simplicity to extrude, shape stability and dimensional accuracy after fabrication. Furthermore, other problems such as compacting issues, anisotropic mechanical properties and poor inter-layer adhesion are the main challenges that need to be addressed.

After rigorous review and analysis of previous and on-going research, trends related with polymer composite based additive fabrication and the associated research gaps are identified. Despite the fact that AM systems are proving to be useful in hard-to-reach locations, such as military bases, the international space station, and also widely employed in the medical applications especially for patient-specific orthopedic implants, there is still a need to fill the gap for many consumer products. Furthermore, many more good parts of this technology are yet to come for the well-being of human needs. Among others, an intensive materials research and development is needed in order to broaden the selection of suitable materials, prepare a database of the mechanical properties of parts fabricated by AM, and determine the interaction between materials and process parameters. The mechanical property of the fabricated parts is still not consistent and the process lacks repeatability of achieved accuracy and surface quality within each machine and across different machine operating under the same principle. Both the applicable design procedures and process modelling and control are considered as critical issues that require closer study in the future research.

In conclusion, parallel with the advances in the fabrication process technology, broadening the versatile use of polymer based additive fabricated products and further investigation of the availability of materials for diverse applications, significant work is needed to get acceptance of the technology in the industry. This needs, among others, changing the mindset in the industrial sector so that the technology gains industrial acceptance.

9th International Scientific Conference
Research and Development of Mechanical Elements and Systems
Kragujevac, Serbia, September 5-7 2019

AUTOMOTIVE RUBBER PART DESIGN USING MACHINE LEARNING

Dávid Huri[1], Tamás Mankovits[2]

[1]University of Debrecen, Doctoral School of Informatics, Kassai út 26, 4028 Debrecen, Hungary, huri.david@eng.unideb.hu
[2]University of Debrecen, Faculty of Engineering, Department of Mechanical Engineering, Ótemető utca 2-4, 4028 Debrecen, Hungary, tamas.mankovits@eng.unideb.hu

Key words: shape optimization, support vector machine, rubber jounce, finite element analysis.

In rubber bumper design one of the most important technical characteristics of the product is the force-displacement curve under compression load. This behaviour is the most critical customer need, in many cases its fulfilment requires general iterative design method. Design engineers can handle this task with the modification of the product shape. This kind of shape optimization problem can be solved with several standard optimization methods, if the parametrization of the design process is determined. Numerical method is a good way to evaluate the working characteristics of the rubber part. Automation of the whole process feasible with the use of Visual Basic for Applications (VBA) which allows to directly access Femap from Excel. Thereby the finite element model pre- and post-processing were controlled with macro running in excel.

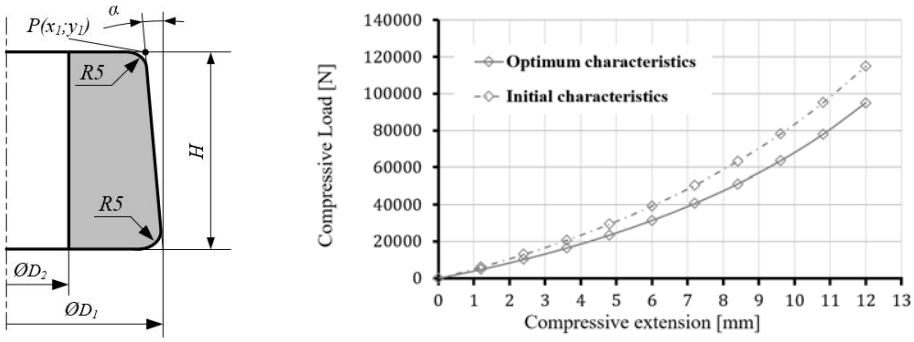

Figure 1. The investigated rubber jounce's geometry and working characteristics with optimum shape and a possible initial shape

Rubber behave as a nonlinear, elastic, isotropic and incompressible material, which can be described accurately with hyperelastic constitutive model. Mooney-Rivlin model with $c_{10} = 1{,}28801\ MPa$, $c_{01} = 1{,}1371\ MPa$ and $\kappa = 1000\ MPa$ values were selected for the finite element investigation of the rubber part. The geometry of the he investigated rubber specimen is axisymmetric, furthermore the boundary conditions are symmetric as well, thereby it is worth choosing axisymmetric element for meshing. The investigated geometry can be seen on **Figure 1** and it was created with $H = 40\ mm, \alpha = 3°, D_1 = 108\ mm$ and $D_2 = 33\ mm$ dimensions.

In many cases the dimensions of the rubber bumper built in air spring are constrained by other parts. During the current investigation, the product's height ($H = 40\ mm$) and draft angle ($\alpha = 3°$) were fixed while D_1 outer diameter and D_2 hole dimeter are variables, see in **Figure 1**. Thus in the shape optimization the design parameters are defined in mm, according to the following conditions:

$$\boldsymbol{D} = (D_1; D_2), where \begin{cases} D_1 \in [70{,}71, \dots 130] \\ D_2 \in [10{,}11, \dots 60] \end{cases} \text{ and } x_1 - \frac{D_2}{2} \geq 15$$

The goal of the shape optimization process is to minimize the $E(\boldsymbol{D})$ difference between the initial characteristics and the desired characteristics see on **Figure 1**. The aim of this research is to investigate the applicability of support vector regression machine, therefore the desired characteristics determined from predefined optimum shape $\boldsymbol{D}_{opt} = (108; 33)\ mm$.
The objective of the machine learning is to discover a function $E = f(\boldsymbol{D})$ that best predict the value of E associated with each value of $\boldsymbol{D}$. At the first step $128{,}36{,}22$ and 8 pieces of vertex pairs (Learning Points) were selected from $\boldsymbol{D}$, than E values were determined by using finite element analysis. Thereby the training set was produced for the machine learning algorithm. Matlab has a Regression Learner application. With the use of this application we could perform automated training to search for the best regression model type. Manual regression model training was ran without validation data set for all available SVM types. The goodness of the prediction highly hinges on the kernel function type. To choose the best model, the root mean square error (RMSE) value was calculated on the predicted set. The best trained model was the Cubic SVM for each set of Learning Points.
Using the different trained Cubic SVM models for different data sets, predictions were made for each combination of design parameters. Due to the verification the error values were calculated by finite element method as well. As it was expected these numbers are different, however the error values are close to zero except for that predictions which one was made by the data set containing 8 pieces of learning points. The rubber bumper working characteristics were also determined for each predicted optimum shape. Compared the different possible optimum shape with the known optimum, it can be stated that each geometry shows nearly the desired characteristics except for the *LP 8.* As a result, it can be stated that support vector machine is a good way to predict the optimum shape of rubber products.

Acknowledgments. The described work was carried out as part of a project supported by the EFOP-3.6.1-16-2016-00022 project. The project is cofinanced by the European Union and the European Social Fund. This research is partly supported by the ÚNKP-18-3 New National Excellence Program of the Ministry of Human Capacities.

9th International Scientific Conference
Research and Development of Mechanical Elements and Systems
Kragujevac, Serbia, September 5-7 2019

ASSEMBLY SYSTEMS PLANNING WITH USE OF DATABASES AND SIMULATION

Stefan Vaclav[1], Peter Kostal[1], David Michal[1], Simon Lecky[1]

[1]Slovak University of Technology, Faculty of Materials Science and Technology, Jána Bottu č. 2781/25, 917 24 Trnava, Slovakia. stefan.vaclav@stuba.sk, peter.kostal@stuba.sk, david.michal@stuba.sk, simon.lecky@stuba.sk

Key words: *assembly systems, databases, simulation*.

By defining the categories, the necessary first format of the database will be obtained, which will be assigned to the individual categories. Each entry must have its own attributes or properties, the properties on which the algorithm will work. Assignment of data properties is based on practice or after discreet simulation.

Mounting workplaces and systems can be designed in two ways:
- from down to top,
- from top to down.

In case of down to top and top to down design, the same database should be used for designing. This can be ensured by assigning such features to data that will focus on component requirements as well as requirements for the assembly system / workplace.

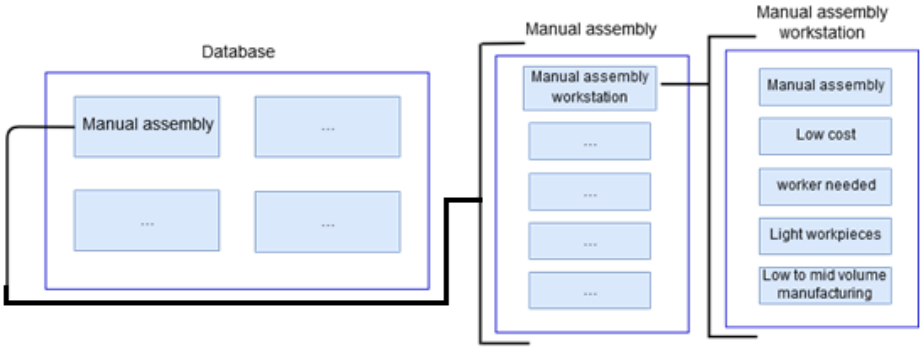

Figure 1. Scheme of attributes in database

The algorithmic solution has the task of correctly identifying data based on the selected properties. After selecting the correct data, it is necessary to perform and evaluate the capacities. This step should be simplified by designing an interactive capacitive calculator that can work on the basis of the algorithm of the selected data.

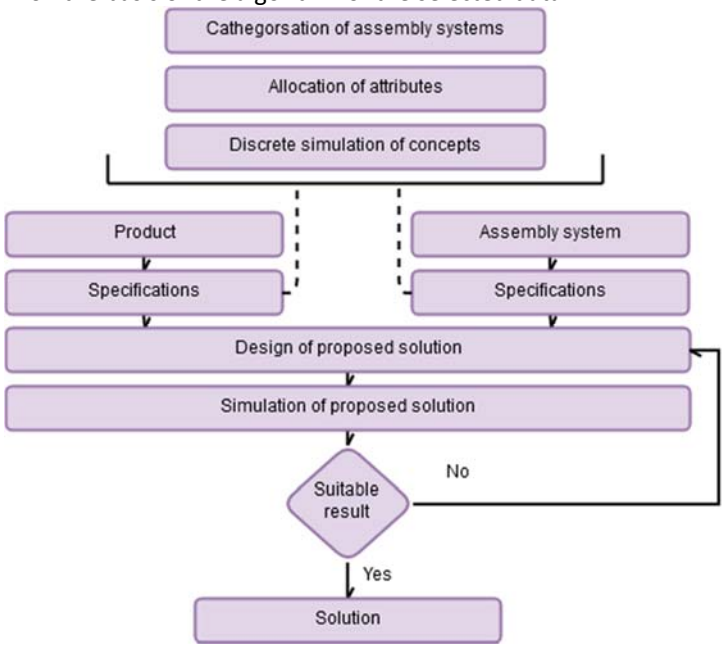

Figure 2. Proposed idea of solution

If the simulation model does not confirm the assumptions, it is necessary to return to the design and change the simulation model and thus the assembly system or workstation. If the simulation model proves to be appropriate and confirms the design assumptions of the assembly system or workplace, we can talk about a design that meets the requirements. Such a model is suitable for future planning of plant or system modifications where it saves time and can also serve as a test model for planning changes in production. In the case of incorporation of the developed methodology into the software solution, we can talk about computer support of design in the field of assembly workplaces and systems.
The article shows the ideological design of the assembly system design methodology. The aim of the work was to clarify and to create a proposal of solutions and partial solutions, which will enable and help the design of the assembly system design methodology. Paper defines access to designing databases that can be used for productbased access or assembly system requirements. Consequently, use the databases in the field of assembly systems to reduce design times.

Acknowledgments. This paper was created thanks to the national grant: KEGA 021STU-4/2018 - Development of a laboratory for the design and maintenance of production systems supported by the use of Virtual Reality.

IRMES KRAGUJEVAC 2019

9th International Scientific Conference
Research and Development of Mechanical Elements and Systems
Kragujevac, Serbia, September 5-7 2019

APPLICATION OF THE MULTI-CRITERIA DECISION MAKING IN THE SELECTION OF MATERIALS OF COMPOSITE SHAFTS

Z Djordjevic[1], S Jovanovic[1], S Kostic[2], M Blagojevic[1], D Nikolic[1]

[1]University of Kragujevac, Faculty of Engineering, Sestre Janjić 6, 34000 Kragujevac, Serbia, zoricadj@kg.ac.rs
[2]Technical College of Applied Studies in Kragujevac, Kosovska 8, 34000 Kragujevac, Serbia, sonja25yu@yahoo.com

Key words: multi-criteria decision making, shaft, material, composite

Thanks to the outstanding combination of construction and special features such as high resistance and stiffness, increased wear resistance to fatigue, higher values of critical speeds, lower mass, long lifetime, and so on, today a growing number of shafts, especially in the automotive industry, are made of composite materials. The optimal values of these parameters can be obtained by selecting the appropriate material.
The selection of materials in the process of product design requires efficient decision-making. In this sense, the use of multi-criteria decision making (MCDM) was used as an adequate tool and support for making optimum decisions.
For the construction of shafts most commonly used general structural steels, tempering steels or cementing steels, depending on the required strength, durability, cost of production, etc. In recent years, due to its good characteristics, composite materials increasingly replace steel in shaft production. The most commonly used shafts are carbon or glass fibers in combination with epoxy or polyester resins or hybrid constructions obtained by combining these fibers. Also, the laminates obtained by the combination of a metal matrix-composite are suitable for high resistance, load and specific stiffness.
When choosing metal materials for shaft production, more criteria must be considered (required load capacity, stiffness, stability, ...). When it comes to composite materials, the problem becomes even more complicated. In order to include as many criteria as possible when deciding on material selection, the multi-criteria decision making process (MCDM) is recommended.
In this case, four different materials (steel, carbon fibers/epoxy resin, fiberglass/epoxy resin, aramid fibers/epoxy resin, respectively) for the production of shafts were analysed the influence of six characteristic values (Young's Modulus E_1 and E_2, Shear Modulus G_{12}, density ρ, max. deflection f, max bending stress σ, respectively) that have the role of criteria in the MCDM process. The values of the x_{ij} are given and in this way the Matrix of the decision is formed. Linear data normalization was made on the basis of the equation from literature

depending on whether the maximization or minimization type is the criterion. On bases on SAW (Simple Additive Weighting Method) which is one of the most well-known and widely used methods, it takes into account the weight coefficients of the criteria. It is necessary to join the weight factor assigned directly by the decision maker or obtained by applying some of the known methods for determining the weight coefficients of the criteria. For each of the considered alternatives, the aggregate characteristic, or the value of the sum of multiplication of relative weight factors and normalized performance values, is calculated according to all criteria. Quotient an alternative with the highest value is the best of the offered solutions, where W_j` represents the normalized value of the weight coefficient W_j:

$$A^* = \left\{ A_i \left| \max_i \sum_{j=1}^{n} W_j' r_{ij} \right. \right\} \qquad W_j' = \frac{W_j}{\sum_{j=1}^{n} W_j}$$

As the final result of the analysis, using the expression above, the values of the aggregate characteristics for the three variants of the weight coefficients of the performances - criteria were obtained. In Table 1 and Figure 1 it is noted that for the values of the first variant of weight coefficients, the carbon fiber composite and the epoxy resin are best chosen.

Table 1. Collective characteristics for different values of weight coefficients

	S	C	F	A
A_{i1}	0.493151	0.722192	0.475890	0.46
A_{i2}	0.666667	0.511668	0.315006	0.24
A_{i3}	0.64	0.637972	0.420144	0.333189

For the second group of weight coefficients, steel was shown as the most favorable material, while in the third case, these two materials were practically identical. The remaining two materials received less or lesser grades in all three variants.

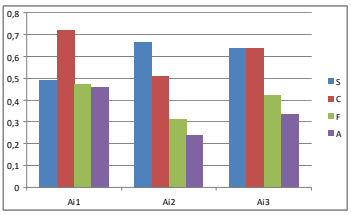

Figure 1. Diagram showing aggregate characteristics for three variants of weight coefficients of preformance - criteria

Based on the analysis presented for the four materials considered and the evaluations of the six selected characteristics, it can be concluded that the steel and carbon fiber composites with epoxy resins are the best estimate of the potential solution.

Acknowledgments. This is result of the TR33015 project, which is investigation of the Technological Development of the Republic of Serbia.

IRMES KRAGUJEVAC 2019

9th International Scientific Conference
Research and Development of Mechanical Elements and Systems
Kragujevac, Serbia, September 5-7 2019

IN APPLICATIVE IMPORTANCE OF THE ARTIFICIAL NEURAL NETWORKS APPLICATION IN KNOWLEDGE ECONOMY

A. Kitić[1], B Anđelković[1], M Milovančević[1], J Stefanović-Marinović[1]

[1]University of Niš, Faculty of Mechanical Engineering, Aleksandra Medvedeva 14, 18000 Niš, Serbia, kitic.ana4@gmail.com

Key words: Gross Domestic Product, corruption, forecasting, artificial neural networks, Corruption Perceptions Index

The area known today as neural networks is the result of a combination of several different directions of research: signal processing, neurobiology and physics. Each computable function can be trained through a neural network, everything that a normal digital computer can do is capable of doing neural networks. The best results can be given in the area of the approximation function classification and problems whose tolerance is imprecise and which have a lot of data for training and which require the rapid application of the appropriate rule depending on the input data. In this paper it will be showen how the artificial neural network can be used to get causality between Gross Domestic Product and Corruption, for the country Chile. The input data are the Corruption Perceptions Index and the output is measured by GDP. The corruption index is measured as a change in the price of food entering the consumer basket and the impact of the change on the household's consumption over a certain period of time. GDP defines the sum of manufactured final products and services (production and non-production) that are provided in a country for a certain period of time (usually one year). Corruption and GDP are terms that by their definitions do not have much to do with each other, but in some works they are connected but the growth of national income and corruption depends on many social factors. If we find a vase between corruption and GDP, we can predict whether a country will have a higher or lower GDP than in the previous year. Therefore, propose measures to reduce corruption if there is a need for this. The data is presented here is from country Chile, which was been chosen by random selection of 32 countries. The data are analysed in ANN network trough training diagrams and relative error diagram. Parameters for ANN network is shown on table 1.

Table 1. Learning parameters.

Element	Parameter
Network data type	Feed-forward backprop
Adaption learning function	TRAINLM
Performance function	LEARNGDM
Number of layers	2
Number of neurons	10

For the purposes of this paper and further commenting, it is necessary to calculate the relative error of our simulation. Usually, a mistake of almost 40% (Figure 1) is considered a major mistake, however, when it comes to corruption and GDP, or indexes that come in depend on some sociological factors, must say that a 40% error is acceptable. The sociological factor is such that it can not be foreseen, but foresight with a 40% chance of error can certainly have an impact on further analysis and should be taken into account.

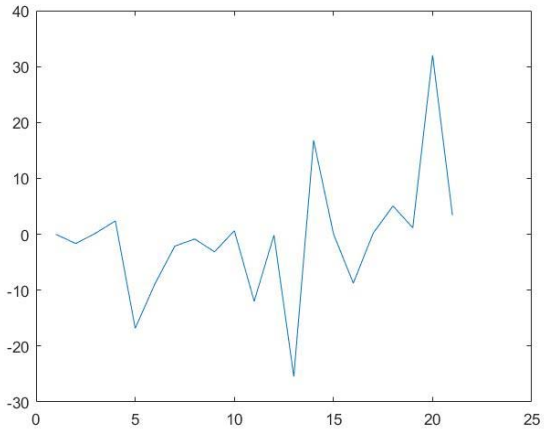

Figure 1. Relative error diagram

However, it can be seen that there are some social factors that have an impact on corruption, and therefore, the country's GDP in this case Chile. As these indices are highly dependent on some internal or external factors, we have analysed the policy of the Chilean government as well as the crises that hit this country. As a suggestion in further research, apart from the data on the Corruption Perceptions Index and GDP of some country, it is necessary to look at some social indexes or to make some index that the "MatLab" program could use in order to determine the link between GDP and the index corruption of a country for a certain period.

IRMES KRAGUJEVAC 2019
9th International Scientific Conference
Research and Development of Mechanical Elements and Systems
Kragujevac, Serbia, September 5-7 2019

DESIGN OF ALGORITHM FOR CREATION OF MODULAR LINES OF SPECIAL PURPOSE MACHINES IN THE AUTOMOTIVE INDUSTRY

Jan Galík[1], Róbert Kohár[1], Tomáš Capák[1]

[1] University of Žilina, Faculty of Mechanical Engineering, Univerzitná 8215/1, 010 26 Žilina, Slovak Republic, jan.galik@fstroj.uniza.sk

Key words: automotive, special-purpose machines, conceptual design, modularity, modular series.

This article deals with modularity of special-purpose machines in the automotive industry, because these machines and devices make up a large part of production and assembly machines, which is the engine of the economy of Slovak Republic. The paper introduces the reader to the issue of special-purpose machines operating in the automotive environment, emphasizing their modularity. The proposed equipment must meet certain criteria and be transformable, as there is great potential for future changes in the automotive industry. Designed devices must be of modular families and must have a wide range, multifunctional, and often perform several tasks, assembly or manufacturing at the same time. Most dedicated equipment transforms inputs into outputs, converting input material, energy, and information to the output materials, energy, and information. (Figure 1)

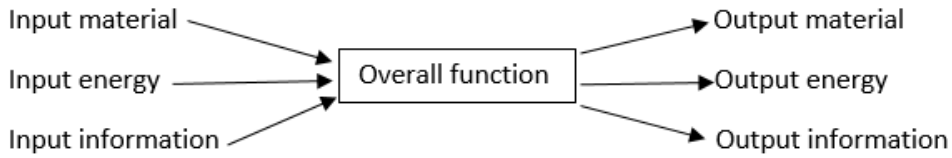

Figure 1. Functional structure of a machine

Any design of a modular or modular system is an effective way to reduce production costs and produce customer friendly machine. It is advantageous for the customer if the machine is made of serial components. This assumes that spare parts and possible failures will be easily repairable and economically inexpensive. In the production is the modularity linked with modular machine centers and big modular lines which are designed to do not need an operator. In assembly is the modularity of special-purpose machines linked with replacing people with machines and often helps people to assemble various components to the car.

How are created modular units is in the chapter 4. The modularity system can be applied in a number of sub-activities such as product design, process design, manufacturing system design, or combinations thereof. The best choice is to combine these three industries, their combinations and their simultaneous use, designing modular products, manufacturing them with modular processes and modular manufacturing processes.

The design of modular systems is possible only on the basis of a thorough analysis and division of the system into basic functional elements that characterize the basic physical principles and are integrated into the components of the modular system and capable of performing their function. This constitutes the basis for the design of the special-purpose machine.

In chapter 5 is described the algorithm and consists of 3 call phases: device planning, concept creation and system design. Each phase is important and must be successive.

Designing using conventional methods does not give designers as many solutions as possible using new methods. In design we want improvement of technical, quality and safety functions, weight and space reduction, reducing economic intensity, reduce delivery time and improving production methods. The importance of these points is different form machine to machine (task). Every new solution is mostly based on new working principles, modifiable in manufacturing methods, based on lower prices and shorter delivery times.

Creating concepts can be said to be one of the most important parts of the equipment design process (often underestimated), because it is precisely in the creation of concepts that we are able to influence future equipment, its shape, cost of production, selling price, performance, and so on. The principles must fulfill the functional requirements, that are based on catalogues, patents and not least engineer experience. From the formulation of construction requirements, we are capable to mapping relationships between working principles. These relationships are very important by the creating matrix. In this matrix are defined modules and from these modules we build a modular design family.

After the concept creation are the modules prepared for designing and the modular product family is assembled. The final product is subjected to a practical assessment. The final product is subjected to a practical assessment. If the design of a modular construction does not meet the requirements, a return to the design process is needed, and more specifically to the point of combination design and selection of device module variants. Subsequently, the design process proceeds to the next points, where the design of the device is detailed.

In the conclusion is described the algorithm, how should the engineer proceed in the theoretical design of the device and should devote sufficient time to this phase. Using the algorithm, we are able to save time, energy, work and money.

Acknowledgments. The research is supported by the Cultural and Educational Grant Agency of the Ministry of Education, Science, Research and Sport of the Slovak Republic under the project No. 046ŽU-4/2018.

9th International Scientific Conference
Research and Development of Mechanical Elements and Systems
Kragujevac, Serbia, September 5-7 2019

TRANSACTION APPLICATIONS OF ENTERPRISE INFORMATION SYSTEM

Vanessa Prajová[1], Mária Homokyová[1], Martina Horvátová[1]

[1]Slovak University of Technology, Faculty of Materials Science and Technology, Institute of Industrial Engineering and Management, J. Bottu 25, 917 24 Trnava, Slovakia

Key words: Enterprise Resource Planning, modules, processes, metrics, ERP effects.

There are various explanations for the concept of process in the literature. However, it can simply be defined as "transforming inputs into outputs". The ISO 9001: 2008 standard characterizes the process as "a set of interrelated or interacting activities that change inputs into outputs." If we look at definitions by author, we understand the process - a set of activities that require inputs and generates value-added outputs for the customer. If we look at this definition, a closer process is not only linked to the production process, as the word process might seem. The process concerns all areas of the business, administrative or non-administrative, and thus, of course, manufacturing. In addition, processes go far beyond the enterprise and thus create and shape relationships with other businesses, partners, customers, employees, government. The process is triggered by an initial event. The event can be created after any activity, with the most important end goal being a customer-oriented outcome. The process or process result is determined by a variety of parameters, such as process costs or process efficiency. In this case, the value for the endpoint - customer. The process owner and the process parameters are responsible for the process. Therefore, three basic process categories have been created:

- key processes: are processes that lead to the company's core vision, to profit, and thus to customer satisfaction;
- supporting processes: these processes are equally important as key processes, they are also customer-focused, but internal. Internal customers are employees of the enterprise and thus one of the inputs to the process;
- side processes: are support processes that can be excluded from the organizational structure of the enterprise and thus can be "outsourced".

The link between the information system and the business process is confirmed by the implementation of enterprise information systems by the need to carry out an "inventory" and, of course, to change all processes in the company, whose activities are affected by the new information system. In today's companies, it is possible to say almost all areas from logistics, business and technical departments, through employee records and all related

tasks - remuneration of merchants based on delivered goods, remuneration of technical workers based on repairs and installations, remuneration. BackOffice workers for their work, to quantify all work and results in the hands of management. As a result, it is not only the achievement of data availability but also the method and thus the processes that obtain and handle the data. Finally, foreign surveys demonstrate this information system symbiosis with processes, which show that the introduction of ERP systems has brought not only cost reductions and quality improvements, but also a space for decision-making in decision-making and customer-driven decision-making. also improve processes throughout the enterprise.

Many IT projects in the past and present in businesses are unsuccessful. The projects do not meet their objectives and do not bring the expected benefits of their introduction. IT support for business processes is so often sceptical. Solutions that were originally intended to bring productivity gains, time savings, cost reductions are often out of control and ultimately do not meet customer expectations. It is no exception if the situation becomes even worse after the introduction of the information system.

Summary of IT Problems by:

- the benefits of introducing new technologies from the IT sphere are not being met;
- implemented systems are not being used properly, failing their possible benefits to the organization;
- many projects are closed or cancelled due to budget or time frame overrun;
- users reject changes in information technology;
- there is a misunderstanding between the needs of business and IT.

One of the key issues encountered in introducing a methodology to measure the benefits of deploying an ERP system or other major change affecting an enterprise is to use an appropriate methodology to evaluate these benefits. As the comprehensive deployment of the new ERP will generally affect all of the company's departments with the desire to cover and optimize key in-house processes, it is appropriate to address a methodology that can quantify the benefits and improvements from a corporate perspective. According to, the metric is a system of parameters or pathways for the quantitative and periodic evaluation of processes that will be measured. Metrics are typically specialized by area of application and cannot be mechanically transferred to other applications.

ERP systems provide efficient business process management at a low cost. They are a solid foundation on which to build and operate new types of enterprise software applications that can provide strategic benefits in the competitive world of today. Only efficiently executed processes are able to move the company to the competition, increase its competitiveness, flexibly respond to constantly changing customer requirements and strengthen the market position. Implementation of modern ERP systems is a means by which it is possible to cope with ever more demanding customer requirements, increase competition pressure, fast technological development and globalization of business.

Acknowledgments. The paper has been written as a partial outcome of the project KEGA No.015 STU-4/2018: “Specialised laboratory suppoted by multimedia textbook for subject: “Production systems design and operation” for STU Bratislava.

9th International Scientific Conference
Research and Development of Mechanical Elements and Systems
Kragujevac, Serbia, September 5-7 2019

RESEARCH AND DEVELOPMENT THAT IS ''LEAVING NO ONE BEHIND'' – THE ROLE OF SCIENCE, TECHNOLOGY, AND INNOVATION IN FULFILLING THE 2030 AGENDA

Danilo Arsenijevic[1]

[1]Cabinet of Minister Without Portfolio Responsible for Demography and Population Policy, Bul. Mihajla Pupina 2a, Belgrade, Serbia, danilo.arsenijevic@mdpp.gov.rs

Key words: Agenda 2030, sustainable development goals, SDGs, research, development.

Leaving no one behind is a motto underpinning the most comprehensive Sustainable Development Agenda adopted by the UN Member States in September 2015. Starting from 1 January 2019, the Governments have agreed to collaborate with all relevant stakeholders in a joint effort to fulfil the commitments enveloped in 17 Sustainable Development Goals (SDGs), 169 targets, and over 230 indicators. Titled "Transforming our World," the Agenda 2030 aims to eradicate extreme poverty in all of its forms, achieve gender equality and reduce inequalities, ensure good health and well-being, and tackle climate change addressing the needs of those most vulnerable who face the risk of being left behind within the next 11 years. The universal, integrative, and transformative SDGs have inherited the Millennium Development Goals broadening both the scope and the body of stakeholders responsible for their implementation with regard to all three pillars of sustainable development: social, economic, and environmental. The overall aim is to foster the creation of an enabling environment that would allow the development of full personal and professional potential of all and everywhere. However, achieving all of the 17 SDGs requires collective and collaborative participation of all. Science, technology, and innovation play one of the pivotal means of implementation of the 2030 Agenda, and open possibilities for its accelerated implementation. This paper aims to review the role of research and development in engineering as an enabling factor for reaching all 17 SDGs, with a special focus on SDG 9: Industry, Innovation, and Infrastructure, and SDG 13: Climate Action.
Industry, Innovation, and Infrastructure have the potential to drive the transition from the current stagnant unsustainable living habits and patterns towards lasting sustainability. SDG 9 verbalizes the need for incorporating innovation in promoting the more effective use of both natural and financial resources through empowering people and bridging the historical gaps. Research and development in engineering aimed at improving health and well-being, transport, irrigation, access to clean and affordable energy, and connectivity, as well as other areas of human activity necessary to reach sustainability are key to ensuring increased

productivity, income and the improvement of the overall quality of living and environment. Industries based on the concept of inclusiveness and sustainability can contribute to creating lasting prosperity for all without compromising the environment and development opportunities for future generations. This type of industrialization is based both on technology and innovations, and embraces research and development. Research and development in engineering framed within the Agenda 2030 commitments can accelerate its implementation through helping businesses switch to sustainable consumption and production patterns as stated in the SDG 12. Whether these innovations would include programming robots to interact with the environment without human assistance using various situation assessments, or creating more effective and affordable clean energy sources, engineering innovations should aim at decreasing the humanmade carbon footprint released by the industry. Carbon neutral circular economy is needed to combat climate change and mitigate its consequences as defined in SDG 13 that stands as one of the greatest challenges of modern times.

Research and development in engineering can help facilitate the change in the lifestyle and manufacturing through innovative, creative, and attractive clean alternatives to the existing unsustainable technologies. They can also help build resilient societies thus mitigating the effects of the extreme weather events, rising sea levels, and other challenges fuelled by the increase of the temperature on the global level. The UN Member States have recognized the hazards arising from the changing climate in the Paris agreement that came to effect starting November 2016. To limit the rise of the global temperature to a maximum of 1.5 degrees Celsius, the Governments could benefit greatly from the development of clean consumer-friendly alternatives to carbon-emitting products in transport and other industries. Engineers can use the Paris agreement to help steer their ideas because this document includes a roadmap for climate action that can reduce carbon emissions and build climate resilience of cities and communities. The need for such an approach is backed by the observed weekly climate changes that follow the artificial human seven-days-working cycle that could not be otherwise linked to natural cycles in any way. It is essential to keep developing more efficient and affordable modes of transport, and energy sources that could lower the negative effects of human activities in the cities thus contributing to reaching the targets underlined by the SDG 11: “Make cities and human settlements inclusive, safe, resilient and sustainable”.

The role of research and development in engineering is to help create an enabling environment for accomplishing all 17 SDGs, thus influencing the change of the way people think encouraging close consideration of the impact that the current human action have on the generations that are yet to come. Research and development are an integral part of the SDG 9 that reiterated the need for switching to sustainable industries and creating the infrastructure resilient to climate change. Engineers now have the possibility to affiliate their efforts to develop clean technologies to achieving SDGs, which could help them access Agenda 2030 funding opportunities that exist around the globe.

9th International Scientific Conference
Research and Development of Mechanical Elements and Systems
Kragujevac, Serbia, September 5-7 2019

TOOLS OF ORGANIZATIONAL-ECONOMIC MECHANISM OF INTERNAL CONTROL FUNCTIONING

Margarita Aristarchova[1], Vadim Fakhrutdinov[1]

[1]Ufa state aviation technical University, Institute of economy and management, department of taxes and taxation, K. Marx St., 12, 450008, Ufa, Republic of Bashkortostan, Russia

Key words: internal control, organizational-economic mechanism, concept.

The need to develop a concept is due to the resolution of a complex practical problem: to ensure the comprehensiveness of internal control (internal control system), i.e. its distribution and coverage of all the activities of the enterprise, including all levels of management, types of activities, risks, as well as the participation in the process of its implementation of each employee regardless of their position within the framework of vested powers.

The structure of the conceptual approach to organizing the organizational and economic mechanism for the functioning of internal control is presented in Figure 1 and includes the following steps:

1. Determining the goals of the organizational and economic mechanism for the functioning of internal control.
2. The formation of the ideology of the philosophy of the organizational and economic mechanism for the functioning of internal control, containing basic values, justification of the interdependence of all subsystems of the enterprise with the mechanism of functioning of internal control, the basic laws of its organization, the requirements for the organization of structural components of the internal control system.
3. Development of tools for the organizational and economic mechanism for the functioning of internal control, which includes: principles, functions, logic, time aspect, controlling, norms.
4. Creating an adaptive organizational structure of the organizational and economic mechanism for the functioning of internal control through the implementation of the developed tools.
5. Building a model of the functioning of the structural unit responsible for the organization of internal control.

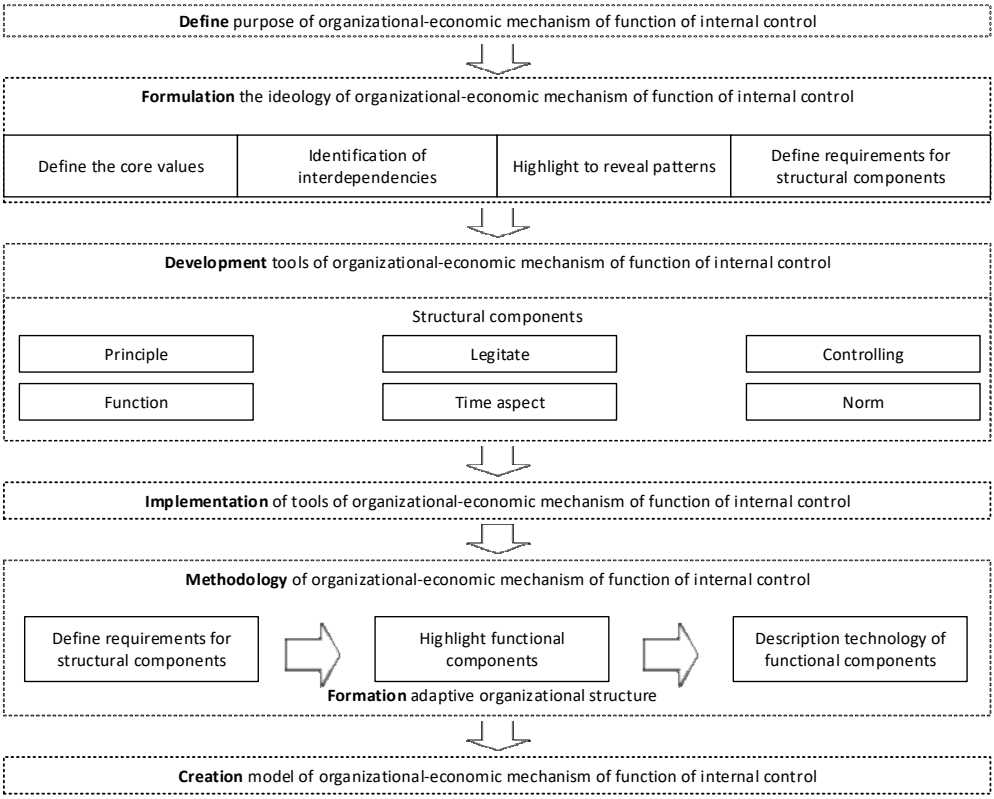

Figure 1. Concept of organizational-economic mechanism of function of internal control.

The presented tools (principle, function, legitimate, time aspect, controlling, norm) are in close interconnection and represent an integrated system, the application of which is determined by the developed methodology for the functioning of internal control, within which three stages of the formation of an adaptive organizational structure have been identified:

- at the first stage, the structural components of internal control are determined;
- at the second stage, the functional components of internal control are highlighted;
- at the third stage, working technologies of each functional component of internal control are developed.

The composition and characteristics of the structural components of internal control, the type of its organizational structure, the forms of organization of internal control will be individual for each enterprise, since all of the above should be consistent with the general organizational structure, and in addition, take into account the wishes of customers and legal requirements.

9th International Scientific Conference
Research and Development of Mechanical Elements and Systems
Kragujevac, Serbia, September 5-7 2019

COST-EFFECTIVE DESIGN OF THE MACHINE PRODUCTS FROM THE ASPECT OF THERMICAL AND THERMO-CHEMICAL TREATMENT

Svetislav Lj. Marković[1], Aleksandar Marinković[2], Bratislav Stojiljković[3], Dragoljub Veličković[4]

[1] Technical College, Čačak, Serbia
[2] Faculty of Mechanical Engineering, Belgrade, Serbia
[3] Nikola Tesla Museum, Belgrade, Serbia
[4] JP EPS, RB Kolubara, Lazarevac, Serbia

Key words: thermical treatment, thermo-chemical treatment, machine products

The responsible machine parts are mostly made from metal, foremost from quality steel. In order to strenghten their mechanical features (firmness, hardness), with these parts chemical and thermo-chemical treatment is usually applied. The development od such machine parts should be adapted to the process of successful thermal and thermo-chemical treatment. The character and the intensity of anomalies made in the process of thermal treatment (high internal pressure, exposed deformity and cracks) depend on the type of thermal or thermo-chemical treatment, type of the metal, as well as the defining the shape of the parts itself. The metal parts put into the treatment should be given such shapes as not to reach the anomalies. This is made by easing the concentration of the pressure in the critical areas, evening the parts of the product and its sections.

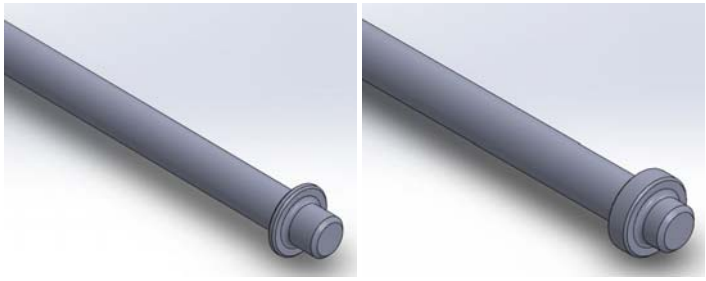

Figure 1. The expansion of the connector in order to avoid the appearance of the crack: left – wrong shape, right – right shape

The enormous difference in measures of certain intersections od parts (the difference lies in their mass) in the process of tempering causes big pressures which lead to distortion and the

forming of cracks. It is therefore necessary to constructively reduce the differences in the thickness of the walls in different intersections (*Figure 1*) [3].

In the process of changing the intersections, sudden crossovers from the flat to thick intersections should be avoided. In the product presented *in Figure 2 – left*, in the process of tempering the chacking is formed due to the sharp angles and not steady intersections. In case of not being possible to provide the construction with gradual transition from flat to thick intersections, and thus provide the substitute, *Figure 2 – in the middle*, then the construction provided in *Figure 2 – right,* should be applied.

Figure 2. The reduction of the resistance to the cracking appearance in the process of tempering: left – wrong, middle and right – right

The dislodgement of the openings on the parts to be tempered should be such that the distance between the centres of the closest openings is no less than the two diameters of the opening.In the process of partial cementry it is possible to provide different arrangement and the relation of the cemented zones. Still, the introduction of the additional protection from the cementry on certain places can lead to raising the price of the production. Because of that, whenever posiible, the cementry of the whole product should be done. [5] The process of firming the surface of high lenght through chemically-thermal procedure leads to the deformity of machine part. In some cases, it is necessary to predict the partial tempering that reduces the deformities, because the existence of soft zones enables the correction of the thermally treated part.

Machine parts that are being firmed through the process of thermal treatment should have such shapes to avoid the appearance of high pressurings, deformations and to avoing the appearance of chackings in the material. It is gained by softening the pressuring concentrations in the critical areas that are thermally or both thermally and chemically treated using different construction measures, including balancing the intersections, reducing the assymetry of the parts, avoiding the sudden transitions from flat to thick intersections and the difference in measurings of certain intersections of the machine part etc.

Acknowledgments. This work has been performed within the project TR 35011. This project is supported by the Republic of Serbia, Ministry of Science and Technological Development, which financial help is gratefully acknowledged.

IRMES KRAGUJEVAC 2019

9th International Scientific Conference
Research and Development of Mechanical Elements and Systems
Kragujevac, Serbia, September 5-7 2019

INNOVATIVENESS OF ENTERPRISES IN KNOWLEDGE ECONOMY

Vanja Vukojevic[1]

[1]University of Nais, Innovation Centre, Univerzitetski trg 2,
18000 Nais, Serbia, vanja.d.vukojevic@gmail.com

Key words: innovation, innovativeness, enterprise, knowledge economy.

After the industrial era has finished, new age in economy begin. Knowledge economy represents new paradigm that is characterized by dynamics and uncertainty. “New situation is best described as 'imperative of change' or, so called, warning, 'innovate, computerize or leave the scene” (Djuricin, Janosevic, 2006). In the knowledge economy, competitive advantage of enterprise is established on their knowledge; knowledge represents key resource which, partially, replaces land, work and physical resources (Krstic, 2009). Contemporary business conditions are characterized by dynamics, uncertainty and continual change. Enterprises in knowledge economy are focused on innovation and flexibility of business. Use of technology has become essential for all the companies wanting to be leaders in their business area. In knowledge economy, innovativeness of enterprises is one of the core preconditions for keeping competitive advantage and *conditio sine qua non* for survival at market competition.

Concept of innovation is in the focus of many authors since the beginning of 20th century, when Schumpeter talked about innovations. Based on his definitions, many others have been made. According to OECD, innovation represents implementation of new or significantly improved product (or service), new marketing method or new organizational method in business practice. Peter Drucker, in his work Innovation and entrepreneurship, emphasizes that innovations are specific instrument of entrepreneurs, which enriches resources with a new capacity to create wealth. He accentuates that innovations are meaningful and systematic search for a change, and systematic analyzing of chances that those changes could get. (Drucker, 2006) Author Bledow by innovation means development and attentional introduction of new and useful ideas, conducted by individuals, teams and organizations. This author emphasizes attentional introduction, i.e. introduction with specific goal. Author West keeps strong difference between innovation and creativity, creativity is development of idea where as innovation is implementation of those ideas in practice, Innovation doesn’t necessarily need to be result of research and development, it

could be substitution of some material in existing product with the material of better quality, better way of selling or distribution of existing product (Stefanovic, 2015). So, innovation doesn't have to be same as invention.

This subject is chosen because of the significance of the innovations for enterprises nowadays. Innovativeness of enterprises in knowledge economy represents one of the key factors for keeping competitive advantage. When we talk about importance of innovation for competitive advantage, we do not look just radical innovation and development of completely new products, but also incremental improvements of business processes and operations that are being conducted daily. For maintaining competitive advantage, it is necessary to continually make innovations in business system, not just production program. Incremental innovation in marketing and organization will cumulatively contribute to better positioning of enterprise in future.

Main aim of this paper is to point out to importance of enterprise innovation, also, to show latest trends and to emphasize differences between activities of strong and weak innovators. Furthermore, this paper contains types of innovations that innovation leaders are focused to. Special emphasis is on the analysis of innovativeness of enterprises in 2018 and present trends in this area. Scientific aim of this work is to, using desk research, trough description and analysis, determine adequate techniques for improvement of innovation process in enterprises. As a primary data source in this research, Boston Consulting Group Annual report for 2018 is used. Also, this paper contains review of relevant literature in the area of innovation.

Results of this work are some of the following conclusions. Analyzing big data is the base for successful innovation process. Use of digital technologies is main difference between weak and strong innovators. Good communication with customers, partners and other stakeholders in every phase of this process is essential. Innovativeness of enterprise is necessity for keeping competitive advantage. It requires presence of certain preconditions such as adequate organizational structure and culture. Nowadays perception of concept of innovation emphasizes importance of daily, incremental improvements of all business operations, not only invention of new products and technologies.

Trends in innovation show that investment in digital technologies is recipe for enterprises to become innovation leaders. In contemporary business conditions, even enterprises in traditional industries are using benefits of digital technologies. This trend will continue in future, by development of artificial intelligence.

Acknowledgments. Project of Ministry of education, science and technological development, no. OI 179066 „Improvement of competitiveness of public and private sector by networking competence during process of integration of Serbia to European Union "

9th International Scientific Conference
Research and Development of Mechanical Elements and Systems
Kragujevac, Serbia, September 5-7 2019

DESIGN OF TESTING RIG FOR PARAMETERS MEASUREMENTSOF ELECTRIC MULTICOPTER PROPULSION SYSTEM

Boris Marković[1], Janko Jovanović[1]

[1] University of Montenegro, Faculty of Electrical Engineering,
Džordža Vašingtona bb, 81000 Podgorica, Montenegro

Key words: electric propulsion system, testing rig, RPAS, multicopter, BLDC motors.

In the last couple of years modern trends in development of new types of small aircraft for transport of cargo and/or people are based on electric powers and multicopter electric technology which proved its success in the field of small RPASs (Remote Pilot Aircraft System).The Multicopter RPAS's Propulsion System, MC-RPAS-PS, as one of main vital part of this type of aircrafts, provides the necessary power to driven propellers for vertical takeoff, hover, horizontal flight and vertical landing.In this moment, in global market it is not possible to find industry gradeMC-RPAS-PS, because market for this type of products is still in early stages.

In this work, our focus is on making testing rig that will be used to simplify the assembling of MC-RPAS-PS from reliable and low-cost components that are widespread in the commercial market. In this manner the final product will be comprehensively tested and optimized for heavy duty work and fine tuned to achieve maximal performance with minimum loss of energy. It is worth mentioning that all of this is needed due to the fact that this type of testing rig forbig MC-RPAS-PS is not commercial available, nor the comprehensive approach for acquiring and analysis of propulsion system parameters.

Figure *1.*Schematics of typical multicopter PRAS propulsion system (battery, RPM controller, ESC and BLDC motor with propeller).

In this paper, architecture of testing rig for performance testing, optimizing and fine tuning of heavy duty MS-RPAS-PS for aircraft with maximal takeoff weight, MTOW, up to 450kg is presented. It can measure all main parameters of MS-RPAS-PS: voltage of power supply, current of power supply,electric power on ESC (Electronic Speed Controller), generated thrust on propeller, rotational speed, temperature of BLDC motor, temperature of ESC motor. It must be noted that importance of temperature measurement and its impact on overall PS performance is essential for reliability of power electric components and BLDC motor's magnets and coils.

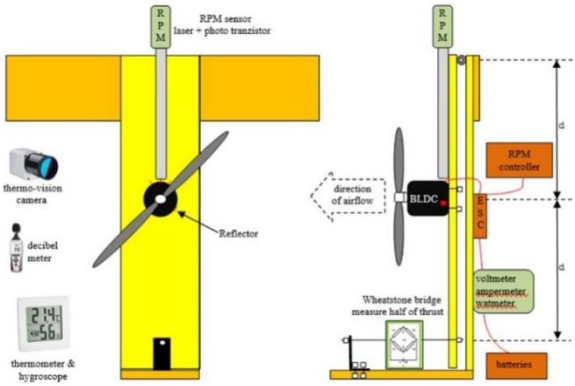

Figure 1. Front and side view of test*ing* rig.

Two MC-RPAS-PSs was tested:1) *BLDC* MP-120100 motor with 34x12, 38x10 and 35x15 propellers; and 2) BLDC T-Motor U15 with 40x13.1 propeller. Both of them were powered with lithium polymer 66.7V, 18Ah, 15C battery and 450A, 90V ESC.

Figure 3. Graph of thrust - electric power dependence for tested MC-RPAS-PSs

Developed testing rig enables easy testing, collecting all necessary data which is used for fine tuning and optimizing performance process of assembling of MC-RPAS-PS. The proposed testing rig was developed for testingPS of manned drone in Montenegro, eq. dodecacopter RPAS, multicopter with 12 propulsion systems, which can carry one passenger and additional cargo, with MTOW up to 400kg.

9th International Scientific Conference
Research and Development of Mechanical Elements and Systems
Kragujevac, Serbia, September 5-7 2019

QUALITY OF EMPLOYEE EDUCATION, TRAINING NEEDS IN SMALL AND MEDIUM ENTERPRISES IN THE SLOVAK REPUBLIC

Oľga Poniščiaková[1], Ivan Litvaj[2], Juraj Makarovič[2]

[1]Department of Economics, The Faculty of operation and economics of transport and communication, University of Žilina, Univerzitná 1, 010 26 Žilina, Slovakia
[2]Department of Power Electrical Systems and Electric Drives, The Faculty of electrical engineering and information technology, University of Žilina, Univerzitná 1, 010 26 Žilina, Slovakia

Key words: education, training, employee education, small and medium enterprises, survey, Slovakia.

Social systems are currently forced to operate in very demanding, variable, and turbulent conditions, characterized by increasing complexity and dynamic change. These changes are of a different nature. The democratic processes of our society were caused by changes in social and political conditions, while the scope of diapason of the changes affect whole society and all its social systems. The result is on the one hand, a number of stimulating impulses for the development of related economic, social, cultural conditions, but on the other hand, the increasing pressure on people operating in social systems towards the necessary adaptation to changing conditions and thus the revaluation of traditional values, value systems and value orientation.

The people, directly concerned, are continually contemplating ways and solutions to the effects of a certain synergistic effect of turbulence. Realizing that changes in traditional functioning affect both social systems and individuals, they strongly support the rise of the value of education and education itself. This process takes on a modified social function and becomes an integral part of social systems. From the traditional perception of education and development, social systems have shifted to the philosophy of lifelong learning and learning beyond the originally age and social groups.

This trend is not random, but it is based on some empirical experience. In particular, it supports the fact that the principle of lifelong learning leads, on the one hand, to the development of both the professional and the personal aspects of the individual. According to Charted Institute of Personnel and Development, the increased adaptability and employability of people are also beneficial [3]. On the other hand, education and training have a socially beneficial effect. It helps to improve economic competitiveness and employability and, according to the Memorandum on Lifelong Learning, it is the optimal way

to combat social exclusion as well as enhance the efficiency and sustainability of the organization.

The philosophy of lifelong learning in Slovakia began to be implemented on the basis of the Lifelong Learning Strategy and Lifelong Guidance in Slovakia. The original version was created in 2007 and has been applied over time at the level of secondary schools and universities, employers as well as by personnel agencies and interested public. The current state of implementation of the Strategy's objectives and the level of success of its implementation has brought empirical surveys into these areas, supplemented by information from interviews with experts from lifelong education field.

Specific objectives were also set within the objective of the empirical survey:

- to identify and analyze implementation of the Lifelong Learning (LLL) and Lifelong Consulting (LLC)in to the real life,
- to identify and analyze opinions and attitudes towards the LLL and LLC,
- to propose corrections and updates to fulfill the mission strategies in accordance with EU policies.

Recommendations in the area of education quality management system

Quality management system recommendations in formal and non-formal education aim at quality management through investment in quality and assessment of teachers and trainers. In terms of employment and readiness for labor market, the recommendations concern the acquisition of a skilled and flexible retraining lecturers through better education, better teacher appraisal, greater focus on skills and technical disciplines, equalization of formal and non-formal education, and, in particular, active school-employer cooperation. The interconnection of subsystems and the recognition of results could be optimized by increasing employers' confidence in certificates acquired through courses, but also by guaranteeing the quality of output of these training programs. Motivation to participate in further education could be unambiguously increased by financial motivations based on recommendations. Following the example of Ambition 2020 from the UK, individual training accounts could be introduced for those who are not educated at ISCED to complete it. Another option is to create vouchers, similar to Germany and Austria. Another option is to create funds by sector, to which employers contribute to education. It is also recommended to introduce grants, loan funds for vocational education and savings and education. In addition to proposals of a financial nature, it is recommended to increase the motivation to educate people with low education and the reasoning behind would be an increase of the financial value after successful completion of courses. It is also very important to increase the availability of training courses for low-income groups. Higher awareness through campaigns is important, by increasing the assurance of use and subsequently evaluating the acquired knowledge and skills, and the public awareness of the general premise to "educate". Answering a question about advisory services revealed a lack of functional advisory institutions and recommendations are aimed at developing advisory services in the choice of employment, and at introducing the position of so-called advisory services. Career advisor in all kinds of schools with formal education.

Acknowledgments. The paper was prepared with the framework of the support of the project KEGA 19-003-00 – Implementation of the Integrated GPS System for Specification and Verification of Products for Teaching Engineering Programs and Practice.

IRMES KRAGUJEVAC 2019

9th International Scientific Conference
Research and Development of Mechanical Elements and Systems
Kragujevac, Serbia, September 5-7 2019

MODEL OF «SHORT CYCLES» AS INNOVATIVE PRODUCT DEVELOPMENT

Elizaveta Gromova[1]

[1]Peter the Great St. Petersburg Polytechnic University, Politechnicheskaya st., 29, St. Petersburg, 195251, Russia, lizaveta-90@yandex.ru

Key words: list model of "short cycles", product development, time to market, innovation, Russian industry.

The fourth industrial revolution is a phenomenon that is actively becoming a reality and that initiates a change in the strategic guidelines of industrial enterprises. The previous strategic indicators such as scale of production, cost and quality have been replaced by a value system such as rapid response, flexibility, disruptive innovation and speed. Currently, great attention is paid to saving time in the course of production and sale of products. Previously, R. Suri proposed the concept of quick response manufacturing. The roots of the concept go to the strategy " time-based competition", which was proposed by G. Stalk and T. M. Hout. Also, many scientists consider agile manufacturing as a concept of production organization based on the foresight of changes in the business environment and timely response to the rapidly changing needs of the market through the effective use of internal and external resources. Today A. Borovkov rightly points out: «The key thesis is time to market. We are now witnessing the window of opportunity slamming in front of entire corporations and industries. The window existed for a year or two, during which time it was necessary to have time to enter the market. If this did not work out for some reason, you will have to wait for the next window». So, the purpose of the study is to offer a product development concept, which will be effective in terms of reducing the time of product market entry in the realities of the Russian industry.

The model of "short cycles" is based on the Deming cycle (PDCA), which is a model of continuous improvement. Each cycle of the development process is a mini-project and includes all the necessary range of operations: design, prototyping, testing, evaluation of results. This project is divided into the required number of "short cycles" depending on the identification of the most appropriate prototype (the standard procedure for product development often consists of one large cycle). It allows to visualize the scope of work and explain to the customer how the finished product will look. The duration of each cycle is from 1 to 4 weeks. The principal feature is the ability to influence each stage of the "short cycle" at any time (figure 1).

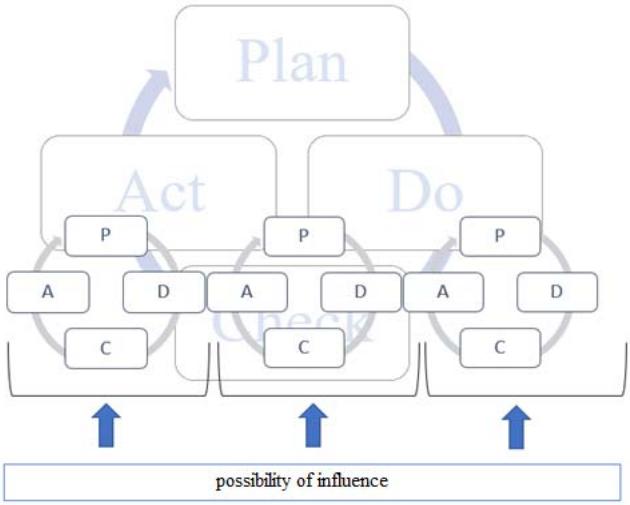

Figure 1. Visualization of the model of "short cycles" (developed by the author)

An interdisciplinary team in cooperation with the customer develops a prioritized list of tasks for the upcoming cycle. The basic rule is that if the team has agreed on a certain number of tasks that need to be performed in one cycle, then it is impossible to add new ones. Small groups of end users have the opportunity to get acquainted with the new prototype and provide feedback. At the end of each "short cycle", a stakeholder assessment will be conducted, which will result in a list of tasks for the next cycle, taking into account the adjustments received through feedback and based on the discussion of the results by the team.

Since the beginning of 2018, PJSC Severstal, as one of the world's leading steel and mining companies, has sold 85.5 tons of new complex products. The project "Product innovations" started in 2017. Product innovations brought $ 12 million in profits only in 2018. In 2019, product innovations are expected to yield about $ 20 million. During the period 2018-2023 Severstal plans to earn more than two billion dollars of additional income. Half will come from product, process and business model innovations.

A pilot project in the development of a new type of product was the development of a new, more durable plastic packaging tape for the production of flat products. Thanks to the model of «short cycles», at the beginning the experts selected the optimal chemical composition, which should satisfy the customers' requirements for the packing tape. Next new product was tested. After the customer and the cross-functional team have reached a final agreement, they will be engaged in the release of a new cold-rolled tape in flat-rolled products. The product creation period was 9 months, instead of 2-3 years, that is, acceleration of product launch to than 3 times. There were 28 short cycles. The product was distinguished by unique properties that gave reason to recognize this product as innovative. Another value is the increased demand among consumers. The pilot project was successful from the company’s management point of view.

The model of "short cycles" can be promising for enterprises of the industrial sector of the Russian economy.

INDICATORS OF TAX RELIABILITY OF INNOVATIVE ACTIVITY

M K Aristarkhova[1], O K Zueva[1], M S Zueva[1]

[1]Ufa state aviation technical University, Institute of economy and management, department of taxes and taxation, K. Marx St., 12, 450008 Ufa, Republic of Bashkortostan, Russian Federation, ninufa@mail.ru

Key words: management, taxes, innovation, indicators, activity

Now the concept – the corporate tax management (CTM) absolutely fairly takes root into practice. According to economic community CTM it is designed to form, optimize and redirect means of tax payments to the government budget.

Now, KNM in structure of business management is represented as the independent subsystem having specific characteristics. The set of the called characteristics can be presented four levels:

The I level – characteristic of corporate tax management; The II level – characteristic of the entered being tax categories (TC);

The III level – characteristic of the structural elements entered by the Tax Code;

The IV level – characteristic of the conditions of achievement entered by the Tax Code. The marked-out characteristics of CTM - tax stability and tax reliability are presented in figure 1.

It is obvious that each structural element can be presented by an independent indicator.

At the same time there is a need of quantitative assessment of these indicators that the corresponding technique which demonstrates interrelation of conditions, elements, components, characteristics on each of the allocated levels represents possible.

This work is offered to be carried out having involved the mechanism of expert estimates. Experts have to put down marks to each condition on a ten-mark scale where the greatest point (Bmax) will be got by optimum conditions for business, i.e.:

$$B_{max} = \sum^{m}_{i=1} 10N_i$$

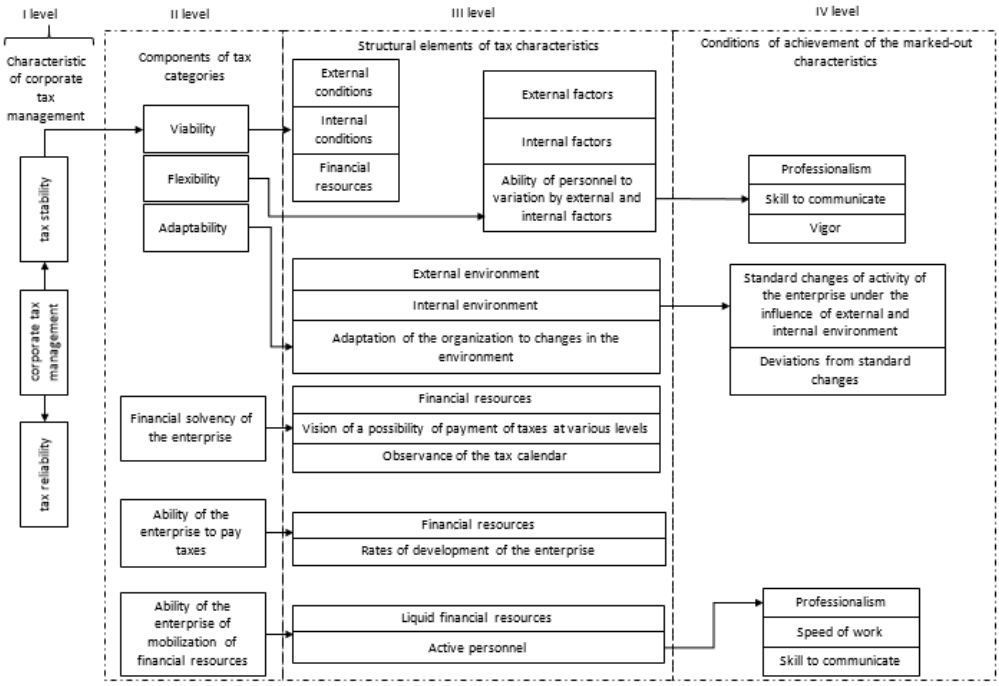

Figure 1. Structural elements of characteristics of corporate tax management

As a result, need and a possibility of introduction of new characteristics of corporate tax management of the enterprise - tax stability and tax reliability are proved and also specific features at each of the entered characteristics are distinguished.

IRMES KRAGUJEVAC 2019

9th International Scientific Conference
Research and Development of Mechanical Elements and Systems
Kragujevac, Serbia, September 5-7 2019

MODELING OF DURATION OF TIME OF DEVELOPMENT AND REALIZATION OF INNOVATIVE PRODUCTS

M K Aristarkhova[1], M S Zueva[1], D A Abzgildin[1]

[1]Ufa state aviation technical University, Institute of economy and management, department of taxes and taxation, K. Marx St., 12, 450008 Ufa, Republic of Bashkortostan, Russian Federation, ninufa@mail.ru, abzgildin-damir@mail.ru

Key words: innovation, modeling, development time duration.

The organization of introduction of innovations is complex therefore processes its accompanying and connected with direct development, creation, introduction of innovations has to be in details investigated. Extent of specification has to be sufficient for allocation of their certain type giving the chance to remove certain regularities. It will make one of prerequisites of implementation of uninterrupted operation of introduction of innovations and will predetermine need of modeling of process of adaptation of innovative solution to conditions of production. In this regard structural components of the period of adaptation – time for mastering skills of practical application of the developed idea and time for bringing to organic unity of the mastered technical tool with the system of its functioning are defined.

The innovative solution or the idea goes through consistently following stages: idea choice, designing, production, adaptation. According to told, duration the cycle of development and realization of the idea (Idea t) will be defined as follows:

T idea= T idea choice + T designing + T production + T adaptation

From all components of formula 1 the last has a certain novelty and this circumstance does necessary its detailed consideration. Usually, in structure of expenses of time such component is not allocated, considering that idea realization all work on its embodiment will be finished. However, with increase in complexity, expansion of dimensions of the developed ideas need of adaptation of the developed idea to conditions of its functioning and also acquaintance with it appears. Otherwise, suspensions of production for the solution of the called problems are possible. [3] According to told, adaptation time (T adaptation) is defined as follows:

T adaptation = T development+ T devices

So far it is possible to state two assumptions:

1. Time of development (Tdevelopment) represents function from the direction of the plan of introduction of an innovation (P), category of complexity of the performed works (C), qualifications of the worker (K)), the size of the production program (PP), etc.

Tdevelopment = f (P; C; K; PP …)

Time for bringing to organic unity of the materialized idea with the system of its functioning can be presented as function from the direction of the plan of introduction of an innovation (P), category of complexity of the performed works (C), qualifications of the worker (K)), etc. factors.

Tdevices = f (P; C; K …)

In relation to this task for creation of correlation and regression model it is necessary to consider several ideas developed by the organization and also to estimate influence of the allocated factors on duration of a cycle of development and realization of the idea. Are carried to number of the factors influencing duration of time of adaptation: direction of the plan of introduction of innovations (P); categories of complexity (C); qualification of the worker (K); size of the production program (PP).

The carried-out correlation and regression modeling allow to create the following model of time of adaptation:

T adaptation = 0.819859*P + 0.555695*C - 023641*K + 0.26084*PP + 0.6454

The correlation and regression analysis made on the stated idea showed that besides the presented criteria for the period of adaptation also other factors which are not presented in this model influence. In this connection, certainly, there are insignificant deviations of time of adaptation actual and time of adaptation planned.

Everything told confirms forecasting effectiveness of time of adaptation on a preparatory phase of production.

We consider that by means of the results received in this research the organizations will have an opportunity to organize continuous innovative development of the production. Though, certainly, they should face need of the solution of a number of the private practical tasks connected with need of accounting of their organizational and economic features too. All this, certainly, moves apart the horizons and opens a way to creativity.

IRMES KRAGUJEVAC 2019

9th International Scientific Conference
Research and Development of Mechanical Elements and Systems
Kragujevac, Serbia, September 5-7 2019

THE IMPORTANCE OF MEDICAL ENGINEERING IN THE IMPLEMENTATION OF THE 2030 AGENDA FOR SUSTAINABLE DEVELOPMENT

Tina Aničić [1]

[1] University of Belgrade, Faculty of Political Sciences, Jove Ilića 165, 11000 Belgrade, Serbia, tinaanicic@yahoo.com

Key words: mammography, non-communicable diseases, breast cancer, Agenda 2030, medical engineering.

Mechanical engineering has been driving the development of human civilization since the early times. From lever as a simple machine, through James Watts' first steam engine, Robert Fulton's first steamboat, George Stevenson's first steam locomotive, to modern computers, PET scanners, and digital mammography. Considering the importance of preventive medicine as an integral part of the Sustainable Development Goal 3, this paper will analyse the mechanical development of a mammograph, its role in the early detection of breast cancer, and the need for its continuous research and development in the light of achieving the goals of the 2030 Agenda for Sustainable Development.

When Wilhelm Conrad Roentgen discovered x-rays in 1895, it made great strides, among other things, in the field of radiology and breast health. A mammograph is a machine that uses x-rays to visualize breast tissue and detect changes in them. Changes that mammography can detect are often very small when patients still do not feel the symptoms that occur in the later advanced stages of the disease. In the last forty years, mammographs as machines have continued to improve, but the basic principle of their operation using x-rays has remained the same. The key innovation in the 21st century was the transition from analog to digital mammography. Although this novelty did not imply any major changes from a patients' perspective, it did allow the image to be created not through a chemical reaction on an X-ray film, but through the conversion of X-rays reaching the digital receptor into electrical impulses that are converted to an image on the monitor screen. Lower radiation dose, better image quality as well as post-processing of the image after exposure (light and contract) that almost eliminates the necessity for additional exposures of patients are just some of the benefits of digital mammography.

Although enthusiasm for the further improvement and advancement of mammography, as a radiological method, is always present among scientific and health care professionals, an additional impetus is created by obligations and agreements at the international level. One such global agreement was reached on September 2015, namely the United Nations Agenda for Sustainable Development by 2030, as a universal call to all states to act to ensure, among other things, healthy lives. Two of the 17 Sustainable Development Goals contained in Agenda 2030, are of specific relevance to the topic of this paper - goal 3 (particularly target 3.4) and goal 9 (particularly target 9.5). Goal 3 is to ensure healthy lives and promote well-being for all at all ages. Goal 9, on the other hand, envisages building resilient infrastructure, promoting inclusive and sustainable industrialization and fostering innovation, with target 9.5. which implies the advancement of scientific research, including, by 2030, encouraging innovation and substantially increasing the number of research and development workers per 1 million people and public and private research and development spending.

Recent mechanical advancements in medical engineering have allowed for a more effective disease diagnostics and treatment that help achieve the commitments of the 2030 Agenda. New generations mammographs can now detect diseases in early stages when treatment is most effective. These developments significantly contribute to achieving the target 3.4 “By 2030, reduce by one-third premature mortality from non-communicable diseases through prevention and treatment and promote mental health and well-being.“ Mechanical advancements of the new-age mammographs also reduce the cost of treatment thus helping countries achieve the SDG 8 (Decent Work and Economic Growth).

All of the above implies that 2030 Agenda is intended, first and foremost, to encourage states to work to reduce the incidence of non-communicable diseases, including breast cancer, as the most common malignancy in women in the world. This can be achieved by supplying hospitals with mammographs and by providing adequate staff for the analysis of mammograms, especially in the least developed and developing countries, and then inviting and motivating women to do mammography through an organized screening program. At the same time, Agenda 2030 commits countries to work on innovation and further development of new technologies. One of the latest examples of new technology, in the field of breast health, is digital breast tomosynthesis, which enables better visualization of breast tissue, better detection of diseases, and reducing the number of false-positive findings. Undoubtedly, in the years ahead we will witness the further development of new technologies in the field of mammography. These machines are a "powerful weapon" with the basic task of saving human lives, which will certainly not change in the future. On the contrary, what will probably change are new targets to further reduce the number of breast cancer patients and deaths in some new document, in some new Agenda. In conclusion, Agenda 2030 opens new possibilities for research and development funding for mechanical engineering advancements in the field of medical engineering.

9th International Scientific Conference
Research and Development of Mechanical Elements and Systems
Kragujevac, Serbia, September 5-7 2019

STUDY ACCURACY OF A TRANSPORTATION SYSTEM POSITIONING OF A TEST RIG FOR AUTOMATED MOUNTING OF LUSTER TERMINALS

R Dimitrova[1], V Zhmud[2], N Petrov[1], T Vakarelska[3]

[1] Technical University, Faculty of Mechanical Engineering, 8 Kl. Ohridski Blvd, 1000 Sofia, Bulgaria, rkd@tu-sofia.bg, khollegh@abv.bg
[2] Novosibirsk State Technical University, Novosibirsk, Russia, oao_nips@bk.ru
[3] Technical University, KEE, 8 Kl. Ohridski Blvd, 1000 Sofia, Bulgaria, vakarelska@tu-sofia.bg

Key words: accuracy, transportation system, automated mounting, luster terminals, WinPISA, experimental studies.

A test rig for study of parameters of a process of automated assembly of luster terminals is designed and developed. The aim of the developed test rig is to study the accuracy of positioning of the transport system during the automated assembly process of luster terminals. On the basis of data collected during the experiments, reliability analysis of the whole system has been made.

Subject to automation is a plastic luster terminal with twelve inputs/outputs and mounting holes. It consists of a body in which brass details are placed with threads, each having two screws. An automated assembly system test rig had been designed and manufactured. It has the following main modules (Fig 1 and Fig.2):

- Magazine - collectors (MC) for each of the three different elements, which are assembled into a final product "luster terminal" - a total of 10 pieces;
- A linear conveyor (LC), which moves the elements between the different positions;
- Interceptors for Element B and Element B (element A is cut off by MC by LC);
- Module for carrying out technological operation (TO) - assembling by threaded connection of 6 pcs. Elements B to 3 pcs. Elements B in position 4.

After the production and purchase of all the necessary items, a test rig for the automated assembly of luster terminals is assembled. For programming of the stand the used program is “WinPISA 4.51” by "Festo". The input and output parameters are responsible for the information sent and received by all pickups, sensors and pneumatic cylinders, connected in the test rig. By using this information and depending on the value of each parameter, the blocks in the prepared block diagram are executed one after the other. Each individual block requires a specific value of one or several parameters in order to send the program signal for a subsequent operation to the test rig and to move to a next block where again the program will require specific values from the input parameters.

After executing one program cycle, it starts again. Each pneumatic cylinder sends a signal of the position in which it is located and this signal is constantly checked by the program. The same applies to the sensors responsible for the presence of elements in the MC. The test rig enters pause mode in case there are no items available in any of the MCs.

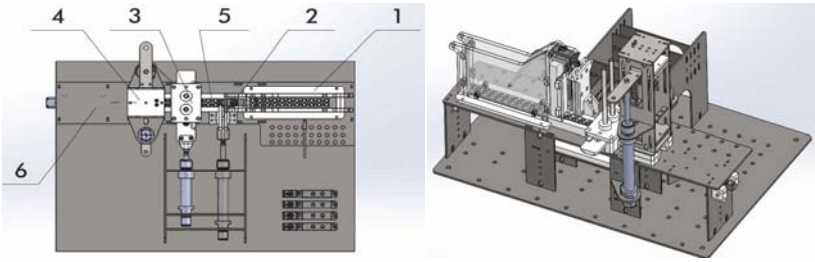

Figure 1. 3D model of a test rig of automated luster terminal mounting: 1 - MC; 2 - MC with interceptor; 3 - Two MCs with interceptor; 4 - Operating position for mounting screw-type element; 5 - Linear conveyor.

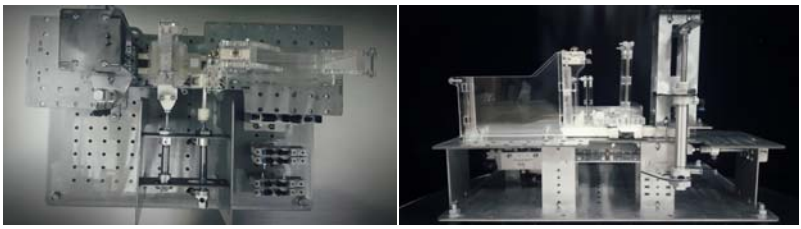

Figure 2. General view of the test-rig.

When performing a certain number of observations or measurements on the subject, the results are obtained x1,x2,…xq, which form an elementary statistical aggregate (elementary statistical order) of volume n. Observed or measured values are the final number of independent random variables that have the same distribution law as the random variable X. The values x1, are called variations, and their ranking in ascending order - ranging order. The resulting statistical set of values xi, (i = 1, 2,..., q) of the random value X together with the absolutes vi and relative frequencies fi form a statistical distribution law. The conversion count of X determines the absolute frequencies - vi, and their relationship to volume determines the relative frequencies fi. In that:

$$\sum_{i=1}^{q} v_i = n, \sum_{i=1}^{q} \frac{v_i}{n} = 1$$

For a continuous random quantity, the statistic is broken down into classes (groups, orders) that are usually of equal lengths of intervals. In this way, an interval statistical sequence is obtained with k - class. The length of the interval h = xi – xi-1 (i = 1, 2,..., k) is determined by the dependence:

$$h = \frac{x_{max} - x_{min}}{k} = \frac{\widehat{R}}{k}$$

9th International Scientific Conference
Research and Development of Mechanical Elements and Systems
Kragujevac, Serbia, September 5-7 2019

AUTOMATION OF CANTILEVER RACKING DESIGNING PROCESS

Rodoljub Vujanac[1], Nenad Miloradovic[1], Pavle Zivkovic[1], Luka Petrovic[1]

[1]University of Kragujevac, Faculty of Engineering, Sestre Janjić 6,
34000 Kragujevac, Serbia, vujanac@kg.ac.rs

Key words: cantilever racking, designing, automation, software.

Cantilever systems are load bearing structures intended for the storage and handling of long or irregular, heavy bodies such as bars, tubing, profiles, plates, wood panel. The main components of racking structure include vertical elements called columns and horizontal elements called cantilever arms and bases. To ensure cross-aisle stability, the base bars usually have the same length as the cantilever arms; in other words, a vertical line running down from the ends of the cantilever arms touches the ends of the base bars. The down-aisle stability of the rack is provided by the cross-bracing. Although components are standardized, they are only standard to each manufacturer. Cantilever racking can be used for internal or external storage. It is generally assumed that rack is serviced by powered handling equipment such as fork lift or side loading trucks and is not hand loaded. The design of the structure or its parts shall be carried out by one of the methods given in relevant standards, FEM codes and/or EN norms. FEM Code 10.2.09 - The Design of Cantilever Racking gives guidelines for the design requirements not covered in more general standard EN 1990 and EN 1993. Information technology and computer technique are present as a standard part of the design phase in modern engineering practice. This paper presents a methodology that enables the automatic generation of a three-dimensional model of cantilever racking using connection between CAD software Autodesk Inventor and spreadsheet software Microsoft Excel. Geometric parameters of the rack structure elements, calculated on the basis of the required input defined in the project assignment in Microsoft Excel as shown on figure 1 and developed automatic procedure of calculation according to standards, are used to generate the 3D model in the Autodesk Inventor environment. The aim of the automation of designing process is to allow easy generation of technical documentation and a complete techno - economic analysis of the developed construction. The ability to quickly, and at the same time easily obtains a number of different variants of complex construction, is another significant advantage of this method of design that make the work of the engineer far more competitive and better.

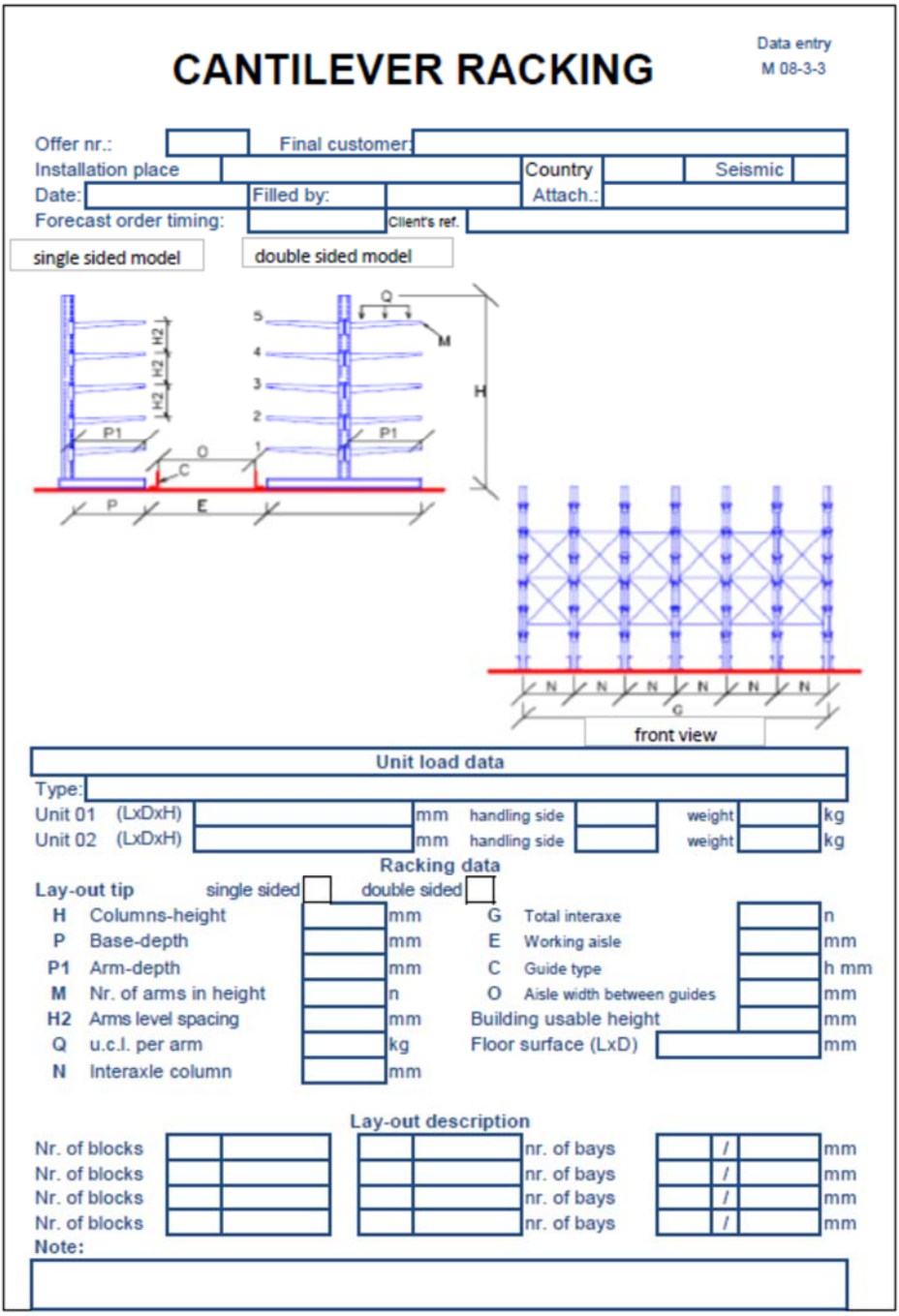

Figure 1. Technical data sheet for cantilever racking

Acknowledgments. This work was funded by the Ministry of Education and Science of the Republic of Serbia under the contract TR 32036.

NEW TECHNOLOGIES AND MATERIALS

CAD/ CAM/ CAE technology, intelligent production systems, robotics and mechatronics, rapid prototyping, new materials

IRMES KRAGUJEVAC 2019

9th International Scientific Conference
Research and Development of Mechanical Elements and Systems
Kragujevac, Serbia, September 5-7 2019

FATIGUE BEHAVIOUR OF FRICTION STIR WELDED AA-2024 ALUMINIUM ALLOY SHEETS

Tomaž Vuherer[1], Janez Kramberger[1], Dragan Milčić[2], Miodrag Milčić[2], Srečko Glodež[1]

[1]University of Maribor, Faculty of Mechanical Engineering, Smetanova 17, 2000 Maribor, Slovenia, tomaz.vuherer@um.si, janez.kramberger@um.si, srecko.glodez@um.si
[2]University of Niš, Faculty of Mechanical Engineering, Aleksandra Medvedeva 14, 18000 Niš, Serbia, milcic@masfak.ni.ac.rs, miodrag.milcic@gmail.com

Key words: Al-alloys; friction stir welding; fatigue; fracture mechanics; experiments.

The presented paper deals with the mechanical and fatigue properties of the alloyed aluminium alloy AA-2024 welded by the Friction Stir Welded (FSW) process. Using the optimized tool and welding procedure, 6 mm thick plates were welded with a constant tool rotation speed n = 750 rpm and three different welding speeds as presented in Table 1. After the welding process was completed, the visual control as well as the radiographic control of welded samples on the weld face and root of the seam were performed. No defects were detected (visually, touch or magnifier).

Table 1. Friction Stir Welding parameters

Sample designation	Rotation speed n [rpm]	Welding speed v [mm/min]	Ratio n/v [rev/mm]
A – I	750	73	10.27
B – II		116	6.47
C – III		150	5

Specimens for the further mechanical and fatigue testing were manufactured from FSW-samples. Tensile tests were carried out at room-temperature under strain rate of 3.3×10^{-3} s^{-1} according to the ASTM E8M standard. Two tensile specimens were tested for each welding regime (A-I, B-II and C-III) and average values have then been considered when determining the mechanical properties of FSW-joints. Fatigue tests were carried out on a servo-hydraulic fatigue testing machine (Shimadzu Servopulser E100kN, Shimadzu Co.) at room-temperature under the stress ratio R=0.1 and loading frequency of 35 Hz. For each welding regime, the fatigue tests have been performed at different stress levels.

Table 2 shows the mechanical properties of welded joints for different welding regimes (A-I, B-II and C-III). It is evident, that the best mechanical properties correspond to the welding regime B-II with the middle welding speed v = 116 mm/min. This welded joint also shows a relative good ductility with elongation at breakage about 7.43 %. On the other hand, a very brittle behaviour (small difference between R_m and $R_{p0.2}$ and extremely short elongation at breakage) under quasy static loading can be observed for welding regime C-III, where the welding speed was the highest (v = 150 mm/min). For welding regime A-I with the lowest welding speed (v = 73 mm/min), the mechanical properties of welded joint can be found in the between of the properties for B-II and C-III.

Table 2. Mechanical properties of welded joints for different welding regimes

Sample designation	Yield strength $R_{p0.2}$ [MPa]	UTS R_m [MPa]	Elongation A_5 [%]
A – I	281.9	371.0	2.29
B – II	330.9	469.1	7.43
C – III	337.6	352.0	0.33

Figure 1 shows the S-N curves for different welding regimes. It is evident, that the highest fatigue strength corresponds to the welding regime B-II (v = 116 mm/min). For this case, the fatigue limit at 10^7 loading cycles is approximately 68 MPa. The S-N curve for welding regime C-III (the highest welding speed) shows a relative high fatigue strength in the area $N < 10^5$. On the other hand, the fatigue strength is for the welding regime C-III significantly decreasing with increase of N. The latter can be explained on the assumption that the hard and brittle material is very sensitive to the high cycle fatigue regime.

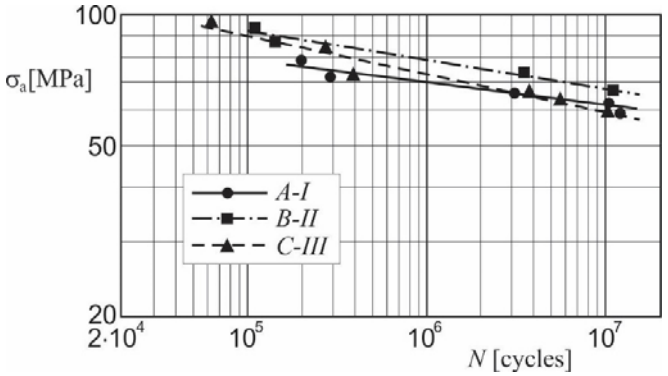

Figure 1. S-N curves for different welding regimes

For future work the influence of the residual stresses on fatigue life of FSW-joint may be addressed. Namely, the higher heat input in the case of low welding speed could induces greater residual stresses which are in high cycle fatigue regime usually not relaxed.

Acknowledgments. The authors acknowledge the financial support from the Slovenian Research Agency (Bilateral cooperation No. BI-RS/14-15-029).

9th International Scientific Conference
Research and Development of Mechanical Elements and Systems
Kragujevac, Serbia, September 5-7 2019

INFLUENCE OF ORIENTATION TO FATIGUE BEHAVIOUR OF STEEL PARTS PRODUCED BY DMLS

Aleksandar Vranić[1], Snežana Ćirić Kostić[1], Nebojša Bogojević[1], Nusret Muharemović[2], Dario Croccolo[3], Giorgio Olmi[3]

[1]University of Kragujevac, Faculty of Mechanical and Civil Engineering in Kraljevo, Dositejeva 19, 36000 Kraljevo, Serbia, vranic.a@mfkv.kg.ac.rs, cirickostic.s@mfkv.kg.ac.rs, bogojevic.n@mfkv.kg.ac.rs
[2]Plamingo d.o.o., Branilaca grada, Gračanica 75320, Bosnia and Herzegovina, nusret.muharemovic@gmail.com
[3]Department of Industrial Engineering (DIN), University of Bologna, Viale del Risorgimento 2, 40136 Bologna, Italy, dario.croccolo@unibo.it, giorgio.olmi@unibo.it

Key words: additive manufacturing, direct metal laser sintering, rotational bending, fatigue strength, stainless steel, maraging steel, build orientation.

This paper presents the results of an ongoing experimental study of the influence of the building orientation on fatigue strength of maraging steel MS1 and stainless steel PH1 parts manufactured using Direct Metal Laser Sintering technology. The study is a part of an extensive research program, which is carried out within the framework of the Horizon 2020 project A_MADAM with the aim to improve understanding of the dynamic behaviour of additive manufacturing products [1]. Additive Manufacturing (AM) technologies represent a family of manufacturing technologies that, unlike more conventional subtractive and forming technologies, produce a product by addition of raw material.
Samples were produced by DMLS machine EOSINT M280 (EOS GmbH – Electro Optical Systems, Krailling-Munich /Germany/) in the "3D Impulse" laboratory of Faculty of Mechanical and Civil Engineering in Kraljevo /Serbia/. The EOSINT M280 machine is equipped with Ytterbium 200W laser. Three sets of samples were manufactured for each of the materials, with longitudinal axis having angles 0°, 45° and 90° with respect to the building plane. All the samples were post-processed by heat treatment, shot-peening and machined. The samples were tested according to the ISO 1143 standard [2].The hourglass shape of the samples with 6 mm diameter at the gauge and 10 mm diameter at the head was chosen as the smallest shape recommended by the standard. All the tests were performed under reverse bending load (stress ratio R=-1) at the frequency of 60 Hz for a life duration of 10 million cycles. The curves for finite life domain were calculated using ISO 12107 [3], and an

estimation of the fatigue limit was made by Dixon method [4]. Dixon method enables estimation of fatigue limit for a small set of samples (two to six).

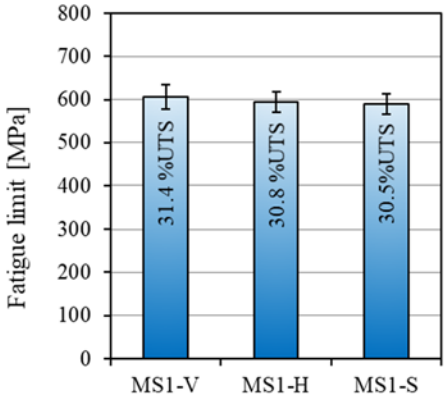

Figure 1. Comparison among the fatigue limits for MS1 maraging steel

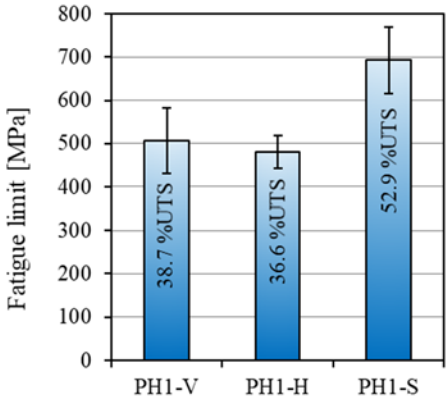

Figure 2. Comparison among the fatigue limits for PH1 stainless steel

Obtained results show that the building orientation has no significant influence on fatigue strength of MS1 maraging steel samples. Fatigue limit were estimated to be close to 30% of ultimate tensile strength for this material (Figure 1.). On the other side, the samples made from PH1 slanted samples have 20% higher fatigue strength in comparison to the horizontal and vertical samples (Figure 2).

The obtained results suggest that the part orientation during production of parts made from MS1 does not have influence on fatigue limits while, for parts produced from PH1 stainless steel may influence on the fatigue limits.

References

[1] "Advanced design rules for optimal dynamic properties of additive manufacturing products", Horizon 2020 project No.734455, www.a-madam.euS.

[2] International Organization for Standardization, ISO 1143:2010 Standard - Metallic materials – Rotating bar bending fatigue testing International Organization for Standardization (ISO) Geneva Switzerland (2010).

[3] International Organization for Standardization, ISO 12107:2003, Metallic Materials – Fatigue Testing – Statistical Planning and Analysis of Data International Organization for Standardization (ISO) Geneva Switzerland (2003).

[4] Dixon W J and Massey F J 1969 Introduction to statistical analysis (Vol. 344). New York: McGraw-Hill.

Acknowledgments. The research presented in this paper has received funding from the European Union's Horizon 2020 research and innovation programme under the Marie Skłodowska-Curie grant agreement No. 734455. Authors S. Ćirić-Kostić, N. Bogojević and A. Vranić wish also to acknowledge the support of Ministry of Education, Science and Technology Development of Republic of Serbia through grants No.TR35006 and No.TR37020.

9th International Scientific Conference
Research and Development of Mechanical Elements and Systems
Kragujevac, Serbia, September 5-7 2019

CAD MODELLING OF THE CLOSING HIGH TIBIAL OSTEOTHOMY

N F Cofaru[1], I I Cofaru[1], V Marjanović[2], N Marjanović[2], M Blagojević[2], R E Petruse[1]

[1]University "Lucian Blaga" of Sibiu, Department of Industrial Engineering and Management, Emil Cioran 4, Sibiu, Romania, nicolae.cofaru@ulbsibiu.ro
[2]University of Kragujevac, Faculty of Engineering, Sestre Janjić 6, 34000 Kragujevac, Serbia,

Key words: closing HTO, CAD modelling, axial deviations, 3D simulation of surgeries

The CAD modelling which we will achieve in our article is applied for simulation of the surgical procedures: Closing High Tibial Osteotomy.
A correct alignment of the bones of the human lower member is defined by collinearity of the line segments which unite the centre of the hip joint, the centre of the knee articulation and the centre of the ankle. Any swerve from this collinearity becomes an axial deviation.
The main cause of this deviation is unicompartimental ghonartrosis. The effect of this malady is the wear of the articular cartilage which leads to an incorrect loading of the knee and thus to the appearance of the deviations. One of the most common surgical procedure used to correct these axial deviations is the surgical technique called High Tibial Osteotomy.
Tibial osteotomy is a surgical technique that involves creating a bone wedge at the proximal tibia level to realign the bones of the lower limb. High tibial osteotomy can be of closing or of opening. Both surgical techniques have advantages and disadvantages.
Taking in account the fact that the closing wedge osteotomy has the important advantage of a more accurate correction with less morbidity, the 3D CAD parameterized modelling of this surgical technique was achieved in this paper.
For the knee affected by axial deviation, the mechanical axis of the leg does not cross the middle of the knee and it is closer to the medial zone of the knee, aspect which needs to be corrected. Generally, patients with ghonarthrosis have a predisposition to a new axial deviations. For this reason the goal of the closing high tibial osteotomy is to lead the mechanical axis of the leg not in the neutral position (50%) but in the point corresponding to the 62.5% of the tibial plateau width. The angle of the correction α is formed by the lines run from the point situated at the 62.5% of the tibial plateau width to the centre of the hip and centre from the ankle.
The establishment of the hinge point CORA is made close to the border of the tibia so that the angular rotation is realized. The first cutting plane is placed parallel to the tibial plateau,

2–2.5 cm below the articular joint line, taking in account the inclination of the tibial plateau. From the bone's lateral it is recommended to leave a distance of 5-10 (mm). The second cutting plane is a normal plane on frontal plane of the knee and makes the correction angle with the first cutting plane. CORA is a line situated at the intersection of the cutting planes.
The presentation of the geometrical elements mentioned above highlights a part of the geometrical parameters which are important for achieving the intervention. These are: the correction angle α, the placement of the hinge point or CORA. So that these parameters are easy to control a parameterized modelling was proposed in the article, with wide possibilities of customising the tibia closing osteotomy.

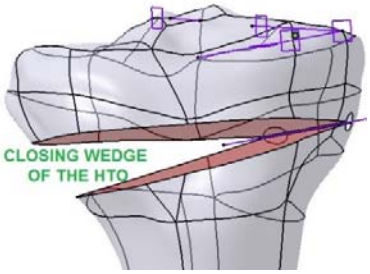

Figure 1. Achieving the closing wedge

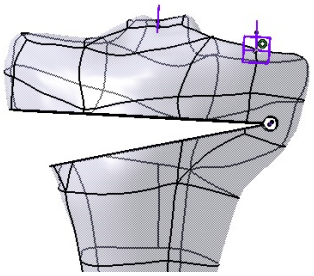

Figure 2. V1=8 mm, V2=14 degree

First steps in our CAD modelling is the creation of planes and lines which help us create and simulate the HTO surgery. These planes are: the sagittal plane of the tibia, the plane which highlight the posterior tilt with a 7° angle of the tibial plateau and another plane perpendicular on the last.
The next step is the execution of the relieving stress hole in the hinge (CORA). This step consists in making a hole which has a double role: eliminating the stress concentrators from the bottom of the osteotomy wedge and limiting the lateral cutting plan. For this a first sketch was made in order to determine the position of the CORA in accordance with the geometrical references presented in the above. The method of modelling that is presented appears complicated but it was created in order to offer a high degree of generality to the model.
The last step is the execution of the closing wedge. Correction angle could also be a variable parameter. In the figure 1 the tibia prepared for closing high tibial osteotomy is shown.
The 3D generalized model allows us to obtain a multitude of cutting possibilities only by modifying the presented parameters. In this case for closing high tibial osteotomy the most important parameters could be the position of CORA related to the tangential plane of the lateral cortical surface of the tibia V1(with values 8, 10 and 12 mm) and the correction angle V2 (with values 6, 10 and 14 degrees). In the figure 2 the simulation of closing high tibial osteotomy for V1=8 mm and V2=14 degree is shown.
The generalised CAD models developed in this article will be used in the further FEM researches in order to establish the best way to perform the surgical procedure CLOSING HIGH TIBIAL OSTEOTOMY.

Acknowledgments
This work is supported by the DiFiCIL project (contract no. 69/08.09.2016, ID P_37_771, web: http://dificil.grants.ulbsibiu.ro), co-funded by ERDF through the Competitiveness Operational Programme 2014-2020.

9th International Scientific Conference
Research and Development of Mechanical Elements and Systems
Kragujevac, Serbia, September 5-7 2019

MECHANICAL BEHAVIOUR OF SMALL LOAD BEARING STRUCTURES FABRICATED BY 3D PRINTING

N Palić[1], V Slavković[1], Ž Jovanović[1], F Živić[1], N Grujović[1]

[1]University of Kragujevac, Faculty of Engineering, Sestre Janjić 6,
34000 Kragujevac, Serbia, nikpa2112@gmail.com

Key words: three-point bending test, bearing structure, PLA, FDM, 3D printing, mechanical analyze.

3D printing enables fabrication of complex 3D structures, by depositing layer upon layer of the material, based on the virtual design of the structure. It belongs to the additive manufacturing (AM) technologies. Process involves adding material, such as liquid or powder layers. One of the main advantages of 3D printing is the ability to produce highly complex structures, from both aspects of design and used materials, based on the CAD model.
One of the mostly utilized polymer materials in FDM 3D printing is polylactic acid or polylactide (PLA). It is low cost material, based on plant starch, and as such is biocompatible. It is widely used in medicine, but also in industry as the replacement of the conventional polymers.
This paper presents the process of design and fabrication of small load bearing structures by FDM 3D printing and verification of its mechanical properties, by using PLA filament. The parameters of the sample print and the setting of the printers have been analysed. Three-point bending test was used to determine mechanical properties of the fabricated elements. Process parameters and results are analyzed.
Three-point bending test was realised at CT3 Texture Analyzer. The instrument has calibrated load cell with maximum load of 500 N with accuracy of 0.5 %.
Test parameters can be monitored in real time within in-built software: load influence on displacement over the test time. Test data are recorded in real time, according to the frequency sampling setup at the beginning of the test. Recorded data enables calculation of stress, strain and strain rate. The sample was tested by placing it on two roller bearings. Speed of the indent was 0.1 mm/s in both directions (in compression and withdrawal regimes) and the compression was stopped and indenter started to withdraw, when specified displacement is reached. Threshold displacement was 17.3 mm, as measured from the horizontal bottom line and the test was stopped when this deflection was reached.
After the bending test is finished, the sample tends to go back to its original shape after deflection, but some deformation stayed, thus showing that this test load resulted in

deformation beyond the elastic limit of the material. The final bending angle was 12°, after material relaxation..

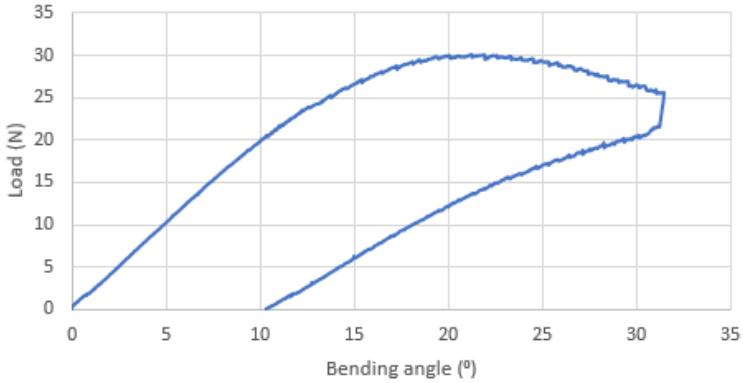

Figure 1. Changes of the bending angle as the function of the compressive load, during the three-point bending test

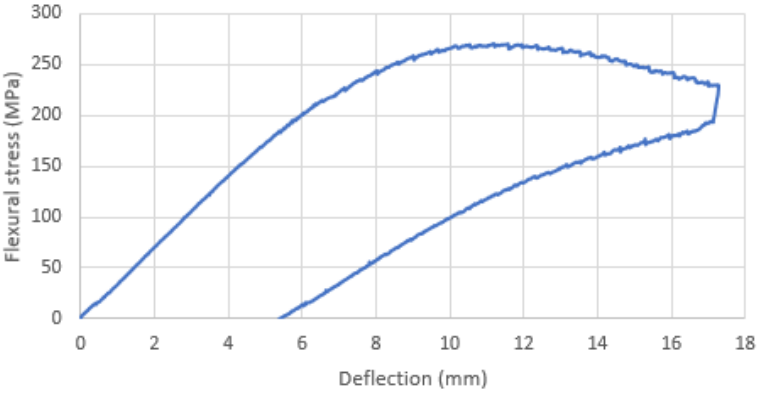

Figure 2. Flexural strength of PLA sample during three-point bending, as the function of the sample deflection

PLA beam was fabricated by 3D printing (FDM), with printing layer of 0.1 mm, and it showed satisfying mechanical properties, under three-point bend testing. Samples were printed with 100% infill and resulting flexural strength was 214 MPa. Elastic limit of the material was reached at around 24N, with bending angle at that point around 12.5°*(Fig. 1 and Fig. 2). The final bending angle of the sample beam was 12°, after material relaxation and finished testing. Experimental and numerical values of the final bending angle were compared and they were in accordance to each other. Infill density during 3D printing significantly influence the resulting mechanical properties and further work will include variation of this parameter to determine closer dependences and provide optimal 3D printing parameters from aspect of mechanical properties of the final object.

Acknowledgments. This work is supported by the national projects III41017, III41007, ON174028 and TR35021, financed by the Ministry of Education, Science and Technological Development of the Republic of Serbia.

9th International Scientific Conference
Research and Development of Mechanical Elements and Systems
Kragujevac, Serbia, September 5-7 2019

MODELING OF 3D TEMPERATURE FIELD IN BUTT WELDED JOINT OF 6060 ALLOY SHEETS USING THE ANSYS PROGRAM

Mateusz Matuszewski

Czestochowa University of Technology, Faculty of Mechanical Engineering and Computer Science, Armii Krajowej 21, 34-201 Częstochowa, Poland, matuszewski@itm.pcz.pl

Key words: aluminium alloy, ANSYS, modeling, temperature field, welding

In work, the modeling of a three-dimensional temperature field in a butt welded joints of two 6060 aluminum alloy sheets using Finite Element Method is presented. Welding tests of single pass butt welded joint of 6060 aluminum alloy sheets were carried out using two methods (in the argon shield): GTA (Gas Tungsten Arc) and GMA (Gas Metal Arc). The welding process involved the manufacture of a butt joint of two 6060 alloy sheets with dimensions of 200x60x5 mm by GMA welding and sheets with dimensions 244x110x4 mm by GTA welding.

In computation of temperature field, the Goldak's double ellipsoidal heat source model has been used. The thermal-mechanical properties of the material were assumed to depend on the temperature. The Workbench, DesignModeler, Mechanical, Fluent and CFD-Post modules of the ANSYS program were used for numerical simulations. The scheme of single-pass butt welding of aluminum alloy sheets is presented in Figure 1.

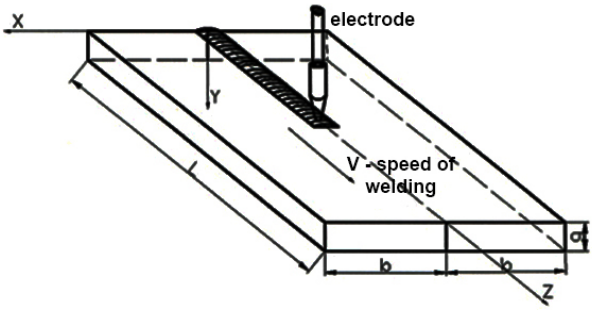

Figure 1. The scheme of single-pass butt welding process.

In the description of the geometry of joints, cube type elements were used, with density of grid in the heat affected zone. The parabolic shapes of face and root were assumed based on the literature and results of the experiment. The temperature distributions in cross-sections of welded joints as well as welding thermal cycles at selected points were analyzed. The results of numerical simulations were verified experimentally. The comparison of experimental and numerical simulations is presented in Figure 2 (for GTA method) and Figure 3 (for GMA method).

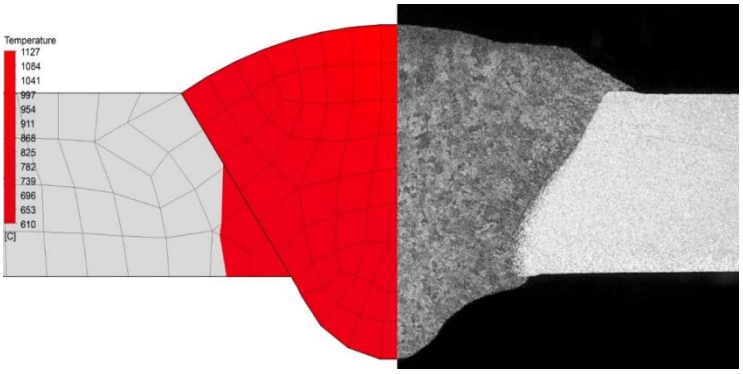

Figure 2. The comparison of calculated fusion zone (left) to the metallographic tests (right) for GTA welding (141) method.

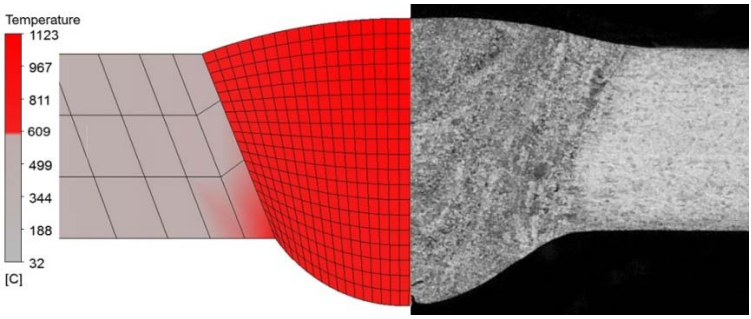

Figure 3. The comparison of calculated fusion zone (left) to the metallographic tests (right) for GMA welding (131) method

Comparison of calculated and obtained in the experiment the characteristic limits of heat affected zones showed satisfactory compatibility. The red color on the left shows the area in which we reached the temperature above the solidus where the material melts. The difference in dimensions obtained in the simulation with respect to experimental tests is below 5%

Numerical simulations of the temperature field in welding processes for sheets made of aluminum alloys allowed to determine the fusion zone of welded sheets in the mentioned welding processes.

The obtained results are the origin point for the calculation of strain and stress states in the welding processes considered in the article.

9th International Scientific Conference
Research and Development of Mechanical Elements and Systems
Kragujevac, Serbia, September 5-7 2019

POSSIBILITIES OF INTELLIGENT FLEXIBLE MANUFACTURING SYSTEMS

Peter Kostal[1], Andrea Mudrikova[1], Dávid Michal[1]

[1] Slovak University of Technology, Faculty of Material Science and Technology, J. Bottu 25, 91724 Trnava, Slovakia

Key words: intelligent manufacturing, control system, machining, intelligent manufacturing systems.

Industry automation continues. Today, it's not just about using classic automation tools, but about a flexible manufacturing system. We can now talk about a new generation of intelligent manufacturing systems.
This new manufacturing paradigm involves a high degree of production automation as well as all processes related to production.
This means that on the one hand (the hardware part) is a highly automated production system on which its various parameters relating to the production itself are constantly monitored, as well as those related to the system's own operation (for example oil temperature, bearing vibration and others).
On the other hand, the software section is an intelligent control system that can handle all of these data and make decisions based on both the production and the manufacturing system itself. (for example, schedule individual activities for regular maintenance, customize the production process to the current system status, and more).
These two parts together form an intelligent manufacturing system that can flexibly respond to and adapt to the current situation.
Machining process monitoring and control is a core concept on which to build up the new generation of flexible self-optimising intelligent NC machines. In-process measurement and processing of the information provided by dedicated sensors installed in the machine, enables autonomous decision making based on the on-line diagnosis of the correct machine, workpiece, tool and machining process condition, leading to an increased machine reliability towards zero defects, together with higher productivity and efficiency. This new generation of manufacturing systems is characterized by the use of a large number of different sensors that constantly gather information about the system itself and its surroundings. These sensors are located in individual production machines as well as in all production system accessories.

In 2013, Germany unveiled its Industry 4.0 strategy, which directed a great deal of global attention to the advances in manufacturing systems technology. In the United States, the government launched the Advanced Manufacturing Partnership (AMP) in 2011. Since then, many other initiatives have been rolled out, including the Advanced Manufacturing Partnership Steering Committee "2.0" in 2013; the National Network for Manufacturing Innovation (NNMI) in 2014; and the Revitalize American Manufacturing and Innovation Act, which was signed into law by the President of the United States in December 2014. Most recently, Manufacturing USA was officially launched by the US government in order to further "leverage existing resources... to nurture manufacturing innovation and accelerate commercialization" by fostering close collaboration between industry, academia, and government partners. In 2015, the Chinese government officially published a 10-year plan and roadmap toward manufacturing: Made in China 2025. The largest international collaborative program, Intelligent Manufacturing Systems (IMS), which is led by Japan, is also rolling out a roadmap for its next step with its IMS2020 project.

Intelligent capability refers to three functions, which operate in an analogy of a human body: sensing, decision-making, and action. With today's rapid advances in sensing and control technologies, there is no lack of sensors or actuators in manufacturing systems.

The challenge is how to process information and knowledge so that the right decision can automatically be made by a computer at the right time and in the right location, with little or no human intervention. New technologies are emerging in this areas, such as big data analytics, machine learning (ML), and cloud computing, which provide great potential for enhanced intelligent capability in manufacturing.

Intelligent manufacturing is a progressive building of integrated production management that connects all technological aspects (sensor use, process control, IT systems, production planning, ...) with the addition of intelligence through modelling, advanced management including cognitive automation concepts, diagnostic tools. Optimization, simulation, and expert knowledge are in harmony and interaction with human intelligence.

The concept of intelligent manufacturing remodels the ability of decision support systems to form generative systems that can acquire knowledge, learn, and adapt to changing environments and the actual composition of system components. A characteristic of smart production is the ability of the system to learn as well as the ability to obtain the information needed to manage an integrated production system.

Acknowledgment:

This paper was written thanks to the national KEGA Grant: 021STU-4/2018 - Development of a laboratory for the design and maintenance of production systems supported by the use of Virtual Reality

9th International Scientific Conference
Research and Development of Mechanical Elements and Systems
Kragujevac, Serbia, September 5-7 2019

WELDING METHOD AS INFLUENTIAL FACTOR OF MECHANICAL PROPERTIES AT HIGH-STRENGTH LOW-ALLOYED STEELS

Andreja Ilić[1], Lozica Ivanović[1], Vukić Lazić[1], Danica Josifović[1]

[1]University of Kragujevac, Faculty of Engineering, Sestre Janjić 6,
34000 Kragujevac, Serbia, E-mail: andreja.coka@gmail.com

Key words: high-strength low-alloyed steels, multipass welded joints, mechanical properties.

In this paper the analysis of welding technology to mechanical properties of welded joints at high strength low alloyed steel S690QL is presented. Experimental testing was done at models with V-groove butt joints that are done by MMA or MIG for root pass and MAG for other passes of multipass welded joints with related parameters and consumables. Yield and tensile strength, so as answer to load of models are determined experimentally in order to analyses the effect of welding technology to resulted mechanical properties. On the basis of the obtained results it can be concluded that welding parameters have significant influence to mechanical properties of welded joints at high-strength low-alloyed steel. Furthermore, it can be concluded that welded joints with root pass done by MIG and other passes by MAG provide better mechanical properties. Presented research point out that welding parameters at high strength low alloyed steels must be selected and controlled precisely to obtain welding joints with adequate mechanical properties. Welding, as dominant method of joining, is primary factor that provide beneficial application of high-strength low-alloyed steels. The paper highlight the influence of material degradation due to welding. This paper point out the importance of analyzing the welded joints at different levels of dimensions, while further, more detailed, research can be continued through development of a numerical model of the welded joints which will complete the experimentally obtained results. As experimentally obtained results correlate to material degradation due to welding it is implicated that future development of high-strength low-alloyed steels must be followed with development and modification of welding processes.

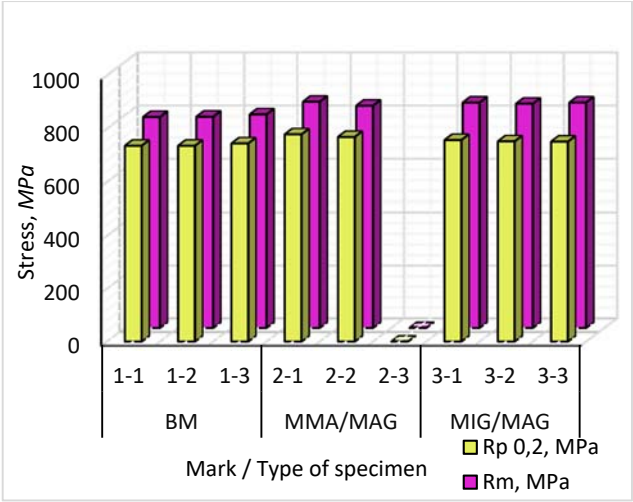

Figure 1. Histograms of yield and tensile strength of tested specimens.

Present norms and standards of welding joints design at high-strength low-alloy steels are based on heterogeneous backgrounds. Limitations are established during design process from different reasons in order to provide welded joint with adequate mechanical properties. Improving resistance of welding joints to forming of defect and inclusions are based on relaxing residual stresses, reducing hydrogen content and obtaining preferred thermal cycles. Zones of welded joints by nature as zones of conditional material discontinuity caused multiple stress concentrations. Redistributions of stresses have local characters. Stress concentrations at welded joints, usually caused increase of stresses, but it can also relax stress-strain state. Experimentally obtained results of mechanical properties showed that both considered MMA/MAG and MIG/MAG welding caused comparable stress concentration. Residual stresses at zones of welded joints are consequence of interaction of different phenomena caused by welding. The basic mechanisms that caused residual stresses at welded mechanical constructions are identified, but estimate of values and distribution is very complex. Mechanical answer to load and values of yield and tensile strength of tested specimens showed that level of residual stresses at considered welding processes are equal. Welding consumables for root pass done by MMA and MIG process with low strength and high plasticity provide relaxing of residual stresses. Solidification processes, mean processes of microstructural transformations under thermal cycles due to welding are most important factor that influent to final microstructure of material at zone of welded joints. Those factors are very similar for both of considered welded processes MMA/MAG and MIG/MAG. Those relations are in focus of research presented in this paper on qualitative level.

From the practical aspect, mechanical characteristics and properties of welded joints at this steel grade is crucial. Joining by welding at high-strength low-alloy steels is complex process with large number of influential factors. Producers of high-strength low-alloy steels due to importance and complexity of welding and sensitivity of those steels to welding also recommend welding processes and parameters.

9th International Scientific Conference
Research and Development of Mechanical Elements and Systems
Kragujevac, Serbia, September 5-7 2019

COMPUTED TORQUE CONTROL FOR A SPATIAL DISORIENTATION TRAINER

Jelena Vidakovic[1], Vladimir Kvrgic[2], Mihailo Lazarevic[3], Pavle Stepanic[1]

[1]Lola Institute, Kneza Viseslava 70a,
11030 Belgrade, Serbia, jelena.vidakovic@li.rs, pavle.stepanic@li.rs
[2]University of Belgrade, Institute Mihajlo Pupin, Volgina 15, 11060 Belgrade, Serbia,
vladimir.kvrgic@li.rs
[3]University of Belgrade, Faculty of Mechanical Engineering, Kraljice Marije 16,
11060 Belgrade, Serbia, mlazarevic@mas.bg.ac.rs

Key words: robot, motion control, computed torque, spatial disorientation

A development of a robot control system is a highly complex task, and many advanced control strategies have been used for the purpose of overcoming nonlinear dynamic coupling between the robot links and uncertainties in robot dynamics. Factors such as characteristics of the mechanical design, applications for which the robot is designed, applied actuators, and implementation requirements have great practical value to a choice of the potential control strategy. The spatial disorientation trainer (SDT), Fig. 1, is a modern combat aircraft pilot training system which examines a pilot's ability to recognize unusual flight orientations, to adapt to unusual positions and to persuade the pilot to believe in the aircraft instruments for orientation, and not in his own senses. This device is modeled as a 4DoF robot manipulator with revolute joints. Regarding a choice of a control strategy for the SDT, given that advanced robot control strategies often entail difficulties in implementation, prospective benefits of their application compared with traditional control approaches need to be analyzed using proper simulation techniques. Herein, computed torque (CT) control, a single joint feedforward control method that implies cancelation of nonlinear coupled terms in robot dynamic model, is considered for tracking of SDT's time-varying trajectories. The performance of the traditional PID controller is compared to CT compensation added to the feedback controller in Simulink. Model of the motor's mechanical subsystem takes into account inertia reflected on the rotor's shaft (effective inertia), calculated from the inverse dynamic model of the SDT for the programmed trajectory of the device. The structure of PI speed controller and limitation of its gains in the simulation model is performed to achieve the fastest response without overshoots and without exciting resonances of the mechanical structure for all possible values of effective inertia. Gains limitation of PI speed controller takes into account the lowest structural natural frequency of the SDT device calculated using CAE software, and saturation is applied at the outputs of controllers on the bases of

maximum torques that chosen motors can achieve. Within CT compensation, the error in load torque calculation from the dynamic model is assumed to be 5%. The reference speed values are given as a series of discrete values obtained from the trajectory planner.

Figure 1. SDT with 4DoF designed in Catia software

In Fig. 2a, trajectory tracking for axes k=1, 2.. 4 using two considered types of controllers are presented. Reference values are given in blue, the controlled process variables obtained by PI speed controller and by CT compensation added to PI speed controller are given in red and green, respectively, and the obtained errors are given in Fig. 2b in the same colors.

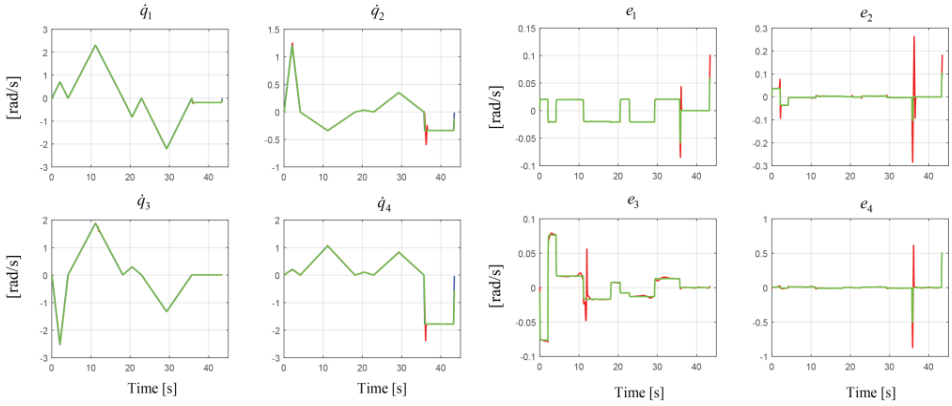

Figure 2. a) Reference and achieved speeds obtained using considered controllers in Simulink, b) Errors in speeds obtained using considered controllers in Simulink

The addition of the CT compensator to the PI speed feedback controller achieved considerable improvement in trajectory tracking in simulation example, for a typical SDT motion. The simulation results are significant regarding the choice of a control method for the SDT, but are also useful regarding the design of the mechanical structure of the manipulator, and consequently the appropriate choice of motors.

Acknowledgments. This research has been supported by a research grant of the Serbian Ministry of Education, Science and Technological Development under numbers TR 35023 and TR 35006.

9th International Scientific Conference
Research and Development of Mechanical Elements and Systems
Kragujevac, Serbia, September 5-7 2019

QUALITY CONTROL OF CLOSED-CELL METAL FOAM PRODUCED BY DIRECT FOAMING

András Gábora[1], Tamás Mankovits[2]

[1]University of Debrecen, Faculty of Engineering, Department of Mechanical Engineering, Ótemető utca 2-4, 4028 Debrecen, Hungary, andrasgabora@eng.unideb.hu, huri.david@eng.unideb.hu
[2]University of Debrecen, Faculty of Engineering, Department of Mechanical Engineering, Ótemető utca 2-4, 4028 Debrecen, Hungary, tamas.mankovits@eng.unideb.hu

Key words: closed-cell metal foam, direct foaming, quality control, statistical evaluation.

Metal foams are relatively new and advanced materials with high stiffness to weight ratio, good thermal conductivity, good acoustic insulation and excellent energy absorption capability which make them ideal materials for a variety of applications. Closed cell metal foams are produced by various methods, but the key step of their manufacture is the inclusion of air in the metal structure. The fact that gas pockets are present in their structure provides an obvious weight advantage and other favourable physical, mechanical, thermal, electrical and acoustic properties. Although metal foams are popular, they are still not sufficiently characterized thanks to their extremely complex structure which is highly stochastic in nature. In this research the influence of the technological parameters on the structure is analyzed. In laboratorial circumstances the production of closed cell aluminum foams depends on several factor. The purpose of the research is to analyze the human factor on the quality of the metal foam specimens.

In our experiments, for the raw material the F3S.20S (AA 359/SiC/20p) aluminum-based metal matrix composite with up to 20% silicon carbide (SiC) particles were used. The most useful features of Duralcan® composites are their high strength, stiffness, wear resistance, thermal conductivity, their improved elevated temperature tensile and fatigue strengths and their low density and coefficient of thermal expansion. The silicon carbide particles are sufficient for viscosity modification. The foaming agent was the titanium hydride.

For the quality of the metal foam specimen (e.g. structure, specimen size, compressive properties) the human factor has great effect. At all experiment the temperature when the TiH_2 is added was 750°C, while the percentage of the TiH_2 to the raw material was 1,5%. The mixing was made manually and human precision was also a factor in the adjustment of cutting cube specimens. After the foaming and cooling processes the samples were cut in

30x30x30 mm^3 cubes. All the investigations were done according to the ISO 13314. To provide information from the cell distribution digital quantitative image analyses were performed using macroscopic records from the specimen's surfaces.

Figure 1. Aluminum foam samples

Applying surface analysis from macroscopic images and the ImageJ software the area percentage of the cells and the number of the cells for all faces of the specimen can be calculated and determined. It can be stated that the above geometrical properties highly depend on the mixing and from where the specimens are cut from the produced sample. All of those have effect on the compressive properties of the aluminum foams.

The compression tests were performed on an INSTRON 8874 type universal testing machine at room temperature. The compression tests were carried out with the application of lubricant. The deformation rate was maintained in quasi-static condition at 8.7mm/min.

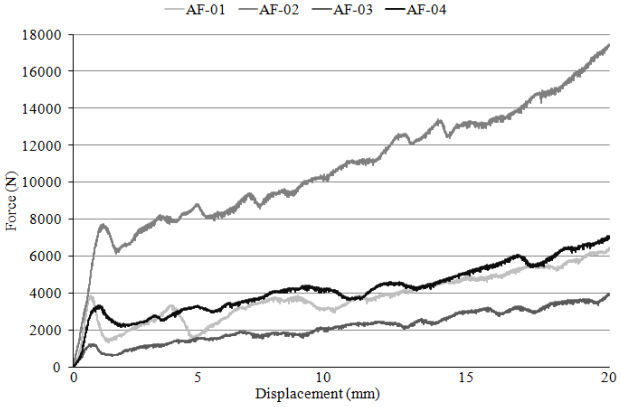

Figure 2. Force-dispalcement curves of the specimens

The force-displacement curves show great deviation thanks to the different geometrical and structural properties of the specimens. The deviation can be observed even in the elastic region of the force-displacement curve which is an essential part for application purposes. This deviation can be explained with the several manual manufacturing steps. The cellular structure of our specimens is not enough homogeneous, so for the future we are planning to change the technological process to more automated, using machines, particularly for the mixing process.

9th International Scientific Conference
Research and Development of Mechanical Elements and Systems
Kragujevac, Serbia, September 5-7 2019

DESIGNING AND OPTIMIZING EXTRACTORS FOR AUTOMATED DISPENSERS

Adrián Hajdučík[1], Lukáš Smetanka[1], Štefan Medvecký[1], Jozef Škrabala[1]

[1] University of Žilina, Faculty of Mechanical Engineering, Univerzitná 1, 010 26 Žilina, Slovakia, adrian.hajducik@fstroj.uniza.sk, lukas.smetanka@fstroj.uniza.sk, stefan.medvecky@fstroj.uniza.sk, jozef.skrabala@fstroj.uniza.sk

Key words: dispensers, extractor, optimization, automation

Currently, the process of manufacturing the goods and then distributing them to the customer is constantly optimized, accelerated and automated. For these aspects, goods handling, and automated storage play a key role. This article focuses on designing and optimizing the mechanisms that are parts of vending machines. As the proposed mechanisms are designed primarily for vending machines and pharmacies, specific requirements that are part of the environment need to be taken into account. Handling mechanisms are primarily intended for supplying and dispensing objects. When designing extractors, it is necessary to pay attention to the shape, weight and other associated operations. When designing the mechanism for supplying the dispenser and for dispensing objects from the dispenser, it was mainly based on the shape diversity of the medicines. For this purpose, we have communicated with pharmacists and worked closely with pharmacies, conducted a survey, and developed an extensive list of the most widely sold drugs. Pharmacies have been involved in the research to provide us with their data. It has also been shown that the marketing of drugs and, in particular, their species is different from the season. For these aspects, a consensus has been created that meets market requirements. Partial goal of data collection was also input conditions for solving problematic packaging forms of some types of drugs.

It has also been found that it is not possible to automate the sale of all kinds of drugs in the present automated device. According to the drug sales list, a formula has been created according to which the design of extractors has started. In general, drug vending machines can automate the sale of 80% of the drugs offered on the market. However, this number may increase over time as mechanical principles are constantly innovated, and drug manufacturers will also consider the shape and packaging of the drug. However, we expect that within a few years we will see more than 90-95% of all drugs automated. The following figures show conceptual designs of a feed extractors (Fig. 1) and a dispensing extractors (Fig. 2).

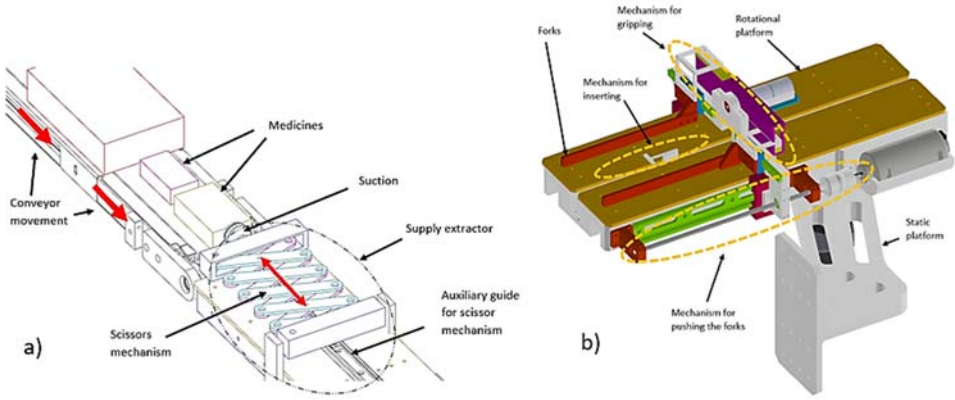

Figure 1. Design of feed extractors with suction and scissors mechanism (a), extractor with forks and slider (b)

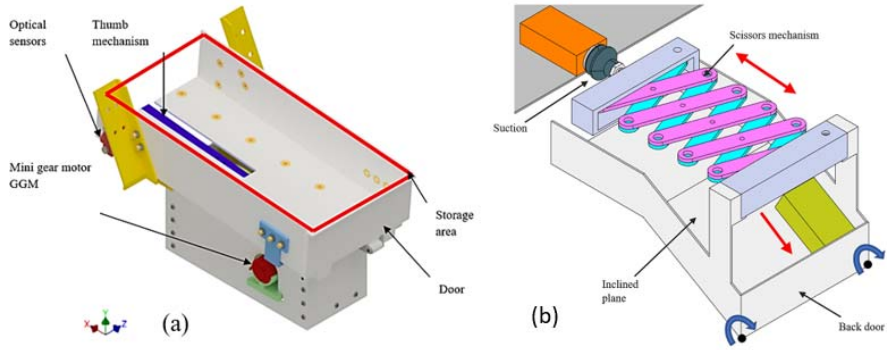

Figure 2. Design of dispensing extractors with "thumb mechanism" (a), suction cup and slip surface (b)

After analyses and calculations, prototypes were produced and tested in practice. We found out that currently the most suitable extractors are extractor with fork and slider for feeding the vending machines and extractor with "thumb mechanism" for dispensing the medicines from gravity shelves.

The article reflects the issue of medicine storage in automated devices. The results of a survey conducted in pharmacies have produced statistics on medicine storage options.

Acknowledgments. This publication is the result of the Project implementation: Competency Centre for Knowledge technologies applied in Innovation of Production Systems in Industry and Services, ITMS: 26220220155, supported by the Research & Development Operational Programme funded by the ERDF.

9th International Scientific Conference
Research and Development of Mechanical Elements and Systems
Kragujevac, Serbia, September 5-7 2019

EFFECT OF REINFORCEMENT ON MECHANICAL CHARACTERISTICS OF A356 ALLOY NANOCOMPOSITES

Sandra Veličković[1], Blaža Stojanović[1], Zorica Djordjević[1], Slavica Miladinović[1], Jasmina Blagojević[1,2]

[1]University of Kragujevac, Faculty of Engineering, Sestre Janjić 6, 34000 Kragujevac, Serbia, sandrav@kg.ac.rs, blaza@kg.ac.rs, zoricadj@kg.ac.rs, slavicam@kg.ac.rs
[2]Metalac a.d., Metalac Inko d.o.o., Kneza Aleksandra 212, 32300 Gornji Milanovac, Serbia, jacab@kg.ac.rs

Key words: A356 alloy, silicon carbide, nanocomposite, nanoindentation, elastic modulus, hardness.

In recent years great attention is paid to aluminum nanocomposites strengthened with particles due to application in the production of parts in the automotive and airplane industry. Metal matrix nanocomposites are a new class of materials that contain a nano-level reinforcement (1-100 nm), e.g. nanoparticles that are often used as an reinforcement in order to achieve superior mechanical characteristics. Based on mechanical characteristics such as hardness, elasticity, elongation, density, porosity and tensile strength, overall characteristics of the test materials are obtained.

The mechanical properties of the nanocomposite and the A356 alloy are tested by penetrating the surface of the test sample. The computer-assisted device for testing of the mechanical properties of the tested materials is Nanoindenter and Micro Scratch Tester. Technical specification of the used nanoindenter is: maximum load 500 mN, load resolution 0.04 µN, maximum depth 40 µm (optional 200 µm), depth resolution 0.04 nm and movement of measuring table XY, 150 x 80 mm. During these tests, Berkovich's three-sided diamond pyramid was used as an indenter. Experimental tests were carried out in the conditions shown in table 1. The chosen type of test is in the form of a matrix, and it is 3x3, which means tests were carried out in 9 points. With this device is possible to continuously measure normal load and movement of the indenter during the hardness testing.

During nanoindentation the following parameters were used: Normal load 50 mN, Maximum load holding time 5 s, Loading speed 100mN/min and unloading speed 100 mN/min.

As the results of nanoindentation a number of representative values can be obtained, in this paper the following will be shown: hardness (HV), elastic modulus (E) and value of maximum indentation depth (hmax). Also, based on the measurements carried out, in figure 1, the diagram of indentation is shown, which represents the dependence of the normal load of the indenter and the maximum depth of penetration.

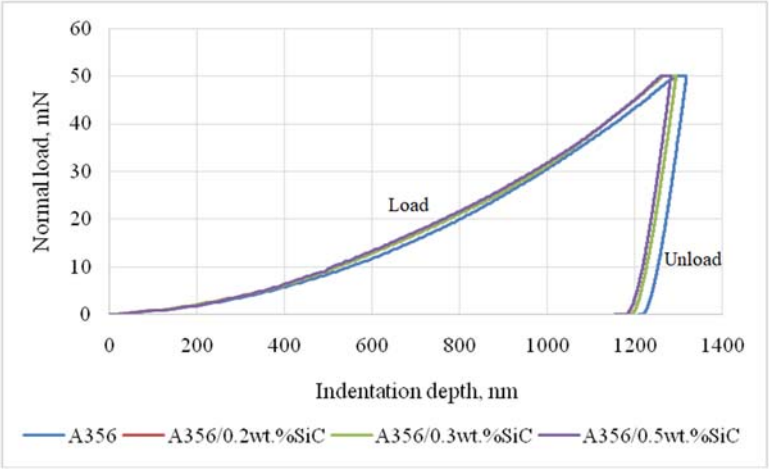

Figure 1. Nanoindentation curves for nanocomposites with SiC reinforcement and A356 alloy.

Based on the curves obtained by nanoindentation of samples of A356 alloys and nanocomposites with reinforcement content of 0.2, 0.3 and 0.5 wt.% SiC, it can be noticed that the obtained values of the hardness of the nanocomposite are higher compared to the base alloy.

Hardness tests were conducted with the aim of analyzing the effect of nanoparticles of silicon carbide as a reinforcement in the A356 base. Based on the obtained values of the hardness in surface layer of the nanocomposites, a noticeable increase in hardness was observed in comparison to the base alloy of the nanocomposite. Increasing the reinforcement content of 0.2, 0.3 and 0.5 wt.% increases the hardness of the nanocomposites ~131, 133 and 134 Vickers, respectively. Also, it can be concluded that the elasticity of the material decreases with the increase of reinforcement content. When comparing the hardness and elastic modulus of the tested nanocomposites there is a small deviation in the results, which is due to the small difference in reinforcement content in the nanocomposites.

However, it has to be noted that the extreme values obtained for eutectic silicon have not been taken into consideration and this requires additional research because it has an impact on the hardness values of the surface layers of the material.

Acknowledgments. This work was funded by the Ministry of Education and Science of the Republic of Serbia under the number TR-35021, Development of the tribological micro/nano two component and hybrid self lubricating composites.

9th International Scientific Conference
Research and Development of Mechanical Elements and Systems
Kragujevac, Serbia, September 5-7 2019

LASER CUTTING OF THE ZN COATED STEEL

Jozef Meško[1], Ružica R. Nikolić[2], Branislav Hadzima[2]

[1]University of Žilina, Faculty of Mechanical Engineering, Univerzitna 1, 010 26 Žilina, Slovakia, Jozef.Mesko@fstroj.uniza.sk
[2]University of Žilina, Research Center, Univerzitna 1, 010 26 Žilina, Slovakia, ruzicarnikolic@yahoo.com; branislav.hadzima@rc.uniza.sk

Key words: laser cutting, steel, Zn-coating, assist-gas, coating degradation, numerical simulation.

Coatings are applied to the original material surface and typically have a different chemical composition and structure than the base material, what creates an interface, which can create problems when applying the coated steels in different technologies. The laser beam cutting technology was earlier considered as inapplicable for cutting of the steels coated with zinc. Here are described two procedures for the laser cutting of the Zn coated steel, with two different assist gases (N2 and O2) and properties of the surfaces thus layered are compared.
The laser cutting parameters, set for cutting of the DX53D galvanized steel are: the cutting speed, the laser beam power, rounding of sharp geometric shapes at border points, the distance of the ignition from the cutting line, method of onset from the inflammation site to the cut curve, procedure of processing the parts, way of creating the inflammation for small contours, the cutting pressure, the type of the assist gas, change of the used nozzle's cross-section, position of the focus point of the laser beam.
The experimental measurements were designed to present the interaction between the amount of the heat input into the cut material and amount of the degraded and sublimed zinc coating material from the vicinity of the cut. In the first phase, the width of the degraded and sublimed zinc coating was measured by a confocal microscope (Figure 1) and in the second phase the immersion corrosion test (70 days in the 3% NaCl solution) was performed. Graphical comparisons of the width of the degraded and sublimed zinc coating dependence on the cutting speed is shown in Figure 2.
The N2 assist gas has a beneficial effect on the width of the region of the degraded and sublimed zinc coating. Its suitability is emphasized due to the large degraded and sublimed width of the zinc coating layer at the laser beam exit side in the case of the O_2 cutting.
The smallest corrosion attack was at the gas pressure p = 0.5 [MPa] for application of the N_2 assist gas and at the gas pressure p = 1.6 [MPa] for the assist gas O_2.

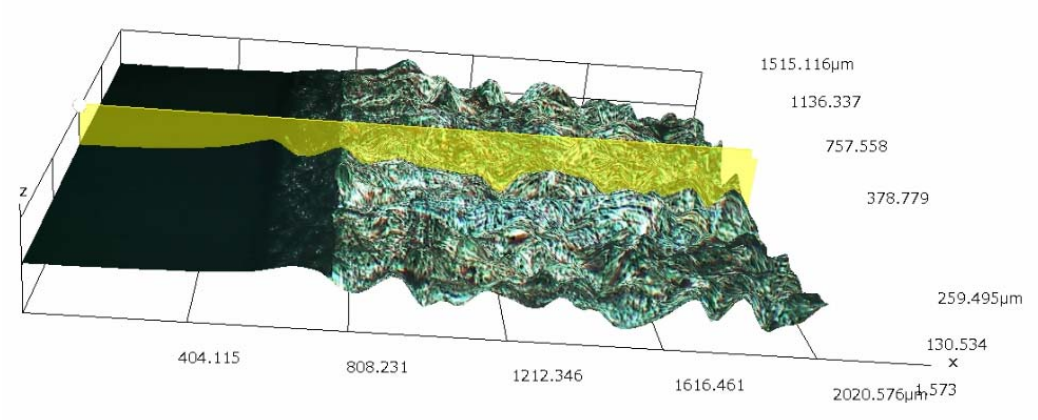

Figure 1. Measuring of the width of the degraded and sublimed Zn coating by use of the confocal microscope at the laser beam entrance side

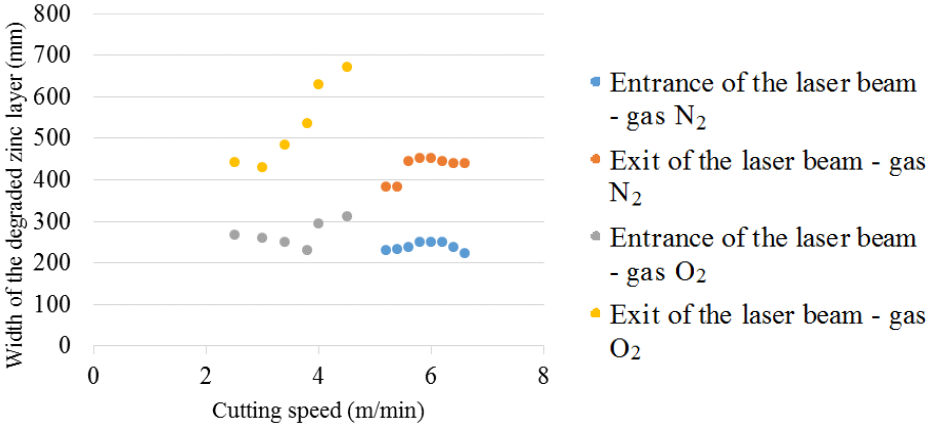

Figure 2. Comparison of the width of the degraded and sublimed zinc coating dependence on the cutting speed for the two assist gases.

Acknowledgements. Research presented in this paper was partially financially supported through project KEGA 014 ŽU - 4/2016 (K-16-00-00) and by the project of Operational Program Research and Innovation: "Research and development activities of the University of Zilina in the Industry of 21st century in the field of materials and nanotechnologies", No. 313011T426, co-funded by European Regional Development Fund.

9th International Scientific Conference
Research and Development of Mechanical Elements and Systems
Kragujevac, Serbia, September 5-7 2019

A REVIEW TO CAST POLYMER COMPOSITE MATERIALS FOR INTERIOR ENVIRONMENTS

Jasmina Blagojević[1,2], Bojan Mijatović[1], Dejan Kočović[3], Blaža Stojanović[2], Lozica Ivanović[2], Sandra Veličković[2]

[1]Metalac a.d., Metalac Inko d.o.o., Kneza Aleksandra 212,
32300 Gornji Milanovac, Serbia, jacab@kg.ac.rs, bojan.mijatovic@metalac.com
[2]University of Kragujevac, Faculty of Engineering, Sestre Janjić 6,
34000 Kragujevac, Serbia, blaza@kg.ac.rs, lozica@kg.ac.rs, sandrav@kg.ac.rs
[3]Metalac a.d., Metalac Posuđe d.o.o., Kneza Aleksandra 212,
32300 Gornji Milanovac, Serbia, dejan.kocovic@metalac.com

Key words: cast polymer composite materials, mechanical properties, manufacturing process, interior environments, design.

The polymer composite materials are modern materials namely advanced composites. It is polymer matrix composites materials in which the polymeric matrix is reinforced with particles. Products of cast polymer composites can be grouped into three categories: engineered composites, solid surface materials and engineered stone. Products of this composite material are distinguished by the materials polymer matrix and type of filler and manufacturing methods used. The paper presents and explains the most common manufacturing method used: gel coated cultured stone modeling and solid surface modeling, with a brief review on design possibilities in interior environments. The paper provides an overview of mechanical and physical properties the cast polymer composite materials. Volume fraction or filler concentration, kind of the particles reinforcement, and particle size, shape of the articles and the interfacial adhesion between the matrix and the particles are the major parameters that influence the mechanical properties of the polymer matrix composites reinforcement with particulates. There are differences between products made with acrylic and polyester of resins. Some of the differences are shown in table 1 for the solid surfaces.

The products of these materials are used for equipping the interior environment – kitchen (figure 1), bathroom (figure 2), laboratory, etc. kitchen sinks, countertop, washbasins, bathtubs, shower tub, sanitation are just some of the products that can be made by these materials. Chemical-resistant materials are therefore used to equip laboratories and kitchens in restaurants. Cast polymer composite materials can use for fabricating products

that are reliable and meet almost all design criteria, some of the designs solutions are presented in the paper.

Table 1. The differences properties solid surface products made with acrylic and polyester of resins

Type resin	Surface hardness	Colour fastness	Water absorption	Fire resistant	Chemical resistant	Heat resistant
Acrylic	Good	Better	Better	Good	Good	Good
Polyester	Better	Good	Good	Better	Better	Good

Figure 1. Applications the cast polymer composites materials in the kitchens

Figure 2. Applications the cast polymer composites materials in the bathrooms

Modern composites become competitors due to the possibility of modeling different design products. Colour, textures and design flexibility of modern polymer composites materials are key factors when choosing materials for large design projects. Further research of these materials is carried out in order to improve their mechanical properties.

Acknowledgments. This paper presents the research results obtained within the framework of the projects TR35021, TR35033 financially supported by the Ministry of Education, Science and Technological development of the Republic of Serbia.

9th International Scientific Conference
Research and Development of Mechanical Elements and Systems
Kragujevac, Serbia, September 5-7 2019

REPARATORY SURFACE WELDING OF THE FRACTURED TOOTH OF THE BUCKET-WHEEL EXCAVATOR GIRTH GEAR

Dušan Arsić[1], Ružica Nikolić[2], Vukić Lazić[1], Aleksandra Arsić[3], Milan Mutavdžić[4], Nada Ratković[1], Branislav Hadzima[2]

[1]University of Kragujevac, Faculty of Engineering, Sestre Janjić 6, 34000 Kragujevac, Serbia, dusan.arsic@fink.rs; vlazic@kg.ac.rs; nratkovic@kg.ac.r
[2]University of Žilina, Research Center, Univerzitna 8215/1, 010 25 Žilina, ruzicarnikolic@yahoo.com; branislav.hadzima@rc.uniza.sk
[3]University of Belgrade, Faculty of Mechanical Engineering, Kraljice Marije 16, 11000 Belgrade, Serbia, aarsic@bg.ac.rs
[4]High Technical School, 24. November bb, 38218 Leposavić, Serbia, mutavdzicmilan57@gmail.com

Key words: reparation, surface welding, fracture, tooth, bucket-wheel excavator, girth gear.

Frequent premature damages and fractures of components or the whole structure of bucket-wheel excavators at open-pit mines occur in exploitation. That is explained either by inadequate design and construction or by insufficient knowledge of the material properties, welded joints or oversights in manufacturing. Besides the direct losses due to damage or fracture of the excavator, the disruption in the power production and supply can cause significant indirect losses. The considered bucket-wheel excavator was employed for 5000 hours, when the fracture of the tooth of the girth gear, which enables the circular motion of the excavator's upper structure, occurred. The gear was made of the cast steel GS 40 MnCrSi3 V. To predict the cast steel resistance to crack propagation, the fracture parameters were calculated, namely the critical value of the stress intensity factor – the facture toughness K_{Ic} and the critical crack length a_{cr}, based on the obtained values of the material's impact energy and the yield stress, according to the Barsom-Rolfe model. The calculated value of the critical crack length was 61.9 mm. After the necessary calculations, the reparatory surface welding technology of the fractured tooth has been proposed. Due to the complex construction solution of the girth gear and its function in exploitation, it was necessary to precisely define a large number of details and carefully consider and execute all the operations in the methodology of manufacturing the new tooth. This was an imperative in order to ensure the safety of the repaired girth gear exploitation, since the smallest oversight, underestimate or improper execution could cause serious problems in

operation of the BWE as a whole. This is the reason why the preparation procedure for the hard-facing technology is presented, as well.

First, the weldability of the cast steel was determined by using various equations. According to equivalent carbon formula of the International Welding Institute, for maximal value of the chemical elements composition of the GS 40 MnCrSi3 V, the limiting value for the good weldability of this material is greater than 0.45. The value obtained by the Ito-Bessyo formula also surpasses the limiting value for the good weldability of 0.30. Based on the obtained results, it was concluded that this steel is prone to cold cracks appearance, what prompted the necessity for the hard-facing of the broken tooth to be performed with preheating and controlled cooling. In addition, according to formula for the Hot Cracking Sensitivity (HCS) it was established that this material is prone to appearance of the hot cracks, as well, since the obtained value for the HCS is less than 4, which is the limiting value for this type of steels with tensile strength of about 700 (MPa). After the detailed investigation of weldability, the hardfacing procedure was proposed, as well as all the preparatory and depositing operations. Due to the girth gear construction (dimensions and mass) and conditions of the hard-facing execution without the heat treatment, for the filling volume greater than 500 (cm3), the recommended preheating temperature is within range 100 to 150 ºC. Depositing of the first layer was executed by the austenitic electrode E 18 8Mn B 22, while the second layer was deposited by the basic electrode E 1-UM-300 (DIN 8555). After the hard-facing, machining of the gears to measures defined by the coordinate measuring device was performed in accordance with clearances (tolerances) prescribed by the excavator manufacturer's documentation.

Reparation of the girth gear tooth of the bucket wheel excavator SRs 2000×32/5.0 by the presented methodology was executed in 2013. The time gap of about 5 years, from the performed reparatory hard-facing to preparation of this paper, appeared due to the fact that the repaired girth gear's behavior was monitored in exploitation. Considering that the new tooth fractured after only a year in operation and that the repaired excavator is still in operation at the open pit mine "Kostolac" (Serbia), it can be concluded that the reparation was successful. It should be emphasized that in this way the large financial effect was realized as well, since the construction of the new girth gear would cost over 500.000 €. If the time, needed for manufacturing the new girth gear, which is about 6 to 9 months, would also be included in this calculation, as well as effect of the electric power that would not be produced in such a long period, the total positive financial effect is about 8.000.000 €.

The presented methodology of the reparatory hard-facing, as well as the welding procedure, can be applicable, with necessary adjustments, for recovery of other parts and structures of the bucket wheel excavator at open pit mines.

Acknowledgments. This research was partially financially supported by the Ministry of education, science and technological development of Republic of Serbia through grants TR 35006 and TR 35024 and by the project of Operational Program Research and Innovation: "Research and development activities of the University of Žilina in the Industry of 21st century in the field of materials and nanotechnologies", No. 313011T426, co-funded by European Regional Development Fund.

9th International Scientific Conference
Research and Development of Mechanical Elements and Systems
Kragujevac, Serbia, September 5-7 2019

EXTENSION OF THE STEEL SIEVE DURING THE SPHERICAL GUN-POWDER SCREENING

Nada Bojić[1], Ružica Nikolić[2], Dragan Milčić[3], Milan Banić[3]

[1]FASIL A. D. Arilje, Svetolika Lazarevića 18, 31230 Arilje, Serbia, nalemfkg@gmail.com
[2]University of Žilina, Univerzitna 8215/1, 010 26 Žilina, Slovakia, ruzicarnikolic@yahoo.com
[3]University of Niš, Faculty of Mechnanical Engineering, Aleksandra Medvedeva 14, 18000 Niš, Serbia, milcic@masfak.ni.ac.rs, banic@masfak.ni.ac.rs

Key words: vibration sieve, spherical gun-powder, screening, mechanical properties, sieve stretching.

The aim of mechanical classification (screening) is to divide particulate material into groups of grains according to their sizes. For this purpose, sieves are equipped with either one or several screens. The selection of a correct sieve for a given particulate material determines the course of screening. The term screening is usually used for continuous sizing operation, while sieving usually means a batch process.
Many factors have been identified that affect the screening, including the size and shape of particles relative to the aperture of the sieve, the mesh size of the sieve itself, amount of material on the sieve surface, direction of the sieve movement, rate of the material movement relative to the sieve surface.
The spherical gun-powder is the nitro-cellulose gun-powder. The basic component is the nitro-cellulose to which the nitroglycerine and stabilizer diphenylamine are added. The whole production process is rigorously controlled, while all the tests are carried out on a daily basis, on the state-of-the-art devices, both in laboratories and on the testing grounds.
The average sieving area (screen) can be made in different ways and from different materials, depending on the material being sown. For screening of the spherical gun-powder, the most commonly used are steel screens with square or rectangular openings.
The sieve represents the wires interlace, which is formed by joining the two systems of wires by weaving, namely by alternate interlacing of the *base* and *weft* wires at a right angle.
The vibration sieve is an above resonant sieve with circular vibrations. Due to the increased impact oscillations, when the spherical gun-powder is poured onto the vibration sieve, stretching, breaking, damage in some places and, in the worst case, breaking of the sieve occurs. The mechanical characteristics of the sieves - stretching (extension) of the steel sieve is analyzed in this paper. The two metal single-layered sieves were used in this experiment

of the same type - TYPE 110, but with different numeration, Table 1. Material for all the wires was WNr. 1.4301.

Table 1. Basic data on two types of sieves.

	Sieve Type 1	**Sieve Type 2**
Base number N_o (wires per cm)	5	30
Base wire diameter (mm)	0.5	0.15
Weft number N_w (wires per cm)	5	30
Weft wire diameter (mm)	0.5	0.15

Test results are given in Table 2 and Figure 1. The data recorded during the test were: a_0 – sample thickness , b_0 – sample width, L_0 – sample length, F_{max} – maximum force, F_{break} – breaking force, ε_{Fmax} – extension at maximum force and ε_{break} – extension at break.

Table 2. Test results

Sieve type	**Sample number**	a_0	b_0	L_0	F_{max}	F_{break}	ε_{Break}	ε_{Fmax}
		mm	mm	mm	N	N	%	%
No. 1 TYPE 110 N_o 5	1	0.3	1.1	150.20	2064.08	1928.44	21.84	21.56
	2	0.3	1.1	150.34	2218.06	2205.97	22.17	22.06
No. 2 TYPE 110 N_o 30	1	0.3	30	150.19	1077.95	969.28	6.32	6.08
	2	0.3	30	150.12	1160.74	1151.64	9.19	9.12

From obtained results one can see that the sieve of type 1, i.e. TYPE 110 N05, has bigger extension for about 50 % and 50 % bigger breaking force that the sieve of type 2, i.e. TYPE 110 N030. Out of the two tested sieves, the better one to be used is the sieve with the smaller wire diameter and the higher number, i.e. the sieve of type 2 TYPE 110 N030.

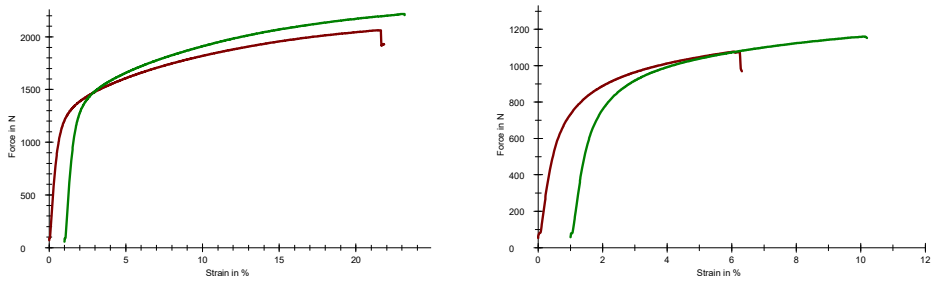

Figure 2. The stress-strain diagram for the sieve TYPE 110 $N_0$5 (left) and sieve TYPE 110 $N_0$30 (right).

Acknowledgments. Research presented in this paper was partially financially supported by the project of Operational Program Research and Innovation: "Research and development activities of the University of Zilina in the Industry of 21st century in the field of materials and nanotechnologies", No. 313011T426, co-funded by European Regional Development Fund.

IRMES KRAGUJEVAC 2019

9th International Scientific Conference
Research and Development of Mechanical Elements and Systems
Kragujevac, Serbia, September 5-7 2019

APPLICATION OF ARDUINO PLATFORM IN TECHNICAL SYSTEM

Natalija Tomić[1], Boban Anđelković[1], Miloš Milovančević[1], Marko Mladenović[1, 2], Ana Kitić[1]

[1]University of Niš, Faculty of Mechanical Engineering, Aleksandra Medvedeva 14, 18000 Niš, Serbia, natalija.tomic@masfak.ni.ac.rs
[2]Harder Digital Sova, Research and development, Bulevar Svetog cara Konstantina 80, 18000 Niš, Serbia

Key words: microcontroller systems, Arduino, technical system monitoring.

Contemporary development of technology and process automation, has increasing need for the development of efficient and economical systems for monitoring production processes and devices. Because of the fact that measurement and monitoring systems have a very high cost an ideal platform for beginners in processing digital signals is Arduino. In 2015 average price for Arduino platform was between 20€ and 52€.The Arduino can be programed with Arduino Integrated Development Environment (IDE) which uses C and C++ programming languages. There are available libraries and open-source codes for large number of sensors to extend the basic capabilities of this controller. In this case Arduino platform will be used for measurement digital and analog signals. An appropriate example of measuring analog signals is measurement of weight. An appropriate example of measuring digital signals is obstacle detection. Obstacle detection is a requirement for many automated systems, in order to detect the presence or absence of elements important for the operation of these systems. Such systems can be diverse, from the system for filling packaging, determining the position of work pieces or the machine elements to the counting system and interacting with the user. The variety of automated systems is followed by the development of sensors that follow their requirements. The aim of this paper is to explain how it is possible to measure digital and analog signals using Arduino platform. Chosen microcontroller is Arduino Uno R3. For the measurement of analogue signals, it is used measuring cell up to 10 kg, so in this way the precision of measurement is ± 10 g. To overcome this problem, it was used Hx711 A/D convertor module with resolution of 24 bits so it can be got more precise results. A coin which value is 1 RSD was used to check the accuracy of code. According to the data of the National Bank of Serbia this coin has a weight of 4.20 grams. The results for weight measurement of coin is presented on Figure 1.

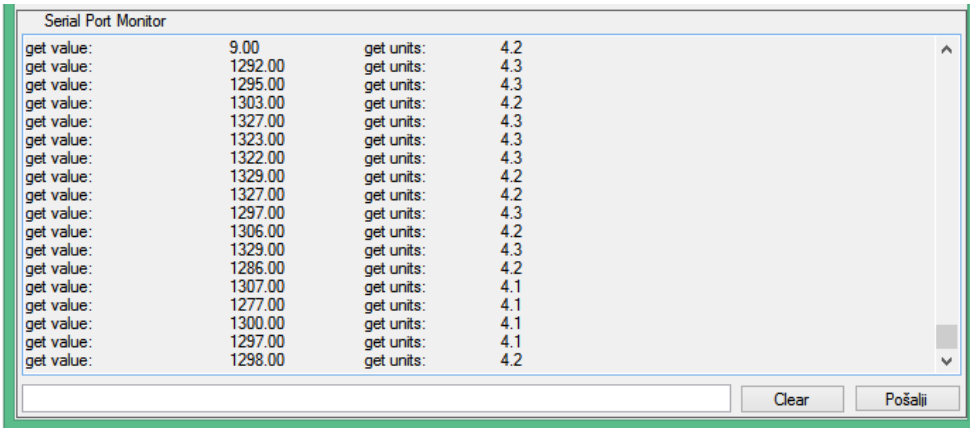

Figure 1. The interface during the weight measurement

To measure digital signals an IR diode sensor was used. The basic elements of IR sensor are: IR diodes, photo diodes, resistors and additional signal gain elements, LED indicators and capacitors. Lighting a photo diodes allows the current in the inverse direction that gives the voltage at the ends of the resistor. Measurement of this voltage determines the brightness of the diode. One such 5V IR sensor module can be directly connected to the Arduino and incorporated into the projected system. The base code allows reading the state of the sensor, and if the presence of an object is detected, the LED on the digital port 13 is switched on. This code exists in the Arduino's software interface library (IDE). To demonstrate the possibility of control with Arduino and computer, as well as storage and retrieval capabilities, the received data is entered in the console. From here they can be easily processed and saved. If there is no obstacle, on display is shown “0”, if there is obstacle, on display is shown “1”, interface in this case is presented on Figure 2.

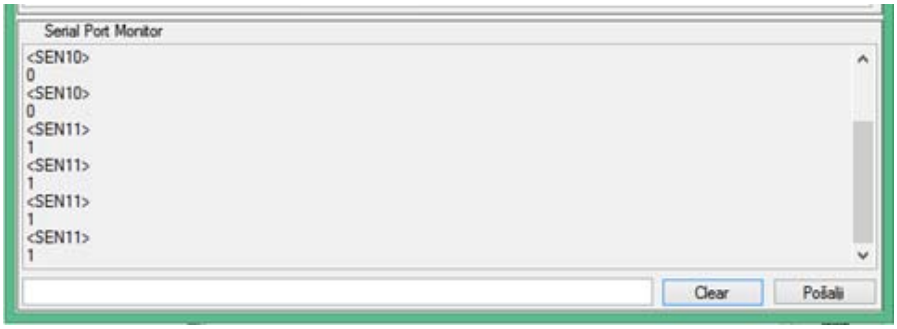

Figure 2. The interface when there is obstacle

The paper presents the basic principles of measurement of different units with the help of Arduino platform, as well as the principle of connecting and realization of communication of Arduino with computer in order to acquire data or management of various processes based on measurement or user command.

9th International Scientific Conference
Research and Development of Mechanical Elements and Systems
Kragujevac, Serbia, September 5-7 2019

DATA ACQUISITION IN ARDUINO SYSTEMS

Natalija Tomić[1], Boban Anđelković[1], Miloš Milovančević[1], Marko Mladenović[1, 2], Ana Kitić[1]

[1]University of Niš, Faculty of Mechanical Engineering, Aleksandra Medvedeva 14, 18000 Niš, Serbia, natalija.tomic@masfak.ni.ac.rs
[2]Harder Digital Sova, Research and development, Bulevar Svetog cara Konstantina 80, 18000 Niš, Serbia

Key words: data acquisition, Arduino systems, data collection

Data acquisition is assumed to mean any measurement or retrieval of data from the environment with the help of sensors. Engineers and scientists commonly use data acquisition hardware and software to research through measurement and analysis. How hardware and software for this purpose mostly have high price, this paper will present data acquisition with a low-cost open-source microcontroller. Since its inception, these microcontrollers are increasingly being used in research across the World in almost all fields of science.

The concept of acquisitions mainly refers to the collection of data and their storage. The data obtained can be stored for subsequent analysis or can be directly used as feedback which reflects the current state of the system in automatically controlled systems, and other forms of data usage as well as their combinations are also possible.

There are analog and digital sensors with the help of which the acquisition takes place. As it is possible to use digital sensors to measure periodic events, for example, rotate a disc with a slot, it is possible to measure some other analog sizes with digital sensors by a certain procedure and store their values for later processing or use for control.

Depending on the need, the complexity of acquisition and data processing varies, so the way and time of programming such an application varies from case to case. Different programs and programming languages can be used to program applications that download and process data from Arduino, because the programming of this application is completely independent of the Arduino platform and does not require a special programming language in order to be achieved. Various software like MatLab, LabView and Mathematica, used for academic and practical purposes, have the ability to achieve this kind of communication with Arduino in a direct or indirect way. Using these programs enables easy processing of large amounts of data, their graphic display and usage. The principle of connecting communication is very similar and can easily be transferred to an environment that is close to us. For the

purposes of this work, a programming language with a light syntax for understanding will be used, it is about Visual Basic.NET, which will show one of the ways of communicating with a computer, data acquisition and control with the help of Arduino.
The basic components of any data acquisition system are:

- The processing unit or controller.
- Sensors or transducers.
- Signal conditioning circuit.

As a controller it will be used Arduino Uno R3 board.
One digital and one analog sensor will be used. In this case, the digital sensor can be an IR sensor or a photo resistor, while the weight sensor will be used as a representative of analogue sensors. Weight sensor will be used to measure mass of RSD 1 dinar coin, which mass is 4,2g acceding to National Bank of Serbia.
The logic diagram for program code is presented on Figure 1.

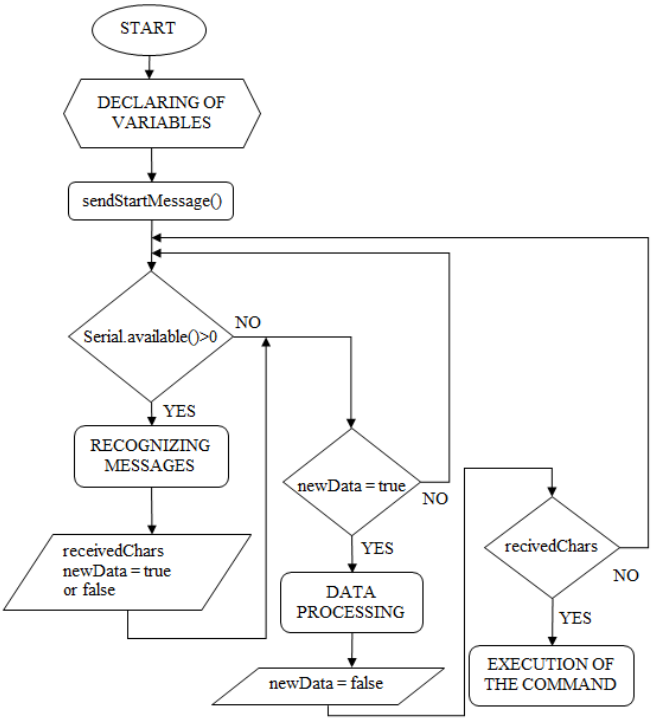

Figure 1. The logic diagram for this program code.

Using Arduino as the mainboard, some sensors and computer, we constructed easily scalable data acquisition and control system which accommodates close range obstacle detection system by IR or photo sensor, and mass measuring with precision of ±0.2g. System can be upgraded to read, store and process all different kinds of sensors such as temperature, acceleration, proximity determination, moisture, gas detection and many more. System has been proven as reliable source of accurate measurements over a series of tests.

9th International Scientific Conference
Research and Development of Mechanical Elements and Systems
Kragujevac, Serbia, September 5-7 2019

DESIGN OF WEARABLE OXIMETER MEDICAL DEVICE SUPPORTED BY MOBILE APPLICATION MONITORING

M Petrovic[1], N Grujovic[1], V Slavkovic[1], F Zivic[1]

[1]University of Kragujevac, Faculty of Engineering, Sestre Janjić 6, 34000 Kragujevac, Serbia, milicaspetrovic92@gmail.com

Key words: Internet of Things, wearable technologies, Oximetry, Arduino, Android application.

In the paper designing process of device and mobile application are presented. Oximeter device is designed to accommodate small dimensions and to allow communication with user through mobile applications. Android application enables user to monitor results (oxygen level) and receive notifications based on measured value (low oxygen level).
The main idea behind the project is to make possible for the user to select multiple sensors and read results using developed application, from any location that have internet access. Portable device described in this paper is used to measure oxygen level. Main advantages of this device are small dimensions, ease of use, and the low price that make it available for larger group of users. This way medical professional can monitor health condition of a remote patient by using developed android application. The device is especially useful in monitoring the health condition of unconscious patient, because it does not require constant presence of the medical professional. The device can be applied on the patient's finger and in the case of a decrease of the oxygen level, inform the competent person who can respond in a timely manner. Mobile application allows access to the data measured by the sensor for any user who has installed application on the Android smart phone. The proposed solution represents an improved measurement method compared to existing bluetooth-based devices. The main advantage of measurement by using ESP8266Wi-Fi module is the possibility of remote monitoring and measurement in comparison to the bluetooth device that requires close proximity of measuring device and measurement point. Methodology used in this project is mainly based on Photoplethismography(PPG) optical non-invasive technique which can detect changes in the blood volume on the micro-vascular tissue level. In photopletismography, skin of the finger is lit by the infrared or red-light LED diode. The light reflected from the skin surface, is detected by the additional photodiode, which allows detection of the changes in the blood. Figure 1 shows the networking of the system elements, with the schematic elements of the device on the left. The device has 3 basic elements: MAX30100 sensor for blood oxygen measurement, Wemos D1 mini with

integrated ESP8266-12f Wi-Fi module and batteries as a power supply. The user applies the device by putting it on a finger. The Wi-Fi module reads data from the sensor, sends it to the appropriate server, from where the user receives the values through the mobile application. Values are available for anyone who has access to the application and internet connection. Remote user can monitor the status of the user who carries devices in real-time on the Android device.

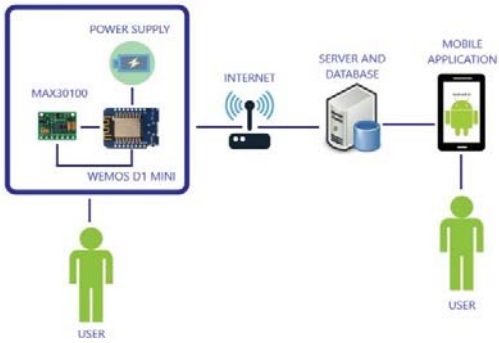

Figure 1. Schematic view of the project.

Data is received in the form of a list that may be printed. Also, the name of the sensor, its measured values, and the notification icons are displayed at the home screen (Figure 2).
The idea is that, depending on the measured amount of oxygen in the blood, a warning signal (mobile notification) is sent to the user if the level of oxygen falls below the normal limit or selected threshold. If there is a need to monitor the health condition over a time period, it is possible to choose sensor from the list menu and print time-level of oxygen diagram.

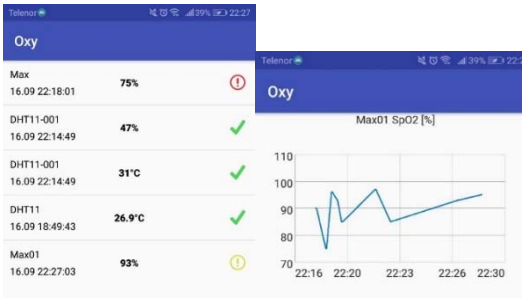

Figure 2. Application screens.

Size, price, ease of use are the main features of this device. Displaying the results in real time via diagrams can be improved by adding an option to store the result history, allowing long-term tracking of the desired parameters. Upgrading the application can get a complex multipurpose product that will be able to send and print results, as well as automatically call the responsible person in the event of alarming notifications. Further improvement of proposed solution may include additional options for the user, custom-made device case and power supply, and display on the device itself. Further research is needed for better power supply with longer battery life and smaller size, to enable small size of the device.

9th International Scientific Conference
Research and Development of Mechanical Elements and Systems
Kragujevac, Serbia, September 5-7 2019

EFFECT OF NANOSIZED PARTICLES ON THE BAINITIC TRANSFORMATION IN AUSTEMPERED DUCTILE IRONS

Valentin Mishev[1], Julieta Kaleicheva[1], Viktor Anchev[1], Zdravka Karaguiozova[2]

[1] Faculty of Industrial Technology, Technical University of Sofia, 8 Kl. Ohriski Blvd, 1000 Sofia, Bulgaria, jkaleich@tu-sofia.bg
[2] Space Research and Technology Institute, BAS, Acad. Georgy Bonchev Str., bl.1, 1113 Sofia, Bulgaria

Key words: nanoparticles, cast irons, bainite, retained austenite

The aim of this study is to investigate the kinetics of the bainitic transformation, the bainitic structure morphology in the upper temperature range of the bainitic area, the hardness and the wear resistance of the austempered ductile cast irons (ADI) containing additives of nanosized particles - titanium carbonitride + titanium nitride (TiCN + TiN), titanium nitride (TiN) and cubic boron nitride (cBN).
The samples tested are made of unalloyed ductile cast iron with the following composition: Fe-3,55C-2,67Si-0,31Mn-0,009S-0,027P-0,040Cu-0,025Cr-0,08Ni-0,06Mg wt. %. During the casting in the cast iron melt nanosized particles of TiCN+TiN, TiN and cBN are added.
Bainitic cast irons are obtained by isothermal quenching in the upper temperature range of the bainitic area, including heating at 900°C for an hour, after that isothermal retention at 380°C, 0,5 h, 1 h, 2 h, 4 h, 6 h. As a result of this heat treatment, the cast iron obtains an upper bainitic structure .The austempered ductile iron samples' microstructure is observed by means of an optical metallographic microscope GX41 OLIMPUS. The microstructure of the austempered ductile irons (ADI) is tested by scanning electron microscopy (SEM) - EVO® MA10. The hardness testing is performed by Vickers method. The austempered ductile iron samples are tested by X-Ray diffraction analysis the retained austenite quantity in the structure to be defined. X-ray powder diffraction patterns for phase identification are recorded in the angle interval 22 ÷104° (2θ), on a Philips PW 1050 diffractometer, equipped with Cu–Kα tube and scintillation detector. For the samples with an upper bainitic structure obtained for 2 hours isothermal retention at 380°C an abrasion test is performed.
Nanosized particles accelerate the transformation of the austenite to bainite. The amount of the retained austenite in the samples without nanoparticles additives for 2 hours isothermal retention at 380°C is 40.4%. In the samples with nanoadditives, the amount of the retained austenite decreases to 30.2÷27.1% for 2 hours of isothermal retention at 380°C.

With the development of the bainitic conversion from 2 to 6 hours, the amount of the retained austenite in all samples tested decrease. The hardness of the tested ADI samples is in the range from 294 to 322 HV10.

For the samples after an isothermal retention for 2 hours at 380°C, an abrasion resistance test is conducted. An increase in the wear resistance for ADI specimens with nanoadditives is found compared to those without nanoadditives. The amount of the retained austenite in the cast iron samples is determined before and after the tribological test (figure 1).During friction the retained austenite transforms partly into strain-induced martensite with the same amount of carbon as in high carbon austenite. This strain-induced martensite is untempered martensite characterised with a high hardness and ability for intensive strengthening by wear.

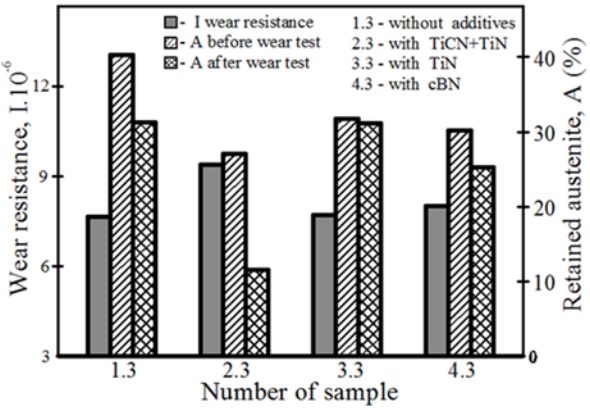

Figure 1. Wear resistance I and retained austenite A of austempered ductile iron samples with and without nanoadditives and after isothermal retention for 2 h at 380°C.

The amount of the retained austenite decreases in all ADI samples tested after the tribological test. Mostly, the amount of the retained austenite decreases in the sample with (TiCN + TiN) nanoparticles - from 27.1% to 11.6%. This specimen also has the highest abrasion resistance (I=9.42.106) (figure 1). The formation of strain-induced martensite from the metastable retained austenite in the frictional area (microtrip-effect), probably is one of the reasons for the wear resistance increase of these materials.

Nanosized additives in the spheroidal graphite cast irons influence on the structure formation in the temperature range of the bainitic area. They alter the kinetics of the bainitic transformation and accelerate the transformation of the undercooled austenite into bainite. Austempered ductile irons (ADI) with nanosized additives possess higher wear resistance (until 23%) in comparison to the samples without nanoadditives. The influence of the nanoadditives on the graphite phase characteristics and on the extent of the transformation of the austenite to bainite explain higher abrasion wear resistance of the tested austempered ductile irons with nanoadditives compared to the same without nanoadditives. Partially transformation of the metastable retained austenite to strain-induced martensite during friction which is observed in the austempered ductile irons also affects their wear resistance.

Acknowledgments. The authors would like to thank the Research and Development Sector at the Technical University of Sofia for the financial support.

9th International Scientific Conference
Research and Development of Mechanical Elements and Systems
Kragujevac, Serbia, September 5-7 2019

PARAMETER OPTIMISATION AND FAILURE LOAD PREDICTION OF RESISTANCE SPOT WELDING OF ALUMINIUM ALLOY 57547

Aleksija Đurić[1], Damjan Klobčar[2], Dragan Milčić[3], Biljana Markovic[1]

[1]University of East Sarajevo, Faculty of Mechanical Engineering, Vuka Karadžoća 30, 71123 East Sarajevo, RS, B&H, aleksija.djuric@ues.rs.ba, biljana.markovic@ues.rs.ba
[2]University of Ljubljana, Faculty of Mechanical Engineering, Aškerčeva cesta 6, 1000 Ljubljana, Slovenia, damjan.klobcar@fs.uni-lj.si
[3]University of Niš, Faculty of Mechanical Engineering, Aleksandra Medvedeva 14, 18106 Niš, Serbia, dragan.milcic@masfak.ni.ac.rs

Key words: resistance spot welding, parameter optimization, response surface modelling

This paper present single objective optimization and failure load prediction of Resistance spot welding of aluminum alloy 57547. The experimental studies were conducted under varying welding currents I, electrode forces F, welding times T, pred preheating currents IA. The settings of welding parameters were determined by using the Taguchi experimental design of L9 Orthogonal array method. For optimization and prediction will be used analysis of Signal-to-Noise (S/N) ratio and Response surface modelling RSM. Sheet metals of aluminum alloy AlMg3 - AW5754 H22 as the parent metal to be lap welded were used in this research. The dimensions of the specimen are defined according to the standard ISO 14273:2016. The experiment involved joining of two sheet metals using RSW machine manufactured by Kocevar & sinovi which is managed using the BOSH 6000 software. Welding was carried out using electrode type A0 with radius 75 mm. Four welding parameters such as weld current *I*, electrode force *F*, weld time *T* and preheating current I_A were selected for experimentation for three levels of factors. Other welding parameters such as squeeze time (SQZ), hold time (HLD), pre-heating time (Pre-Weld), Cool Time (CT), Up Slope Time (UST) and Down Slope Time (DST) were constant during the experiment. The tensile-shear tests were performed according to standard ISO 14273:2016 at cross-head speed of 2mm/min with a Beta 50-7 / 6x14 testing machine. As per the L9 orthogonal array for each combination of process parameters results obtained from the test are given in table 1. The optimum levels of different control factors for higher failure load are weld current at level 3 (35 kA), electrode force at level 1(3,68 kN), weld time at level 3 (0.2 s), and pre-weld current at level 3 (10 kA).

Table 1. Experimental layout using L9 OA and result from tensile-shear tests (Failure load)

Runs	Weld current *I* [kA]	Electrode force *F* [kN]	Welding time *T* [ms]	Pre-heating current I_A [kA]	Failure load *F* [N]
1	20	3,68	80	6	1504
2	20	4,91	140	8	1830
3	20	6,14	200	10	1638
4	28	3,68	140	10	2046
5	28	4,91	200	6	1581
6	28	6,14	80	8	1316
7	35	3,68	200	8	2719
8	35	4,91	80	10	1989
9	35	6,14	140	6	1862

The plot of S/N ration is showed in figure 1. It can also be concluded from table 3 that the welding current has the greatest influence on the failure force, while the pre-weld current has the slightest influence on the meaning of this force. The plot of S/N ration is showed in figure 1. Using the analysis of variance (ANOVA), the previous assertion that the most influence on failure load has a weld current is confirmed (43.65 %).

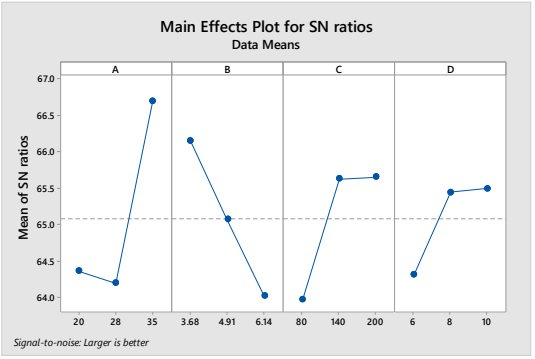

Figure 1. Plot of S/N ratio

The response surface model (RSM) for failure load F has been developed from the experimental response values obtained using L9 OA experimental matrix. The above-mentioned model is presented below as the equation:

$$F = 1971 - 253A + 505,2B + 12,59C + 800,5D + 5,246A^2 + 31,4B^2 - 0,03375C^2 - 46,25D^2$$

Using RSM, the corresponding parameters that yielded maximum value of failure load are weld current 35 kA, electrode force 3,68 kN, weld time 0.1866667 s, and pre-weld current 8,667 kA.

Acknowledgments. The authors gratefully acknowledge partial support by CEEPUS network CIII-BG-1103-04-1920-M-133090 – Modelling, Simulation and Computer-aided Design in Engineering and Management.

9th International Scientific Conference
Research and Development of Mechanical Elements and Systems
Kragujevac, Serbia, September 5-7 2019

THE INFLUENCE OF DIFFERENT LAMINA POSITIONS ON BUCKLING PROPERTIES OF COMPOSITES PLATES UNDER BIAXIAL COMPRESSIONT

Dejan Jeremić[1], Nebojša Radić[1]

[1]University of East Sarajevo, Faculty of Mechanical Engineering East Sarajevo, Vuka Karadžića 30, 71123 East Sarajevo, Bosnia and Herzegovina, dejan.jeremic@ues.rs.ba

Key words: buckling, composites plates, fiber orientation angle, critical buckling force.

The present work focused on the buckling of composite plates subjected to biaxial compression using Classical Laminated Plate Theory (CLPT). The two composite plates are bonded by an elastic medium. CLPT is utilized for deriving the governing equations. Difference between 4-ply symmetric lamination scheme with different material properties and fiber orientation angle (0° and 30°) is shown. The main contribution of this work is to perform a composite laminated plates analysis by using the CLPT.

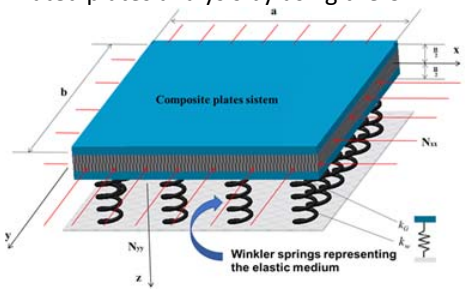

Figure 1. Schematic diagram of composite plates system subjected to biaxial compression

Composite plates are assumed to be coupled by an elastic medium and subjected to biaxially compression. The composite plates are surrounded by external elastic medium. The external medium is modeled as Pasternak-type foundation which is equivalent to Winkler modulus parameter k_w and shear modulus parameter k_G of polymer matrix. Bending displacements of the plate-1 and plate-2 are $w_1(x, y, t)$ and $w_2(x, y, t)$, respectively. It was assumed that each composite plate had the length, a and width, b. We assume that composite plates are biaxially compressed by forces N_{xx} and N_{yy} in the directions of x and y axes, respectively (figure 1). The governing equation for biaxially compressed orthotropic composite plate embedded in an elastic medium, which is based on Classical Laminated Plate Theory CLPT, have following form

$$D_{11}\frac{\partial^4 w}{\partial x^4}+2(D_{12}+2D_{66})\frac{\partial^4 w}{\partial x^2\partial y^2}+D_{22}\frac{\partial^4 w}{\partial y^4}+N_x\frac{\partial^2 w}{\partial x^2}+N_y\frac{\partial^2 w}{\partial y^2}+k_w w-k_G\left(\frac{\partial^2 w}{\partial x^2}+\frac{\partial^2 w}{\partial y^2}\right)=0$$

The composite plate system is subjected to both biaxial as well as biaxial compressive forces. The cases studied will be composite plates buckling with out-of-phase (asynchronous); in-phase (synchronous); and when one of the composite plates is considered to be fixed. Critical buckling load for asynchronous type of buckling can be written as

$$N_{cr}=\frac{D_{11}\alpha^4+2(D_{12}+2D_{66})\alpha^2\beta^2+D_{22}\beta^4+2k_w+2k_G(\alpha^2+\beta^2)}{(\alpha^2+\delta\beta^2)}$$

Critical buckling load for synchronous type of buckling can be written as

$$N_{cr}=\frac{D_{11}\alpha^4+2(D_{12}+2D_{66})\alpha^2\beta^2+D_{22}\beta^4}{(\alpha^2+\delta\beta^2)}$$

and critical buckling load for this type of buckling when one of the two composite plates is stationary can be written as

$$N_{cr}=\frac{D_{11}\alpha^4+2(D_{12}+2D_{66})\alpha^2\beta^2+D_{22}\beta^4+k_w+k_G\left(\alpha^2+\beta^2\right)}{(\alpha^2+\delta\beta^2)}$$

Based on CLPT, in this paper was analyzed influence of aspect ratio a/b, fiber orientation angle and lamina positions on the non-dimensional buckling load on biaxial compressed composite plates embedded in elastic medium. In this paper, there are analytical expressions for non-dimensional buckling load for three characteristic cases of buckling of simply supported composite plates. Two types of materials are combined:

-Kevlar 49/CE 3305 (material M1)

-Graphite-Epoxy AS-1/3501-5A (material M2)

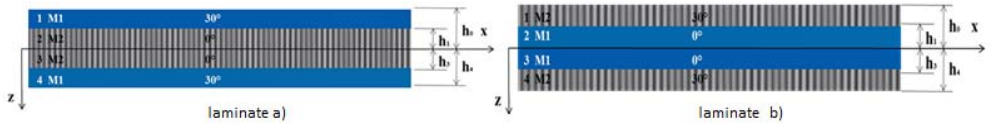

Figure 2. Schematic layout of composite laminate

It was shown that the increase of Winkler modulus parameter and shear modulus parameter also increases the nondimensional buckling load for all three characteristic buckling cases. The layout of the lamina inside the laminate has a significant effect as well as fiber orientation angle on the buckling and cannot be ignored. It has been shown that with the change of lamina positions in the laminate, the value of the non-dimensioning critical load is changed for all three characteristic buckling cases. Laminates have different minimum and maximum values of non-dimensional critical force at the same value of aspect ratio. For asynchronous type of buckling non-dimensional critical buckling force has the highest value in both schemas of laminate plates. The study shows that the mechanical properties of the composite materials depending on the fiber orientation angle and lamina positions.

9th International Scientific Conference
Research and Development of Mechanical Elements and Systems
Kragujevac, Serbia, September 5-7 2019

FRACTURE ANALYSIS DIAGRAM IN INTEGRITY ASSESSMENT OF HIGH-FREQUENCY WELDED CASING PIPES MADE OF API J55 STEEL

Ljubica Lazić Vulićević[1], Živče Šarkočević[2], Aleksandar Rajić[1], Milenko Stašević[1]

[1]Technical College of Applied Sciences in Zrenjanin, Đorđa Stratimirovića 23, 23000 Zrenjanin, Serbia, lazic.ljubica@yahoo.com
[2]University of Priština, Faculty of Technical Sciences, Kneza Miloša 7, 38220 Kosovska Mitrovica, Serbia, zivcesarkocevic@yahoo.com

Key words: welded casing pipes, axial surface crack, fracture behavior, integrity assessment, Fracture Analysis Diagram – FAD.

The reliability of the oil wells system is important not only because of economically oil exploitation, but also to preserve the environment. This paper presents the integrity analysis of welded casing pipes from exploitation made of API J55 steel with outside axial surface crack. Analyzed tube was in operation at an oil rig and was withdrawn during the process of reparation, after a period of about 70 000 hours (8 years). This period is much shorter than the projected service life, which is up to 30 years. The Fracture Analysis Diagram (FAD) provides a simple integrity analysis of the welded casing pipes and it can be reliably concluded that the exploited welded pipe is safe of the mutual interaction of brittle fracture and plastic collapse.

Mechanical properties of API J55 steel were determined on specimens taken from exploited pipes. The measurement process is performed using electromechanical testing machine SCHENCK-TREBEL RM 100. The result shows the exploited base material tensile properties degradation. The tests of the modified CT specimens were carried out at room temperature on a machine SCHENCK-TREBEL RM 100. Modified CT specimen thickness is d = 6.98 mm (equal to the pipe wall thickness). Using value J_{Ic}, the critical values of stress intensity factor K_{Ic}, and further the values of critical crack length (a_c), for base material (BM), heat affected zone (HAZ) and weld metal (WM) are calculated. The conclusion is that the lowest resistance to the crack initiation and propagation has the base material, and further analyses were conducted only for the base material.

The integrity analysis of welded casing pipes (diameter of the pipe Ø139.7 mm and nominal wall thickness 6.98 mm) is performed for the pipe model with an axial surface crack in the base material on the outer surface of the pipe. The initial crack dimensions are: depth a = 3,5 mm and length $2c$ = 200 mm. The concept with two failure criterion was introduced to

describe the mutual interaction of brittle fracture and plastic collapse implemented through the Fracture Analysis Diagram - FAD. Starting point of this diagram is modified strip yield model for through crack in an infinite plate, which connects the effective stress intensity factor K_{eff} with distant stress:

$$K_{eff} = \sigma_Y \sqrt{\pi a} \left[\frac{8}{\pi^2} \ln \sec \frac{\pi}{2} \frac{\sigma}{\sigma_c} \right]^{1/2}$$

In real structures yield strength σ_Y should be replaced with collapse stress σ_C, which, in addition to the material, depends on the geometry of the structure, including crack. The next step is an expression of effective stress intensity factor in dimensionless form as K_{eff}/K_I. And finally we have dimensionless variables $S_r=\sigma/\sigma_c$ and $K_r=K_I/K_{Ic}$ which represents the abscissa and ordinate in the modified fracture analysis diagram, and the equation becomes:

$$K_r = S_r \left[\frac{8}{\pi^2} \ln \sec \left(\frac{\pi}{2} S_r \right) \right]^{-1/2}$$

If the material is totally ductile, the structure breaks in plastic collapse S_r=1, while for the failure of the structure of completely brittle materials K_r=1. In all other cases there is interaction between plastic collapse and brittle fracture. If the structure is safe from failure, the K_r and S_r values are less than 1, and the pairs of corresponding values are inside the border line. The obtained values for K_r and S_r in this calculation marked the point with coordinates (0.7; 0.35), which is located in a safe part of the diagram **(Figure 1.** Fracture Analysis Diagram - FAD for pipe with axial surface crack).

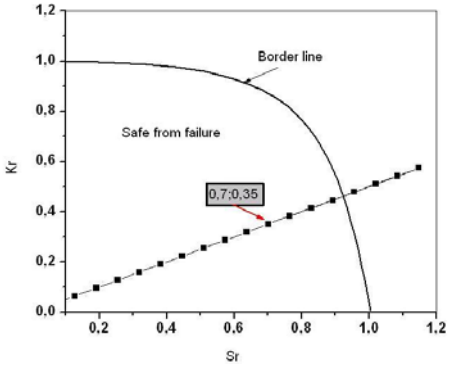

Figure 1. Fracture Analysis Diagram - FAD for pipe with axial surface crack

Having in mind the conservative analysis of FAD it can be concluded that the welded casing pipes are safe not only of brittle fracture, but also of plastic collapse. It is important to notice that the Fracture analysis diagram (FAD) provides a simple analysis of integrity that can reliably determine whether the welded casing pipe, and thus the casing string, is safe from failure under condition that the geometry and the load presented on the conservative way. On the other hand, if you cannot prove integrity, it does not mean that the casing string is useless. In that case they need additional and more complicated analysis.

9th International Scientific Conference
Research and Development of Mechanical Elements and Systems
Kragujevac, Serbia, September 5-7 2019

NON-WOVEN COMPOSITES INTENSIFICATION PROPERTIES FOR AIR FILTERS BY PLASMA PRE-TREATMENT

M P Neznakomova[1], M-L Klotz[2], D N Gospodinova[3]

[1]Technical university – Sofia, Department of Material Science and Technology of Materials, 8 Kliment Ohridski Blvd., 1000 Sofia, Bulgaria
[2]Rhine-Waal University of Applied Sciences, Department Werkstoffe, Qualität und Ökologie, Marie-Curie-Straße 1, 47533 Kleve, Germany
[3]Technical University – Sofia, Faculty of Electrical Engineering, 8 Kliment Ohridski Blvd., 1000 Sofia, Bulgaria, dilianang@abv.bg

Key words: non-woven industrial textile, electrospinning, surface modification, cold plasma treatment.

Figure 1. Structure of double-layer gas filter media.

The use of nonwovens in the automotive market has increased significantly in recent years and nonwovens can be engineered to have specific properties. Method for changed porosity fibrous materials obtaining is the electrospinning process that provides applying on the surface substrate a nanofibres layer. The pad hydrophpbic balance affects the adhesion between mat and layer. Plasma surface modification is carried out to change: hydrophilicity/hydrophobicity, surface roughening, grafting and surface functionalization.
After processing in cold plasma, the hydrophilic properties of the, non-woven needle-punched textile materials with varying area and volume widely used in the automotive industry, change. It can be seen that plasma exposure leads to changes in the polymer composition surface - free radicals formation, activated species of inert gas surface graft polymerization, and functional groups incorporation. The present work attempts to elucidate these complex and simultaneous changes in the materials.
Good adhesion property can be achieved if between the two layers, in our case needlefelt non-woven fabric and a nanofibre mat, can initiate a boundary contact area, figure 1.
The aim of the work is to define empirically the changes in nonwoven fabric (filters) designed for pad of the nanofibres layer. Presented results are related to the change of cation-exchange properties after plasma chemical modification (Wp = 0.5-2.0 kW, P = 80 Pa; gas consumption G = 0.04-1.2 g/s; f = 1.76 MHz, time t = 1 and 2 min and plasma- forming gases - Ar and O2).

Mechanical, physical, chemical, and electrical properties of the treatment of textile are changed simultaneously. Sample thickness of the plasma-treated non-woven fabric are presented in table 1 and the change is greater at O2 and 2 min treatment time. At the same

conditions studied samples have different moisture content, figure 2. In that study differential scanning calorimetry analysis of treated samples is performed and the change in PET fibres shows the difference in the amount of heat required to increase the temperature, table 2.

Table 1. Change in thickness depending on the type of gas used.

No	Untreated	Plasma treatment in oxygen (O_2) for 1 min	Plasma treatment in oxygen (O_2) for 2 min	Plasma treatment in argon (Ar) for 1 min	Plasma treatment in argon (Ar) for 2 min
Thickness average value $\bar{x}$ (mm)	1.948	1.929	2.043	1.853	1.910
Dispersion s (mm)	0.042	0.027	0.057	0.024	0.032

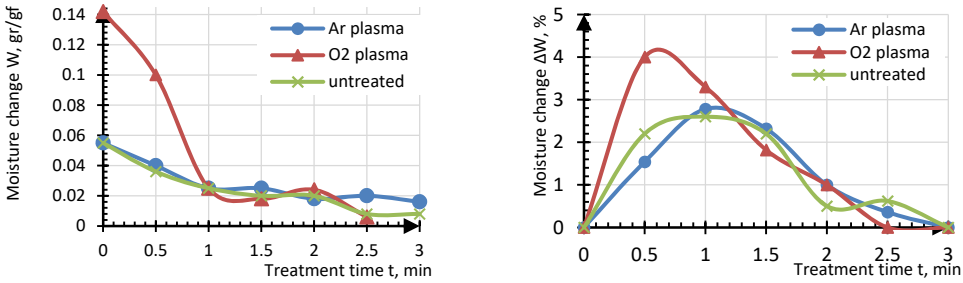

Figure 2. Experimental data on the change of moisture in the samples at P = 80 Pa and O2 and Ar gases.

Table 2. DSC evaluation of plasma treated PET non-woven samples.

No	Type of plasma-forming gas	Plasma treatment duration *t*, min	Entalpy Δ H, J/g	Peak Area, mJ	Max. peak value °C	Peak height, mW
1	Ar	1	60.4969	120.994	252.11	6.8683
2	Ar	2	62.2919	124.584	251.25	7.3700
3	O_2	2	70.3840	126.691	251.66	6.7632
4	O_2	1	63.0338	125.461	251.21	6.0325
5	Untreated	0	80.1161	208.302	240.31	8.7330

After the plasma treatment the PET fibres surface are activated and the CEC increases (table 3). Plasma treatment leads to additional O2-containing functional groups.

Table 3. CEC (cation exchange capacity) evaluation of plasma treated PET non-woven samples.

No	Type of plasma-forming gas	Treatment time *t*, min	CEC, mEq/100g
1	Ar	1	10.9
2	Ar	2	11.2
3	O_2	2	19.3
4	O_2	1	18.6
5	Untreated	0	7.8

Cold plasma activation in O2 and Ar was used for polyester non-woven modification, designed to produce high-grade double-layer dust filters for automobile industry. Plasma activation is an environmentally friendly (green) technology for filter functionalization to improve hydrophilicity, wettability, wicking, and ion exchanging interaction. Polyester plasma activation produce different new functional groups on the surface of the fibres. Experimentally, as a result of pre-treatment in plasma, the adhesion between the two layers of the double layer gas filter has been improved. The most significant change in the values of moisture observed in the samples in O2 medium.

Acknowledgments. The authors would like to thank the Research and Development Sector at the Technical University of Sofia for the financial support.

9th International Scientific Conference
Research and Development of Mechanical Elements and Systems
Kragujevac, Serbia, September 5-7 2019

ESTIMATION OF LASER CUTTING PROCESS EFFICIENCY

Constantin Cristinel Girdu[1], Laurentiu Aurel Mihail[1], Mircea-Viorel Dragoi[1]

[1]Transilvania University of Brașov, Manufacturing Engineering Department,
Bdul Eroilor 29, 500036 Brasov Romania

Key words: metal laser cutting, specific energy, efficiency indicators, Hardox steel.

Generally speaking, efficiency of machining processes is a relative vague concept. It can be interpreted in terms of economical or technical aspects, it can refer to different specific processes, or to a certain material. In the technical literature, the efficiency of machining processes is approached mainly from the perspective of the ways to increase it. A survey of literature reveals different kinds of the concept's approach. Thinking about the specific of laser processing, different types were found: cutting, remote cutting, laser-assisted machining. The present paper proposes a discussion on different ways to interpret efficiency as effectiveness, and how it is directly, or indirectly influenced by the cutting parameters.
To narrow down the area of research, and to be more specific, the present paper focusses on laser cutting of metal. For this particular category of materials, the process consist mainly of metal melting, and removing the melt. The volume previously filled by the melt becomes the so called kerf that separates the part and the metal sheet. In this context, efficiency can be interpreted in different ways, or expressed by different indicators, as follows:

- Effectiveness, that is how fast a part is produced;
- Linear specific energy (E_l). This expresses one way to appreciate the measure the process is friendly to environment. This can be estimated by the quantity of energy spent to process a unit of length of part edge. Of course, the lower the linear specific energy is, the more environmentally friendly the process is considered to be;
- Surface specific energy (E_s). This indicator is intended to take into account the thickness (h) of metal sheet. It expresses the energy spent to process a unit surface on the side of cut part.
- Volume specific energy (E_v). This is a third mean to appreciate the measure the process is environmentally friendly. This can be estimated by the quantity of energy spent to melt a unit of volume, and is interpreted in the same way as the previously specified indicator.

These indicators are influenced by some input parameters as: laser power (P), cutting speed (v), pressure of the assistant gas (p), the processed material itself (characterized by different properties as specific heat, conductivity and other), the metal sheet thickness (h). It is important to note that these parameters influence directly by their values the efficiency indicators, but also indirectly, by means of their combined effect/interaction (especially the

couple power-speed). The cutting parameters can be directly adjusted in the process, to influence in a direction or in the opposite one any efficiency indicators. Some other data are given, and cannot be changed for a specific batch, e.g. the part material itself or the thickness of the metal sheet. This is the reason for that the given data are not involved in computing efficiency indicators.

A case study was conducted to illustrate using the indicators of laser cutting processes efficiency. Hardox 400 and Hardox 450 steels have been cut with different combinations of input data. Combinations of laser power and cutting speed levels were selected from data sets, according to design of experiments (DOE) procedures. The combinations used limit values for P and v, which were determined by means of initial test screening trials, as to be sure that cutting process develops properly, that means that the part is completely cut (separated from the sheet material) and the machined surface's roughness is appropriate. Even if the combinations where the extreme low, or extreme high values for both the input parameters were coupled, the part output quality was acceptable. Analysing the output data, some conclusions have been drawn:

1. It is obvious that for both the materials, the linear specific energy E_l, which depends exclusive on P and v, the highest value of E_l is recorded for the combination with lowest P and highest v; the difference in terms of E_l value between the two materials is given by their different properties.
2. The influence of h on surface specific energy E_s, shows that this indicator becomes more useful when it is to compare in terms of cutting efficiency related to environment protection parts made of different materials and having different thickness
3. Criterion based on volume specific energy E_v. comes with some apparently random results. Being involved more input data, it is almost impossible to appreciate without this indicator which is the least and most energy consuming sample. According to this criterion, the best combination is: Hardox 400, thickness of 10 mm, laser power medium, and cutting speed at its highest value. The worst sample (the most energy consumer per melted volume unit) is Hardox 450, thickness of 12 mm, laser power at its lowest value, and cutting speed at its lowest value. In this context, referring to lowest and highest value of a parameter we mean the extreme value used for a certain material. This is an important remark, because from technological reasons, different minimum-maximum P and v values must be set up for different materials, depending on their physical properties.
4. It is important to select correctly the indicator used to appreciate a certain case (set of part samples), according to the input variable data that can be controlled. We have to keep in mind that in certain cases, some input data could be fixed, they may not be changed (e. g. material, or thickness of the part).

Nowadays, when environment protection becomes a stringent problem, taking care about energy consumption is an important task. In this context, the energy consumption becomes an important criterion of optimization in manufacturing. The technical/technological criterion remains the most important, but the environment protection cannot be neglected anymore. The research presented here has proved that even respecting the technological restrictions, that is obtaining parts conform to specifications, still optimization in terms of energy consumption can be performed. The task is not easy, because of the many input data involved and of the particularities specific to each application apart. A mean to appreciate the efficiency of laser cutting of metals are the efficiency indicators, which have to be selected correctly, according to the specific available input data.

9th International Scientific Conference
Research and Development of Mechanical Elements and Systems
Kragujevac, Serbia, September 5-7 2019

SELECTION OF WELDING PROCESS FOR ASSEMBLING THE ALUMINUM TRUSS USING THE CES SELECTOR SOFTWARE

Dragan Adamović[1], Jelena Živković[1], Miloš Lazarević[1], Bogdn Nedić[1], Miroslav Živković[1], Fatima Živić[1]

[1]University of Kragujevac, Faculty of Engineering, Sestre Janjić 6, 34000 Kragujevac, Serbia, adam@kg.ac.rs

Key words: materials selection, process selection, aluminum, welding, CES selector.

Three new activities are equally represented in the new product development: structural design, material selection and selection of manufacturing process. By combining different types of materials, shapes and dimensions of products and manufacturing processes, various product solutions are obtained. An increasing number of materials and manufacturing processes make the construction process more complex and responsible, and it is very often expected from them to decisively influence the properties and behavior of the product. Therefore, designers are increasingly turning to the methodical process of material selection, and less to experience, although it is still necessary in some phases of decision making. For each possible solution, a specific manufacturing process is determined and the choice of materials is often determined by the criteria of technology and costs. Product development methods simultaneously analyze different design-manufacturing variants, varying the design forms, materials and methods of manufacturing. Structural design, material selection and the selection of manufacturing processes are inseparably linked activities. The choice of the manufacturing process is a difficult task because the same part can be formed in several ways, with different quality, manufacturing time and costs. The manufacturing process must achieve the desired quality for the selected material, shape, dimensions, tolerances and workpiece surface conditions with minimal costs and manufacturing time. In doing so, the constructor should be provided with information about the possibilities of the available manufacturing processes in order to select the most favorable process in the given circumstances.

CES Selector is one of the most commonly used Expert Systems (ES) for material or process selection. It is a PC application that enables both constructors and material experts, and other engineers, to find proper materials or process that will constitute the optimum solution for their product. This product is of great help in decision making about materials in the early stage of product design, redesign or replacement of existing material with a new one.

The joining process selection will be shown in the case of a roof truss structure. The material selected for this construction is aluminum. The structure should be composed of tube profiles of different lengths. The construction must be strong, without the occurrence of damage during use. The joining can be performed using inseparable (welding, soldering, gluing) or separable (rivets, screws) connections. Separate connections are less suitable than inseparable due to lower endurance, and also because of the higher execution costs. Welding is certainly the most appropriate inseparable bonding, but due to the number of welding methods it is necessary to choose the most suitable one.

For the welding of the aluminum truss, it is necessary to choose the optimal welding procedure. Table 1 shows the technical and economic constraints that the welding process must meet.

Table 1. Welding process requirements

Function	**Welding of the truss rods**	**Constraints**
Constants	Material: aluminum Type of welded joint: butt and corner joint. Type of welded joint loading: compression, tension and bending. Shape: circular; Mass: 0,5 – 100 kg; Radius: R = 15 mm; Pipe wall thickness: d = 4 mm Process type: discrete	Technical constraints
Goal	Cost reduction	Economic constraints
Free variables	Process selection Process work conditions	

Table 2 lists the processes that meet the before mentioned requirements.

Table 2. Processes that meet the requirements

Welding process	**Comment**
Friction welding	Friction welding is not applicable in more complex shapes of truss. In the case of truss structures there is an approach problem.
Submerged arc welding	It was not found that this method can be used for welding of aluminum. This procedure is used in large batches. Welding is carried out in a horizontal position.
MIG welding	The possibility of a better approach and according to Table 1 it is suitable for welding of aluminum.

According to Table 2, it can be concluded that the MIG welding procedure is the optimal solution, both in technical and economic terms.

The illustrated example of selecting the welding process of the roof truss construction using the CES Selector indicates that the mentioned software can be used effectively, among other things, for the selection of the welding process.

Acknowledgments: This work was funded by the Ministry of Education and Science of the Republic of Serbia under the contract TR32036, TR34002 and TR35021.

RESEARCH AND DEVELOPMENT IN FIELD OF VECIHLES AND TRANSPORT

IRMES KRAGUJEVAC 2019

9th International Scientific Conference
Research and Development of Mechanical Elements and Systems
Kragujevac, Serbia, September 5-7 2019

- PAPER BY INVITATION -

ADVANTAGES OF USING DRONES VS HELICOPTERS IN CIVIL AIR TRANSPORT

Petar Mirosavljević[1], Miloš Marina[1], Dalibor Pešić[1], Radomir Mijailović[1]

[1]University of Belgrade, The Faculty and Transport and Traffic Engineering, Vojvode Stepe 305, 11000 Beograd, Serbia, perami@sf.bg.ac.rs

Key words: drone, helicopter, momentum theory, ground effect.

This paper presents the important annual characteristics of the drones, primarily quadcopters, as the dominant solution for drilling. The aim of the paper is to show the drones themselves and to demonstrate the benefits of using trunks in relation to helicopter of civil air transport. Particular attention is paid to the stability of drones during basic operations and during near-surface operations and ground effects.
The analysis of the use of drones, as well as its ability to replace traditional aircraft, was done primarily for their expansion use. So far, this topic has not been given too much attention, and one of our goals has been to focus attention on them. A special thing that should be of concern is the integration of drones into civil air traffic. The issue of integration is open for the time being and it is inevitable that it will one day arise.
The beginning of the work is related to the modern structures of drones, first of all the quadcopter structure. In addition to the appearance of the structure itself, the paper outlines certain requirements that the structure must satisfy in order to be adequate for use. Part of the paper is devoted to the creation of buoyancy force and the theory of the ideal rotor. After this analysis, we moved on to the possibilities of movement and control of drones in space. The hovering phase was analyzed, as well as the effects of forces and moments in the lateral and rotational motion of the drones. At the very end of the paper, an analysis of the effect of ground efect on drones was performed and a comparative alasis of this effect on helicopters.
The main advantages of using a quadcopter, as the dominant solution for the structure of drones, are the very features of the structure and especially the effects of the creation of aerodynamic force. The quadcopter is constructed so that the adjacent rotors rotate in opposite directions, while the opposite rotors rotate in the same directions. An illustration of the rotor orientation can be seen in Figure 1. This rotor orientation avoids the possibility of generating torque around the structure due to the creation of buoyancy force on the rotors themselves. In the case of a quadcopter, there is no need to hire an additional engine to respond to torque, such as in the case of helicopters.

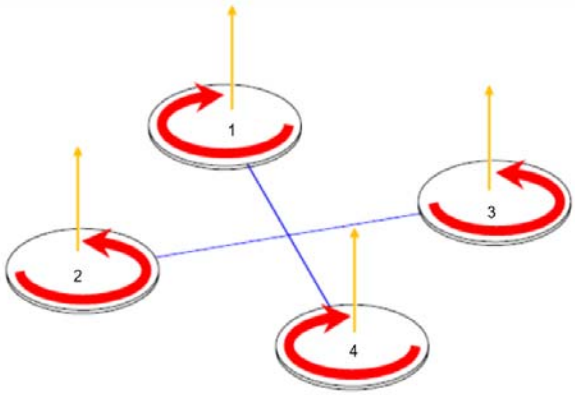

Figure 1. The direction of rotation of the quadcopter rotor

The angular groun effect was only thoroughly processed for helicopters until almost thoroughly. Drones-related research on this topic has hardly been done. This effect implies that the rotor blades near the ground are not capable of fully developing downward stance. Thus, a significant increase in buoyancy occurs and less engine power is required to create aerodynamic buoyancy to overcome aircraft weight. This effect occurs near the ground, more precisely during landing and take-off, that is, the most critical phases of aircraft flight. The quadcopter is largely non-expressive, as is the case with helicopters. The main contribution to this is primarily the structure of the quadcopter, namely that the buoyancy force is created on four rotors. Because the force is created on four rotors, the rotor diameters are smaller than when using one rotor to create buoyancy force. Considering that the cluster effect is pronounced near the ground, more precisely at altitudes less than the radius of the rotor, we come to the very reason that this effect is almost absent from the quadcopter.

The entire analysis was done to show the basic principles of the operation of drones, as well as their basic capabilities when used in comparison with traditional aviation vehicles.

9th International Scientific Conference
Research and Development of Mechanical Elements and Systems
Kragujevac, Serbia, September 5-7 2019

VEHICLES OPTIMIZATION REGARDING TO REQUIREMENTS OF RECYCLING *EXAMPLE: BUS DASHBOARD*

Saša Milojević[1], Radivoje Pešić[1], Jovanka Lukić[1], Dragan Taranović[1]
Tomas Skrucany[2], Blaža Stojanović[3]

[1]University of Kragujevac, Faculty of Engineering, Department for Motor Vehicles and IC Engines, Sestre Janjić 6, 34000 Kragujevac, Serbia
sasa.milojevic@kg.ac.rs, pesicr@kg.ac.rs, lukicj@kg.ac.rs, tara@kg.ac.rs
[2]Department of Urban Transport, University of Žilina, Slovakia
tomas.skrucany@fpedas.uniza.sk
[3] University of Kragujevac, Faculty of Engineering, Department for Mechanical Construction and Mechanization, Sestre Janjić 6, 34000 Kragujevac, Serbia, blaza@kg.ac.rs

Key words: bus dashboard, dismantling, optimization, recycling.

In 2016, more than 22.5 million of trucks and busses (approx. 7.5 million in U.S.) and approx. 72.1 million of personal cars (approx. 4.2 million in U.S.) were produced globally. According to prognosis, a total of around 107 million vehicles will be manufactured worldwide in 2020.

Parallel the number of end-of-life vehicles (ELV) arising constantly, and there are gaps between the numbers of deregistered and ELV in many countries. There is no detailed information available because of a certain number of de-registered vehicles are commercially exported to the underdeveloped countries as second hand.

If current trends continue and no relevant legislation from design to disposal vehicles, The Globe can become overloaded vehicles at the end of the service cycle. Vehicle recycling and reuse of materials incorporated is very important from that point of view and presents a solution the problem. On this manner it is possible reuse of consisting materials and optimization of End-of-Life Vehicles.

In European Union has defined targets to be achieved in the future for the recycling rate of vehicles at the end of their service cycle. Directive of the European Parliament and of the Council 2000/53/EC regulate waste management in the vehicle sector. This manuscript presents in global the international legislative in this field, regarding to the situation in Republic of Serbia. As contribution, during production of domestic city bus running on natural gas, performed the replace of material for bus dashboard on the basis of plastic and

polyurethane foam, with ecological material with carbon inserts. The requirements for dismantling, reuse and recycling are integrated in the design of new bus.

Regarding dismantling (consisting of collection, depollution and crushing) of ELV in Europe, two main aspects have to be considered.

First, there is evidence suggesting that ELV are treated illegally in some cases. However measures which make the disposal of an old vehicle in the country of de-registration more attractive, such as refunds obtained in a deposit-refund system, would help reduce illegal shipments of ELV.

Second, there is evidence suggesting that even in authorized treatment facilities dismantling (specifically depollution) is not in full compliance with the relevant requirements of the existing ELV Directive.

Domestic recycling industry is in this moment in the stage of development. The problem is the design of the vehicles, which does not allow an adequate and rapid implementation of the process of dismantling, and the lack of unified system.

Due to existence of several domestic bus manufacturer in the market solution to the problem of recycling these vehicles is very important. Designing regarding to recycling demands inside ELV Directive allow not only to meet domestic ecological requirements, but also to contribute to the increase in the export potential of the vehicle trademark.

During researches, redesigned is local city bus running on natural gas. Dismantling information for the correct and environmentally sound treatment of ELV formed, too.

An example of modeling the dismantling of plastic parts of the city bus type (203 CNG-S) podium dashboard is shown in Figure 1.

The result is the catalog for the dismantling of city bus, which meets the requirements of the EU regulations on the suitability of vehicles for disposal.

Figure 1. Integrated platform with new design of podium dashboard for city bus

Acknowledgments. The paper is a result of the research within the project TR 35041 financed by the Ministry of Science and Technological Development of the Republic of Serbia.

9th International Scientific Conference
Research and Development of Mechanical Elements and Systems
Kragujevac, Serbia, September 5-7 2019

ASSESSMENT OF DYNAMIC PROPERTIES OF A CARRIAGE USING MULTIBODY SIMULATION CONSIDERING RIGID AND FLEXIBLE TRACK

Ján Dižo[1], Miroslav Blatnický[1]

[1]University of Žilina, Faculty of Mechanical Engineering, Univerzitná 8215/1, 010 26 Žilina, Slovak Republic, jan.dizo@fstroj.uniza.sk, miroslav.blatnicky@fstroj.uniza.sk

Key words: carriage, multibody system, dynamic properties, rigid and flexible track, wheel forces.

Recently, we cannot imagine investigation and analysing mechanical properties of railway vehicles without using state-of-art tools. They are implemented in whole process of design, analysing, verification, testing and optimising of railway vehicles. Such an approach saves time for development, production costs and finds application across whole spectrum of produced types of railway vehicles. In order that the approach based on simulation computations can reliably simulate the reality, a virtual model of a railway vehicle has to take into account as many factors as important.

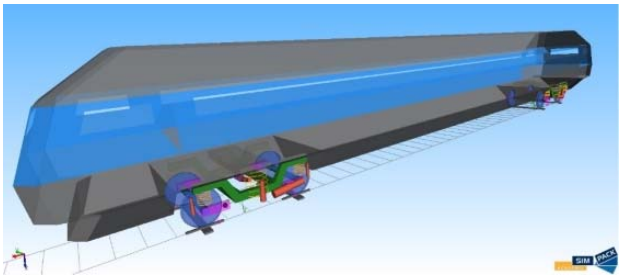

Figure 1. A virtual model of the analysed passenger car created in Simpack software

When we investigate behaviour of a railway vehicle in terms of dynamics, we used the multibody approach for creating its computational model. The goal of this article is evaluation of output quantities of a passenger car from the dynamics point of view. The main objective is assessment of selected values for rigid and flexible models of a track. There are evaluated quantities, which belong to main assessed outputs for investigation of dynamic properties of a passenger car. There are values of vertical forces in the wheel/rail contact as the indicator of dynamic load of a railway track as well as the bodies of a railway vehicle.

This contribution introduces a study of influence of flexible track on dynamic response, i. e. selected output quantities. The multibody models of a passenger car and a track have been created in Simpack program package. There is a commercial program, which enables to an user building up many kind of virtual models, which can be quite simple subsystem of any transport mean, e. g. individual parts of suspension system, partial systems of a drive mechanism, such as an engine, gearbox, etc., or there can be a bogie of a railway vehicle, even an entire train sets. In our work we have submitted a passenger car to simulation computations. Its model created in the Simpack software package (figure 1).

We have selected only several speeds, which can concrete show influence of different running speed on waveforms of output quantities and for various track flexibility foundation, i. e. with constant values of stiffness-damping coefficient and with stiffness-damping coefficients given by a sinusoidal function even with softer and stiffer values.

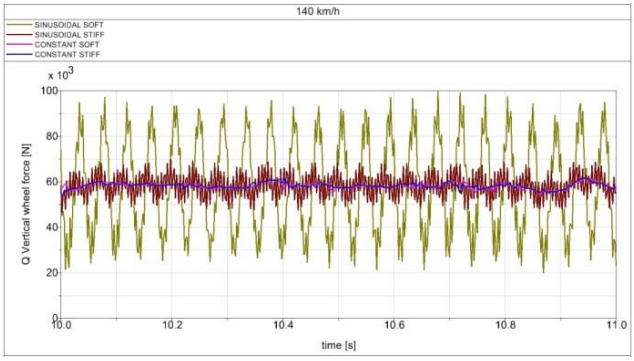

Figure 2. Waveform of the dynamic vertical force for various track flexibility foundation, 140 km/h

In our research we have focused on dynamic response of a passenger car running on a track represented by the dominant forces, which act in the railway wheel and railway track during operation of a railway vehicle, namely the vertical wheel force. This force affects significantly the dynamic loads of a track as well as dynamic loads of main structural units of a railway vehicle.

Based on reached results we have found out that the dynamic response of the passenger car, which indicate the track loading as well as the railway vehicle loading depends on the credibility of input data for track flexibility foundation.

Acknowledgments. This work was supported by the Cultural and Educational Grant Agency of the Ministry of Education, Science, Research and Sport of the Slovak Republic of the Slovak Republic in the project No. KEGA 077ŽU-4/2017: Modernization of the Vehicles and engines study program. The work was supported by the Slovak Research and Development Agency of the Ministry of Education, Science, Research and Sport of the Slovak Republic in the project No. VEGA 1/0558/18: Research of the interaction of a braked railway wheelset and track in simulated operational conditions of a vehicle running in a track on the test bench.

9th International Scientific Conference
Research and Development of Mechanical Elements and Systems
Kragujevac, Serbia, September 5-7 2019

DETERMINING OF THE DRIVE POWER OF A TRANSPORT MACHINE FOR DISABLED PERSONS USING A COMPUTATIONAL MODEL

Miroslav Blatnický[1], Ján Dižo [1]

[1]University of Žilina, Faculty of Mechanical Engineering, Univerzitná 8215/1, 010 26 Žilina, Slovak Republic, miroslav.blatnicky@fstroj.uniza.sk, jan.dizo@fstroj.uniza.sk

Key words: transport machine, stair lift, drive power, electric motor, computational model.

The article deals with calculation of a stair lift drive and its design. The aim is the determining the necessary power of the used electric motor depending on the variable input values such as a passenger weight, a gradient of the seat lift etc. Calculating the required power for operation of the equipment is essential for selecting the optimal drive motor. In practice, the mathematical-physical principle of solving a problem such as drive calculation is often neglected. This results in the use of excessively powerful propulsion equipment, and thus in excessive financial cost in mass production. Consequently, by designing a drive-train, it will be possible to design the entire drive mechanism, i.e. motor, gearbox, gear module, etc. A significant part of the overall solution will be the design of the shaft for the drive pinion and its analytical dimensional calculation in comparison with the numerical solution. This will fulfil the prerequisites for optimizing the current shaft design by reducing its mass from the current value of 1.185 kg while the safety and reliability conditions of the construction are still met.

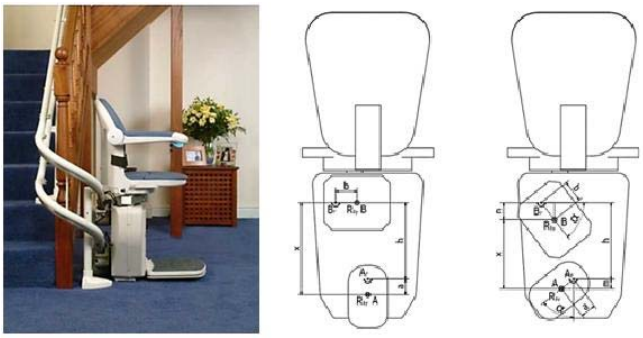

Figure 1. A real model of SA Alfa stair lift (left), schematic change of geometry when the carriage is tilted due to the ascent of the track (right)

One of the social aspects of a modern advanced society is its ability to help those in a difficult situation. One subset affliction of people is a restriction of a person's mobility. Several devices have been contrived for people with disabilities to facilitate surmounting various obstacles. A stair seat can also be found between these devices, which are also the subject of the issue solution (figure 1).

Such a handling machine is usually made of more kind of material to reach suitable mechanical properties of particular components in combination with required lifetime and acceptable price. There are most often used combination of standard steel, high strength steel, light metals, mainly such as aluminium alloys, plastics etc.. The latest types of stair lifts have the automatic process of tilting and they dispose of a remote control. The drive-train is composed of an electric motor, a gearbox and a gear wheel, which is in the mash with a rack.

Numerical calculation of stress in shaft was performed by means of the finite element method. The mesh was created with 2 mm long elements and was formed by 53 684 nodes and 31 234 elements (figure 2 left). The equivalent (von Misses) stress was selected as output and then the calculation was started. The calculation results are shown in figure 2 right.

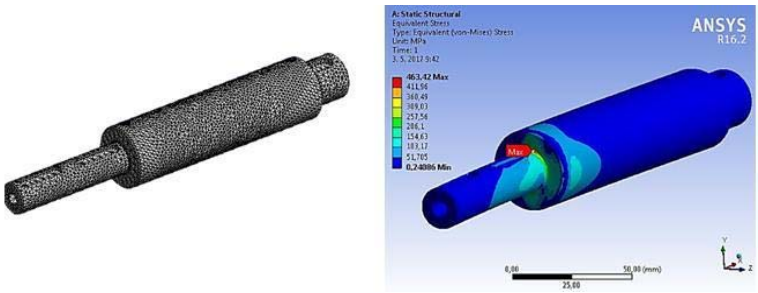

Figure 2. FEM mesh of the analysed shaft (left) and the stress distribution in the shaft (right)

The shaft material used is steel 1.7131 (16MnCr5, STN 14 220) with tensile strength R_m = 780 – 850 MPa and with the minimum yield strength R_{emin} = 550 MPa. The maximum stress value determined by the simulation is σ_{max} = 463.42 MPa.

The analysis proved the suitability of the used shaft for the specified operation, but also revealed the space for its optimization because of the minimum stress values in the bulk of the shaft volume.

Acknowledgments. The work was supported by the Cultural and Educational Grant Agency of the Ministry of Education of the Slovak Republic in project No. KEGA 077UU-4/2017: Modernization of Vehicles and Engineers Study Program. The paper was prepared within the framework of the grant project of the Ministry of Education of the Slovak Republic KEGA, n. 018ŽU-4/2018: „Innovation of didactic approaches and content of subjects of technical diagnostic as a tool for enhancing the quality of professional knowledge for practice needs."

IRMES KRAGUJEVAC 2019

9th International Scientific Conference
Research and Development of Mechanical Elements and Systems
Kragujevac, Serbia, September 5-7 2019

TECHNICAL SOLUTION OF THE UNDER LOCOMOTIVES VISUAL INSPECTION SYSTEM

Aleksandar Miltenović[1], Dušan Stamenković[1], Milan Banić[1], Miloš Simonović[1]

[1]University of Niš, Faculty of Mechanical Engineering, Aleksandra Medvedeva 14, 18000 Niš, Serbia, aleksandar.miltenovic@masfak.ni.ac.rs

Key words: visual inspection system, locomotive, product development, technical concept.

In recent years, liberalisation of rail cargo operators market brought to the position of a number of small rail operators that are operating on rail infrastructure. Most of them are relatively small with specific cargo transport products, limited number of locomotives and wagons and with limited service resources. Independently of the cargo operator size, they are also obligated to have regular inspections according to the cargo regulations. According to railway regulations, railway vehicles, primarily locomotives, should be inspected relatively frequently, and inspections differ from those in which the visual inspection is sufficient to those for which it is necessary to measure something or open a part of the vehicle.

Smaller inspections like “service inspection” of electric locomotives includes:

- Visual control (from inspection pit and exterior) of boxes and equipment on it
- Visual inspection of handrails, axle assemblies, wheel rims, traction engine covers, rubber shock absorbers, winding springs and hydraulic shock absorbers.

In order to develop the appropriate system for visual inspection of the railway vehicle from the bottom on a track without inspection pit, research of technical solutions has been carried out, which can be applied with specific requirements on the railway.

The conceptual solutions of the system are elaborated on the basis of two initial conditions:

- The system is mobile (mobile) and the locomotive is static (no moving) or vice versa
- At the location where the visual control is carried out, it is possible to set the appropriate surface

In total, four conceptual technical solutions have been developed: ”rod”, “tray”, “runway” and “trolley” (Figure 1).

a) “rod” b) “tray” c) “runway” d) “trolley”

Figure 1. Overview of technical solutions

The technical solution "rod" is based on similar products used for inspection and control of passenger vehicles and trucks at border crossings, where the solution is adapted to the needs of inspection of railway vehicles and on-line inspections.

Technical solution "tray" is an improved technical solution "rod" based on the installation of the entire device on the rails.

The technical solution of the "runway" is designed as a solution in which it is possible to easily position the camera to the desired location below the locomotive. For this purpose, a frame was constructed that would be placed between the rails and would be placed on the surface with 3.6 m or 18 m lenght.

The technical solution of the "trolley" is designed as a solution where the camera with the device would move on the profiles back and forth and thus allow for longitudinal movement, and for the transverse movement on the device there are motors that allow the remote control to position the camera to the desired place.

Evaluation of the concepts has been done according to following criteria: price, user friendliness, degree of automatization, inspection speed and mass. For every factor is determined weight coefficient.

According to evaluation the best grade has concept “trolley”. The lowest grades have concepts “runway” due to their price. Concepts “rod” and “tray” are having a little lower Sum of grades than “trolley”.

9th International Scientific Conference
Research and Development of Mechanical Elements and Systems
Kragujevac, Serbia, September 5-7 2019

IMPROVEMENTS OF THE RANGE EXTENDER FOR A 48V ELECTRIC VEHICLE

Marcin Noga[1], Paweł Gorczyca[1], Radosław Hebda[1]

[1]Cracow University of Technology, Faculty of Mechanical Engineering, Institute of Automobiles and Internal Combustion Engines, Jana Pawła II 37 Avenue, 31-864 Kraków, Poland, noga@pk.edu.pl

Key words: electric vehicle, range extender, overall efficiency, spark ignition engine, three-way catalyst conversion efficiency, noise reduction.

The article describes a further stage of development work of the range extender (RE) designed at the Cracow University of Technology (CUT) for a 48V electric light commercial vehicle. The range extender is an auxiliary power unit with a maximum output power of 2.65 kW. It was built on the basis of a three-phase alternating current generator driven by a single-cylinder spark-ignition engine. A general view of the developed range extender attached to the body of vehicle is presented in Figure 1.

Figure 1. The developed range extender (yellow rectangle) attached to the vehicle body

As part of further development work, the engine was equipped with a muffler with an integrated three-way catalytic converter (TWC) to reduce an emitted noise, as well as to reduce exhaust emissions. In order to be able to efficiently process exhaust gas in the catalytic reactor, modifications of the fuel system were introduced, enabling feeding with a stoichiometric air-fuel mixture. The principle of operation of the air-fuel ratio (AFR) correction system consists in a dilution of the rich mixture formed in the carburetor using the air fed downstream from the carburetor. The system works in a closed-loop with an exhaust oxygen sensor.

Applied modifications of the range extender had a significant impact on minimizing the effect on the environment by reducing the noise level and toxic components of exhaust gases. In addition, the use of the exhaust gas correction system has made it possible to improve the overall efficiency of the unit, which is important in terms of reducing carbon dioxide emissions and reducing the costs of generating electricity necessary to drive the vehicle. The results confirmed that the developed AFR correction system properly performs the assigned task. In a figure 2 the selected results of research are presented.

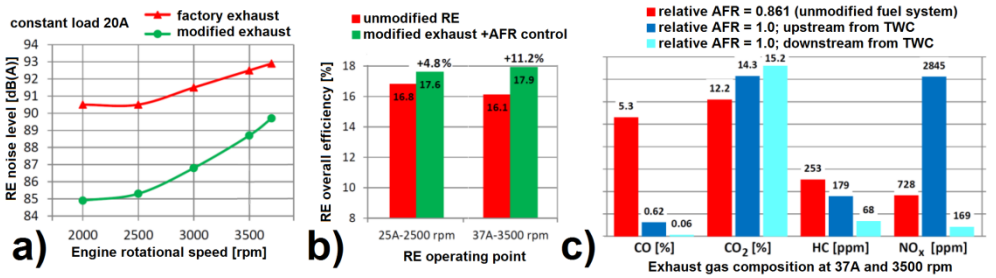

Figure 2. Selected comparisons of the results obtained for unmodified and improved range extender; a) noise level, b) overall efficiency, c) exhaust composition.

The tests of the general efficiency of the auxiliary power unit allowed to indicate the points in which the range extender operation is the most effective, which allows the development of a favorable algorithm for the control of the assembly depending on the current state of the battery and the driver's needs. Despite the use of a simple generator and belt transmission control, a more beneficial result of the overall efficiency of the range extender developed at CUT was obtained than the device offered commercially [2].

Dynamic tests of the charging unit carried out after completion of the stationary part showed its correct operation. The energy supplied to the vehicle's electrical system by range extender after depleting the energy stored in the vehicle battery enabled the use of full range in all-electric mode without the user's fear of not reaching the destination. In addition, during the second attempt, the start-up of the range extender and its continuous operation from the moment of using half of the energy stored in the battery allowed for a two-fold increase in the range of the vehicle.

In the further development phase of the project, it is also planned to use the integrated electronic ignition - injection system and engine modifications, which will further increase efficiency and reduce exhaust toxicity also in transient states (start-up, heating, speed and load change, engine shutdown). Ultimately, consideration is also given to using the alternative fuels for the range extender, such as a mixture of gasoline with bioethanol - E85 or natural gas, which will reduce CO_2 emissions due to the more favorable ratio of hydrogen to carbon for these fuels compared to gasoline.

References (for the extended abstract)

[1] Noga M and Gorczyca P 2019 Development of the range extender for a 48 V electric vehicle, Combustion engines **177**(2) 113-121

[2] Range Extender, the future of electric vehicles, www.elp-power.com/en/chanpinzhongxin-248659-98591-item-423690.html (accessed on Jun. 2019)

9th International Scientific Conference
Research and Development of Mechanical Elements and Systems
Kragujevac, Serbia, September 5-7 2019

ANALYSIS AND FORMING COMPUTATIONAL MODEL OF ZIPLINE

Jovan Vladić[1], Tanasije Jojić[1], Radomir Đokić[1], Anto Gajić[2]

[1]University of Novi Sad, Faculty of Technical Sciences, Trg Dositeja Obradovića 6, 21000 Novi Sad, Serbia, tanasijejojic@uns.ac.rs
[2]Mine and Thermal Power Plant, 76330 Ugljevik, Bosnia and Herzegovina, antogajic@yahoo.com

Key words: zipline, catenary, computation model, computer simulation, motion resistance.

The term "zipline" represents a system containing a tightened steel rope by which a person is carried by high speed travelling trolley. The trolley and the person are moving under the influence of their own weight. The main aim is causing increasing excitement, as in so-called adrenaline sports (*Jojić T, Vladić J and Đokić R 2018 Specific machines and devices with horizontal rope as carrying element – zipline, Proceedings of the Faculty of Technical Sciences, Vol. 33, No. 1, pp. 13-16*). Figure 1 shows a schematic representation of a zipline with main notions.

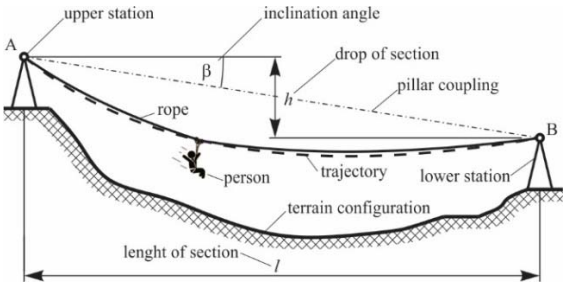

Figure 1. Schematic representation of zipline

The computational model is based on the catenary theory which represents an elastic flexible thread freely suspended between two supports located on the horizontal (*l*) and vertical (*h*) distance and loaded with its own weight. As the use of hyperbolic functions is relatively complicated for engineering practice, the catenary is replaced by the appropriate parabola:

$$y = \frac{q \cdot x \cdot (l - x)}{2 \cdot H \cdot \cos \beta} \cdot k + x \cdot tg\beta$$

The relevant computational model is formed by neglecting small quantities of high order, so the computational model, shown on figure 2, can be represented as a movement of a concentrated mass along the trajectory determined for static conditions (*Alamoreanu M and Vasilescu A 2014 Theoretical Aspects of Zip Line Analysis, Proceedings of VIII Triennial International Conference Heavy Machinery - HM 2014 pp. 131-136 and Kožar I and Torić M N 2014 Analysis of body sliding along cable, Coupled Systems Mechanics, Vol. 3, No. 3, pp. 291-304*).

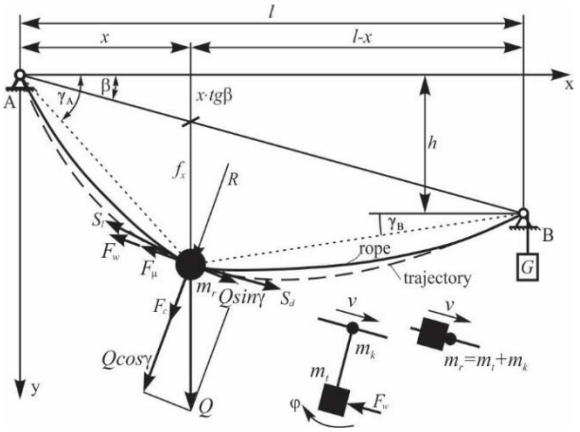

Figure 2. Computational model of a zipline

The air resistance and rolling resistance are acting on the concentrated mass while moving in the direction which is always opposite to the direction of movement.

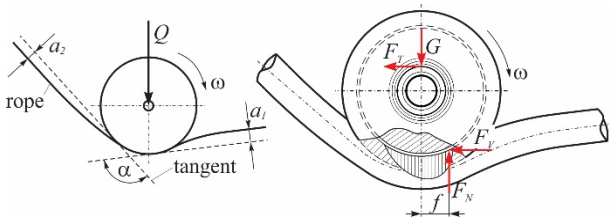

Figure 3. Model of wheel rolling along steel rope

The analysis was made by computer simulations for specific conditions of zipline whose installation was planned on Fruška Gora (*Vladić J, Đokić R and Jojić T 2017 Elaborats I,II i III - Analysis of the zipline system in Vrdnik*).

It is notable that increase of tension rope force increases reach, but reduces maximal achieved velocity. On the other hand, for a given tensile force, heavier passengers are achieving higher maximal velocity.

9th International Scientific Conference
Research and Development of Mechanical Elements and Systems
Kragujevac, Serbia, September 5-7 2019

MATHEMATICAL MODELS OF VERTICAL TRANSPORT MACHINES AND METHODS FOR ITS SOLVING

Radomir Đokić[1], Jovan Vladić[1], Tanasije Jojić[1]

[1]University of Novi Sad, Faculty of Technical Sciences, Trg Dositeja Obradovića 6, 21000 Novi Sad, Serbia, djokic@uns.ac.rs

Key words: machines of vertical transport, mathematical models, numerical simulation.

Analysis of the vertical transport systems and machines means that we must form mathematical models with systems of differential and algebraic equations. The paper presents the issues with mechanical models of the vertical transport systems (elevators and the mining elevators) and numerical methods for formed mathematical models solving according to basic parameters of exploitation facilities in mines. Analysis of the vertical transport systems and machines means that we must form mathematical models with systems of differential and algebraic equations.
The proper dynamic model for describing dynamic behavior of the device with a driving pulley is shown in figure 1.

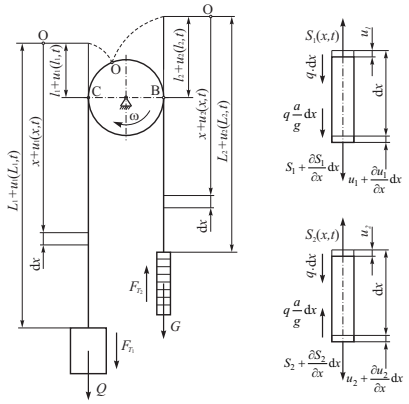

Figure 1. Dynamic model of elevators (ref. [2] and [3] in full paper)

The model takes into account the influence of the rope free length variations on both the incoming and outgoing pulley side. The variations in rope free length (shortening or lengthening) directly affect the rope stiffness, and therefore also the dynamic behavior of

the rope, which is of significant importance in the systems with high lifting velocities. This paper deals with Koepe system because the experiments were performed on a mine elevator in RTB Bor mine (Serbia). Forming a representative model for the analysis of dynamic behavior implies simplification of the model so as to exclude the small influences of the "higher" order and to keep only the most influential (representative) parameters (*Vladić J and Đokić R 2017 Characteristics of mathematical methods and specialized software systems for dynamic analysis of elevators and mining elevators, IMK-14 – Research and development in Heavy Machinery 23(2) EN31-38*). Numerical solving of a partial differential equation is generated in the form of a table of approximate values for the requested function $u(x,y)$ for the equidistant values of independent variables.

To consider the specific cases, such as elevators and exploitation facilities in mines, we are going to take a look at the one-dimensional partial differential equation of the hyperbolic type of the second order.

$$\frac{\partial^2 u}{\partial t^2} - a(x,t)\frac{\partial^2 u}{\partial x^2} = f(x,t)$$

By taking into consideration a special case (homogenous differential equation where $f(x,t)=0$, we get a simple system of algebra equations:

$$(1+\alpha)u_n^{k+1} - \frac{1}{2}\alpha u_{n+1}^{k+1} - \frac{1}{2}\alpha u_{n-1}^{k+1} = 2u_n^k + \frac{1}{2}\alpha u_{n+1}^{k-1} - (1+\alpha)u_n^{k-1} + \frac{1}{2}\alpha u_{n-1}^{k-1}$$

The solution of differential equations lies in the application of specialized software systems for dynamic analysis (MSC ADAMS). As an illustration of the possibilities of dynamic analysis, the following figures show the diagrams for changes in certain values, done in MSC ADAMS software, while using the real experimental data.

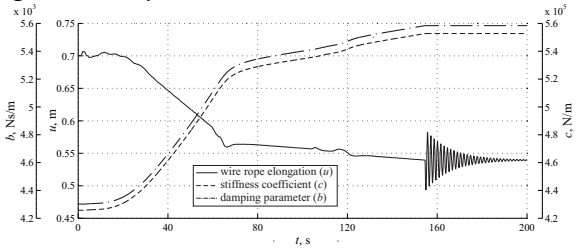

Figure 2. Diagrams of the change in hoisting ropes elongation, stiffness coefficient and damping parameter.

Due to a significant influence of rope free length changes, due to its slipping over the driving pulley and for the reason of its mechanical characteristics, it is impossible to apply a classical dynamic model of longitudinal oscillations for homogenous stick of a constant length, especially by the elevators with large velocities and large lifting heights (express and mine elevators).

In order to do the analysis of the dynamic behavior of the system during the movement (variable stiffness and nonholonomic boundary conditions) it is necessary to apply the specialized software packages with specifically defined (adjusted) parameters of dynamic models that can be obtained through measuring at vertical transport real systems.

9th International Scientific Conference
Research and Development of Mechanical Elements and Systems
Kragujevac, Serbia, September 5-7 2019

TANK CAR TESTING FOR DANGEROUS CARGOES TRANSPORTATION

Musij Kelrykh[1], Oleksij Fomin[1], Juraj Gerlici[2], Pavlo Prokopenko[3], Kateryna Kravchenko[2], Tomas Lack[2]

[1]State University of Infrastructure and Technology, Faculty of Infrastructure and Railway Rolling Stock, St. Kyrylivska, 9, 040071, Kyiv, Ukraine,
vagon.getut@ukr.net, fomin1985@ukr.net
[2]University of Zilina, Faculty of Mechanical Engineering, St. Univerzitná 8215/1, 010 26, Zilina, Slovak Republic,
juraj.gerlici@fstroj.uniza.sk, kkatherina@ukr.net, tomas.lack@fstroj.uniza.sk
[3]Branch "Research and design and technological Institute of Railway Transport "PJSC"Ukrzaliznytsya", St. Ivana Fedorova, 39, 030 38 Kyiv, Ukraine,
rokopenko1520mm@gmail.com

Key words: tank car, dangerous goods, tests, cargo capacity, service life.

The experience of the operation of rail transport shows that a significant part of emergency situations with significant negative environmental consequences are related to tank cars carrying liquid goods of a wide range, including liquefied gas, petroleum products, concentrated acids, toxic and explosive products of chemical origin. The article presents the peculiarities and result of carrying out of the corresponding tests. In order to address the question of the possibility of further safe operation of tank cars in the over-term period, their technical diagnostics and control tests are carried out. In this case, the control of the technical condition includes visual inspection of the tank wagon, measurements of the thickness of the metal at the control points of the boiler and the frame of the car, conducting of the magnetopowder, ultrasonic and acoustic emission control of the bearing metal constructions. Control tests include static vertical load tests, test for a low cyclic load by boiler pressure, typical, resource shock tests, and possible emergencies testing.

In recent years, there has been a significant aging of the Ukrainian fleet of freight cars, including tank wagons for dangerous cargoes transportation. In conditions of Latvian railway the main damages of the barrels of oil tank wagons and their quantity are: cracks of welding seams of shaped pads – 50%, barrel damages in area of supports – 30%, damages of welding seams of the barrel – 15%, unfastening of shaped pads – 5%.

Currently, on the Ukrainian railways network, tank wagons with a service life that exceeds the deadline set by the manufacturer and even extended service life are in operation.

Therefore, the urgent issue is either the replacement of rolling stock or the extension of the service life of the operated rolling stock.

It is necessary to form the necessity of conducting data of controlling tests of flat wagons.

After analyzing the park and the technical condition of tank cars for the particularly dangerous goods transportation, it was established that the main part of the park consists of tank cars of model 15-1407 - for transportation of propane (Fig. 1), 15-1408, 15-1408-01, 15-1408-02, 15 -1440, 15-1597, 15-1619 - for transportation of ammonia, 15-1409, 15-1556 - for transportation of chlorine (Fig. 2), 15-1519, 15-1780 - for transportation of propane-butane, and they are in good technical condition. The above-mentioned tank cars are structurally different from each other by the following features: the material from which the tank boiler is made, the diameter of the boiler, the number of shells in the boiler, the protective equipment of the bottom of the boiler from damage during accidents and protection of the boiler armature.

The purpose of the article. Illustration of theoretical and practical features of conducting technical diagnostics, control tests and tests with simulation of emergency situations of tank cars for the carriage of especially dangerous cargoes.

Taking into account the operational experience and the results of the inspection of the technical condition, it is possible to determine the probability of failure of the elements of the frame of the tank car, Pi (i = 1, 2, 3 ... N, where N is the number of elements) by the formula:

$$P_i = \frac{\sum_{1}^{k} \frac{R_H}{R}}{k},$$

where *k* - the number of surveyed wagons;

R_H - number of defective elements of the same type in the wagon.

On the basis of technical diagnostics and control tests of the tank-wagon it was established that the tank-wagon is technically a typical representative of the operational fleet of Ukrainian railways, which have completed their intended service life. The tensile condition of the boiler of the tank-wagon from the action of normative static and shock loads did not exceed the permissible 236 MPa. When testing on a low-cycle load on a boiler with pressure from 0 to 2 MPa, 225 cycles were carried out, which corresponds to 5 years of operation. In tests with simulation of emergency situations: the impact on the bottom of the tank, the creation of a limit pressure in the tank, up to 6 MPa, an impact on the auto-coupling device of a tank carriage at a speed of 22 km/h, damage and depressurization of the boiler tank-tank was not detected.

IRMES KRAGUJEVAC 2019

9th International Scientific Conference
Research and Development of Mechanical Elements and Systems
Kragujevac, Serbia, September 5-7 2019

DETERMINATION OF THE STRENGTH OF THE CONTAINERS FITTINGS OF A FLAT WAGON

Oleksij Fomin[1], Juraj Gerlici[2], Alyona Lovska[3], Kateryna Kravchenko[2], Yuliia Fomina[2], Tomas Lack[2]

[1]State University of Infrastructure and Technology, Faculty of Infrastructure and Railway Rolling Stock, St. Kyrylivska, 9, 040071, Kyiv, Ukraine, fomin1985@ukr.net
[2]University of Zilina, Faculty of Mechanical Engineering, St. Univerzitná 8215/1, 010 26, Zilina, Slovak Republic, juraj.gerlici@fstroj.uniza.sk
[3]Ukrainian State University of Railway Transport, Department of Wagons, 61050, Feuerbach Square 7, Kharkov, Ukraine, alyonaLovskaya.vagons@gmail.com

Key words: flat wagon, container, fitting for container, corner casting, combined transport.

The article presents the results of the dynamic loading and strength study of the fittings for containers of a flat wagon loaded with containers during shunting. It has been found that with impact interaction of corner castings with fittings, there are increased stresses, both in structural components of a flat wagon and in containers. To provide the strength of the fittings of a flat wagon and corner castings of containers, it has been proposed to install elastic-viscous linkage between them. This solution is implemented by installing elements having appropriate properties in the corner castings. Mathematical modeling has been performed to determine the dynamic loading of the flat wagon and containers. The obtained values of dynamic loads were taken into account when determining of the strength indexes. It has been established that, the maximum equivalent stresses in the fittings and corner castings are within acceptable parameters taking into account the proposed solutions. The studies will contribute to provide the strength of the structural components of flat cars and containers during shunting, to reduce the cost of their unscheduled repairs, as well as to create recommendations for design of rolling stock with improved technical and economic indexes.

The creation of foreign economic relations between the Eurasian states determined puting into operation of intermodal transport systems. At present container transportation is one of the most common transportations, owing to containers intermodality as vehicles.
Containers are transported by flat wagons equipped with fittings for container with respect by main tracks. The study of regulatory documents standardizing the containers dynamic

loading in operation allows for the conclusion that one of the most loaded modes is a shunting collision of a flat wagon with containers placed on it. In this case, both the corner castings damage and the flat wagon container fittings damage may occur. To improve the efficiency of container transportation and reduce the cost of unscheduled flat wagons and containers repair types, at the current stage of the transport industry development it is important to introduce new alternative solutions for the design features of vehicles, their interaction patterns.

The purpose of the article is to determine the strength of the container fittings of a flat wagon loaded with containers during shunting. To achieve this goal, the following tasks are defined: 1. To investigate the flat wagon dynamic loading taking into account the improved interaction scheme of container fittings with corner castings by means of mathematical modeling. 2. To investigate the flat wagon dynamic loading taking into account the improved interaction scheme of container fittings with corner castings by using computer simulation. 3. To calculate the strength of the flat wagon, taking into account the improved interaction scheme of container fittings with corner castings.

Based on the research we can draw the following conclusions:

1) The dynamic loading of the flat wagon has been investigated taking into account the improved scheme of interaction of container fittings with corner castings using mathematical modeling. Mathematical models have been designed taking into account the presence of viscous and elastic-viscous couplings between fittings and corner castings. It has been established that the maximum accelerations acting on the flat wagon are about 40 m/s2 (4g), that is, they are within the allowable range. 2) The dynamic loading of the flat wagon has been investigated taking into account the improved scheme of interaction of container fittings with corner castings by using computer simulation. The finite element method, implemented in the CosmosWorks software, has been used in a calculation. The dislocation areas of accelerations acting on the flat wagon supporting structure with containers placed on it are determined. Verification of the designed models is made by the Fisher method. 3) The flat wagon strength has been calculated taking into account the improved scheme of interaction between container fittings and corner castings. It has been established that in case of viscous interaction of container fittings with corner castings during flat wagon shunting, the maximum equivalent stresses are about 270 MPa and are concentrated in the zone of interaction between the center girder and the bolster beam. Maximum displacements occur in the middle parts of the main longitudinal beams of the flat wagon frame and are 12.1 mm. When using elastic-viscous interaction of fittings with corner castings during flat wagon shunting, the maximum equivalent stresses are about 260 MPa, the maximum displacements are about 11.0 mm. The research will contribute to improving the efficiency of container transportation, reducing the cost of unscheduled flat wagons and containers repair types, as well as creating recommendations for designing of modern rolling stock.

9th International Scientific Conference
Research and Development of Mechanical Elements and Systems
Kragujevac, Serbia, September 5-7 2019

TRANSPORT AIRCRAFT MAINTENANCE INFLUENCE ON AIRCRAFT MARKET VALUE

Petar Mirosavljević[1], Nebojša Bojović[1], Dalibor Pešić[1], Radomir Mijailović[1], Miloš Marina[1]

[1]University of Belgrade, The Faculty and Transport and Traffic Engineering, Vojvode Stepe 305, 11000 Beograd, Serbia, perami@sf.bg.ac.rs

Key words: maintenance, market value, aircraft, annual report.

Airline companies, insurance agency, banks and aircraft owners often need neutral, objective assessment of actual market value of their primary assets aircraft. The reasons for this are insurance, mortgage or airline sales. For airline companies, the main reason is to determine the capital value of an aircraft due to an annual report on the value of a company for the purpose of recapitalization, sale or other reason. The paper presents a systematic approach to estimating the value of aircraft that is in maturity of exploitation. with the remaining system, engine and structure resources. The paper presents the importance of investment in the maintenance of aircraft components and raising the market value of aircraft over the years of exploitation. The balance between investing in maintenance of the structure and the engine is also shown in order to achieve a quality extension of sensitive components resource

The process of assessing the market value of aircraft, associated engines and spare parts is a highly responsible, difficult and delicate job that requires knowledge of a large number of data that are time-varying. Standard market analysis has been set up by large companies, the core business, which defined the level of market value estimates of the aircraft through the most common six levels of estimation. An estimation that is sufficiently promising, quick and inexpensive to realize is the third level of detail.

By studying the lifespan of a plane that was in a mature era of exploitation, it was noticed that the plane of the aircraft (airframe) differs from the runoff (by FH and FC) of each individual engine and auxiliary drive group APU. Therefore, it always approached the separation of the price of the aircraft structure from the engine price and APU. According to the reference data available in the aircraft manufacturer's bases [1], the price of a new airplane is read on the basis of yearly production and serial number of aircraft or S / N planes. The decline in value for the year is determined by the Standard Depreciation Act or the SYD-Standard Year Depreciation:

$$SYD = \frac{(price - rest) * (all\ maintenance\ periods - \ current\ period + 1) * 2}{all\ maintenance\ periods * (all\ maintenance\ periods + 1)}$$

In the equation the following variables have the given values:

- Changing Price is the purchase price of the aircraft
- Changing The remainder is the value of the remainder at the end of the amortization cycle
- Changes All depreciation periods are the number of instalments for depreciation
- Changing Current period is the current instalment rate for the depreciation payment

The basis of each value assessment is the verification of the available technical documentation of the airplane located in the technical base of the airline. The review of the documents must be grounded. The classic methodology for creating an airplane maintenance documentation technician is approaching paperwork while modern systems involve software and digital database documents, so work is significantly faster and in the second case. In technical documentation on aircraft maintenance, it is revealed that the aircraft element is structured that generates the value of the complex. Usually it is concluded that the structure of the aircraft, the engine and the APU is very complex because they are usually different from the original ie Manufacturers. Usually, there is a difference in the production cycle if it is a mature exploitation period of about 15 to 20 years of exploitation. The implications of this are the split in consideration of the change in the value of the aircraft, engine and APU structure and other investments related to the implementation of the Airworthiness Directive -AD as prescribed by EASA and Service Bulletin -SB.

The structure, engines and APUs are maintained regularly and pedantic about what is recorded in the Aircraft Log Book CAP 408 and the Aircraft Modification Book CAP 395 if also in the Engine Log Book. All major surveys and maintenance of the structure are C1, C2, C3, C4 check and 6 year maintenance as well as 12 year structural maintenance. Other A and B considerations do not have significant value and are included in inspections and maintenance to preserve the airworthiness and safety of aircraft exploitation without any significance for aircraft value.

9th International Scientific Conference
Research and Development of Mechanical Elements and Systems
Kragujevac, Serbia, September 5-7 2019

CONSTRUCTION OF THE HELICOPTER SIMULATOR AS A SCIENTIFIC RESOURCE

Petar Mirosavljević[1], Miloš Marina[1], Dalibor Pešić[1], Radomir Mijailović[1]

[1]University of Belgrade, The Faculty and Transport and Traffic Engineering, Vojvode Stepe 305, 11000 Beograd, Serbia, perami@sf.bg.ac.rs

Key words: simulator, construction, helicopter, modelling, simulation.

The best form of learning is practical work. If we have limited resources, the best visuals for realizing reality are simulators. The basic use of the simulator is that certain experiments can be performed by mapping the image of the real world. The theme of this paper is the modelling, construction and construction of a helicopter simulator. This paper presents the entire process. Special attention is paid to the advantages that simulators provide, as well as their disadvantages. The fact is that the use of simulators as a scientific tool in the education of engineers is also realized through work.

The paper presents the whole process of placing a flight simulator as a scientific tool. The process itself took about three months. The first part consisted of significant design and drawing of the selected model in AutoCad. The design process of the simulator was then used. While, eventually, checks and tests were performed to determine if the simulator could be used for scientific purposes.

One part of the paper is devoted to significant simulation and model. In addition to the fact that simulation can be used in education, it can also be used to solve problems from real situations with the engagement of smaller resources. Even more problems are impossible to discern without simulating it or reconstructing it in reality. From all it can be concluded that designing and making a flight simulator is of great knowledge for the education of future engineers.

The construction itself is made of a combination of aluminum and iron elements. Robinson R66 was used to make the same construction as the benchmark. When choosing a benchmark model to build a simulator, they were placed on the following headings:

- The cabin must be such that it has two seats in the first place - pilot, co-pilot;
- Possibility of real model display;
- Possibility of construction;
- Available drawings and sketch for the given model.

Flight controls are identified as an object in the selected benchmark model.. While creating this simulator, it is possible to set universal flight and joystick controls.
With the completion of the simulator assembly process, the process of simulator testing has begun. The processes were proven and the examination consisted of two parts. The first part deals with the static and dynamic checking of the simulator structure. The second part of the check was to examine the control system and the command response itself. After a series of tests and correctness, classic iteration processes, when satisfactory levels of commands and transmissions are achieved on the system unit. The final appearance of the simulator can be seen in Figure 1.

Figure 1. Complete operative flight simulator

Based on all the tests performed, the team concluded that the simulator could be used for scientific purposes. As the subject is a self-build simulator, it cannot now be used in helicopter pilot training. Considering the construction costs, which are far less than the cost of purchasing one such simulator, this project can be considered very successful. Of course it has to be said that this is not the humble attitude of the team that worked on him, but time will tell that he was right or not.

IRMES KRAGUJEVAC 2019

9th International Scientific Conference
Research and Development of Mechanical Elements and Systems
Kragujevac, Serbia, September 5-7 2019

ESTIMATION OF THE INFLUENCE OF THE INTERACTION OF FACTORS PAIRS ON THE COEFFICIENT OF ROUTE EXECUTION POSSIBILITY

Volodymyr Puzyr[1], Oleksandr Krasheninin[1], Denis Zhalkin[1], Yurii Datsun[1], Oleksandr Obozny[1]

[1]Ukrainian State University of Railway Transport, Faculty of Mechanics and Energy, Feierbakh Square 7, 61050 Kharkiv, Ukraine, sasha.obozny@gmail.com

Key words: coefficient of route execution possibility, full factor experiment, electronic passport of the locomotive, technical condition of the locomotive, reliability.

The analysis of the reliability of the work of locomotives in the operation indicates a rather high level of their failures in the route. It indicates that before the departure of the locomotive to the route, there is no assessment of its ability to successfully complete the route under the influence of various factors. Denials on the route may result in significant material losses that could have been avoided even at the stage of route preparation. First, before sending the locomotive to the route, it is necessary to analyze its actual technical condition and to ensure that the state of its nodes allows executing the route without fail. For this purpose an electronic passport of the locomotive can be used. Secondly, it is necessary to make sure of sufficient qualification of the locomotive crew in order to avoid the failure of the locomotive due to improper actions of the locomotive crew. Thirdly, it is necessary to take into account the influence of operational parameters of the future route to change the technical condition of the locomotive and its knots. As a tool that will allow simulating and analyzing the interaction of various factors, the method of a full factor experiment can be used. As a tool that will allow simulating and analyzing the interaction of various factors, the method of a full factor experiment can be used. Methods of the theory of experiment are used to find optimal conditions and obtain formulas reflecting the interaction of factors. Experiment planning applies for searching for optimal conditions, building interpolation formulas, choosing significant factors.

The purpose of this article is to analyze the influence of the interaction of a pair of factors on the coefficient of route execution possibility and ranking of selected factors by degree of influence.

As factors that influence on the value of the coefficient of route execution possibility were selected: x1 – the profile of the area, x2 – experience of the driver, x3 – the length of the shoulder, x4 – the weight of the train. Accepted values of the zero level, the interval of variation, the upper and lower levels of factors are given in Table 1.

Table 1. Values of variables and variables range

Levels and interval of variation of factor	Factors			
	x1	x2	x3	x4
	i, ‰	T, years	L, km	Q, t
Zero level	0	10	300	4000
Interval of variation	10	10	200	2000
Lower level	-10	0	100	2000
Upper level	10	20	500	6000

The formula for determining the coefficient of route execution possibility with the interaction of factors x_1 and x_2 will have the following form

$$k = 0.8958 + 0.0025x_1 + 0.0108x_2 + 0.0075x_1x_2$$

The formula for determining the coefficient of route execution possibility with the interaction of factors x_3 and x_4 will have the following form

$$k = 0.8715 - 0.0057x_3 - 0.0014x_4 - 0.0033x_3x_4$$

The formula for determining the coefficient of route execution possibility with the interaction of the factors x_4 and x_2 will have the following form

$$k = 0.8837 - 0.0218x_4 + 0.0315x_2 - 0.0089x_4x_2$$

The formula for determining the coefficient of route execution possibility with the interaction of the factors x_2 and x_3 will have the following form

$$k = 0.8948 - 0.0253x_2 - 0.0071x_3 - 0.0105x_2x_3$$

The formula for determining the coefficient of route execution possibility with the interaction of the factors x_4 and x_1 will have the following form

$$k = 0.8919 - 0.0165x_4 + 0.0043x_1 - 0.0203x_4x_1$$

The obtained formulas are valid for the variables in the intervals of variation given in Table 1. According to them, it is possible to calculate the value of the coefficient of route execution possibility at different combinations of a pair of factors. In this case, the coefficient of route execution possibility takes the value from 0.85 to 0.926. The minimum value of the coefficient corresponds to the interaction of the maximum values of x4 and x1, the maximum value corresponds the interaction of the maximum value of x2 and the minimum value of x4. By the force of influence on the coefficient of route execution possibility, the factors are arranged in the following order: experience of the driver, the length of the shoulder, the weight of the train, the profile of the area.

9th International Scientific Conference
Research and Development of Mechanical Elements and Systems
Kragujevac, Serbia, September 5-7 2019

APPLICATION OF DIGITAL HUMAN MODELS IN DETERMINATION OF THE PEDAL FORCE WHILE DRIVING

Slavica Mačužić [1], Jovanka Lukić[1]

[1]University of Kragujevac, Faculty of Engineering, Sestre Janjić 6,
34000 Kragujevac, Serbia, s.macuzic@kg.ac.rs

Key words: digital human model, pedal force, vehicle.

One of the most important tasks of the car manufacturer is the design of the interior space of the vehicle. Anthropometric characteristics of drivers are also important for designing cars. In this paper the determination of the pedal force has been performed. The force determination was made on digital human models for different populations, a total of 11 different populations of men and women [Table 1]. Analyzing was done in the software package Ramsis and subjects were presented using "mannequin".

Table 1. The anthropometric data of 5% female and 95% male population

Population	Height [mm]		Sitting height [mm]		Foot length [mm]	
	5%	95%	5%	95%	5%	95%
West Africa	1440	1785	741	881	212	278
North India	1450	1765	771	919	205	270
Eastern Europe	1540	1845	831	959	225	285
North Europe	1585	1910	846	999	227	280
Australia	1565	1885	831	979	220	280
South East Europe	1525	1825	811	949	220	285
Central Europe	1560	1805	826	989	220	288
South East Africa	1480	1775	771	909	210	280
Middle East	1529	1800	801	944	222	280
South India	1395	1715	746	874	200	265
North Asia	1504	1820	801	961	207	275

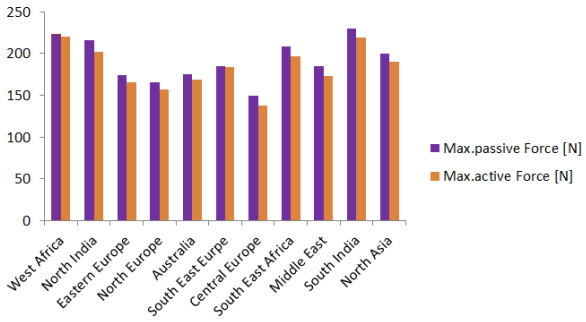

Figure 1. The maximum foot pedal force (active and passive) of eleven female 5% populations

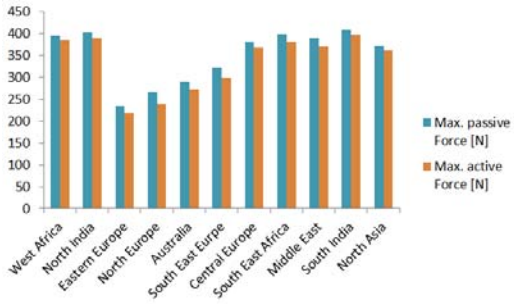

Figure 2. The maximum foot pedal force (active and passive) of eleven male 95% populations

Using this software package, car makers have the opportunity, before the first prototype, to graphically display how the model interacts with its environment inside the car. Results (Figure 1 and 2) show that the smallest value of the active and passive force has population from Eastern Europe and North Europe 218.1 N and 238.5 N, respectively for active force, and 233.8 N and 266.2 N for passive force. The South India, North India and West Africa populations have the highest values of active and passive forces. Maximum value of active force was 397.1 N (South India male 95% population), while the maximum value of passive force was 408.7 N. By increasing the height of the male or female drivers, it can be concluded that there is a decrease in the active and passive force values required to activate the pedal. By calculating Pearson R coefficient in both populations, female 5% (R^2 = 0.84) and male 95% (R^2 = 0.72), it can be concluded that there is a good correlation between active foot pedal force and driver's height. Also, in case of maximum values of passive forces R coefficient in both populations also has a good correlation between passive pedal force and driver's height (over 0.69).

Acknowledgments. This research supported by the Ministry of Education, Science and Technological Development of Republic of Serbia through Grant TR 35041.

9th International Scientific Conference
Research and Development of Mechanical Elements and Systems
Kragujevac, Serbia, September 5-7 2019

INDOOR POSITIONING AND NAVIGATION SYSTEM FOR AUTONOMOUS VEHICLES BASED ON RFID TECHNOLOGY

Michal Regus[1], Rafal Talar[1], Remigiusz Labudzki[1]

[1]Poznan University of Technology, Institute of Mechanical Technology,
60-965 Poznan, Piotrowo 3 Str., Poland, michal.j.regus@doctorate.put.poznan.pl

Key words: indoor positioning system, autonomous vehicle, RFID.

The last few decades have brought a great technological progress. At present time, a strong trend of automation and data exchange process within the production area can be observed. This tendency is considered as a 4th Industrial Revolution (called also Industry 4.0). The concept of Industry 4.0 is based on the production environment where people and machines create the cyber-physical system, within which they communicate, cooperate and self-organize their job [1]. It is worth to mention that one of the major direction of Industry 4.0 is Human Robot Collaboration (HRC). According to this concept, collaborative robots (called also *cobots* or *co-robots*) - equipped with safety and collision avoidance systems – assist the human co-workers in the most physically difficult and monotonic tasks within one workspace. No additional safety fence is required. In the face of above mentioned idea, reliable and accurate Indoor Positioning System (IPS) seems to be indispensable component of modern production environment. Tracking of goods during the production process, navigation and localization of people, robots and autonomous vehicles are only a few potential applications of IPS in modern production plants.
It is worth to mention, that not only the industrial environments have changed over last few decades. We are the witnesses of changing lifestyle and living conditions. Nowadays, our society lead sedentary lifestyle. A huge percentage of people spend our time sitting at home in front of their computers, TVs and smartphones. They do the shopping through the internet and even build the relationships. It is predicted that in the near future people will spend more than 70% of their lifetime within indoor environments [2]. Consequently, reliable and accurate indoor positioning systems are highly demanded to complement widely used satellite-based technologies and to ensure tracking within outdoor environments. Such hybrid system would provide real-time monitoring of objects and people position regardless they are within in- or out-door environment.
The Global Positioning System (GPS) is the most commonly used localization system based on the satellite technology. Nowadays, GPS receivers are built-in most of everyday use devices, like smartphones, watches or vehicles. The GPS system contains mainly 31 satellites

and receivers. The satellites are evenly deployed in the Earth orbit and constantly broadcast the radio signal about their position and current time. The signals from multiple satellites, which arrive to the receiver are processed in order to calculate its current position. The object position can be calculated as long as an unobstructed line of sight to four or more satellites is assured. As a consequence, GPS technology is not sufficient for indoor applications [3, 4]. Furthermore, indoor environments are usually more complex and susceptible for noises which decrease the reliability and accuracy of positioning systems. All the obstacles like, walls, furniture, electrical devices or human being influence the propagation of electromagnetic field. In reference to above mentioned issues, it can be stated that appropriate solution for positioning within indoor environments became a new challenge for the present day.

Recently, the real time indoor positioning systems have become an object of interest for many scientist centers. Despite the huge progress in regards to IPS that has been done over last decades, a reliable, accurate, cost-effective, simple and flexible indoor location system is still searched for [3]. One of the biggest challenge that must be faced nowadays is not only to develop reliable and accurate positioning system containing advanced and highly specialized sensors but also to implement hybrid system which would be based on currently existing technologies and commonly used devices [2]. WLAN-based (Wireless Local Area Network) indoor positioning system can be mentioned as an example of such approach. WLAN technology reuses the devices and networks which are widely used almost everywhere. Consequently, any additional equipment or infrastructure are not required to implement IPS utilizing WLAN. Another approach which comes from an idea of reusing already deployed technologies are smartphone-based IPSs [5]. These are only two examples of many different indoor positioning systems (based on IR, RFID, WLAN, Bluetooth and other technologies) which have been already designed and implemented. More examples of locating systems are given in the further part of this article.

The following paper contains a general overview of currently existing indoor positioning systems as well as the authors concept of 2D wireless indoor positioning and orientation system dedicated for autonomous vehicles based on Radio Frequency Identification (RFID) technology.

References

[1] TUV Austria, *Safety in Human-Robot Collaboration 2016*, www.tuv.at/i40 (accessed on May 2019).

[2] D Dardari, P Closas, P M Djurić 2015 Indoor Tracking: Theory, Methods, and Technologies, IEEE Transactions on Vehicular Technology **64**(4) 1263 – 1278.

[3] Y Gu, A Lo, I Niemegeers 2009 A Survey of Indoor Positioning Systems for Wireless Personal Networks, IEEE Communications Surveys & Tutorials **11**(1) 12 – 32.

[4] H Liu, H Darabi, P Banerjee, J Liu 2007 Survey of Wireless Indoor Positioning Techniques and Systems, IEEE Transactions on Systems, Man, and Cybernetics, Part C (Applications and Reviews) **37**(6) 1067 – 1080.

[5] A Mulloni, D Wagner, I Barakonyi, D Schmalstieg 2009 Indoor Positioning and Navigation with Camera Phones, IEEE Pervasive Computing **8**(2) 22 – 31.

9th International Scientific Conference
Research and Development of Mechanical Elements and Systems
Kragujevac, Serbia, September 5-7 2019

SIMULATION OF VEHICLE'S LATERAL DYNAMICS USING NONLINEAR MODEL WITH REAL INPUTS

Danijela Miloradović, Jasna Glišović, Nadica Stojanović, Ivan Grujić

University of Kragujevac, Faculty of Engineering, Sestre Janjić 6,
34000 Kragujevac, Serbia, neja@kg.ac.rs

Key words: vehicle, lateral dynamics, simulation, nonlinear model, real inputs.

Lateral dynamics of vehicles has been studied since 1950's. A very often-used single-track vehicle lateral dynamics model, frequently referred to as "Riekert-Schunk single-track model", was developed back in 1940. Analysis of simple single-track models can explain a large part of dynamic behaviour during handling of the vehicle, especially during stationary ride. This enables faster testing and analysis of vehicle behaviour during ride and easy translation of the models to the language of simulation programs. Although they contain certain reductions, the single-track models of vehicle lateral dynamics are nowadays used in the design of steering system control units. However, due to their nature, these models do not take into account the redistribution of weight in the lateral direction, nor the angular oscillations of the vehicle around the longitudinal axis.

The linear single-track models contain simplifications regarding the assumption of small angles and linear dependence between wheel forces and slip angle. In addition, they do not take into account nonstationary nature of vehicle vibrations induced by variable vehicle velocity or road roughness. Considering the previous limitations, a nonlinear nonstationary single-track model of the vehicle was used for simulation of vehicle's lateral dynamics in this paper, Figure 1. The used model considered larger values of body slip angles and tire slip angles, in which case the linearized equations of motion were no longer valid. In addition, the selected model considered longitudinal, lateral and yow motion of the vehicle, under the assumption that the vehicle travels over even road and that there was negligible lateral weight shift and roll of the vehicle.

The following differential equations describe relations between different parameters of motion in the adopted nonlinear single-track model of lateral dynamics and parameters of vehicle and tires, when only front wheels are steered:

$$\dot{\theta} = \dot{\varepsilon} - \frac{1}{m \cdot v}\left\{k_1 \cdot \left[\lambda_1 - \operatorname{arctg}\left(\frac{a \cdot \dot{\varepsilon} - v \cdot \sin\theta}{v \cdot \cos\theta}\right)\right] \cdot \cos\left(\lambda_1 + \theta\right) + k_2 \cdot \operatorname{arctg}\left(\frac{b \cdot \dot{\varepsilon} + v \cdot \sin\theta}{v \cdot \cos\theta}\right) \cdot \cos\theta\right\},$$

$$\ddot{\varepsilon} = \frac{1}{J_z}\left\{k_1 \cdot \left[\lambda_1 - \text{arctg}\left(\frac{a \cdot \dot{\varepsilon} - v \cdot \sin\theta}{v \cdot \cos\theta}\right)\right] \cdot \text{a} \cdot \cos\lambda_1 - k_2 \cdot \text{arctg}\left(\frac{b \cdot \dot{\varepsilon} + v \cdot \sin\theta}{v \cdot \cos\theta}\right) \cdot \text{b}\right\}.$$

These equations were the basis for development of MATLAB/Simulink program for simulation of lateral vehicle dynamics for nonlinear nonstationary vehicle model with real inputs.

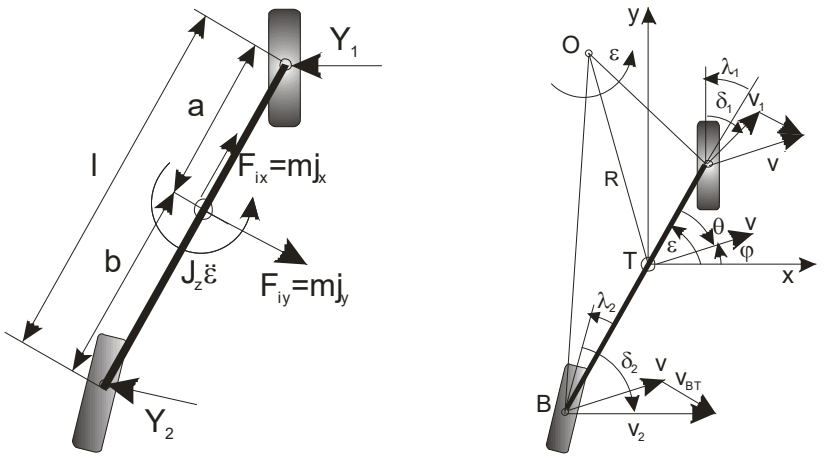

Figure 1. Nonlinear single-track model of the vehicle: (a) forces acting on vehicle, (b) definition of the observed angles and velocity directions.

The developed nonlinear model of vehicle lateral dynamics was used for simulation with real, experimentally obtained inputs: variable vehicle longitudinal velocity, v_x, and steering wheel angle, β_v (used to calculate necessary steered wheel angle, λ_1) in the form of quasiharmonic curve. Model offers simulation results for several output variables that are important for understanding the vehicle lateral dynamics: yaw angle, ε, body slip angle, θ, tire side slip angles (δ_1, δ_2), lateral dynamic reactions on the front and rear wheels (Y_1, Y_2), vehicle lateral acceleration, $\ddot{y}$ and lateral inertial force, F_{iy}.

The obtained results show that all output curves have a wave character that corresponds to the model's basic excitation - steer angle of the front wheels. In addition, all simulated curves have the same dominant frequency as the input curve of the front wheels steer angle. The influence of variable velocity and system nonlinearities can not be clearly seen in the time domain, so further analysis in spectral domain is necessary.

Acquired experimental data and the developed single-track model of the vehicle lateral dynamics may serve as a basis for application of estimation techniques in system parameter identification and for solving the problem of optimal control with the aspect of estimation of lateral vehicle dynamics.

Acknowledgments. The Ministry of education, science and technological development of the Republic of Serbia funded this research through grant number TR35041.

9th International Scientific Conference
Research and Development of Mechanical Elements and Systems
Kragujevac, Serbia, September 5-7 2019

RAILWAY CARRIAGE MASS IMPACT ON RETARDER NOISE

Peter Zvolensky[1], Marian Kollar[1], Lukas Lestinsky[1] and Jan Dungel[2]

[1]University of Zilina, Faculty of Mechanical Engineering, Univerzitna 1, 01026 Zilina, Slovakia, peter.zvolensky@fstroj.uniza.sk, marian.kollar@fstroj.uniza.sk, lukas.lestinsky@fstroj.uniza.sk
[2]CEIT, a.s., Univerzitna 6A, 01008 Zilina, Slovakia, jan.dungel@ceitgroup.eu

Key words: retarder, marshalling yard, acoustic power, frequency analysis, railway carriage, noise.

The paper is focused on railway carriage mass impact on retarder noise. In the ŽSR railway network, many marshalling yards classified as a hump yards are using retarders. Those retarders are sources of noise, which can have negative impact on surrounding municipalities. The paper is showing measurements how acoustic power of the retarder depends on railway carriage mass, and possibilities of negative impact reduction. Measurements were performed on PHB 04-S0 (RO) retarder. This type of retarder is used in many ŽSR marshalling yards.

Figure 1. PHB 04-S0 (RO)

Measurements were performed with multiple railway carriages mass ranges in Teplička nad Váhom marshalling yard. Also impact of noise on surrounding municipalities was measured. Mass of the railway carriage significantly affects acoustic power. This is present even more, when set of multiple carriages is braked. In graph bellow, noise levels during braking of single carriage (mass 21t - red) a triple carriage set (single unit mass 89t – blue) are shown. As one can see, even in comparison of single 89t and 21t carriage there are significant differences in peak noise level. Also frequency analysis was performed. Dominant frequency of the noise is reducing with increasing weight of the carriage. Lighter carriages achieved frequencies in the range of 3200, 5400, 6200 Hz. Heavier carriages achieved frequencies in the range of 1600, 2100, 3500 Hz.

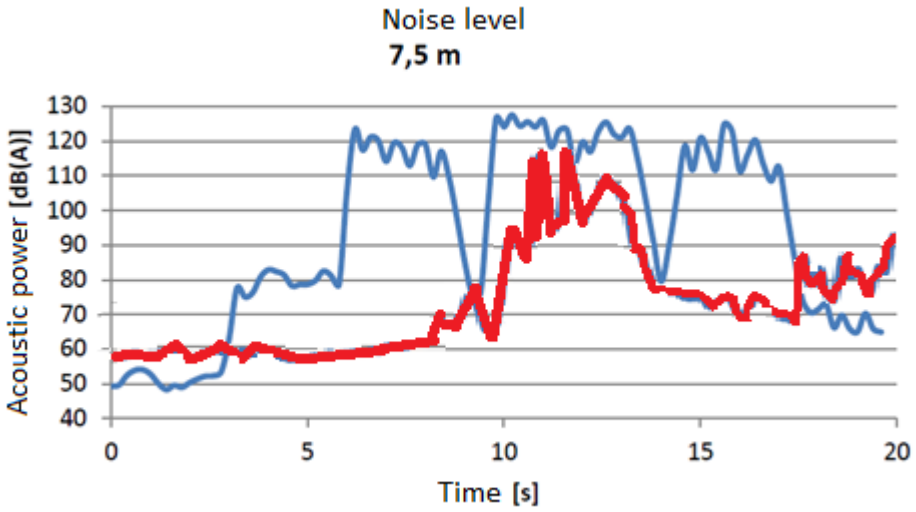

Original idea was to modify marshalling to prevent multiple heavy weighted carriages braking or make schedule for marshalling, so that heavier carriages could not be marshalled during night. But this would not be possible because of effective operation of marshalling yard. In this case, the ideal solutions are to build sound reducing barriers or other objects such as buildings, vegetation. With combination of these solutions it is possible to reduce impact of the marshalling yard on surrounding municipalities.

Acknowledgments. This work was created by the implementation of the project “Low Cost Logistic System Based on Mobile Robotic Platforms for Industrial Use”, ITMS: 26220220205 supported by the Operational Programme Research and Development and by the European Fund for Regional Development.

9th International Scientific Conference
Research and Development of Mechanical Elements and Systems
Kragujevac, Serbia, September 5-7 2019

OPTIMIZING THE BRAKING SYSTEM FOR HANDLING EQUIPMENT

Daniel Varecha[1], Róbert Kohár[1], Tomáš Gajdošík[1]

[1]University of Žilina, Faculty of Mechanical Engineering, Department of Design and Machine Parts, Univerzitná 8215/1, 010 26, Žilina, Slovak Republic,
daniel.varecha@fstroj.uniza.sk

Key words: braking system, automated guided vehicle, braking distance, braking time

Introduction. The paper is focused on optimizing the friction disc plates of the braking system integrated into the space of the drive wheel of an automated guided vehicle (see figure 1). At present, these handling vehicles are braked by an electric engine. This method of braking is sufficient only to a certain extent. It is not possible to brake safely with an electric engine at higher speeds and heavy loads. The research and development of the AGV brake system is relevant to practice.

Figure 1. Automated guided vehicle (Handling equipment)

Solution of the topic. The inside space of the wheel of the transport handling device forms an unused space. (see figure 2). This space was used to install the friction brake (see figure 3). The type of braking system is inspired by the braking system from planetary gearboxes. However, the principle of brake operation will vary. In the planetary gearbox, the rotary movement must be stopped immediately by friction plates. In this case, the braking force will be applied gradually. During braking, the handling equipment must control the braking force to prevent the wheels from locking. The literature of several authors has been used to develop this braking system. The most used source is the book "The machine part and mechanisms", that was needed when designing the brake. The book "Modeling and simulation of Mechanisms with computer support" was also very important to the

simulation of braking AGV. Last but not least, the experience of my older colleagues and all listed references.

Figure 2. Drive wheel of AGV

Figure 3. Drive wheel with the braking system

In the first step, boundary conditions (e.g., space of inside wheel, speed, the pressure between friction disc plates during braking, etc.) were determined. Four friction plates were designed according to the inside space of the wheel (see figure 2). Subsequently, all friction disc plates were subjected to mathematical calculations. This step is very important for the correct design of the braking system. Graphically view of the axle with the final braking system is in the figure below (see figure 4).

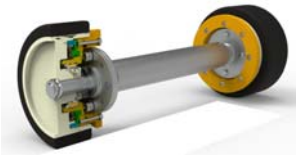

Figure 4. Drive axle with the braking system in cross-section

Subsequently, the calculated values were compared to the boundary conditions and evaluated. Two friction disc plates did not comply with the boundary condition. The other two friction disc plates were simulated in Matlab software under assigned specified boundary conditions. The software generated a graph using the iterative method. This way of solution generates a sequence of approximations. The graphs show distance, speed, and deceleration.

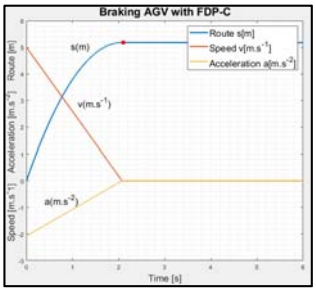

Figure 5. Simulation of braking with FDP-C

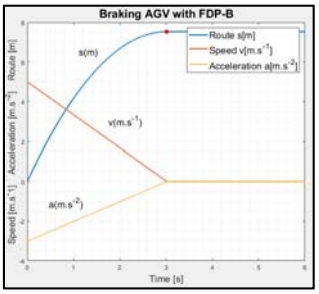

Figure 6. Simulation of braking with FDP-B

Conclusion. From the above graphs (see figure 5 – 6), it will be evaluated for which version of the friction disc plates the research will continue. Keep in mind that optimizing the brake system is a complex problem that is affected by a number of technical factors.

Acknowledgments. The research is supported by the Cultural and Educational Grant Agency of the Ministry of Education, Science, Research and Sport of the Slovak Republic under the project No. 046ŽU-4/2018.

9th International Scientific Conference
Research and Development of Mechanical Elements and Systems
Kragujevac, Serbia, September 5-7 2019

MEASURING THE WEIGHT OF A VEHICLE BY MONITORING THE DYNAMIC TORQUE OF A HEAT ENGINE

Stefan Ionita[1], Corneliu Hagiescu[1], Bogdan Iovu[1], Stefan Velicu[1], Paul Paunescu[2]

[1]Polytechnic University of Bucharest, Faculty of Engineering and Mangement of Technological Systems, Splaiul Independentei 313, Bucharest, Romania
[2]Polytechnic University of Bucharest, Faculty of Electronics, Telecomunications and Informaton Technology, Blvd Iuliu Maniu 1-3,Bucharest,Romania

Key words: road, safety, infrastructure, asphalt, low cost.

The main objective of this paper is the theoretical and experimental study of the connection between the value of the rotation moment developed by the motor of a vehicle and the value of the forces existing in the process of interaction between the traction wheels of the vehicle and the road surface (the wear layer of the road), when pulling away from the curb on a flat road. Following up the (experimental) determination by calibration of the rotation moment values depending on the different masses (weights) that the vehicle may have, with the upper limit represented by the maximum value registered in the documents, the road damage can be limited/reduced in due time by forbidding the access. The results of the research make possible the development of some intelligent systems on all the vehicles, with low costs and maximum benefit that consists of the permanent monitoring of the mass (weight) in different zones with heavy traffic and the elimination /diminution of the road damage level (as a result of mass exceeding on the axis) or the compensation by charging the overweight.

The research paper presents a computer assisted measurement system meant to simulate the operation conditions of a vehicle. This model will be used to check the mathematical relations shown above that associate the weight of the system (vehicle) with the engine moment required by its movement. The system was designed on the basis of the direct method using a torque transducer.

In order to obtain data similar to the data of the research system, we took into consideration a modular system that can be very easily modified, depending on the data we need. As shown in the figures before, we highlighted a series of variants of simulation by means of the Simulink Library of the software, selecting from the multitude of solutions the one that

is closed to the studied phenomenon. Several simulations were made in order to reveal a certain behavior of the system submitted to the perturbing component (weights).

The results of the research will provide the vehicles manufacturer with the information necessary for the development of an intelligent system for low-cost monitoring of the weight, with maximum benefits, consisting of the monitoring of vehicle active components, the permanent monitoring of its mass and the elimination/reduction of roads damage (resulted from exceeding the mass on the axis) by access interdiction, fines or maximum charging of the transport.

9th International Scientific Conference
Research and Development of Mechanical Elements and Systems
Kragujevac, Serbia, September 5-7 2019

EXAMINATION OF VEHICLE IMPACT AGAINST STATIONARY ROADSIDE OBJECTS

S Karapetkov[1], L Dimitrov[2], Hr Uzuniv[1], S Dechkova[1]

[1] Technical University of Sofia, Faculty and College – Sliven, Bulgaria,
skarapetkov@yahoo.com, hvuzunov@gmail.com, sdechkova@tu-sofia.bg
[2]Technical University of Sofia, 8 Kliment Ohridski bulv., Sofia 1000, Bulgaria,
lubomir_dimitrov@tu-sofia.bg

Key words: car, impact, roadside barrier, MATLAB, SolidWorks-Simulation, FEA.

In statistical analysis reports of traffic accidents, automobiles hitting against semi-rigid barriers and flexible barriers get a particularly large share. The impact phase between the vehicle and the metal crash barrier is considered to be a deformation phase between two bodies whereas the transformed kinetic energy as deformation energy. The objective is to find an approach to estimate the deformation energy of the vehicle as well as the deformation energy of the metal crash barrier separately, the residual energy of the vehicle after the impact, making the automobile pass a certain distance. The method is based on the law of conservation of mechanical energy, which is as follows:

$$\frac{m_1.V_1^2}{2} = \frac{m_1.u_1^2}{2} + \frac{I_1.\omega_1^2}{2} + E_1 + E_2$$

According to the functional dependence two options are possible: there is lack of residual kinetic energy or there is manifestation of it after the impact. If residual kinetic energy is manifested, the stopping distance travelled by the vehicle is found by means of the center-of-mass motion theorem.
Equation clearly shows that not only the deformation energy of the two bodies, but also the post-impact vehicle velocity of the center of mass and the angular speed of the vehicle are exhibited. If we apply the center-of-mass motion theorem, it would be a rather inaccurate approach, for it would not be possible to estimate the kinetic energy for the rotation of the vehicle after the impact.
The deformation energy of the metal crash barrier (Figure 1) is determined from equation by integrating the finite element method. This method is used as a universal tool for calculating and analyzing the behavior of mechanical structures in power and heat loads as

well as for solving problems in fluid mechanics, heat engineering, theory of electric and magnetic fields, acoustics, nuclear physics, etc.

Figure 1. Models for identification of impact

In this paper, a model of a car impact against a metal crash barrier is presented and discussed. The energy of the rigid barrier deformation was estimated by using the finite element method, and the energy absorbed by the deformed car body was examined by performing impact phase reconstruction in a series of car crash tests against a metal crash barrier.

After considering the mass inertial parameters, the solution to the post-impact vehicle motion is obtained. Initial conditions for the velocity of the center of mass and the angular velocity of the vehicle, satisfying the differential equations for vehicle motion, determine the residual energy of post-impact vehicle motion.

Solution to a common engineering task necessary for legal analysis and widely used in case law is provided. It determines the pre-impact speed of a vehicle following roadside objects/barrier impact and the loss of longitudinal stability after the impact. Traditional methods analyzing such crashes, which are generally applied to modern impact investigation and accident reconstruction, do not meet accuracy and precision requirements.

The proposed FEM approach is a modern innovative means of solving similar engineering tasks in order to identify traffic road accidents. It is based on credibility and justification of facts and evidence.

This method for investigating and analyzing head-on vehicle impact with a rigid barrier can also be applied to other vehicles and trucking fleets - trailers and semitrailers. The solution to the task requires precise post-impact mechanical and mathematical model for vehicle crashes, which represent the motion of the composition of the vehicle fleet.

9th International Scientific Conference
Research and Development of Mechanical Elements and Systems
Kragujevac, Serbia, September 5-7 2019

OPTIMALIZATION OF TRACTION UNIT FOR LOW-COST AUTOMATED GUIDED VEHICLE

Tomáš Capák[1], Róbert Kohár[1] Jozef Škrabala[1], Ján Galík[1]

[1]University of Žilina, Faculty of Mechanical Engineering, Department of Design and Mechanical elements, Univerzitná 8215/1, 010 26 Žilina, Slovak Republic, tomas.capak@fstroj.uniza.sk

Key words: Industry 4.0, modularization, AGV system, optimization, traction unit.

The automated logistics system, a comprehensive solution for logistics automation in the industrial area, has been the subject of many industrial companies using this solution in recent years. At present, the company CEIT a.s. (AGV manufacturer) is looking for a solution to the demand for a low-cost version of the undercarriage with multiple ways of transporting cargo without using a peripheral. This article describes the design and optimization of the traction unit for this version of the automated guided vehicle.
The device is based on a 6-wheel chassis with a traction unit (the axle) in the middle of the chassis. This orientation of the traction unit also serves as the equivalent of a mechanical differential used mainly for small and low-cost robots working indoor. It is independent control of traction wheels driven most often by DC electromotors with encoders or stepper motors. When designing a traction unit, it is necessary to identify the conditions in which the equipment will be operating. The AGV traction unit must overcome the driving resistance while driving. The higher the driving resistances, the greater the power of the traction unit's electric motors, and the increased electric power consumption.
The nominal torque of the selected electric motor when the AGV acceleration is 1,12 Nm. Check of the total output torque (T_{TO}) of traction unit was performed as follows:

$$T_{TO} = 2 \cdot (T_{Total} \cdot i_G \cdot \eta_G)$$

$$T_{TO} = 68{,}32\ Nm > T_{Total} = 57{,}2\ Nm$$

The resulting total torque of the traction unit is higher than the calculated torque required. Traction unit drive is dimensioned correctly and will be able to operate in the event of a small overload. The equipment test conditions result from the required operating parameters, load: 432kg (batteries) and max. speed: 0.7 m/s. 14 measurements were made after setting the measuring technique. The following figure 1 shows the position of the traction unit on the AGV frame and figure 2 shows the way how to measure the ductility of a device.

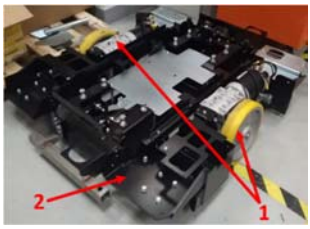

Figure 1 Position of the traction unit
1 – traction unit, 2 - frame

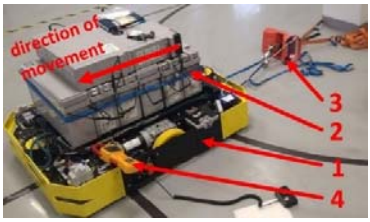

Figure 2 AGV with load
1 – AGV, 2 – load (batteries), 3 – industrial scale, 4 – clamp multimeter

The measured traction force at the stopped electric motor is equivalent to the maximum traction force needed to start the AGV. The measured traction force values of the AGV confirmed that the designed parts of the traction unit (DC electric motor and worm gearbox) are suitable for a low-cost version of medium-class AGV equipment. The traction force of the AGV is 1000N and the electric motor torque of 1.12Nm will be sufficient for the start acceleration AGV (see figure 3 and 4) because it is greater than the calculated maximum torque.

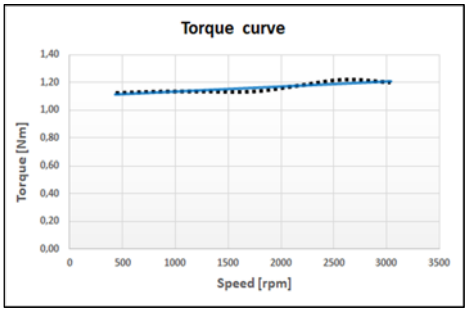

Figure 3 Torque curve – 1. measurement

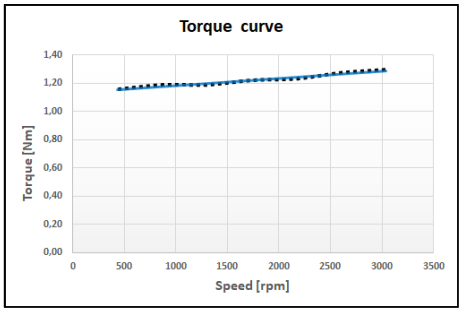

Figure 4 Torque curve – 2. measurement

In low-cost solutions, economic point is a major factor affecting those solutions. The main aim of the paper is to design a simple solution of parts of the traction unit and verify the proposed solution by physical measurement for the required parameters of the equipment. Testing of the equipment takes place in the laboratory of CEIT a.s., which developed this equipment. The measurement results showed that the designed type of traction unit is a suitable equivalent of servomotors and it can be usable as AGV's drive.

References

Nicholas P, Chironis 1991 *Mechanisms and Mechanical devices sourcebook.*
Ullrich G 2014 *Automated guided vehicle systems*
Robot Platform, *Wheel control Theo*ry,
Kučera Ľ, Gajdošík T 2014 *The vibrodiagnostics of gear*
Lukáč M, Brumerčík F, Krzywonos L, Krzysiak Z 2017 *Transmission system power flow model*

Acknowledgment. This publication is the result of the Project implementation: Competency Centre for Knowledge technologies applied in Innovation of Production Systems in Industry and Services, ITMS: 26220220155, supported by the Research & Development Operational Programme funded by the ERDF.

9th International Scientific Conference
Research and Development of Mechanical Elements and Systems
Kragujevac, Serbia, September 5-7 2019

CONTROL STRATEGY FOR AFTERMARKET ELECTRONIC THROTTLE CONTROL

Jelena Prodanović[1], Boris Stojić[1]

[1]University of Novi Sad, Faculty of Technical Sciences, Trg Dositeja Obradovića 6, 21101 Novi Sad, Serbia, jelena.prodanovic@uns.ac.rs

Key words: throttle-by-wire, electric drive, hybrid drive, project-based learning, student project.

This paper presents the development of control approach for aftermarket electronic throttle control device, provided for use in an experimental light hybrid-electric vehicle that was made in the scope of ongoing student project of developing and creating a light hybrid-electric vehicle as a platform for educational and research work. The vehicle is configured as a parallel hybrid with IC engine power at the rear axle and two electric hub-motors at the front axle. Originally, the IC-engine throttle system was operated by means of mechanical linkages and cable, which is not appropriate for optimal control of the simultaneous operation of both the IC engine and electric motors. Therefore prototype of new electronic throttle control system has to be developed, exerting control of both IC engine and electric hub motors by using the single accelerator pedal (Figures 1-3).

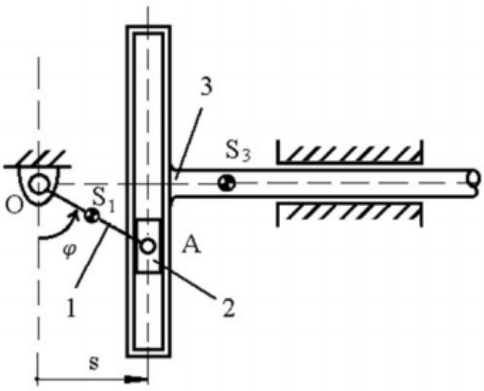

Figure 1. Working principle of a Scotch yoke mechanism **Error! Reference source not found.**

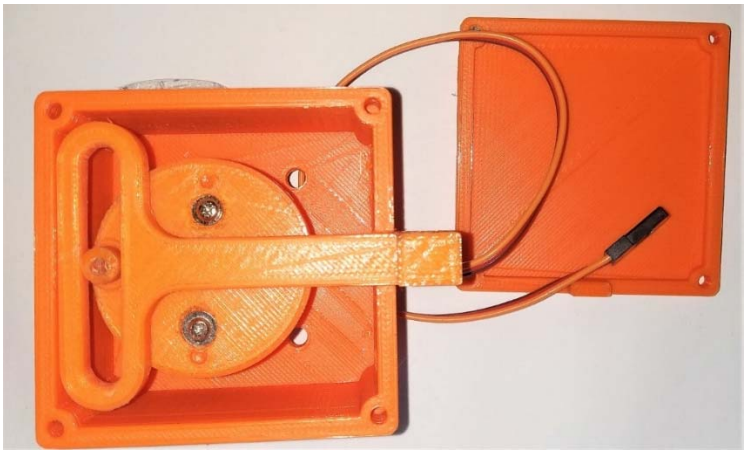

Figure 2. Servo motor and the Scotch yoke 3D printed mechanism

This way full exploitation of hybrid drive potentials can be enabled. The new control system also has to use a controller with appropriate software for conversion of the control signal to the actuator displacement. In the scope of this paper, the development of a closed-loop based control algorithm is described.

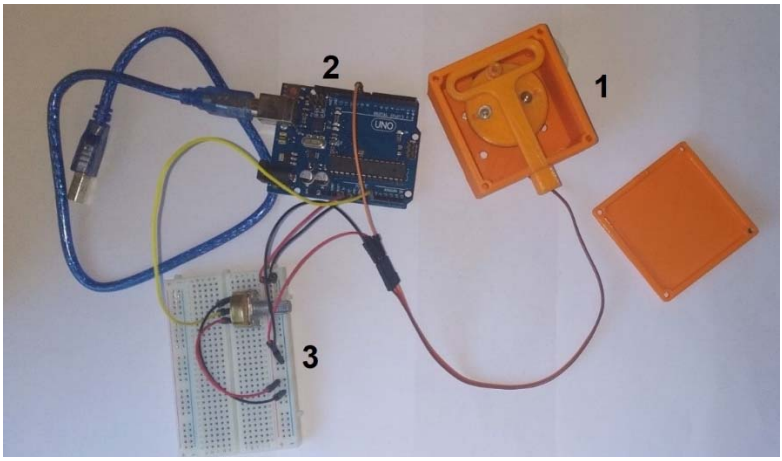

Figure 3. Prototype

Acknowledgments. This paper was done as a part of the researches on the project TR35041 – "Investigation of the safety of the vehicle as part of cybernetic system: Driver-Vehicle-Environment" and the project TR31046 " Improvement of the quality of tractors and mobile systems with the aim of increasing competitiveness and preserving soil and environment", supported by Serbian Ministry of Education, Science and Technological Development.

9th International Scientific Conference
Research and Development of Mechanical Elements and Systems
Kragujevac, Serbia, September 5-7 2019

OPTIMIZATION OF MAINTENANCE OF VEHICLES BASED ON COSTS

Vojislav Krstić[1], Božidar Krstić[2]

[1]Faculty of Transport and Traffic Engineering, University of Belgrade, Vojvode Stepe 305, 11000 Beograd, Serbia
[2]Faculty of Engineering University of Kragujevac, Sestre Janjić 6, 34000 Kragujevac, Serbija, bkrstic@ kg.ac.rs

Key words: motor vehicles, preventive maintenance, strategy.

Optimization of the maintenance system should be understood as looking for a compromise solution that will be most acceptable in maintaining the technical systems available. Optimizing the maintenance system, using a preventive maintenance model, is usually reduced to asking for an answer to the question of whether it is useful to apply preventive maintenance, and if yes, after a certain amount of time it is necessary to apply preventive maintenance procedures. If it is possible to determine the legality, to which the reliability distribution function is subject, it is possible to determine all other parameters of reliability. An optimal maintenance strategy for the technical system can be determined if there are data on the failure of the technical system during its use. Finding an adequate mathematical model that can present the legality of the behaviour of the technical system from the aspect of the occurrence of malfunction is one of the basic elements for forecasting its behaviour in the future and optimizing its maintenance system.
Since the correctness of establishing the reliability distribution model is dependent on all further conclusions and decisions related to taking appropriate measures in order to maintain the required level of reliability of the technical system. This stage of analysis should be given special attention. The aim of the paper is to find an optimal strategy for maintenance of the technical system, based on the indicator of its reliability, which is based on data from exploitation.
We will consider the basic principles for the development of a preventive maintenance plan (implementation of works according to the regulations) for long-term use vehicles. It is known that complex vehicles consist of a large number of blocks of different types, sub blocks, as well as some dismantling mechanisms, modules and parts. Preventive maintenance of such vehicles reduces the degree of its utilization. Using the aforementioned methods for determining the preventive maintenance characteristics shown in this paper, it is possible to make a plan for the dynamics of vehicle maintenance. In doing so, it is necessary to implement the following steps:
1. Based on the analysis of statistical data on the causes of malfunctioning and failure of vehicles obtained during factory tests and experimental research, the character of

malfunction is determined. They are precisely defined and finally determined by the laws of changing the forecasting, outgoing or general parameters, statistical data are processed which determine the law of distribution of the working time without the cancellation of vehicles when the determination of forecasting parameters is difficult.

2. On the basis of data on the nature of the malfunction, as well as on the basis of experimental research, the methods for monitoring the accumulation of malfunctions in the process of use are determined and define the acceptable (possible) methods for their detection.

3. Optimum preventive maintenance characteristics for each group of vehicles are determined: the periodicity and duration of preventive measures are determined.

4. The budget for the harmonization of preventive measures is being implemented. Integration of individual operations into a common complex of preventive measures is carried out either by periods of operation without cancellation, or by calendar dynamics. In doing so, the total time of the works during which the vehicles are excluded from exploitation is determined, and the degree of its exploitation is estimated.

5. The quantity of additional spare equipment, additional forecasting equipment and control provided for by the continuous maintenance system is determined if the level of utilization of the analysed vehicle is below the required level.

An optimal vehicle maintenance strategy can be determined if there are data on the occurrence of a cancellation of a vehicle during its use. Finding an adequate mathematical model that can present the legitimacy of vehicle behaviour from the aspect of defects is one of the basic elements for forecasting its behaviour in the future and optimizing its maintenance system. Since the correctness of the reliability distribution model is based on all further conclusions and decisions related to taking appropriate measures in order to maintain the required level of vehicle reliability. This stage of analysis should be given special attention.

Analysis of reliability, and in general failure of parts of the vehicle, can be achieved by statistical and / or instrumental methods of forecasting. Starting from the minimum cost value necessary for the prevention of preventive maintenance procedures, in this paper, the methodology for determining the optimal periodicity of the replacement of parts using the statistical method, as well as the methodology for determining the optimal periodicity of forecasting using the instrumental method is presented.

As a basic characteristic, which allows taking into account the impact of the length of preventive maintenance, the correctness of the vehicle and the determination of its optimum duration, it is possible to take the efficiency of using the vehicle.

In determining the periodicity of the implementation of the procedures of preventive maintenance technology, it is necessary to bear in mind that increasing the number and time between consecutive preventive maintenance procedures, only to a certain value, leads to an increase in the effectiveness of the vehicle. Too many implementations of preventive maintenance procedures, reduces the likelihood of failure of the vehicle, but increases the costs of its exploitation, and therefore reduces its effectiveness. Using the methodology shown in this paper, the dependence of the cost of implementing preventive maintenance procedures can be determined, depending on the characteristics of the vehicle reliability. By applying the methodology presented, it is possible to determine the value of the minimum cost of preventive maintenance that corresponds to the optimal reliability reserve and the length of the forecasting period.

IRMES KRAGUJEVAC 2019

9th International Scientific Conference
Research and Development of Mechanical Elements and Systems
Kragujevac, Serbia, September 5-7 2019

THEORY AND EXPERIMENTAL RESEARCH OF OPTIMAL CHARACTERISTICS OF HYDRODYNAMIC TRANSMISSIONS OF MOTOR VEHICLES

Vojislav Krstić[1], Božidar Krstić[2]

[1]Faculty of Transport and Traffic Engineering, University of Belgrade, Vojvode Stepe 305, 11000 Beograd, Serbia
[2]Faculty of Engineering University of Kragujevac, Sestre Janjić 6, 34000 Kragujevac, Serbija, bkrstic@ kg.ac.rs

Key words: motor vehicle, turbotransmissions.

From the emergence of Fetinger's principle, to date, the development of hydrodynamic power transducers (HDPS) has gone upward, with intense or less intense periods of development, in order to experience a booming development over the past few decades. In the previous period, thanks to the large number of researchers in this field, many types of these notebooks have been developed and today it is almost impossible to list all types and models designed for different applications. New concepts in the treatment of power transfer have led to the vigorous development of HDPS. The fundamentally analysed power transfer of HDPS, and not only based on currently observed characteristics, has led to the creation of conditions for mass production and their wide application in all industries. Such an approach leads to the final affirmation of Fetinger's principle of power transfer and development, on this principle of a whole series of transmissions for a wide variety of applications. The numerous theoretical and experimental investigations in the field of HDPS, as well as the monitoring of their behavior in exploitation, confirmed the importance and justification of their application in almost all areas of the technique. The favorable characteristics of this type of power transfer, confirmed in exploitation, have enabled them massive application, and today there is virtually no industry in which they are not applied or justified they cannot apply.

In the study of the influence of geometric parameters on fluid flow parameters in the turbine working area, an indirect measurement method was used, which is based on the definition of pressure on the walls of the velocity probes. Non-regulating turbodiesel D-370, active circulation diameter 370 mm, with different the position of the blades (radial and slanted) of the production industry of "14. Oktobar" from Krusevac. The number of pump blades is 45 and turbine 43. In order to carry out these investigations, it was necessary to create an original experimental plant, which is described in more detail in. Its components include: asynchronous electromotor type OPS 80/4 "Sever" -Subotica, accepting device of the research facility, hydraulic braking device of the hydrodynamic type ut-30 of the German

company Schenk-Heker, a five-stage mechanical gear and measuring equipment. The accepting device represents the original conceptual and constructive solution of the author. The following measuring equipment was used: Pressure transmitter P.4AK, for measuring range 0-20 bar, production of the German company HBM, and with a cylindrical probe connected by a hose of 8 mm diameter; Universal digital meter for electrical quantities of HBM production; Six channel (KWS 673.A4) and dual channel (KWS 85.A1) analogue HBM production amplifiers; Temperature thermo par produced by Swedish company SVEMA; Measuring shaft T30 FN 3/5 production of HBM.

The investigations were carried out at the angular speed of rotation of the pump circle 107.02 s-1, the gap between the blades of 4.5 mm, the slip coefficient of 3.5% and the filling of the turbocharger with 85% mineral oil of a viscosity of 21 mm2 / s at 323 K.

Using a single-channel cylindrical probe of 3mm diameter, with a diameter of 0.6mm, the values of current and stop of the pressure, as well as the angle, which defines the direction of flow velocity of the fluid are measured. Using the known connections between the pressures and the flow velocity of the fluid, the velocity of the flow velocity in the plane parallel with the axis of rotation is determined. Then, on the basis of the measured (pd, ps) and the calculated the size of the cartoon diagrammatic dependence of the changes in the measured and calculated values with the change of the position of the measuring point in relation to the rotation axis.

The obtained results of the investigation of the influence of the position of the wheel blades and the gap between the blades on the shape of the flow in the working area of the hydrodynamic couplings indicate the following conclusions:

- At a lower value of the gap between the HDS blades, higher values of the volume and meridian components of the absolute fluid flow velocity are obtained, as well as the lower value of the angle of convection of the working fluid current when it is released from the HDS blades. Then, the less value of the coefficient of current leakage is obtained, and thus the higher value of the effort and the degree of utilization of HDS work circuits;
- HDS with tilted blades has considerably more unfavourable HDS flow rates with radial blades;
- The two previous findings, based on the results of the experimental research, suggest that the geometric parameters of the HDS workspace have a decisive influence on the flow mode in them.
- The highest total fluid pressure occurs near the smallest and largest diameter of the HDS workspace, and its smallest value appears in the interval (0.73 0.95). That indicates the existence of the so-called center of the meridian stream in that area. In this area, there may be a cavitation in the HDS pump circulation, both in the starting mode and in the turbine circuit.
- The value of the volume component of the absolute velocity of fluid flow in the HDS workspace is smaller, over the entire width of the blades, of the value of the transmission speed and for HDS with radial blades and code HDS with sloping blades. This finding indicates the occurrence of the fluctuation of the working fluid current over the entire width of the HDS blades;
- The value of the meridian component of the working fluid flow rate increases from the so-called the center of the meridian flow to the minimum and maximum circulation diameter;
- The values of the angle of working fluid flow in HDS with radial blades, under the same other conditions, are less than the value of this angle in HDS with sloped blades.

RESEARCH AND DEVELOPMENT IN FIELD OF ENERGY AND ECOLOGY

IRMES KRAGUJEVAC 2019

9th International Scientific Conference
Research and Development of Mechanical Elements and Systems
Kragujevac, Serbia, September5-7 2019

DETERMINATION OF OPERATING PARAMETERS OF TURBINES FOR MICRO HYDROELECTRIC POWER PLANTS FOR OPTIMAL USE OF HYDROPOWER

Milutin Prodanović[1], Aleksandar Miltenović[2], Miroslav Nikodijević[1]

[1] JP EPS Beograd, Ogranak Održivi razvoj, Belgrade, Serbia
[2] University of Niš, Faculty of Mechanical Engineering, Aleksandra Medvedeva 14, Niš, Serbia, aleksandar.miltenovic@masfak.ni.ac.rs

Key words: turbines, micro hydroelectric power plants, hydropower.

The basic function of the turbine is the transformation of the kinetic energy of the water into the mechanical energy of the rotating parts of the turbine. The operating conditions of the turbine depend on a large number of influencing parameters such as field configuration, possible flow and fall combinations, etc. Many different types of turbines have been developed to cover a wide range of working conditions. It can be said that turbines used in small hydropower plants are a reduced version of turbines used in conventional large hydroelectric power plants.

According to the qualification of the turbines according to the delivered electricity of the micro hydro power plants, they include a power range of 5 to 100 kW.

Considering that in the case of micro-flow hydroelectric power plants, the flow of water varies widely, which is why water turbines are chosen that work efficiently at wide flow limits.

Crossflow turbines are pulse turbines in which water passes twice over the blades of the impeller. It has a simple construction with three main components: Rectangular introductory device, which directs the flow of water over two profiled blades placed side by side; Impeller drum with arched profiled shovels; enclosures that, in accordance with the flow of water, surround the impeller and on which the impeller of the impeller is clamped.

With the Francis turbine, the introducer device is a fixed wheel, where the introductory blades are located. The blades are articulated so that the turbine operation can be controlled. The water is fed by a circular channel and directs it to the impeller via the opening blades. The impeller is connected to a shaft that is clamped over the main bearing of the turbine and connected to the gear and generator.

The Kaplan turbine impeller is similar to a propeller. It is primarily intended for low altitude falls, where it has a good degree of efficiency. The blades of the impeller at Kaplan's turbine

are attached to the hub so that their position can be adjusted. The impeller is most often placed in the spiral housing so that the water flows radially through the input device and radially through the impeller. A complete turbine can be integrated into the pipeline, which enables a compact construction.

Selection of turbine is significantly influenced by the available flow and its change during the year. In this regard, the following cases should be distinguished:

• Constant flow - a turbine with a fixed hole is selected at the input of the propeller turbine (Kaplan's with fixed inlet blades) and Pelton to a constant diameter of the nozzles.

• Small change of flow - turbine is relatively little exposed to variable flow. A Fransis or Kaplan turbine is selected with a fixed fixed hole at the inlet for maximum efficiency.

• A large change in flow - turbine very often does not have enough water. Despite the reduced efficiency, it is recommended to use a flow turbine or a Fransis turbine. Pelton turbines with multiple nozzles, as well as Kaplan turbines with 2 degrees, can be used as they can be adjusted according to the flow.

From the aspect of optimal exploitation of the available hydroelectric power plant, it is necessary, in accordance with hydrological conditions, to harmonize the choice of the turbine itself, its construction parameters with the parameters of the machine plant or the generator itself. It should be noted that the working speeds of the turbine circuits are not fixed and can be changed within certain limits by changing the design parameters of the turbine.

The current generator is connected to a network having a constant network frequency of 50 Hz. Therefore, it is necessary that the number of revolutions of the generator does not change and that it is harmonized with the other parameters of the hydroelectric power plant. The following should be taken into account:

• With the increase in the speed, the centrifugal force increases significantly, and therefore the mechanical mapping of the machine group, and therefore the nominal speed is limited to 1500 min^{-1}.

• When applying a generator with a rotational speed below 600 min^{-1}, the overall dimensions and therefore the specific price of the genarator are growing, while at the same time reducing the energy efficiency due to magnetic losses.

• It is therefore recommended that, with turbine speeds below 750 min^{-1}, using a multipixer power transmission, the rpm rises to 1500 min^{-1} or 1000 min^{-1} and optimally exploits available hydropower.

From the aspect of optimal use of the available hydroelectric power plant, it is necessary, in accordance with hydrological conditions, to harmonize the choice of the turbine itself, its construction parameters with the parameters of the machine plant or the electricity generator itself. In this regard, the application of the generator with the numbers of revolutions of 1500 min^{-1} or 1000 min^{-1} is purposeful, with adequate harmonization with the speeds of the turbine circuits with the use of a power transmission - multipixer.

9th International Scientific Conference
Research and Development of Mechanical Elements and Systems
Kragujevac, Serbia, September5-7 2019

IMPACT OF SOURCE TEMPERATURE AT ELECTRIC FLOOR HEATING PANELS

Dragan Cvetković[1], Aleksandar Nešović[1]

[1]University of Kragujevac, Faculty of Engineering, Sestre Janjić 6,
34000 Kragujevac, Serbia, aca.nesovic@gmail.com

Key words: ANSYS Workbench, finite volume method, heat flux, heat transfer, floor panel, electric heating cables.

Among the panel systems, floor heating is the most widely used in Serbia because it offers characteristic advantages in terms of thermal comfort and final energy consumption. The uniform distribution of room temperature, lower temperature regime, easy installation, long service life, simple control, and the current low price of electricity are the reasons for the increasing use of electric heating cables (EHC) in floor heating systems. The application of low-temperature electric floor heating panels (LTEFHP) is limited to hygienic requirements (Table 1, Table 2), therefore the surface temperature of the floor should be uniform and within certain limits. The field of application of EHC in the construction of floor heating panels (Figure 1, Table 3) was investigated taking into account their mutual axial distance and temperature regime. The complete research was conducted numerically, using the finite volume method (FVM) in the ANSYS Workbench 14.5 software.

Table 1. The maximum floor temperature limit values depending on the LTEFHP application

Room category	Type of room	$t_{S\text{-}MAX}$ [°C]
I	In working rooms where a longer period of time is mostly standing	25
II	In residential and office spaces	28
III	In exhibition and similar halls	30
IV	In the bathrooms and swimming pools	32
V	In rooms where short stays, or through which only passes	35

Table 2. Simulation scenario

t_{IN} [°C]	30	35	40	45	50
L [mm]	70; 80; 90; 100; 110; 120; 130; 140; 150; 160; 170; 180; 190; 200				

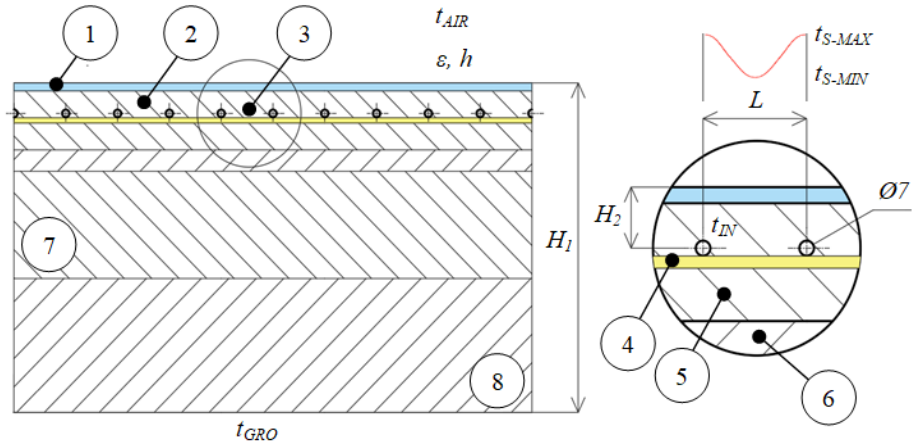

Figure 1. Initial boundary conditions before simulation of LTEFHP

Table 3. Characteristics of materials in the construction of the LTEFHP

Ordinal number	Material	H [m]	ρ [kg/m^3]	c_P [J/kgK]	λ [W/mK]
1	Granite plates	0.012	2700	920	3.5
2	Cement screed	0.05	2200	1050	1.4
3	EHC	-			
4	PVC foil	0.001	1200	960	0.19
5	Styrofoam	0.05	33	1500	0.035
6	Reinforced concrete	0.04	2400	960	2.04
7	Ggravel layer	0.2	1700	840	0.81
8	Stone layer	0.25	1750	840	2.035

The results showed that LTEFHP can easily be used to heat residential and office space (category II) if the input temperature is 30°C in the floor heating panel. If the input temperature is 35°C, then it can be used to heat the exhibition and sports hall (L=115-200 Heating rooms IV and V category is possible with an input temperature of 40°C, but the application limit is quite shifted (L=163-200 mm for category IV). With an inlet temperature of 45°C it is possible to heat only the rooms of the V category, if the distance between EHC is 150-200 mm. Due to hygienic requirements, LTEFHP has no application for the input temperatures in the panel ≥50°C.

Acknowledgments. This investigation is a part of the project TR 33015 of the Technological Development of the Republic of Serbia. We would like to thank the Ministry of Education, Science and Technological Development of the Republic of Serbia for their financial support during this investigation.

IRMES KRAGUJEVAC 2019

9th International Scientific Conference
Research and Development of Mechanical Elements and Systems
Kragujevac, Serbia, September5-7 2019

INTEGRITY EVALUATION FOR THE AIR TANK OF THE REGULATION SYSTEM OF TURBINE AT HYDROPOWER PLANT

Miodrag Arsić[1], Vencislav Grabulov[1], Mladen Mladenović[1], Dušan Arsić[4], Zoran Savić[1]

[1]Institute for materials testing, Boulevard vojvode Mišića 43, 11000 Belgrade, Serbia, miodrag.arsic@institutims.rs
[4]University of Kragujevac, Faculty of Engineering, Sestre Janjić 6, 34000 Kragujevac, Serbia, dusan.arsic@fink.rs

Key words: non-destructive tests, damage repair, strength calculation, integrity evaluation.

Vertical Kaplan turbines with nominal power of 200 MW, made in Russia, have been installed at 6 hydroelectric generating sets of "Djerdap 1". Most of the components were made of steel in accordance with GOST and ASTM standards. During the rehabilitation of the hydroelectric generating set A6 non-destructive testing methods were performed on parent material and welded joints of the main oil/air tank and air tank with the auxiliary oil/air tank, which acts as pressure accumulator in the regulation system, in order to carry out the analysis of the current state and integrity evaluation for the regulation system of the turbine. Regulation system supplies the turbine regulator with oil and regulates the movement of guide vane apparatus vanes. It also regulates the position of runner blades and number of revolutions of the turbine shaft (Figure 1). Shells of all 3 tanks were made of steel Č 1205, while bottoms were made of Russian steel St 20K. Tests were also performed on pipeline elements (pipes and elbows). In order to carry out the analysis of the current state and evaluate the integrity of the air tank, which is a component of the regulation system of A6 turbine at hydro power plant "Djerdap 1", non-destructive tests were performed. These tests were supposed to confirm the adopted value of quality factor of the welded joint v = 1, because for this value no damages on parent material and welded joints of pressure equipment are allowed.

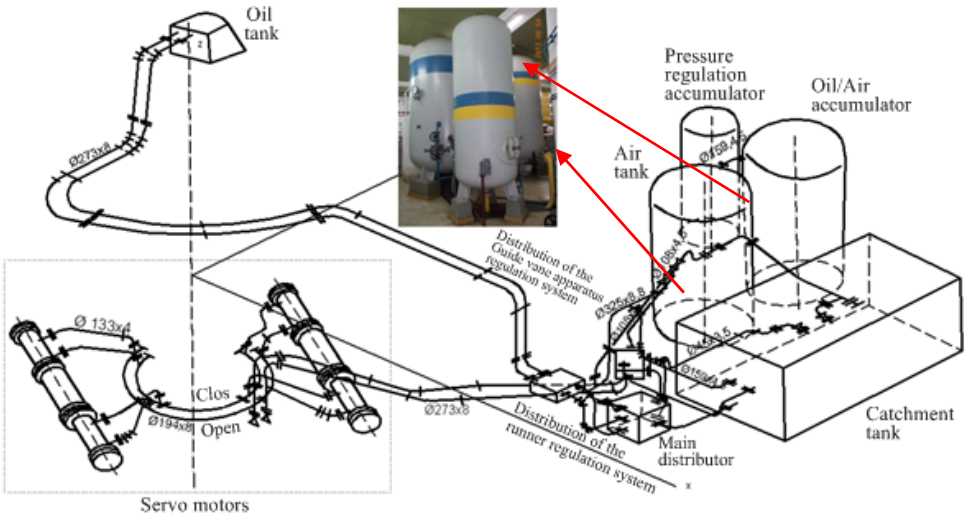

Figure 1. Appearance of tanks which are integral parts of the regulation system of A6 turbine

The results of non-destructive tests performed on air tank are presented in this paper. Mechanical damages were detected by visual inspection at parent material of the shell and at the upper bottom, as well as discontinuous and incompletely welded joints on the inside and outside of the tank. Surface linear crack type indications were detected through magnetic particle testing at intersections of welded joints on the inside of the tank. Internal crack type defects were detected through ultrasonic testing of welded joints. On the basis of test results the technology of reparatory welding / surface welding of parent material and welded joints was created, while on the basis of the analytical calculation of tank strength the evaluation of its integrity for the following 40 years of operation was obtained. Integrity of structures is a relatively new scientific and engineering discipline which, generally, comprises the state analysis, behavioral diagnostics, service life evaluation and rehabilitation of structures. It means that, aside from the usual situation in which the integrity of the structure needs to be evaluated when the defect is detected, this discipline also comprises the stress state analysis of the crackless structure. This approach is especially relevant for welded structures subjected to operating conditions suitable for crack initiation, such as fatigue and corrosion.

Acknowledgments. The authors are thankful for the financial support from the Ministry of Education, Science and Technological Development of Republic of Serbia trough project TR 35002.

9th International Scientific Conference
Research and Development of Mechanical Elements and Systems
Kragujevac, Serbia, September5-7 2019

COMPUTER-AIDED DESIGN OF 30 KW HORIZONTAL AXIS WIND TURBINE

D N Jovanović[1*], V M Šušteršič[1]

[1]University of Kragujevac, Faculty of Engineering, Sestre Janjić 6,
34000 Kragujevac, Serbia, davorjovanovic94@gmail.com, vanjas@kg.ac.rs

Key words: Betz, BEM, Schmitz, Weibull distribution, annual energy production.

In this paper we analyze blade geometry optimization for 30 kW wind turbine with 6.5 tip speed ratio via Betz and Schmitz formulas, using "QBlade" software. Numerous studies were conducted using simple Blade Element Momentum (BEM) theory for horizontal three-bladed wind turbines. In "*The Performance Test of Three Different Horizontal Axis (HAWT) Blade Shapes Using Experimental and Numerical Methods"* by Hsiao et al., experimental and numerical methods were used to test three different horizontal axis wind turbine blade shapes. In "*Comparison of Qblade and CFD results for small-scaled horizontal axis wind turbine analysis"* by Koc, Günel and Yavuz, a unique approach was developed using BEM method to obtain the optimal twist angle and chord length for small wind turbine design.

Chord will be calculated according to the following Betz formulas:

$$c(r) = \frac{16 \cdot \pi \cdot R}{9 \cdot B \cdot C_L(\alpha) \cdot \lambda} \cdot \frac{1}{[(\lambda \cdot \frac{r}{R})^2 + \frac{4}{9}]^{1/2}}$$

Blade optimization after Schmitz will also be conducted, according to the equation:

$$c(r) = \frac{16 \cdot \pi \cdot R}{B \cdot C_L(\alpha) \cdot \lambda} \sin^2\left(\frac{1}{3} \cdot \tan^{-1}(\frac{R}{\lambda \cdot r})\right)$$

Annual energy production (AEP) can be computed via equation:

$$AEP = \sum_{i=1}^{N-1} \frac{1}{2} \cdot (P(v_i + 1) + P(v_i)) \cdot f(v_i < v < v_{i+1}) \cdot 8760$$

In the conducted simulations the blades are divided into 100 elements. After both blades are calculated and 3D models are created, BEM analysis is conducted for both blades. In figures 1 and 2 is shown power curve for both cases, which are generated after BEM theory is applied on 100 aerodynamically independent elements. Note that cut-in wind speed is 3 ms^{-1} and cut-out is 30 ms^{-1}.

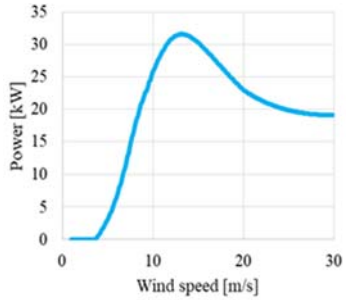

Figure 1. Power curve generated for Betz optimized rotor

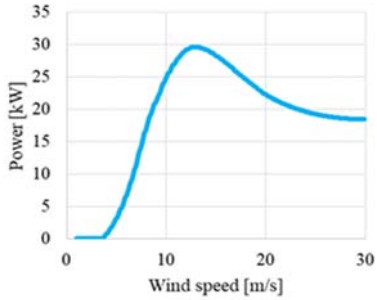

Figure 2. Power curve generated for Schmitz optimized rotor

Betz optimised rotor has the highest power generation at 13.1 ms^{-1} with 31.55 kW, while Schmitz optimized rotor has highest power generation at 12.9 ms^{-1} with 29.56 kW. This gap close to 2 kW will have some effect in annual energy production.

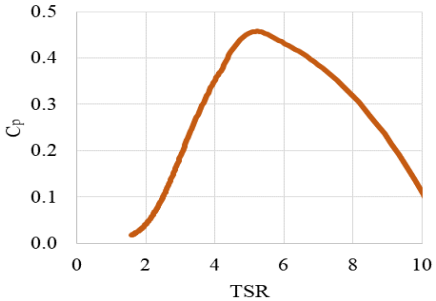

Figure 3. Power coefficient generated for Betz optimized rotor

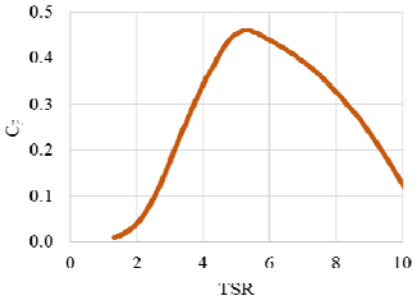

Figure 4. Power curve generated for Schmitz optimized rotor

By analysing figures 3 and 4, small C_p difference can be noticed. Highest C_p ratio for Betz optimised rotor is 0.458 at 5.23 TSR, while for Schimtz optimised rotor C_p ratio is 0.46 at 5.3 TSR. While these are highest values of C_p ratio, at rated TSR (6.5) according to which both rotors are calculated these values are 0.416 and 0.418 for Betz and Schmitz optimised rotor, respectively.

By using software "QBlade", power curve of wind turbine with rated power of 30kW, TSR of 6.5 and rated wind speed of 9.8 ms^{-1} is analysed using Betz and Schmitz formulas for blade geometry optimisation. Chord distribution is optimised, while twist angles are same for both cases when calculated and optimised so angle of attack has maximum value. 3D models of blades and rotors are generated and BEM analysis is conducted (for 100 elements blade discretization), thus, calculating power curves and power coefficients. Weibull distribution is used to calculate probability for certain wind speeds to occur (parameters k and c are the same for both cases with values of 2.38 and 8.5 ms^{-1}). AEP for Betz optimised rotor is 124142 kWh, while for Schmitz optimised rotor AEP is 120775 kWh. It is noted that, observing wind turbine of 30kW differences in power curves and power coefficients have 2.79% AEP for Betz optimised blades, compared to Schmitz optimisation.

9th International Scientific Conference
Research and Development of Mechanical Elements and Systems
Kragujevac, Serbia, September5-7 2019

LIFE CYCLE ASSESSMENT OF THE CAR TIRE WITH ECO-INDICATOR 99 METHODOLOGY

A Pavlović[1], D Nikolić[1], S Jovanović[1], G Bošković[1], J Skerlić[1]

[1]University of Kragujevac, Faculty of Engineering, Sestre Janjić 6,
34000 Kragujevac, Serbia, djina1107@gmail.com

Key words: LCA, Eco-indicator 99, product, tire

The concept of the product life cycle (PLC) was introduced in the fifties of the last century in scientific researches. The existence of the biological life cycle is implemented on the products. Namely, the PLC represents one cycle or the process from birth to death. The product life cycle is an important phenomenon because it describes all the phases through which it passes. In each phase, the product is interdependent with the society, economy and environment, and it encounters a number of limitations.

From the point of view of the environment, the current economic model is based on the transformation of resources into ready to use products and their disposal. This economic model, ie the product life cycle is not eco-friendly.

The previously mentioned fact can be proved by certain analyzes, such as life-cycle assessment (LCA). The LCA is a technique to evaluate environmental impacts related to all the phases of a product's life cycle. This assessment takes into accountnumerous activities:from extraction the raw material and its production, manufacturing of a product, product use, end-of-life disposal and all of the transportation activities thathappen between all mentioned phases.

Today the automotive industry is a driving force for the development of national economics so the number of a vehicle increases expeditiously. As an integral part of the vehicle, tires are generated annually in large amounts all over the world. The growth of the car tires production affects the environment and also the growth of non-degradable waste which has a large energetic potential but which currently is not fully used.

The aim of this study is to evaluate the environmental impact of car tire during its whole life cycle. That analysis can be achieved throughout its service life, from the acquisition of the raw materials through to the recycling of the worn tire, because the tire constantly interacts with the environment. Approaches to effectively reducing the negative environmental impact can be demonstrated only on the basis of detailed knowledge of this interaction.

This is why a life cycle assessment quantifies the material and energy flows in the different stages of a tire's life cycle (life cycle inventory analysis) and describes the interaction with

the environment (impact assessment and interpretation). In this study, the environmental impact is evaluated by using methodology Eco Indicator (EI) 99, which is one of the most widely used impact assessment methods in LCA. The EI was developed to connect the life cycle inventoryresults with procedures for determining weight coefficients, with the aim of presenting LCA results at all levels.

In this paper, EI 99 methodology is done for a single tire with an average service life of 50,000.00 km over a four-year period. The car tire is assumed to weight approximately 6.5 kg.

The main phases of the life-cycle tires that are analyzed in this research:

Phase 1. Production of raw material: the feedstock for tires is manufactured from mineral, fossil, and reused resources.

Phase 2. Production/manufacture of the tire: includes the production of the structural parts of the tire and its packaging.

Phase 3. Distribution/transport of the tire: involves all activities that are undertaken in the transport, storage and distribution sector.

Phase 4. Use of the tire: includes using process scenarios and processes such as maintenance, repair, cleaning of the tires, etc.

Phase 5. End-of-life tires: includes activities that are associated with collecting the worn tire and its disposal.

Phase 6. End-of-life processing: involves all activities that are established on waste management and treatment.

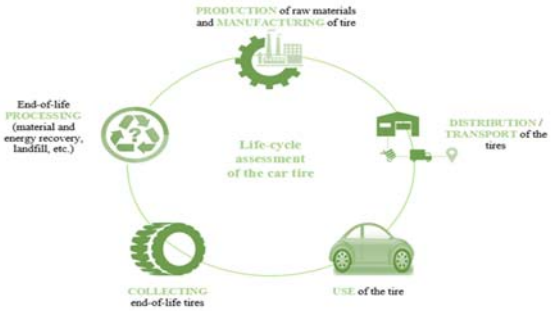

Figure 1. Life-cycle of the car tire

In this research, the above-mentioned phases are analyzed expect phase 5. and 6. Due to insufficient data, the EI was not calculated for the disposal phase but it is known that the car tire has a big negative impact on the environment in this phase.

According to the calculation which is done in software Microsoft Excel, it is concluded that the biggest environmental impact and expenses have the “production” phase.

Based on the obtained results, can be summarized that the way of production of the car tire is necessary to be changed and improved. One of the solutions for that is implementing the circular model of production, ie using the worn tires in the production process.

Life-cycle assessment is very important because based on values which are obtained from analysis, it is possible to identify activities in life-cycle phases that can be improved and on that way it is possible to reduce the negative impact of the tire on the environment.

9th International Scientific Conference
Research and Development of Mechanical Elements and Systems
Kragujevac, Serbia, September5-7 2019

ENERGY PERFORMANCE OF THE SERBIAN AND ESTONIAN FAMILY HOUSE WITH A SELECTIVE ABSORPTION FACADE

Nebojša Lukić[1], Aleksandar Nešović[1], Novak Nikolić[1], Andres Siirde[2], Anna Volkova[2], Eduard Latosov[2]

[1]University of Kragujevac, Faculty of Engineering, Sestre Janjić 6, 34000 Kragujevac, Serbia, lukic@kg.ac.rs
[2]Tallinna Tehnikaulikool, Energiatehnoloogia instituut, Ehitajate tee 5, 19086 Tallinn, Estonia, anna.volvkova@taltech.ee

Key words: heating energy consumption, selective absorption façade, Serbian and Estonian family houses.

The aim of this paper is to examine the possibilities of using selective absorption facades in the construction of Serbian and Estonian houses in order to reduce the energy consumption during the heating season. Defined simulations will be carried out by EnergyPlus. This software is a collection of many program modules that work together to calculate the energy required for building heating and cooling, using a variety of systems and energy sources. It does this by simulating the building and associated energy systems when they are exposed to different environmental and operating conditions. The core of the simulation is a model of the building that is based on fundamental heat balance principles.

The subject of research is the family house shown in Figures 1 and 2. The net area of the house is 180.75 m^2. The net conditioned building area is 171 m^2 (storage room and closet are unconditioned rooms). The total surface of the thermal shell is 432 m^2 and window-wall ratio is 14%. The family house has two floors (ground floor and first floor).

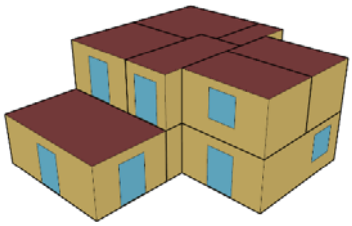

Figure 1. Northwest facade

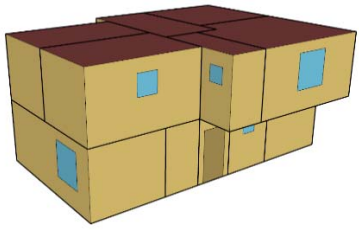

Figure 2. Southwest facade

According to simulation procedure, four simulation scenarios are performed. Since, the minimum regulation requirements of thermal characteristics are different for Serbian and Estonian house, all simulations are carried out for two houses, separately. Initial scenario (DHM) has been implied two houses (Serbian and Estonian), built according to current regulations of building thermal characteristics as minimum requirements (the highest allowed heat transfer coefficients). Thermal and solar absorptance (and emittance) are adopted as usual for a building façade, 0.9 and 0.7, respectively. This means that building façade of DHM absorbs solar radiation and emits thermal (infrared longwave) radiation very well. Other three simulation scenarios has been implied two houses with changed absorptance characteristics of the south (S), south and west (S, W) and south, west and east oriented wall. In Figure 3 the percentage savings of the monthly heating energy consumption of Serbian and Estonian house using different insulation thickness and selective façade is given. For this review the warmest and coldest heating season months in Kragujevac, Serbia (April and January, respectively) and Tallinn, Estonia (October and January, respectively) are considered. For all presented cases the simulation scenario is S (selective south façade). Figure 13 shows that in case of Serbian house for the warmest heating month (April) the percentage savings are positive even for south wall without insulation layer. The maximum energy savings (8.51%) Serbian house achieves with maximum insulation thickness (south selective façade). For the coldest month (January) only for south wall without insulation layer savings are negative (-4.00%). Also, figure 13 shows that in case of Estonian house for the both considered heating months (October and January) the percentage savings are positive only for maximum insulation thickness. In case of the coldest month (January) and maximum insulation thickness the energy savings effects of south selective façade are insignificant (0.41%).

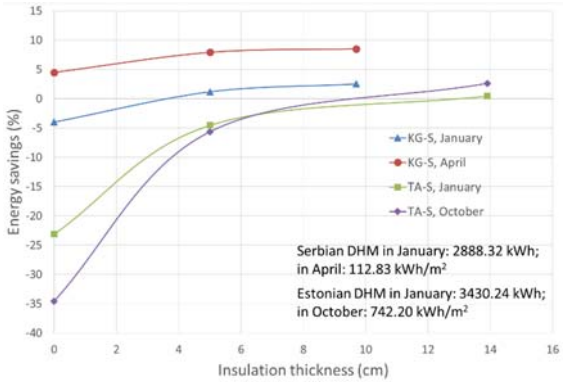

Figure 3 Percentage savings of the monthly heating energy consumption of Serbian and Estonian house using different insulation thickness and selective façade for selected months

Acknowledgments. This work was funded by the Ministry of Education and Science of the Republic of Serbia under the contract TR 33015.

9th International Scientific Conference
Research and Development of Mechanical Elements and Systems
Kragujevac, Serbia, September5-7 2019

APPROXIMATION OF THE BRIDGE DECK DIFFUSION COEFFICIENT AND SURFACE CHLORIDE CONCENTRATION FROM FIELD DATA

Petr Koneny[1], Petr Lehner[1], Dita Vorechovska[2], Martina Somodikova[2], Marie Hornakova[1], Pavla Rovnanikova[2]

[1]VSB – Technical University of Ostrava, Faculty of Civil Engineering, Ostrava-Poruba, Czech Republic
[2]Brno University of Technology, Faculty of Civil Engineering, Brno, Czech Republic

Key words: Analysis of field data, reinforced concrete, chloride ingress, diffusion coefficient, numerical modelling, surface chloride content.

Bridges are the typical constructions exposed to the combined effect of carbonation, chloride ingress and mechanical load. Such structures are prone to corrosion that threatens their durability and reduces the service life and bearing capacity. Even though the physical law for the analysis of the penetration of agents inducing steel reinforcement corrosion, such as chlorides or carbon dioxide, are known, the modelling still contains lot of unknowns, especially in case of heterogeneous material, such as concrete.
Numerical modelling of chloride penetration might be simplified using deterministic 1D numerical diffusion model called Crank's solution applied by Collepardi:

$$C_{z,t} = C_0 \left[1 - \mathrm{erf}\left(\frac{z}{\sqrt{4 D_c t}}\right)\right],$$

where $C_{z,t}$ is concentration of chlorides [% by mass of concrete], C_0 is concentration of chlorides [% by mass of concrete] at the surface of concrete, D_c is apparent diffusion coefficient of chloride ions in concrete [$m^2 \cdot s^{-1}$], t is chloride exposition time [s], z is depth of the layer from the concrete surface [m].

In this paper, the data from the regular inspections of 5 highway bridges in the Czech Republic were analysed with respect to the corrosion related durability aspects and modelling of reinforced concrete. In each location, the samples were taken from three different depths of 0–10, 10–20 and 20–30 mm from the concrete surface. Subsequently, the value of pH and the amount of water-soluble chlorides were measured in water leaches in laboratory.
Suitable chloride profiles, that are characterized by decreasing value of chloride concentration, were selected for the subsequent regression analysis.

The lacking parameters, that are in this case the diffusion coefficient D_c and the chloride concentration on the surface C_0, were determined iteratively by the analogy to the least square method:

$$S_j = \sum_i^N \Delta C_{(i)}^2 = \sum_i^N \Delta (C_{m(i)} - C_{c(j,i)})^2,$$

where S_j is sum of the squares in the j-th iteration [(% by mass)^2], N is number of layers in profile, $\Delta C_{(i)}$ is difference between the measured and calculated concentration of chlorides in the N-th layer [% by mass of total cementitious materials], $C_{m(i)}/C_{c(j,i)}$ is measured/calculated concentration of chlorides [% by mass of total cementitious materials].

The full length paper contains description of the above mentioned numerical procedure in detail, including demonstration in case of selected single pole bridge No. 55I-030. The trend of the ratio between chloride ingress rate and the diffusion coefficient is not proportional (Figure 1). Based on the visual assessment of the bar chart, it cannot be proved that the diffusion coefficient is correlated to the concentration of chloride ions. Thus, it can be concluded that for the successful determination of the diffusion coefficient three measured values are not sufficient and the analysis is burdened with a numerical error. For more precise determination of diffusion coefficient is recommended 6 measurements for every drilled core.

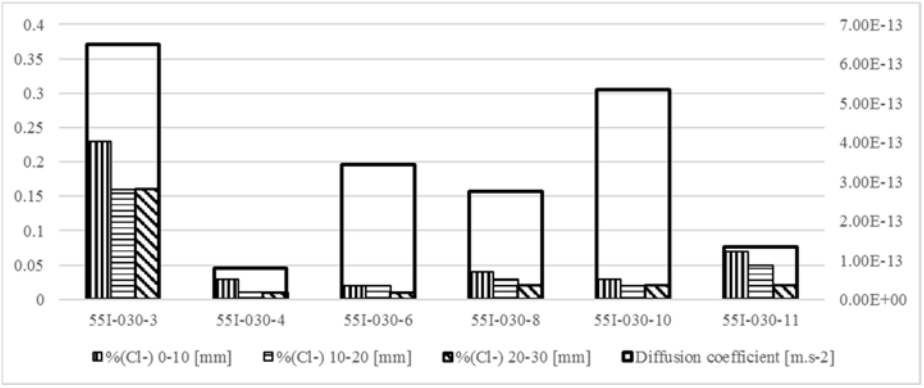

Figure 1. The chloride profile and calculated diffusion coefficient D_c for selected samples of the bridge No. 55I-030.

The visual comparison of the ratio between the diffusion coefficient and chloride profile values was used to evaluate the quality of approximation. This procedure with quantified measurement might be tested in the future research as the tool for the assessment of the quality of chloride profile data.

Acknowledgments. This contribution has been developed as a part of the research project GACR 18-07949S "Probabilistic Modeling of the Durability of Reinforced Concrete Structures Considering Synergic Effect of Carbonation, Chlorides and Mechanical Action" supported by the Czech Science Foundation. We are grateful to Mr. Igor Suza from Mostní a silniční, s.r.o. company that enabled the processing of presented data from in-situ measurements carried out by him and his colleagues.

9th International Scientific Conference
Research and Development of Mechanical Elements and Systems
Kragujevac, Serbia, September5-7 2019

INNOVATIVE SOLUTION OF FINE HORIZONTAL TRASH RACK FOR SMALL HYDROELECTRIC POWER STATIONS

Aleksandar Miltenović[1], Milutin Prodanović[2], Livia Beju[3], Vojislav Miltenović[4], Nikola Velimirović[5]

[1]University of Niš, Faculty of Mechanical Engineering, Aleksandra Medvedeva 14, Niš, Serbia, aleksandar.miltenovic@masfak.ni.ac.rs
[2] JP EPS Beograd, Ogranak Održivi razvoj, Belgrade, Serbia
[2]University "Lucian Blaga" of Sibiu, Department of Industrial Machines and Equipment, Emil Cioran 4, Sibiu, Romania
[1]University of Niš, Innovation center, Univerzitetski Trg 2, Niš, Serbia
[1] State University of Novi Pazar, Department for Technical Science, Vuka Karadžića bb, Novi Pazar, Serbia

Key words: hydroelectric power station, trash rack, product development

Alternative energy sources have a number of advantages over energy derived from fossil and nuclear power plants. Large potential from this aspect has small hydropower plants, which are not expensive, they can be installed on small rivers, and in this way the received electricity is much cheaper. One of the problems that need to be solved is to prevent the penetration of impurities into turbine plants. This is solved by placing protective trash rack on water intakes. The paper presents an innovative solution for horizontal fine trash-rack with cleaning function for small hydro-electric power stations.

For solving prevention of impurities into turbine plants, three conceptual solutions are developed and for further work was chosen third solution.

Choosen conceptual solution (Figure 1.) is the transmission of the drive from the working point to the trash-rack is not carried out directly by mechanical connection, but indirectly by electrical means. A current generator 7 is installed on the impeller of the impeller through the corresponding multiplier. The drive unit is now running via an electric motor with gearbox 8, which is connected to the chain drive chain. This variant is more expensive compared to variants 1 and 2, but provides a number of advantages.

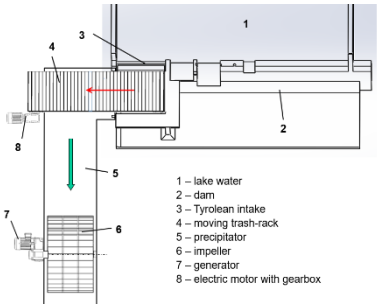

Figure 1. Trash-rack – variant 3

The complete plant for autonomous electrical energy production consists of side panels and sheet metal, the function of which is to direct the flow of water properly. The shape of the sheet metal is harmonized with the construction of the Poncelet wheel. A water flow control mechanism is also installed with the appropriate guides of the stop plate (plate closure). The flow can be regulated via a threaded spindle. On the side are the mounts on which the impellers of the impeller are fixed.

The torque transfer from the impeller to the generator is carried out over the stepped shaft. The link of the shaft with the impeller is made via conical clamping rings and with the generator via the coupling.

The horizontal fine trash-rack with cleaning function is constructed according to the model of conveyor belts with movable perforated plates.

The basic components or components of the trash-rack are:

1. Perforated plates are mutually articulated with rollers for operation and guiding
2. A supporting structure of the trash-rack, which has a guide function;
3. Set the sprocket with the drive, ie the driven shaft
4. Protective sheet for trash-rack, with a brush for removal of impurities and waste from the grid;
5. Electric motors for the peripheral motor (24V / 600W DC motors), connected to the set of drive sprockets 3a.

Due to the power generated by the Poncelet impeller (Pt = 612W), the following type of 24V / 600W DC motors, PM296 of the Ningbo Jirun Electric Machine Co. Ltd. The generator is supplied with the multiplier to increase the speed with n_t = 16.2 min^{-1} at n_G = 1450 min^{-1}.

The generator current is charged with AKU batteries and is powered by an electric motor to drive the trash-rack.

IRMES KRAGUJEVAC 2019

9th International Scientific Conference
Research and Development of Mechanical Elements and Systems
Kragujevac, Serbia, September5-7 2019

CALCULATION METHODOLOGY AND RESULTS OF PIPELINE STRESS ANALYSIS, SUPPORTS AND STEAM PIPELINE HANGING RECONSTRUCTION FOR RA FRESH STEAM PIPELINE AT POWER PLANT KOSTOLAC B WITH INCREASED FRESH STEAM FLOW RATE OF 1060 T/H AND NEW OPERATIONAL CONDITIONS

Dragan Živić[1], Vladimir Stevanović[2], Sanja Milivojević[2], Milan M Petrović[2], Đura Kesić[3]

[1]JP Elektroprivreda Srbije - Ogranak „Termoelektrane i kopovi Kostolac“, Nikole Tesle 5-7, 12208 Kostolac, Serbia
[2]University of Belgrade, Faculty of Mechanical Engineering, Kraljice Marije 16, 11120 Belgrade, Serbia
[3]Termoenergo inženjering d.o.o, Bulevar Kralja Aleksandra 298, 11050 Belgrade, Serbia

Keywords: static and dynamic loads, calculation methodology, allowable stress design /analysis, safety analysis.

In order to reach designed power output of 2 x 348.5MW at two units of the Thermal power plant Kostolac B, a number of modernization and reconstruction activities are performed as well as static and dynamic fresh steam pipeline stress analysis. All overhauls and retrofits are conducted with aim to increase plant efficiency and reduce environmental pollution. In order to reach the design power, it was determined that it is necessary to increase the fresh steam flow rate from 1000 t/h to 1060 t/h. In this paper, the calculation methodology and obtained results of pipeline stress analysis of the fresh steam pipeline with new operational conditions are presented. Maximal fresh steam pipeline loads are determined in cases of transient conditions. The results of the pipeline stress analyses are presented together with the determined support loads and hangings. The steam pipeline operational parameter are analysed during trips and shut-offs, cold and hot start-ups and drainage conditions. Obtained results are support for the safety analyses and operational conditions determination.

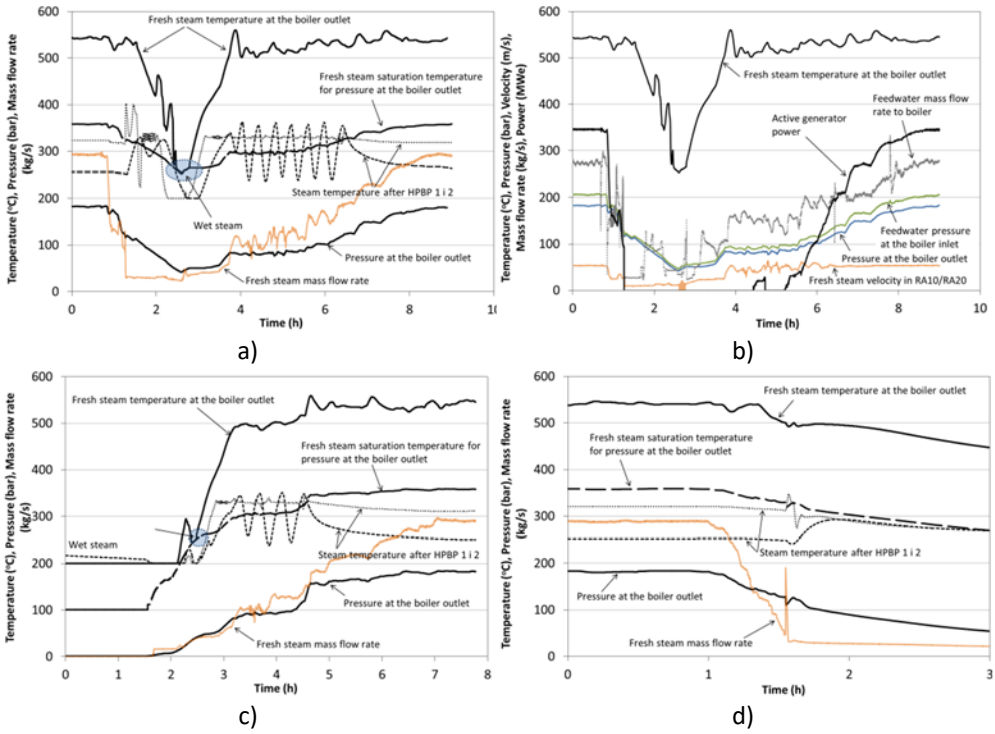

Figure 1. Parameters of fresh steam in RA steam pipeline in case of a) unit shut-off from full-power and hot start-up, b) unit shut-off from full-power and hot start-up, c) cold start-up and d) unit trip from full-power.

IRMES KRAGUJEVAC 2019

9th International Scientific Conference
Research and Development of Mechanical Elements and Systems
Kragujevac, Serbia, September5-7 2019

INSULATION IMPACT ON APPLIANCE ACOUSTIC CHARACTERISTICS

Peter Zvolensky[1], Lukas Lestinsky[1], Jan Dungel[2], Juraj Grencik[1]

[1]University of Zilina, Faculty of Mechanical Engineering, Univerzitna 1, 01026 Zilina, Slovakia, peter.zvolensky@fstroj.uniza.sk, lukas.lestinsky@fstroj.uniza.sk, juraj.grencik@fstroj.uniza.sk
[2]CEIT, a.s., Univerzitna 6A, 01008 Zilina, Slovakia, jan.dungel@ceitgroup.eu

Key words: increasing rigidity by insulation, insulation on panels, stiffness simulation, FEM simulation.

The quality of appliances is crucial in their purchase, which puts considerable pressure on their manufacturers, which are forced to invest significant resources in their development. Consumers have much greater opportunity to compare individual products with each other, either through the parameters on the label in a stone shop, or through online e-shops and their search engines, where individual parameters can be freely chosen. The possibility of a real comparison of appliances allowed a customer to search a wide range of products and the manufacturers are forced to modify already sold appliances in order to overcome or differentiate themselves by selling their products.

Figure 1. Appliance Store

This article is concerned with impact of insulation rigidity on washing machine acoustic characteristics. Washing machine body is affected by forces during washing cycles which originate from mass of water and laundry. The forces also originate from an unbalance inside the washing machine tub. The unbalance is changing after every inner tub stoppage during a spin cycle. Unbalance inside the washing machine tub creates a big acoustic issue, not only for increased noise, but also for increased load of components. Also, rigidity of the washing

machine body has big impact on overall noise. If there is no excessive relative movement of panels and other components there is no excessive noise also.

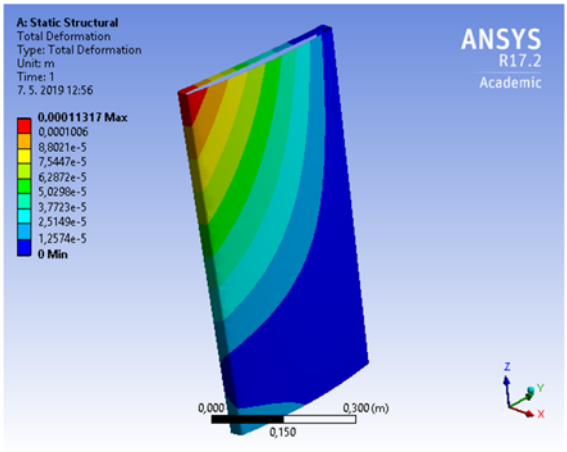

Figure 2. Front panel with upgraded insulation

Washing machine body is usually well designed in terms of deformation resistance. Panels are equipped with many extrusions which improves their rigidity. Panels of different producers differ in thickness also. Thickness of panels has also big impact on the washing machine rigidity. In ideal conditions, washing machine body should be as robust as possible, to prevent deformations. If producers want to achieve higher level of a robustness, they have to invest into production of the washing machine body. But there is an issue of increased production costs. Efficient way is to use current panels in production and improve their rigidity without big intervention into its structure. The proposed solution is to use noise insulation as a panel stiffener. Nowadays, washing machines have got installed noise insulation on the panels, but the insulation has not got any measurable impact on the panel rigidity. Production costs increase would be significantly smaller than production of the thicker panels. New solution relies on a new way of gluing insulation on the panels. To secure solid connection between an insulation and a panel, the insulation is equipped with a crosshatch. The crosshatch, made of glass-fabric, secures solid connection between panel and insulation and allows to transfer forces from panel to insulation, so the insulation can serve as the stiffener. For determination of the insulation impact on the panel stiffness, 3D models of the panels were made. The 3D models were exposed to strength analysis in the FEM software Ansys. The biggest impact on a rigidity of a panels was achieved on the side panels, which on a top loader washing machine transfer majority of the forces.

Acknowledgments. This work was created by the implementation of the project “Low Cost Logistic System Based on Mobile Robotic Platforms for Industrial Use”, ITMS: 26220220205 supported by the Operational Programme Research and Development and by the European Fund for Regional Development.

9th International Scientific Conference
Research and Development of Mechanical Elements and Systems
Kragujevac, Serbia, September5-7 2019

VIBROMECHANICAL DIAGNOSTICS OF URICANI MINE HOIST MACHINES

Mihai-Carmelo Ridzi[1], Răzvan-Bogdan Itu[1], Wilhelm Kecs[2], Vilhelm Itu[1]

[1] University of Petroșani, Faculty of Mechanical and Electical Engineering, University Street 20, 332006 Petroşani, Romania, ridzim@yahoo.com
[2] University of Petroşani, Faculty of Sciences, University Street 20, 332006 Petroşani, Romania, wwkecs@yahoo.com

Key words: vibromechanical diagnostics, mine hoist machines.

This paper presents some technique and its applications of modern digital computer monitoring and control for safety mining production process. The technique has been used in the full digital monitoring and automation control for hoists coal mining machines. With the technique, it has been achieved the better economical and social benefits in safety mining production. The aim of vibration monitoring is the detection of changes in the vibration condition of the object under investigation during its operation. The cause of such changes is mainly the appearance of a defect. Machine condition monitoring is conducted first of all using low frequency and middle frequency vibration that propagates very well from the point of its origin up to the point of its control. The number of such points can be reduced to one or two for each object to be monitored if there is a common casing. The vibration measurements can be conducted without any change in the operation mode of the object. The vibration signatures are analyzed from the two parameters, namely Absolute Vibration of Bearing casing and Relative shaft vibration of bearing housing and the shaft. Most of the defects encountered in the rotating machinery give rise to a distinct vibration pattern (vibration signature) and hence mostly faults can be identified using vibration signature analysis techniques. For the diagnosis it is use peak to peak or rms values to monitor the condition of the machine. But it has been found that any defect developed may not show any indication in time domain unless it deteriorates to an advanced condition. But in frequency domain signal not only registers the problem early in its growth but actually tells, with certain probability, the nature of impending faults like misalignment, or bearing failure. The developed system integrates the different channel vibration data and frequency analyzed output through on-chip FFT analysis. Figure 1 shows possible functional diagram of such a Vibration analysis system. The acquired data comprise 9-vibration signals. 6 vibration signals are acquired from bearing sensors and 3 vibration signals from shaft sensors. The signal values are tapped from on-line monitoring system. These data were available from a Uricani Mining Plant of Romania for experimentation. The vibration channels are set with a

predetermined threshold level. Each vibration signal is represented by samples at a sampling frequency higher than the process signal. Thus the vibration signal acquired for a total of a second gives sufficient data for converting vibration signals from time to frequency domain. Each signal also carries information regarding whether the signal is taken due to threshold crossing (upper or lower) and if so, which signal crossed the threshold. This information is maintained by the front-end software when it updates trend plot data.

Figure 1. Functional Diagram of vibration analysis system

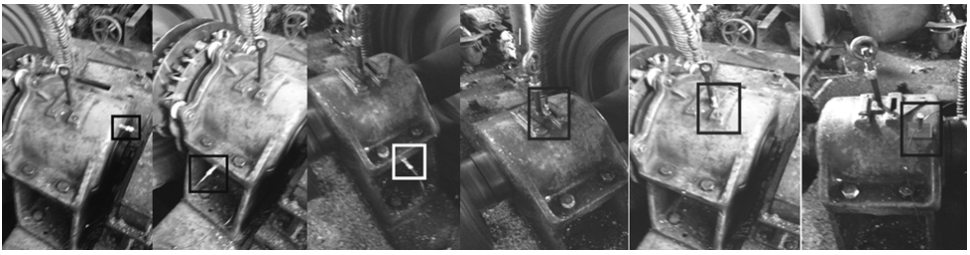

Figure 2. Points of measurement

The Fast Fourier Transform is performed on each of the 3 bearing vibration data. The rms value computed from the time domain signal and amplitude of vibration at predominant frequencies of interest obtained from frequency domain signal of the 6 signals are stored in trend record format. This information is useful for the purpose of trend monitoring. The trend data can be segregated in four separate files, namely, the previous day file, the last week file, the last month file and the last year file. Points of measurements is presented in Figure 2. The According to the development status of coal industry, this paper presents some technique and its applications of modern digital computer diagnosis monitoring and control for safety mining production process. The technique has been used in the full digital monitoring and automation control for hoists in mining production process. Implementing the on-line real time vibration analysis system requires collection of vibration data (bearing or shaft) over a long period, (at least one year) to get the behavioral history of machine. In conclusion we may say that vibration analysis for mining machine can prevent catastrophic breakdown if fault diagnosis is done in time

Acknowledgments. This work was possible thanks to the support of the Uricani Mining Plant and belonging to the Hunedoara Energetic Complex.

9th International Scientific Conference
Research and Development of Mechanical Elements and Systems
Kragujevac, Serbia, September5-7 2019

TECHNICAL CHARACTERISTICS, INVESTED FINANCIAL FUNDS AND EFFECTS OF THE PERFORMED MODERNIZATIONS OF THE FIRST INSTALLED EQUIPMENT OF TPP KOSTOLAC B

Miroslav Crncevic[1], Dragan Zivic[2], Milivoje Cvetkovic[2]

[1] Institut Mihajlo Pupin, Volgina 15, 11000 Beograd, Serbia, miroslav.crncevic@institutepupin.com
[2] JP EPS, TE-KO Kostolac, Nikole Tesle 5-7, 12208 Kostolac, Serbia, dragan.zivic@te-ko.rs

Key words: modernizations, invested funds, energetic, economic, environmental effects.

Thermal power units, fired on coal as fuel, are very complex production capacities for electricity generation. They consist of several individual, according to technical-technological characteristics, mutually harmonized plants and systems. When designing thermal power units, all necessary and complete project bases for the technical characteristics of fuel (coal and auxiliary liquid fuel) and water, which will be used for the operation of the units, will be used. The projected lifetime of the equipment is 150,000 operating hours, i.e. 25 years of operation of the units. The discrepancy of the designed characteristics, especially coal, (which occurred in practice) results in an inadequate function and short service life of the equipment. Two units of TPP Kostolac B with the designed nominal power output of 2 x 348.5MW, since commissioning (1988 and 1991) worked with reduced power, with many operating problems and some exceedance of the allowed levels of the environmental pollution. Also, new more strict regulations and rules were brought for the allowed influence of pollution to environment. Based on the research of the causes for not reaching the guaranteed technical characteristics of units and based on researches regarding technological solutions for meeting the new changed regulations and rules regarding environmental protection, in the first installed systems and equipment of TPP Kostolac B (2 x 348.5MW) in accordance with planned modernizations in TPP and EPS, several adaptations and rehabilitations of equipment were performed as well as upgrade of new systems and plants of TPP Kostolac B. On the first equipment of the two units TE Kostolac-B, from the term of the first synchronization of the units on the network of the electric power system (unit 1 - 30 December 1988 and unit 2 - September 23, 1991), through trial and regular drives, monitoring of work and necessary testing of technical, primarily guaranteed, characteristics of equipment and plants were performed. For the identified shortcomings in the work of the equipment, the research of optimal possibilities and technical solutions for their deviations were performed and the following goals were set:
The achievement of the nominal power of the unit 348.5 MW with increasing efficiency of the unit; Securing the reliable operation of the unit of the next 150,000 hours; Bringing

availability to the level of modern units in the world; Shortening the duration of planned downtime; Increasing energy efficiency; Compliance with environmental protection requirements.

Modernization of equipment and systems – adaptation and rehabilitation of first installed equipment and erection of new plants were performed on the base of preparation work design and the following design technical documentation:

- Project ECO RAM Phase I and II 2007 and 2008 (done by Alstom and TPP Kostolac B)
- Feasibility studies with the Preliminary Design of Works on units B1 and B2 TEKO B,

The activities foreseen in the Preliminary Project, and in relation to unit B2, are divided into the following groups of activities:

Modernization of the MRU system, Capital overhaul of turbines and generators and auxiliary turbine plants, Boiler plant, steam and pipelines, Electric power plant part and Reconstruction of electrofilter.

- Main project "Adaptation of unit B2 in TE Kostolac B with reconstruction of ESP".

Technical characteristics of performed modernizations were described in chapter 3.0:

Equipment for the coal fired boiler systems; Boiler pipe systems, steam super heaters and steam pipelines; Feed water pumps; Installation of new ESPs; Reconstruction of the systems for collection, transport and deposition of ash and slag; Replacement of turbine housings and some blades, connecting steam pipelines and condenser pipes and modernization of generator; Installation of new distribution DCS system; Management and control of CWT and CCT processes; Erection of new plant for FGD; Design of new plant for service water and sanitary waste water; Replacement or adaptation of electric power equipment.

Invested financial funds for the performed modernizations were shown in the work by tables. According to tables given in the work, for removal of technical shortcomings and reaching the design power of units 336,749,000 EUR was spent, and for improvement of environmental protection 297,454,000 EUR was invested.

Effects of the performed modernizations were shown in chapter 5.0 and especially production and technical effects in 5.1. Average power output of the units is increased, time on grid extended and efficiency coefficients enlarged (for exploitation, power, production, reliability and availability).

-Ecological effects – item 5.2 Monitoring and impact to the environment.

in accordance with the law regulation regarding environmental protection a Monitoring program for supervision of pollutant emission in the area of Branch 'TE-KO Kostolac' and its surroundings.

At the end of the work the following conclusions were made:

-By the performed modernizations, replacement of components of unreliable equipment and upgrade of new plants, the capacity of boilers was enlarged from 1000 to 1060t/h of steam and permanent nominal power output from 348.5 to 350MW

- Boiler efficiency rate was increased as well as reliability and power efficiency of units and the level of unit operation automation. These make significantly higher results in production of electric power and the economic effect is bigger too
- Environmental protection is now better. Installed monitoring for measurements of pollution shows lower pollution than permitted, and with erection of waste water treatment plant which is currently under construction we will have conditions for getting the ecological permit for operation of TEKO B.
- Units' lifetime is prolonged for 150,000 working hours more.

SPECIAL SECTION

"Toward a Sustainable Mobility"

Section Editor: **Ana Pavlović** - *Interdepartmental Center for Industrial Research on Advanced Mechanics and Materials, University of Bologna, Italy*

European Union

Ministry of Foreign Affairs and International Cooperation

9th International Scientific Conference
Research and Development of Mechanical Elements and Systems
Kragujevac, Serbia, September 5-7 2019

TOWARD A SUSTAINABLE MOBILITY: A SOLAR VEHICLE FOR A NEW QUALITY OF LIFE

Giangiacomo Minak[1], Marko Lukovic[2*], Stefano Maglio[3], Sinisa Kojic[4]

[1]InterDept. Centre for Industrial Research on Advanced Mechanics and Materials, Alma Mater Studiorum University of Bologna, Forlì, Italy
[2] Industrial Design Department, University of Arts Belgrade, Belgrade, Serbia, marko-design@hotmail.com
[3] Onda Solare Association, Castel San Pietro (BO), Italy
[4] Polytechnic School Kragujevac, Kragujevac, Serbia

Key words: vehicle mobility, sustainable mobility, solar car.

The vehicular mobility causes 15% of greenhouse gases emission: one million tons of carbon anhydrite per hour. In addition, it produces CO, NOx, fine powders, carcinogenic and mutagenic elements: these substances will disappear in the presence of solar vehicles. And solar mobility would also mitigate indirect effects: fuel used to transport fuel, energy for the distillation of hydrocarbons, gas leaks, even fracking, explosions, rivers and oceans. In contrast, electric and hybrid vehicles do not allow this improvement in the quality of life. In almost all modern countries, the energy mix is strongly unbalanced towards fossil fuels: massive electrification would not make mobility sustainable, but rather risks worsening its effect on the environment by shifting the problem of emissions from cities to power plants. The Sun, indeed, can guarantee long-term sustainable mobility: for every circulating solar vehicle CO2 production is really zero. From July to today, our solar racing car has travelled 3000 km, avoiding to emit half a ton of CO2: reporting these data to a conventional use, each solar vehicle would avoid the release of 1.5 tons of CO2 per year: like planting 10 large trees for each month in our garden. This study describes how to transform a solar super-car into an ordinary vehicle for urban and everyday mobility.
The expression "quality of life" has been used since 1980 with reference to signs indicative of urban decay and criminality, and therefore of diminishing quality of life. In the years after 2000 the concept of quality of life was often compared to the concept of sustainable development, especially in relation to the growing awareness of the limited nature of energy reserves related to oil and coal and to the negative effects of many modern technologies on the natural environment and resources.

Public opinion is beginning to wonder if all technological advances are always convenient, or if, on the other hand, long-term damage will nullify its immediate advantages, and even threaten the quality of life of future generations.
In these terms, another interesting expression more and more related to the modern idea of quality of life is the “Seventh Generation Standard”. It proposes that the government should take into consideration the effect its decisions will have in the long term, up to the seventh generation, that is about a century later.
A restricted, but emerging technology is represented by the solar vehicles. A solar car consists of an electrical powertrain supplied by photovoltaic panels: the vehicle is able to extract all the energy it needs from the Sun and this energy is directly used through electric motors that transform it into motion, without passing by a combustion.
Therefore, all emissions characterizing combustion engine vehicles will disappear in the presence of solar vehicles. And this exclusivity remains true regardless of the particular fuel with which the comparison is proposed: petrol, diesel, methane, alcohol and so on, but only solar vehicles are able to guarantee a real zero-emission policy, for real, both at local and global levels.

Figure 1. Multi-occupant solar car, made by the University of Bologna.

For instance, the solar car, recently designed and developed by the University of Bologna (Fig.1) for the American Solar Challenge 2018, won this 2700 km competition travelling with four occupants at an average speed over 60 km/h. It is characterized by advanced design, light materials and efficient energy solutions. This development has been largely reported in several investigations.
The development of solutions capable of making solar mobility increasingly valid and efficient should represent a goal of primary interest. At this time, solar vehicles are mainly seen as a curious attraction, but their performances should attract much more than this. Our solar racing car, for instance, has travelled 3000 km with without emission. Reporting these data to a conventional mobility, each solar vehicle would avoid the release of 1.5 tons of CO_2 per year. This results can be obtained, according to the authors’ opinion, transforming the solar extra-efficient prototypes, currently used inside solar races, in something more similar to the ordinary light vehicles, suitable for the urban and everyday mobility.

Acknowledgment. This research is funded by the Italian Ministry of Foreign Affairs and International Cooperation thought the Joint Research Projects as Particular Relevance, with a project named ‘Two Seats for a Solar Car’ within the Executive Programme of Cooperation between Italy and Serbia in the field of Science and Technology.

iRMES KRAGUJEVAC 2019

9th International Scientific Conference
Research and Development of Mechanical Elements and Systems
Kragujevac, Serbia, September 5-7 2019

PASSENGER CAR STEERING PULL AND DRIFT REDUCTION CONSIDERING SUSPENSION TOLERANCES

Mariano De Rosa[1], Alessandro De Felice[2], Cristiano Fragassa[3], Silvio Sorrentino[2]

[1]Product Development, Maserati SpA,
Via Emilia Ovest 911, Modena, Italy, mariano.derosa@maserati.com
[2]University of Modena and Reggio Emilia, Department of Engineering "Enzo Ferrari",
Via Vivarelli 10, Modena, Italy, {alessandro.defelice, silvio.sorrentino}@unimore.it
[3]University of Bologna, Department of Industrial Engineering,
Viale Risorgimento 2, Bologna, Italy, cristiano.fragassa@unibo.it

Key words: handling, pull to side, steering wheel misalignment, drift leeward.

Among handling anomalies affecting passenger cars travelling on a straight path, the Pull to side (PTS, lateral deviations from straight trajectory with steering wheel correctly aligned), the Steering wheel misalignment (SWM, straight trajectory with steering wheel not aligned) and the Drift leeward (DL, lateral deviations due to the effects of uneven ground surface on the rear suspensions) are particularly relevant. Even though they do not constitute safety problems, however they represent a cost factor in the automotive industry, occurring in small but not negligible percentage of the overall car production.
Several studies are devoted to investigate the contribution of tire characteristics on Pull to side and Steering wheel misalignment (also referred to as drift). On the other hand, the literature aimed at investigating the contribution of tolerances of suspension systems on Pull to side and Steering wheel misalignment is less extensive, considering simulation–based dimensional tolerance optimization processes applied to specific cases [1 – 4].
The present contribution is focused on understanding which are the causes and on reducing the extents of PTS, SWM and DL as handling anomalies due to suspension component and assembly tolerances, in the case of vehicles with front Double wishbone suspension and rear Five arms suspension.
The vehicle assembly process is first analyzed in terms of errors and tolerances by means of a design of experiment analysis (DOE), aimed at identifying in which proportion each suspension parameter is influenced by tolerances (Fig. 1, case of Ride steer).
A sensitivity analysis by multibody virtual modelling is then performed, aimed at understanding how and at which level the relevant suspension parameters can affect the straight path handling of the vehicles under study (generating PTS, SWM and DL).

Finally, the results of simulations are correlated with experimental data from presetting and wheel aligner benches, for setting tolerance thresholds able to keep the anomalies under study within acceptable bounds.

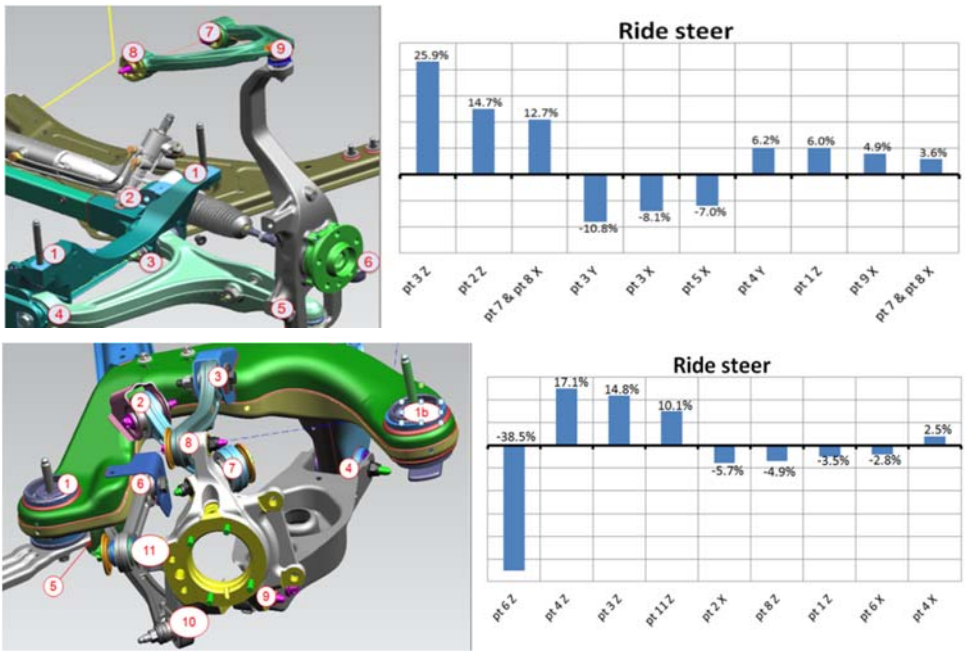

Figure 1. Front (top) and rear (bottom) suspension: tolerance contributions to Ride steer.

Virtual analysis put in evidence that PTS and SWM are mainly related to the set up phase of wheel angles. In particular, both anomalies can be explained by the contribution that vehicle geometry gives to the sideslip angle. Front camber angles influence PTS, while front and rear toe angles influence SWM. Main cause of DL has been identified with (rear) ride steer, which in turn can be generated by components out of tolerances or/and presetting variation. By improving all the set up process (presetting bench and wheel aligner bench) on a whole production line, the number of vehicles affected by PTS, SWM and DL was strongly reduced: from 3% down to about 1% of the production.

[1] Kim Y Sand Jang D Y 2009 Optimization of geometric dimension & tolerance parameters of front suspension system for vehicle pulls improvement, *Transactions of the Korean Society of Mechanical Engineers A*, 33(9) 903–912.

[2] Murari T B et al. 2016 Vehicle steering pull: from product development to manufacturing, *Product Management & Development* 14(1) 22–31.

[3] Cho Y G 2010 Steering pull and drift considering road wheel alignment tolerance during high–speed driving, *International Journal of Vehicle Design* 54(1) 73–91.

[4] Park K S, Heo S J and Kang D O 2013 Robust design optimization of suspension system considering steering pull reduction, *International Journal of Automotive Technology* 14(6) 927–933.

9th International Scientific Conference
Research and Development of Mechanical Elements and Systems
Kragujevac, Serbia, September 5-7 2019

EXPERIMENTAL ANALYSIS OF JET SLURRY EROSION ON MARTENSITIC STAINLESS STEEL

Galileo Santacruz[1, *], Antonio Shigueaki Takimi[1], Felipe Vannucchi de Camargo[1, 2], Carlos Pérez Bergmann[1]

[1] Federal University of Rio Grande do Sul - UFRGS, Post-Graduation Program in Mining, Metallurgical and Materials Engineering, Osvaldo Aranha 99, Porto Alegre, RS 90035-190, Brazil.
[2] University of Bologna, Department of Industrial Engineering, Viale del Risorgimento 2, 40136, Bologna, Italy, galileo.santacruz@ufrgs.br

Keywords: jet slurry erosion; martensitic stainless steel; tribology; wear; mechanical properties.

Due to their enhanced tribological properties that contribute to the increased useful life of components, martensitic stainless steels are an excellent option for industrial applications such as hydroelectric, petrochemical, civil construction, and mineral processing plants. In the present investigation, the erosive wear of AISI 410 martensitic stainless steel is evaluated after thermal treatment by quenching and tempering by mass loss, under erosive attack at 30° and 90° incidence angles, using a self-made jet slurry erosion equipment controlling parameters such as speed, volume of fluid, temperature and concentration of erosive particles of erodent. The characterization of the eroded samples was carried out in terms of the microstructure (SEM) and microhardness as well as the particle size distribution (LG) and morphology of the erodent. It was possible to establish the relationship between the slurry erosive wear and the physical properties inherent of stainless steel for this particular experimental configuration, concluding that the steel presents better resistance to jet slurry erosion wear when compared to austenitic steel commonly used in the industry.

Thus, the ideal choice of engineering materials is important in order to decrease the wear rate and to improve their tribological behavior. Among the different alternatives for such applications, the most current being studied is the austenitic and martensitic stainless steels. Austenitic stainless steels are used in many components where corrosion resistance is crucial. However, under the mechanical action of hard particles, they present a high plastic deformation and wear. On the other hand, martensitic stainless steel presents better mechanical resistance to erosive particles than austenitic steel, with the compromise of lower corrosion resistance.

In the present investigation, it was possible to evaluate the erosive wear of the martensitic stainless steel AISI 410 thermally treated with quenching and tempering, evaluating the volume loss under jet slurry erosion conditions at incidence angles of 30° and 90° between the axis of symmetry of the fluid flow and the surface of the samples, via the control of parameters such as angle and speed of impact, test temperature and concentration of erosive particles in the suspension. In this case, electrofused alumina was used as erodent.

The materials were characterized with regard to their microstructure by scanning electron microscopy (SEM), roughness, microhardness, and the particle size distribution analyzed with laser granulometry (LG) and morphology of the erodent.

The jet slurry erosion tests were carried out in a modified commercial high-pressure washer which is based on ASTM G-76 standard and adapted in the nozzle of the gun a system of feeding of erodent particles using an inner Venturi accelerator of particles inside a test chamber. This equipment allows controlling the angle of impact, the speed of impact, the concentration of erosive particles in the suspension and test temperature, all important parameters to determine the distribution of frictional energy along a surface.
The tests were performed using water between 25 and 28°C of temperature with 960 g of (Al_2O_3) erodent. The samples were placed at the nozzle output to guarantee the incidence of impact fluid and mean jet velocity of erosive material in the suspension of 77 m/s. This velocity was calculated using flow rate, time and nozzle area measurements of flow output. The incidence angles studied were 30° and 90° between the axis of symmetry of the fluid flow and the surface of the samples. In all cases, the concentration of particles in the slurry was 7 wt%. The erosion resistance was determined from the volume loss results per unit of time from the difference of mass loss considering the relation of the apparent density of the studied material (7.73 g/cm^3 for AISI 410 stainless steel). Mass losses were measured every 1 min by using a scale with 0.01 mg resolution. The total duration of each test was 4 min. The samples were cleaned in an ultrasonic bath with deionized water before and after each test and dried and weighted afterward.
From the results obtained in the accomplishment of the experimental work, it is possible to infer the following conclusions:
An experimental erosion wear simulation equipment of the jet slurry type was developed, considering conditions that allowed the control of the test parameters such as impact angle, impact velocity, erosive particle concentration in the suspension and test temperature, all significant variables in the determination of the behavior of the materials. The AISI 410 martensitic stainless steel presented a higher rate of accumulated volumetric erosion in the impact angle of 30°, presenting a predominantly ductile behavior, and higher resistance to jet slurry erosion at the impact angle of 90° with the compromise of deeper eroded area.

Acknowledgments. The authors express their gratitude to the following laboratories: Laboratory of Ceramic Materials (LACER), Laboratory of Physical Metallurgy (LAMEF), Laboratory of Design and Selection of Materials (LdSM) and the Laboratory of Conventional Machining (LUC) of the Federal University of Rio Grande do Sul (UFRGS) for the investigation support and to the Research and Technology Center of Rijeza Metallurgy. G. Santacruz and F.V. de Camargo thank the Coordination of Improvement of Higher Education Personnel of the Brazilian Ministry of Education (CAPES/MEC) for the doctorate scholarship grants 88882.345871/2019-01 and 88882.345831/2019-01, respectively.

9th International Scientific Conference
Research and Development of Mechanical Elements and Systems
Kragujevac, Serbia, September 5-7 2019

SOLUTION COMBUSTION SYNTHESIS OF Mo-Fe/MgO - INFLUENCE OF THE FUEL COMPOSITION ON THE PRODUCTION OF DOPED CATALYST NANOPOWDER

Rúbia Young Sun Zampiva [1], Carlos Pérez Bergmann [1], Annelise Kopp Alves [1], L Giorgini[2]

[1]Programa de Pós-Graduação em Minas, Metalurgia e Materiais, PPGE3M, Universidade Federal do Rio Grande do Sul-UFRGS, Porto Alegre, RS 90035-190, Brazil, rubiayoungsun@gmail.com
[2]Department of Industrial Chemistry "Toso Montanari", University of Bologna, Viale del Risorgimento 4, 40136, Bologna, Italy

Key words: catalysts; nanoparticles; fuel influence; low-cost synthesis; high-crystallinity.

Among the techniques for producing oxide catalysts, the solution combustion synthesis (SCS) has been widely used to produce, at low-cost, high-quality nanostructured powders. SCS mainly consists of combining, in solution, a fuel (organic precursor) and an oxidizing agent (usually nitrates). The mixture is heated at ≤ 500°C reaching ignition in a fast and highly exotherm reaction. At the end of the process, unagglomerated and crystalline nanopowders are typically formed. The product is then heat treated in order to organize the crystalline structure and to burn out residual fuel. Through SCS, due the high exothermic energy liberated in the ignition, it is possible to homogeneously incorporate dopants ions into the catalyst. Besides, SCS allows the production of nanopowders with sizes in the decimal scale, which is extremely important for powdered catalysts. The smaller the particle is, the larger the surface area is. In this paper, in order to efficiently produce nanostructured catalysis by SCS, we studied the correlation of the oxidizer/fuel ratio, and the use of glycine and polyethylene glycol (PEG) as fuel in the SCS of Fe-Mo/MgO nanopowder catalyst.

0.96 mols of Iron nitrate nonahydrate, 0.004 mols of ammonium heptamolybdate tetrahydrate and 1 mol of magnesium nitrate hexahydrate were used as precursors and oxidizing agents. Glycine and PEG concentrations, as fuel, were calculated according to the chemistry of propellants, as presented on table 1. The precursors were individually dissolved in distilled water and then mixed. The solutions were heated at 60°C during 5 min under constant stirring and then were inserted in a 400 °C pre-heated electric muffle furnace

during 15 minutes reaching self-ignition point. To finalize, powders were heat treated at 1100 °C.

Table 1. Composition and concentration of the fuels in the SCS, Ø = Oxidizer/Fuel.

Sample	Fuel	Ø	Description	Concentration (mol)
G1	Glycine	0.66	Rich	3.975
G2		1	Stoichiometric	2.615
G3		2	Lean	1.3
P1	PEG	0.665	Rich	0.855
P2		1	Stoichiometric	0.57
P3		1.995	Lean	0.285

Samples morphology and physicochemical properties were characterized by X-ray diffraction, electron microscopy, granulometry and surface area analysis. The results indicated high crystallinity for the samples produced with PEG, as shown in the diffractogram (figure 1) and a wide variation on the nanoparticles sizes depending on the fuels properties.

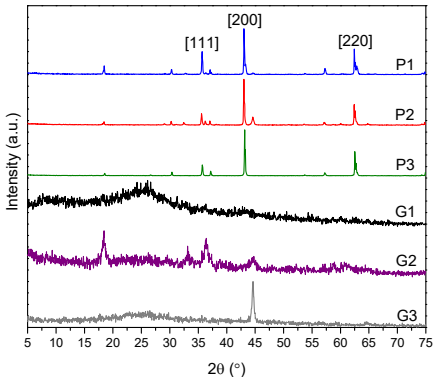

Figure 1. Samples diffractogram correlating the crystalline structure and SCS fuel concentration and composition. The peaks [111], [200] and [220] belong to periclase.

Nanostructured oxide catalysts were successfully obtained through the SCS method using PEG as fuel. Through the analyses was possible to observe that the concentration of fuel strongly influences the properties of the final product. We concluded that not necessarily the stoichiometric formulation is the best path to produce nanomaterials. In the case of Fe-Mo/MgO catalyst, the best formulation was the PEG fuel-lean that presented the largest surface area among the samples.

Acknowledgments. The authors would like to thank the Coordination for the Improvement of Higher Education Personnel - CAPES for the financial support. The present paper was presented inside the 'Toward a Sustainable Mobility' special session as part of the 'Two Seats for a Solar Car' research project, an action funded by the Italian Ministry of Foreign Affairs and International Cooperation within the Executive Programme of Cooperation in the field of Science and Technology between the Italian Republic and the Republic of Serbia.

9th International Scientific Conference
Research and Development of Mechanical Elements and Systems
Kragujevac, Serbia, September 5-7 2019

SYNTHESIS OF COBALT FERRITE ($COFE_2O_4$) BY COMBUSTION WITH DIFFERENT CONCENTRATIONS OF GLYCINE

C G Kaufmann Junior[1,2], R Y S Zampiva[1], A K Alves[1], C P Bergmann[1,2], L Giorgini[3]

[1]Post-Graduation Program in Mining, Metallurgy and Materials Engineering (PPGE3M), Federal University of Rio Grande do Sul, Osvaldo Aranha 99, 90035-190, Porto Alegre, Brazil
[2]Post-Graduation Program in Production and Transport Engineering, (PPGEP), Federal University of Rio Grande do Sul, Osvaldo Aranha 99, 90035-190, Porto Alegre, Brazil
[3]Department of Industrial Chemistry "Toso Montanari", University of Bologna, Viale del Risorgimento 4, 40136, Bologna, Italy

Key words: cobalt ferrite, glycine, combustion synthesis, XRD, MEV.

Ferrite is a ceramic material produced from burning large proportions of iron (III) oxide (Fe_2O_3) blended with small concentrations of one or more metallic elements, such as cobalt, manganese, nickel, magnesium, and zinc. Ferrites usually present a spinel structure with the formula AB_2O_4, where A and B represent various metal cations, including iron (Fe) [2]. Solution combustion synthesis (SCS) has been increasingly applied in the production of oxide catalysts due to the possibility of producing low-cost, highly pure and homogeneous nanostructured powders. Many studies on ferrites nanoparticles including $CoFe_2O_4$ spinel have been recently presented due to their distinct magnetic and electronic properties. Among the wide range of applications of Cobalt Ferrite ($CoFe_2O_4$), its usage for the manufacturing of modern electronic devices such as solar panels, capacitors and batteries has been studied lately. Hence, solar-powered vehicles, which strongly rely their performance on energy efficient electronics, is a sector that could particularly benefit from enhanced applications of such material In this work, the synthesis of Cobalt Ferrite was studied by means of Solution Combustion Synthesis (SCS) using iron nitrate nonahydrate and cobalt nitrate hexahydrate as precursors, and glycine as fuel. The nitrates were dissolved in distilled water and placed under stirring and heating for 5 minutes; when the temperature reached 60°C, glycine was added; after complete homogenization, the solution was placed in an electric oven (400°C) until complete combustion (approximately 15 minutes). Three syntheses were carried out using different concentrations of fuel: lean, stoichiometric and rich. The product crystallite size and composition were investigated in order to determine

the influence of the fuel concentration on the structure of the produced cobalt ferrite. The diffractograms (Figure 1) shows the characteristic crystal peaks corresponding to the cobalt ferrite phase for all samples. The stoichiometric and rich samples showed the formation of a second phase of cobalt oxide. The fuel-lean sample was the only one that produced a nanometer pure phase of $CoFe_2O_4$. This sample is promising for applications in the electronics field, such as on solar-powered electric vehicles, since pure particles and good crystallinity are crucial in this area.

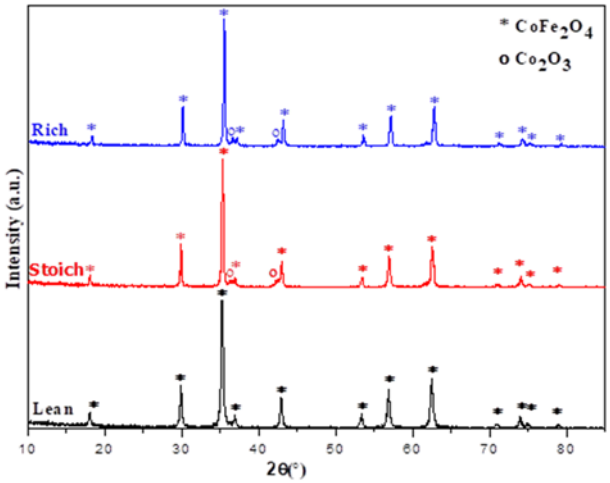

Figure 1. Diffractograms of the $CoFe_2O_4$ catalysts for different fuel concentrations.

Acknowledgments. The authors would like to thank the Coordination for the Improvement of Higher Education Personnel - CAPES for the financial support. The present paper was presented inside the '*Toward a Sustainable Mobility*' special session as part of the '*Two Seats for a Solar Car*' research project, an action funded by the Italian Ministry of Foreign Affairs and International Cooperation within the Executive Programme of Cooperation in the field of Science and Technology between the Italian Republic and the Republic of Serbia.

IRMES KRAGUJEVAC 2019
9th International Scientific Conference
Research and Development of Mechanical Elements and Systems
Kragujevac, Serbia, September 5-7 2019

FIRST ASSESSMENT ON SUSPENSION PARAMETER OPTIMIZATION FOR A SOLAR POWERED VEHICLE

Silvio Sorrentino [1], Alessandro De Felice[1], Pasquale Grosso[1], Giangiacomo Minak[2]

[1]University of Modena and Reggio Emilia, Department of Engineering "Enzo Ferrari", Via Vivarelli 10, Modena, Italy, {silvio.sorrentino, alessandro.defelice, pasquale.grosso}@unimore.it
[2]University of Bologna, Department of Industrial Engineering, Viale Risorgimento 2, Bologna, Italy, giangiacomo.minak@unibo.it

Key words: solar powered vehicle, vertical dynamics, comfort, road holding.

The interest in solar–powered vehicles arose as a topic of study mainly developed by academic institutions with the aim of promoting sustainable mobility. The main challenges of designing such cutting–edge vehicles [1] consist in electrical systems, solar array design, structural materials and mechanical sub–systems such as suspensions. Focusing on suspension systems, the load due to passengers, electric batteries and solar panels can be even higher than the total weight of the remaining parts of the vehicle, making the choice of suspension stiffness and weight distribution quite challenging in order to get good performances in terms of vehicle dynamics. These technical demands becomes extreme in the case of multi–passenger vehicles recently introduced in solar–powered car competitions. In fact, compared to more traditional single–seater solar cars, cruisers present a total weight from four to five times higher, as well as higher centre of gravity [2].
The solar–powered car considered in this study was designed and manufactured for racing by the University of Bologna. It represents one of the lightest multi–occupant solar cars ever built: a vehicle with total mass of 300 kg allows to transport 320 kg due to four occupants [2]. However, this vehicle still needs further mechanical improvements: the suspension system, in particular, has to be designed considering the necessity to provide adequate levels of handling, road holding, comfort and vibration control.
Focus of the present contribution is a first assessment on optimization of the main parameters affecting comfort and road holding, which are the equivalent stiffness and damping of the suspensions, for the solar–powered car designed and manufactured by the University of Bologna.
To this purpose, with the adopted design parameters (mass distribution, partial wheelbases), the equivalent vertical stiffness of the front and rear axles were tuned in order to fit the

basic requirements for comfort in terms of natural frequencies and mode shapes of bounce and pitch [3]: (1) natural frequencies of bounce and pitch modes falling in the range 1.0 – 1.5 Hz; (2) pitch mode with its node located at about the front seats.

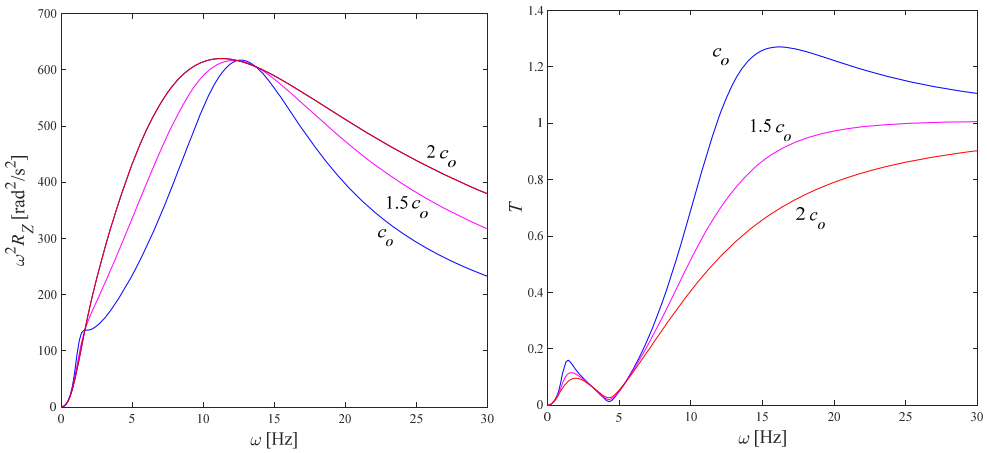

Figure 1. Amplification factor for vertical acceleration of the sprung mass m_s ($\omega^2 R_Z$) as a function of frequency (left) and transmissibility T for ground vertical force amplitude N as a function of frequency (right), for different values of suspension damping.

The optimization of suspension damping was then addressed [4], for reaching a good compromise between comfort and road holding. A value close to what can be considered the best choice for the damping coefficient c in terms of comfort optimization was identified (c_o = 3734 Ns/m), to be increased to some extent for improving road holding. To this purpose the following frequency response functions were considered: (1) receptance R_Z between amplitude Z (vertical displacement of sprung mass m_s) and amplitude H of ground harmonic input ($\omega^2 R_Z$ yielding a measure of the vertical acceleration of m_s, to be minimized for comfort optimization, as displayed in Fig. 1 left); (2) transmissibility T between ground vertical force amplitude N, and force pH (where p is the vertical stiffness of the tires; T to be minimized for road holding optimization, as displayed in Fig. 1 right). The results (as shown in Fig. 1) are comparable to those of standard passenger cars.

[1] Thacher E F 2015 *A Solar Car Primer: A Guide to the Design and Construction of Solar–Powered Racing Vehicles*, Springer.

[2] Minak G, Brugo T M, Fragassa C, Pavlovic A, Vannucchi de Camargo F and Zavatta N 2019 Structural Design and Manufacturing of a Cruiser Class Solar Vehicle, *Journal of Visualized Experiment* **143** 1–15.

[3] Olley M 1934 Independent wheel suspension – its whys and wherefores, *SAE Transactions* **34**(3) 73–81.

[4] Bourcier de Carbon C 1950 *Theorie mathématique et réalisation pratique de la suspension amortie des véhicules terrestres*, Troisieme Congres Technique de l'Automobile, Paris, France.

9th International Scientific Conference
Research and Development of Mechanical Elements and Systems
Kragujevac, Serbia, September 5-7 2019

SYNTHESIS OF $Bi_2Fe_XNbO_7$ FILMS APPLIED AS A CATALYST FOR HYDROGEN PRODUCTION USING VISIBLE-LIGHT PHOTO-ELECTROLYSIS

Allan Scharnberg[1], Ana Pavlovic[2], Annelise Alves[1]

[1]Laboratory of Ceramic Materials, Department of Materials, Federal University of Rio Grande do Sul - UFRGS, Osvaldo Aranha 99, Porto Alegre, RS 90035-190, Brazil, allan.ambiental@outlook.com.
[2]Interdepartmental Center for Industrial Research on Advanced Mechanics and Materials, University of Bologna, Viale del Risorgimento 2, 40136, Bologna, Italy.

Key words: Bi_2FeNbO_7, photo-electrolysis, H_2 production, PEC, clean energy.

Nowadays, oil, coal and natural gas (fossil fuels) are the three main sources of global supply of energy, accounting for over 80% of all consumption. In addition, the energy demand has been growing continuously. This growth has given rise to a series of environmental problems, mainly due to the emission of greenhouse gases (GHG). CO_2 emissions from fossil fuels have increased exponentially in the last decades. This phenomenon can lead to glacier melting, rising and acidification of the ocean, coral extinction, epidemics of temperature-making diseases, tropical storms and extreme snowstorms. Besides, fossil reserves are finite, subject to geopolitical conflicts, and there are more noble applications for them, such as the petrochemical industry. Due to these facts, there is a need to develop new technologies for clean energy generation. Representing a major cause of pollutant emissions, research on urban mobility has seek to take advantage of the solar energy to produce innovative, safe, lightweight and zero-emission vehicles.

One of the most interesting proposals to attain that goal is the photo-electrolysis, which also consists in the usage of the solar energy, but to produce hydrogen, since it presents the possibility of storage and association with other renewable sources of energy. Photo-electrolysis is the conversion of solar light into useful chemical energy (H_2). A photo-electrolytic cell (PEC) is composed of a semiconductor device that absorbs solar energy and generates the voltage necessary to split the water molecules. Photo-electrolysis integrates the generation of solar energy and electrolysis of water in a single photo-anode and is considered the most promising renewable method for hydrogen production. This technique has begun in 1972 using TiO_2 as photo-anode. Several studies have pointed out oxides with possible relevance for use in this process; many of them present difficulties as cost, obtaining and toxicity. The semiconductor must have short band gap value to absorb a large part of visible light irradiation, be stable in operation and allow electron mobility.

Researchers explore catalysts that can be activated under visible light, such as coupled semiconductors, doped semiconductors and mixed metal oxide semiconductors, such as bismuth-based mixed oxide semiconductors, which have attracted interest because of their excellent stability, visible light absorption and photocatalytic properties. In order to develop photocatalysts based on bismuth, iron and niobium oxides for hydrogen production via photo-electrolysis of water, in this research, thin films were synthesized and characterized regarding their morphology and optical properties.

In order to develop and characterize photo-anodes based on bismuth, niobium and iron, thin films were synthesized by the sol-gel method and deposited by dip coating on fluorine-doped SnO_2 (FTO) glass substrates. Four compositions were proposed: one without iron and with 0.8, 1.0 and 1.2 mole of iron. The samples were dried at room temperature for 15 h and heat-treated at 600°C (2°C min^{-1}) by 1h. Morphological studies were performed using SEM. The band gap (Eg) of the samples was evaluated by Kubelka-Munk method using UV-Vis diffuse reflectance data. Solar spectrum percentage was calculated as proposed by ASTM G173-03 (2012). Table 1 demonstrates the most important results.

Table 1. Characteristics of the synthetized photo-electrodes.

$Bi_2Fe_xNbO_7$ x =	Band Gap (eV)	Equivalent wavelength (λ_{eq}) (nm)	Solar spectrum percentage (%) (AM1.5 Global)
0	2.01	617	35.95
0.8	1.32	939	70.24
1.0	1.21	1025	75.36
1.2	1.06	1170	82.16

All films presented semiconductor behaviour with Eg values lower than 2.01 eV. It decreases with the increment of iron, typical red shift. The adding of iron produces intermediate energy levels between the valence and conduction band, thus absorbing more light, up to 82% of the solar spectrum, what increases the photo-catalytic activity. SEM studies show that the surface presents some cracks, possible due the presence of nitrates and residual tensile stresses. The cracked surface can be beneficial in the process of photo-electrolysis, mainly due to the greater surface area, directionality in the transport of electrons and the availability of electron-holes (h^+) for water oxidation. However, if necessary, it is possible to manage by changing the parameters of the heat treatment.

Further analyses should be performed to better understand their properties, however, based on data from UV-Vis spectroscopy and morphology studies, the photo-electrodes show high photo-catalytic activity under visible and even infrared light, which places them as potential candidates for photo-anodes, being able to overcome the barrier that the low absorption of visible light imposes to the hydrogen production by photo-electrolysis.

Acknowledgments. This work was financially supported by the Brazilian National Council for the Improvement of Higher Education (CAPES). The present paper was presented inside the 'Toward a Sustainable Mobility' special session as part of the 'Two Seats for a Solar Car' research project, an action funded by the Italian Ministry of Foreign Affairs and International Cooperation within the Executive Programme of Cooperation in the field of Science and Technology between the Italian Republic and the Republic of Serbia.

9th International Scientific Conference
Research and Development of Mechanical Elements and Systems
Kragujevac, Serbia, September 5-7 2019

COMPARING THE ACCURACY OF 3D SLICER SOFTWARE IN PRINTED END-USE PARTS

Milan Šljivić[1], Ana Pavlović[2], Milija Kraišnik[3], Jovica Ilić[1]

[1]University of Banja Luka, Faculty of Engineering, S. Stepenovića 75, 78000 Banja Luka, R. Srpska, B&H, milan.sljivic@unibl.rs, jovica.ilic@mf.unibl.org
[2]University of Bologna, Department of Industrial Engineering, Viale del Risorgimento 2, Bologna, Italy, ana.pavlovic@unibo.it
[3]University of East Sarajevo, Faculty of Mechanical Engineering, Lukavica 71126, Republika Srpska, B&H, milijakraisnik@yahoo.com

Keywords: FDM, 3D Slicer, Simplify3D, Cura, Slic3r, comparing, accuracy

The Fused Deposition Modeling (FDM) process of Additive Manufacturing (AM) is a newly developed, innovative technology based on the Rapid Prototyping process that evolved and expanded its use to produce end-use parts and products that are applied from medical applications up to the automotive industry. The FDM has achieved a large increase in all spheres of applications nowadays, from the professional one to the amateur domain. This study aims to compare the accuracy offered by 3D Slicer Software in printing end-use parts inside a Fused Deposition Modeling process of Additive Manufacturing. The purpose is to check the surface quality and dimensional stability of the printed parts using the processing tools: *Simplify3D*, *Cura* and *Slic3r 3D* Slicer software. In the integration with a 3D printer, good 3D slicer software is very important. If a good slicer tool is used, it will surely get better results, even from a mediocre 3D Printer. Otherwise, any valid 3D slicer tool will create a geometry based on an STL-file successfully, describing coordinates, printed speed, nozzle and bed temperatures, advanced dimensional accuracy, support requirements and other accuracy variables. The application of the appropriate slicer software for processing has a direct impact on the quality of the printed parts, as in the case shown in Figure 1.

Figure 1. RP in-scale model of a Solar Car [Minak at al. 2019]

Printed parts have been analyses and the accuracy, time of production and consumption of material through the 3D Slicer tools are compared. In Figure 6 (I) and (II) the locations used for measures are shown. Observations on the achieved results for the accuracy of the printed parts analyzed were made for each used slicer tool.

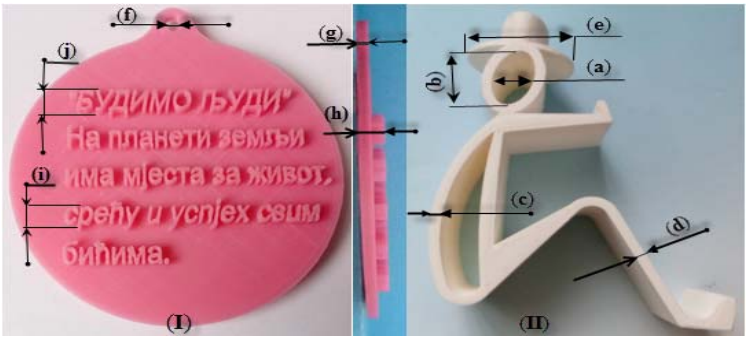

Figure 2. (I) Locations measured with the calliper by the pendant and (II) Locations measured with the calliper by the phone holder

For quality test comparison, the corresponding parts that were printed on a low-cost 3D printer were selected and processed from three 3D slicer software: *Slic3r* and *Cura* (Open source and free) and *Simplify3D* (Powerful and Professional). The comparison of the precision in the printed parts showed significant differences in the quality achieved with the three tools used. The *Slic3r* software according to the metric for measuring parts deviations in terms of dimensional accuracy in the surface normal has done from 0.10 mm to 0.61 mm which belongs to the class from small deviation. But if it takes visual visibility as an indicator of surface and letter-quality then the Slic3r software has not achieved satisfactory quality. The *Cura* (*version 15.04*) software was achieved better dimensional accuracy than the Slic3r slicer tool. The dimensional deviation between the 3D model and the printed parts was done from 0.05 mm to 0.36 mm, which is also in the range of small deviation. The surface and complex letters of parts, Cura was done with good quality and achieved a high level of detail. The *Simplify3D* slicer software has achieved the best quality and dimensional accuracy of printed parts. The dimensional deviation has done in the range from 0.02 mm to 0.28 mm. The visually analyzed quality of surface and letters of the printed parts are corresponding and close to the original shape. We can conclude that Slicer *Cura* gave good, but not necessarily accurate results. Results, graphically and visually presented, show significant differences in the dimensional and surface accuracy with an optimum outcome offered by the *Simplify3D* as best 3D slicer tool. The *Simplify3D* slicer has essential advantages in printed end-use parts because creates the 3D models with significantly better accuracy and quality support.

Acknowledgement: This research has been supported by the Italian Ministry of Foreign Affairs and International Cooperation thought the Joint Research Projects as Particular Relevance, with a project named 'Two Seats for a Solar Car' within the Executive Programme of Cooperation between Italy and Serbia in the field of Science and Technology.

9th International Scientific Conference
Research and Development of Mechanical Elements and Systems
Kragujevac, Serbia, September 5-7 2019

SEQUENTIAL DEPOSITION METHOD OF TIO_2/$CH_3NH_3PI_3$ FILMS FOR SOLAR CELL APPLICATION

A E R T P Oliveira[1], F Bonatto[2], A K Alves[1]

[1]Graduate Program in Mining, Metallurgy and Materials Engineering (PPGE3M), Federal University of Rio Grande do Sul, Osvaldo Aranha 99, Porto Alegre, Brazil, anne.targino@ufrgs.br
[2]Graduate Program of Production and Transportation Engineering (PPGEP)/ Federal University of Rio Grande do Sul, Osvaldo Aranha 99, Porto Alegre, Brazil, fernando.bonatto@ufrgs.br

Key words: Perovskite, solar cells, TiO_2, organic lead halide.

The development of sustainable energy sources has become critical, since most of the global energy still relies mostly on fossil fuels, whereas a scenario of an industrial sector considerably dependent on coal and the urban mobility that almost entirely leans on polluting fuels such as gasoline and diesel can be verified. Within this context, solar energy is increasingly becoming an attractive energy alternative, causing a significant increase in research and development of more efficient and inexpensive photovoltaic devices, either for industrial plants or, more recently, solar-powered zero-emission vehicles. Seeking to study innovative solar cell compositions to reach the highest energy efficiency level attainable, the aim of this study was to develop a synthesis route to obtain a solar cell composed by hybrid perovskite ($CH_3NH_3PbI_3$), using a sequential deposition method through the technique of spin-coating. Initially, the deposition of PbI_2 (2000, 3000 and 4000rpm velocity) thin film of was performed over FTO/glass substrate coated with TiO_2 paste, which was subsequently converted into perovskite crystals through spin coating using a CH_3NH_3I (MAI) solution. The TiO_2 paste was obtained by grinding 50 g of TiO_2-P25 (Evonik), 20 g of titanium isopropoxide (97 %, Sigma-Aldrich), 2.5 g of carboxymethyl cellulose (Sigma-Aldrich), 80 mL of terpineol (Sigma-Aldrich), 4 mL of acetylacetonate (Sigma-Aldrich) and 5 mL of ethanol (99 %, Zeppelin) for a period of 12 h, so the paste was fully homogenized. For the preparation of PbI_2 solution a two-steps methodology was used: 1 M solution was obtained dissolving PbI_2 in anhydrous *N, N*-dimethylmethanamide under agitation at a temperature of 70 °C. For the second stage of two-step deposition, a solution was prepared composed of 10 mg/mL CH_3NH_3I in anhydrous isopropanol, stirred for 10 min, in which all MAI was dissolved. The whole process was performed without temperature and ambient pressure control. The influence of the PbI_2 layer thickness on the formation of $CH_3NH_3PbI_3$ crystals was evaluated.

The hydrophilic characteristic of TiO_2 affects the distribution of the crystals nucleation sites, since PbI_2 possesses a non-polar liquid characteristic. The characterization of the perovskite thin films showed that thickness affects the bandgap and the surface morphology directly, revealing the presence of dendritic structures and acicular crystals. Both growth and coverage increased for thinner layers of PbI_2. It was also possible to observe an increased uniformity in the film for smaller PbI_2 layers. There was a variation in the optical band gap for the lower velocity layer due to the greater presence of deposited material (PbI_2). It can be noted that the diffraction signal related to the formation of perovskite $CH_3NH_3PbI_3$ in 2θ = 14° is the most intense, and confirms the high crystallinity of the synthesized film can be identified, in addition to the anatase peaks at 2θ = 25.2° and rutile at 2θ = 26.4°, belonging to TiO_2 film from the substrate. Analysis of this data provided an average grain size of approximately 91 ± 3 nm. The film prepared at 3000 rpm presents a greater absorption (UV-Vis) compared to the other films corroborating the results of SEM where it is possible to observe a higher homogeneous formation of perovskite. It is also possible to observe the mesoporous layer of TiO_2 below the grains and dendrites of formed perovskites. The results show that, through the established route, it was possible to obtain the thin films that can be used in organometallic solar cells, with the best results obtained for the 3000 rpm deposition sample.

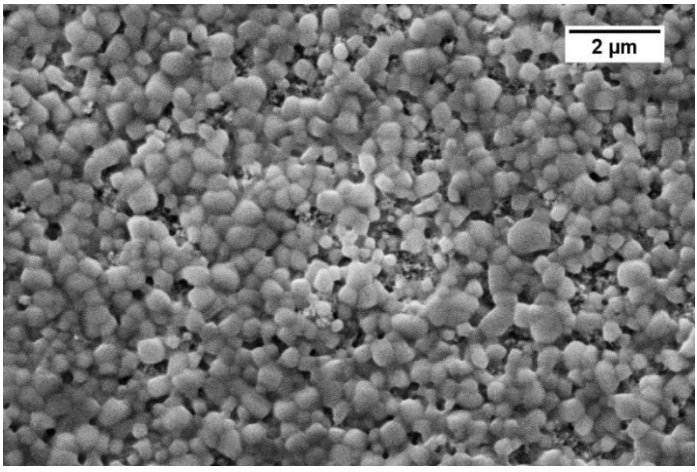

Figure 1. SEM image of $CH_3NH_3PbI_3/TiO_2$ films, 3000 rpm deposition velocity.

Acknowledgments. The authors would like to thank the Coordination for the Improvement of Higher Education Personnel – CAPES, the National Council for Scientific and Technological Development – CNPq and the Foundation of Support to Research of the State of Rio Grande do Sul – FAPERGS for the financial support. The present paper was presented inside the '*Toward a Sustainable Mobility*' special session as part of the '*Two Seats for a Solar Car*' research project, an action funded by the Italian Ministry of Foreign Affairs and International Cooperation within the Executive Programme of Cooperation in the field of Science and Technology between the Italian Republic and the Republic of Serbia.

9th International Scientific Conference
Research and Development of Mechanical Elements and Systems
Kragujevac, Serbia, September 5-7 2019

NEW METHOD FOR MODELING THE TOPOGRAPHICAL PROPERTY OF METALS AND ITS APPLICATION IN ROBOT LASER HARDENING WITH OVERLAPPING

M Babič[1*], G Lesiuk[2], L Giorgini[3]

[1]Faculty of Information Studies, 8000 Novo Mesto, Slovenia
[2]Department of Mechanics, Materials Science and Engineering, Wroclaw University of Science and Technology, 50-370 Wroclaw, Poland
[3]Department of Industrial Chemistry, University of Bologna, 40136 Bologna, Italy

Key words: robot laser hardening, pattern recognition, modelling.

Robot laser surface hardening is the part necessary for hardening instantly absorbs light energy, turning it into thermodynamic, due to which the temperature rises and austenite forms, then, after instant cooling, the martensite microsubstance is obtained. Due to the technology of heat treatment, it is possible to obtain other high-strength layers. The combination of laser hardening technology with the advantages of high cooling rate, uniform temperature distribution, minimum thermal stress, high strength, wide processing capabilities of various parts, etc. made this machine advanced in the processing of molding tools and many other industries. The study of laser technology involves the study of principles of light energy in physics. Laser is an acronym for Light Amplification by Stimulated Emission of Radiation. Laser hardening [1-4] is a metal surface treatment process complementary to conventional flame and induction hardening processes. A high-power laser beam is used to heat a metal surface rapidly and selectively to produce hardened case depths of up to 1,5mm with the hardness values of up to 65 HRC. It is used exclusively on ferrous materials suitable for hardening including, steels and cast iron with a carbon content of more than 0.2 percent. Laser beam hardening is employed to locally improve the surface properties of components. Use of this treatment can increase wear and fatigue resistance in parts of steel and cast iron. Through a locally restricted heat treatment arises a minimum heat input, thereby minimized distortion. The associated high heating and cooling rates result in fine microstructures with good mechanical properties. During the laser skin hardening, the material (carbonaceous material) is heated up for a short time above austenitizing temperature and is transubstantiated by fast cooling down into the martensite

structure. Different tool steels are widely used in industrial applications due to good performance, a wide range of mechanical properties, machinability and wear cheapness. With the laser hardening surface of the material, we can significantly improve their wear properties. Heat is generated by absorbing the laser radiation on the surface and the material is quenched by heat transportation inside. In the equipment of laser hardening a flat semiconductor laser is used as a heat source. The laser, in turn, has a high photoelectric conversion efficiency, has a short wavelength, low energy consumption and other advantages. In this article, we present technology of robot laser hardening with overlapping and new method for modeling topographical property of overlapping hardening process. The paper presents application of intelligent system methods in process of robot laser hardening with overlapping. We present hybrid method of intelligent system to predict topographical property of robot laser hardened specimens. The main findings can be summarized as follows: For prediction of the hardness of hardened specimens we use neural network and support vector machine methods, with the hybrid method of intelligent systems, we increase production of the process of laser hardening, because we decrease the time of the process and increase topographical properties of materials and we describe the relationship between hardness and the parameters of the robot laser cell. This finding is important with regard to certain alloys that are hard to mix, because they have different melting temperatures; however, such alloys have better technical characteristics. By varying different parameters (e.g., temperature), robot laser cells produce different patterns.

IRMES KRAGUJEVAC 2019
9th International Scientific Conference
Research and Development of Mechanical Elements and Systems
Kragujevac, Serbia, September 5-7 2019

PIEZOELECTRIC PVDF SENSOR AS A RELIABLE DEVICE FOR STRAIN/LOAD MONITORING OF ENGINEERING STRUCTURES

Sakineh Fotouhi[1], Roya Akrami[2], Keean Ferreira-Green[3], Mohamed Gamal Ahmed Naser[3], Mohamad Fotouhi[3], Cristiano Fragassa[4]

[1]Department of Mechanical Engineering, University of Tabriz, Tabriz, Iran
[2]University of Peyamnoor, Tehran, Iran
[3]Department of Design and Mathematics, University of the West of England, Bristol BS16 1QY, UK
[4]Department of Industrial Engineering, University of Bologna, Viale Risorgimento 2, 40136 Bologna, Italy

Key words: load monitoring, PVDF, passive sensors, fatigue cycle counter.

Engineering structures, such as aircraft, wind turbines, marine vessels, buildings and offshore platforms, are experiencing a range of uncertain dynamic loadings during their life time, due to changes in operational and environmental conditions, etc. These structures are usually over- engineered in order to prevent failure. This is because there is not an appropriate and cost efficient devices to monitor the subjected loads, and therefore not possible to predict the fatigue life of these structures.

This research is investigating the feasibility of replacing strain-gauges with Piezoelectric PVDF (polyvinyldiene fluoride) piezoelectric film, as a dynamic load gauge. The overall aim is to develop a monitoring-based method for fatigue life assessment with use of long-term monitoring data by PVDF. The PVDF sensor can be made in any shape/size and are flexible. In addition, the PVDF sensor is passive and offer the advantage of requiring no power to function.

As shown in Figure 1, the experiment was coordinated by attaching the PVDF sensor attached to a piece of mild steel and subjecting it to cyclic tensile tests with different load levels. The examined sample was created by mounting the PVDF sensor 20mm from the midpoint of the steal which was cut to length of 300mm. This was followed by another sensor mounted on the other side of the mild steel to compare the results. The PVDF sensors were manufactured by TE Connectivity (part number 1-1002910-0) and the employed data acquisition system was Vishay Model 6100 scanner.

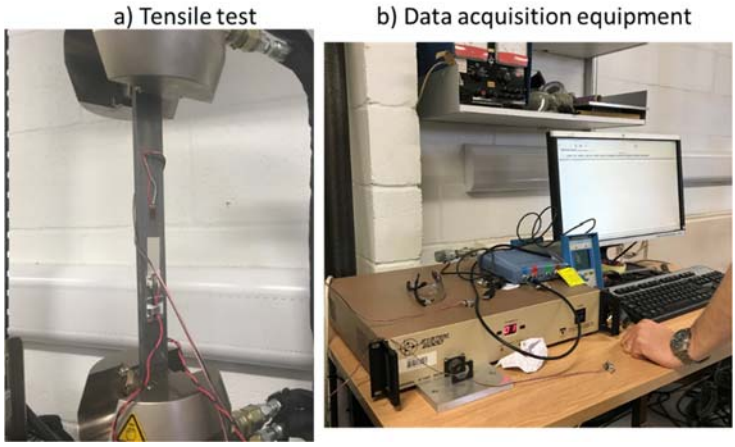

Figure 1. Experimental setup a) The tensile test and b) The data acquisition system.

Figure 2 shows the amplitude dependence of the PVDF sensor and strain gauge according to the magnitude of load. The loads for this test ranged from 2 kN to 10 kN. The output varied linearly with a peak amplitude of 0.11 volts being achieved for 2 kN of force and 0.39 volts for 10 kN. Results also show that PVDF was more sensitive to sense deformation than strain gauges giving it an advantage over strain gauge technology.

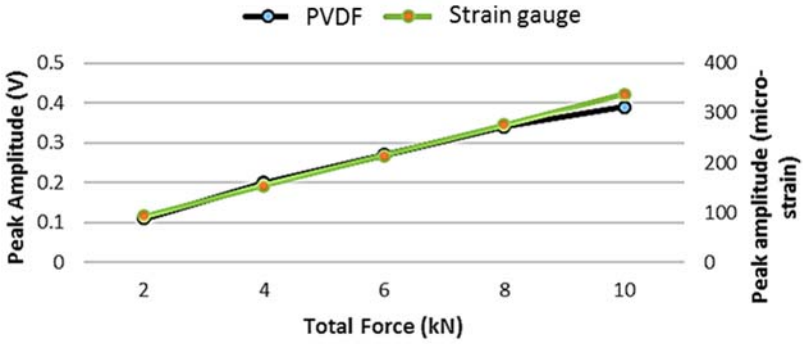

Figure 2. PVDF output dependence on amplitude compared with strain gauge.

Monitoring the load level of steel sample with PVDF sensors, the output of the sensors was found to vary linearly with applied load. A similar pattern was observed for the strain gauge measurements. It was concluded that the PVDF piezoelectric sensor is a good alternative to conventional strain gauges in order to measure dynamic loadings for structural health monitoring purposes. The PVDF sensors offer the advantage of needing no power to function and the sensors can be made to suit any size and geometry, therefore reducing the size and cost of the load monitoring device.

9th International Scientific Conference
Research and Development of Mechanical Elements and Systems
Kragujevac, Serbia, September 5-7 2019

INNOVATION IN SOLAR VEHICLES: FROM CONCEPT TO PROTOTYPE IN LESS THAN 24 MONTHS

S Maglio[1], M Lukovic[2], N Zavatta[3*], A Leardini[3]

[1] Onda Solare Association, Castel San Pietro Terme, Bologna, Italy
[2]Industrial Design Department, University of Arts Belgrade, Belgrade, Serbia
[3]Interdepartmental Center for Industrial Research on Advanced Mechanics and Materials, Alma Mater Studiorum University of Bologna, Bologna, Italy, nicola.zavatta2@unibo.it

Key words: solar vehicle, 3D CAD modelling, hybrid manufacturing.

The present article describes the integrated path used for the conceptual, functional and constructive design of an exclusive multi-occupant solar-powered vehicle. The project was based on the massive implementation of concurrent engineering and quality tools, rarely used in such an integrated way, featuring a novel and attractive design, 3D CAD modelling, structural and fluid dynamics validations, in-scale rapid prototyping, functional tests, multi-objective optimization, parts manufacturing and assembly. Thanks to this approach, the solar car prototype presented high technological contents, especially in terms of materials, structures and processes. Furthermore, large CNC-machined multi-material molds and hybrid manufacturing solutions were adopted to speed up the production phase allowing to move from the initial concept to the final prototype within 24 months. Since June 2018, the solar vehicle is on the road transporting 4 people, weighing less than 300kg, reaching speeds of 120km/h and able to travel hundreds of kilometers with zero-emission and no fuel consumption.

This work briefly summarizes the realization of the design (Fig.1 and 2) and construction of one of the few multi-occupant solar vehicles in the world and its use to cross a large part of the United States, carried by a group of researchers from the University of Bologna and supported by partner institutions. Everything started from the sporting passion for automotive competitions and from the previous experience in the field of solar vehicles, which led to the creation of a solar single-seater in recent years. With this vehicle, we took part in several races on different continents bringing back valuable successes. However, the category of single-seater solar vehicles did not seem to represent a real technological challenge as it appeared to be the category of multi-passenger vehicles. Known under the name of 'cruiser' car, this relatively recent category in the racing scene obliges designers to face particularly complex technical problems, linked to the specific needs of solar mobility.

Figure 1. Aesthetic design: some proposals from the design competition (©Filip Relic).

Solar cars have to be imagined by the designers around the fundamental concept of energy efficiency. This condition requires important technical and design choices that, combined with the race regulation requirements, lead to exclusive and highly innovative prototypes. Besides, everything was made possible only thanks to the use of concurrent engineering and its design tools, within a more general approach to Total Quality Management (TQM) in automotive. This path is here briefly presented together with a list of references, able to provide full details on specific aspects.

(a) (b)

Figure 2. Aesthetic final design (a) and patented version with rendering effect (b) (©Marko Lukovic).

The final result is a 4-seater, electric solar-powered vehicle. Size 4.6x1.8x1.2m; empty mass (including batteries) of 230 kg and a maximum of 600 kg. Main structure and components in carbon fiber reinforced polymers (CFRP), with some parts in kevlar, titanium and ergal. Front surface of 1.60 m2 with a 0.20 drag coefficient. Maximum expected speed 100 km/h, average consumption of 21 Wh/km (at 55 km/h), range of about 750 km (at 55 km/h). Photovoltaic panel in monocrystalline silicon, 5 m2 with 326 SunPower cells, maximum efficiency 24% (at 25°C) and maximum panel power of 1.1kW. Converter with 98% efficiency. Battery pack: 83 kg positioned in the central tunnel, 1344 Samsung lithium ion cells with a nominal capacity of 3.4 Ah; rated voltage 48V, intensity 331.2 Ah, total energy 16.1 kWh; 2688 temperature sensors. Two synchronous motors with permanent magnets on the rear wheels: external rotor coupled directly to the wheel, and stator on the structure. Each 11kg motor has a nominal power of 1300 W and a maximum of 3000 W (nominal torque of 35 Nm and a maximum of 125 Nm); expected efficiency 97%. These performances permitted to cross the United States, from the Missouri river to Portland, passing through the Rocky Mountains in less than 10 days, with an average speed of approx. 65 km/h, inside the American Solar Challenge 2018 (Figure 7). As a synthesis, thanks to the design approach, it was possible to: design and build a four-wheeled light vehicle; include it in the standard category of quadricycles; minimize the overall dimensions of space; maximize the space where to locate the solar panels; carry 4 passengers safely; balance weights and vehicle dynamics; provide adequate space for vehicle components such as steering and suspensions; provide adequate space for electrical components such as engines and battery; guarantee fast-access systems in case of maintenance; optimize the aerodynamic profile by reducing air resistance; guarantee a phenomenon of downforce in order to reduce the rolling resistance; correctly convey part of the air for cooling and ventilation; ensuring the internal liveability of the spaces and the installation of auxiliary devices; insert elements such as doors, air vents, lights, arrows, license plate in line with the standards; use shapes that can be built with available materials and technologies; provide for the possibility of registration of the vehicle.

Acknowledgment. The research is part of a larger action, managed by the University of Bologna (with references Cristiano Fragassa and Giangiacomo Minak), aiming at demonstrating the potentialities of the solar energy for a sustainable mobility. This publication has been supported by the Italian Ministry of Foreign Affairs and International Cooperation thought the Joint Research Projects as Particular Relevance, with a project named 'Two Seats for a Solar Car' within the Executive Programme of Cooperation between Italy and Serbia in the field of Science and Technology. Special thanks to Mauro Sassatelli and Ruggero Malossi (Onda Solare).

9th International Scientific Conference
Research and Development of Mechanical Elements and Systems
Kragujevac, Serbia, September 5-7 2019

TESTING METHODS AND EQUIPMENT FOR PALLETIZED PRODUCTS

A Greco[1], A Renzini[1], M Vaccari[1]

[1] Technology Lab Robopac, Aetna Group Spa, Via Cá Bianca, 1260, 40024 Castel San Pietro (BO), Italy, mvaccari@robopac.com

Key words: palletized products, palletizing scheme, stability of the load.

The ability to present cutting-edge solutions for packaging in the field of palletized products has to be considered as the result of the investments in research infrastructures and advances in applied researches. In the present article, in particular, it is detailed the main equipment and all the other testing facilities that can be used to optimize the way a palletized product is realized. Tests are implemented in accordance with standard and less standard procedures up to fully innovative methods. This approach is able to provide advice both on the most appropriate palletizing scheme to pack the load, either on the best packaging methods able to conserve intact the product to the consumer. For customer it represents a great added value that allows to experience first-hand palletizing solutions, packaging and stability of the load, reducing production costs and optimizing efficiency.
Over the years, the packaging industry has become increasingly important. At the beginning, the essential aspect was to guarantee a safe, functional and aesthetically appreciated product packaging. Later, and rather recently, the packaging has covered additional aspects such as environmental sustainability of transport and the integrity of the goods transported. In this regard it is usual to differentiate a 'primary packaging', the one intended to contain the product in contact with it (e.g. bottles, blisters, etc.), from a 'secondary packaging', used to collect and protect the goods during transport. For this second form of packaging it is common to group primary containers (e.g. bottles, blisters, etc.) in bundles, consolidated through heat-shrink material, and then in pallets. These pallets are wrapped in prestressed films of plastic material that stabilize the package.
This secondary packaging process is characterized by a significant number of parameters, such as, for example, the type and thickness of the film, the number of layers, the strength of pre-stress and so on. Transport by ship, by train, by truck are just some of the different options that identify the specific load spectra to which a package is subjected during transport. In the various studies the attempt is to categorize these solicitations around some bases of reference, such as, for example, the geographical area, America, Asia or the type of route travelled (highway vs secondary roads. This is joined by all that is present although less intuitive. This relates, for example, to secondary handling, including shocks (expected or not), storage inside or outdoors (changes in temperature, humidity and irradiation with modification of the properties of the film.

This problem is so worthy of attention that innumerable standards have arisen. Among many of others it is interesting to mention: EUMOS 40509 for evaluating the load unit rigidity; the ASTM D4003 as test method for horizontal impacts of containers; ASTM D5276 for drop tests on containers; the ISTA list on procedures for simulating the effect of different mean of transportations.

Regardless of the characteristics of the packaging considered to be the most suitable and the stresses expected during the trip or their theoretical models, there will always be a time when all these considerations must be tested through an experimental approach.

Figure 1. Moog hexapod configured for test simulation.

In other words, we will always need a laboratory equipped to test packages. This goal is not obvious in terms of feasibility, especially considering how the packaging subject to analysis can be very large and heavy, and must be subjected to rather significant impulsive loads, capable of reproducing stresses similar to those present during transport, including events such as shock.

Some regulations help simplifying real loads by considering them equivalent or less burdensome than those provided through standard tests. Several studies and even our experience suggest that these tests are not to be considered equivalent, nor more rigorous.

Figure 2. Results on wrapping load after test on vibrating platform.

The success of the first simulations and the potentiality to replicate every type of transport or critical event thanks to the developed measurement system combined with Moog hexapod (Fig.1) has led the laboratory to represent a first-class test environmental for this special products. Therefore this machine is added to the current one, able to study by standard tests the effect of transport on the stability due to wrapping of the palletized load (Fig.2). Meanwhile an instrumented pallet will be used to extend the available data related to transports, for every kind of product, transport, road and other parameters and configurations required by the customer.

Acknowledgments. The authors wish to acknowledge the assistance and encouragement from colleagues from the Department of Industrial Engineering at the University of Bologna.

STUDENT SECTION

9th International Scientific Conference
Research and Development of Mechanical Elements and Systems
Kragujevac, Serbia, September 5-7 2019

- STUDENT SECTION -

VIRTUAL DEVELOPMENT PROCESS OF POWER GEAR TRANSMISSION

Nikola Rucić[1], Miloš Stanković[1], Damjan Rangelov[1], Miloš Stevanović[1], Jovan Aranđelović[1], Dragan Milčić[1], Milan Banić[1]

[1]University of Niš, Faculty of Mechanical Engineering in Niš, Aleksandra Medvedeva 14, 18000 Niš, Serbia, dragan.milcic@masfak.ni.ac.rs

Key words: virtual development process, power gear transmission, CAx, 3D printing, fused deposition modeling.

All products have a limited life expectancy, so it is necessary to constantly develop new products that will replace the existing ones and keep the company's competitiveness in business. Just as the product life cycle has different phases, the development of new products is also broken down into several specific phases (Figure 1).

Figure 1. Phases of new product development

Product development today can not be imagined without the use of numerous CAx tools in the virtual product development process. CAD is a key tool used to create product geometry in a virtual environment. CAx includes a wide range of product calculation, simulation, optimization and planning processes in several disciplines (e.g. mechanics, electrics, electronics, optics), which are performed parallel to the geometry creation. Of course, throughout the virtual development cycle, design always goes hand in hand with computational engineering processes. In some literature, virtual development in general is denoted as CAx (computer aided technologies). The combination CAD and different of CAx processes can be displayed as process chains (Figure 2).

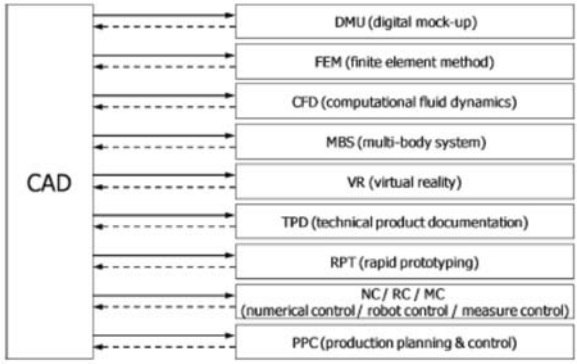

Figure 2. CAD-CAx workflows

In the process of virtual development of power gear transmission, the calculation of all gear elements of the gearbox is carried out in the software Power Transmission Design (PTD), developed at the Faculty of Mechanical Engineering in Niš. Based on the results of the calculation, all parts of the gearbox, the assembly gearbox, and the documentation of parts were made in the CAE software Autodesk Inventor Professional 2019. In Figure 3, a 3D model of a power gear transmission is given.

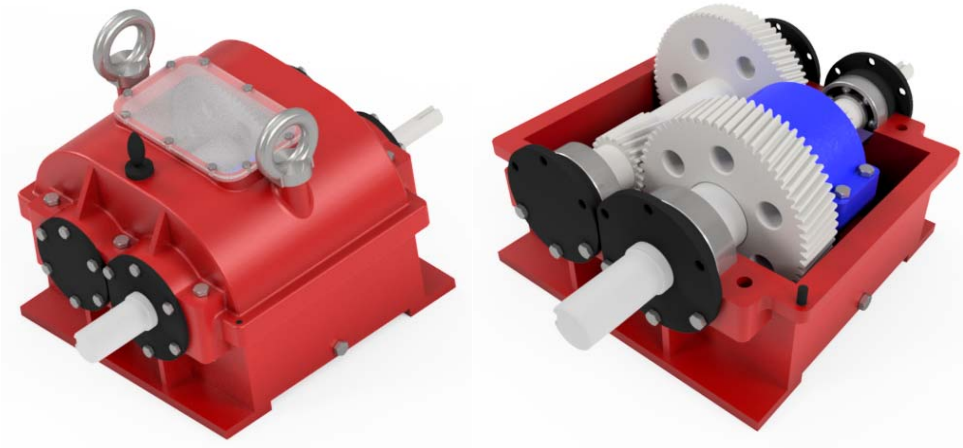

Figure 3. 3D model of power gear transmission

Based on the 3D model of parts of power gear transmission, the physical parts are obtained by 3D printing. 3D printing (3DP) technologies can be divided in the following groups: inkjet printing, fused deposition modelling, polymer jetting and so on. In this paper the focus is on 3DP applications, mainly fused deposition modeling (FDM).

Acknowledgments. This paper presents the results of the research conducted within the project ‘‘Research and development of new generation machine systems in the function of the technological development of Serbia’’ funded by the Faculty of Mechanical Engineering, University of Niš, Serbia.

9th International Scientific Conference
Research and Development of Mechanical Elements and Systems
Kragujevac, Serbia, September 5-7 2019

- STUDENT SECTION -

PROOF OF CONCEPT FOR DESIGN OF NOVELTY HANDHELD VACUUM CLEANER GADGET USING ADDITIVE MANUFACTURING TECHNOLOGIES

Predrag Cvetković[1], Marko Pavlović[1], Tomica Mutavdžić[1], Kristina Milojević[1], Lozica Ivanović[1]

[1]University of Kragujevac, Faculty of Engineering, Sestre Janjić 6, 34000 Kragujevac, Serbia, pedjacvetkovic1@gmail.com

Key words: product development, industrial design, handheld vacuum cleaner, 3D print

3D printing technology significantly saves the time in development of functional product. This paper presents the use of 3D printing for prototype production of handheld vacuum cleaner. The aim was to improve our knowledge in fields of product development and manufacturing technologies by making a novelty handheld vacuum cleaner. Beginning of product development was based on sketching potential models of handheld vacuum cleaner by using "Brainstorming" method. After selection of four alternative solutions, analyses of their best characteristics with aim to combine them into the one solution was made. Figure 1, a shows a sketch of final solution, while in figure 1, b the corresponding 3D model of handheld vacuum cleaner is presented.

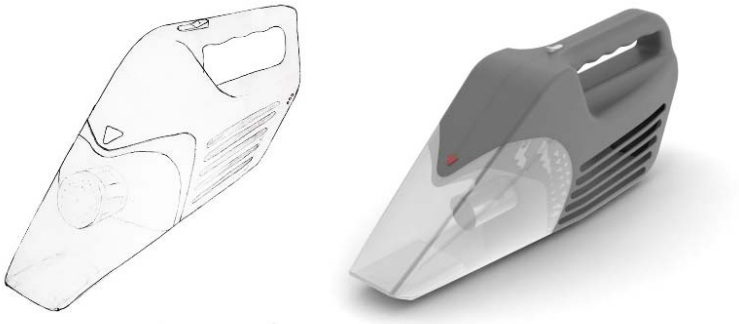

Figure 1. Sketch (a) and 3D model (b) of handheld vacuum cleaner

In order to showcase the appearance and have a proof of concept for the handheld vacuum cleaner, a prototype of it was made. For efficient 3D printing, model presented in figure 1, b

was adjusted to production process for corresponding 3D printer. Printed component from prototype of handheld vacuum cleaner is presented in figure 2.

Figure 2. Printed component of handheld vacuum cleaner

The current model was made with the purpose of being used as a desktop gadget in the office or at home. As the device is a product of 3D printing, it is possible for anyone who possesses a 3D printer to print and assemble their own following given instructions and purchasing the required motor and battery.

Further development will require testing design efficiency and functionality of handheld vacuum cleaner, as well as eliminating weak points and sections, it was planned to make functional prototype with use of different materials.

What it created motivation for work is existence of possibility to extend knowledge in fields like industrial design, construction and product development, as well as gaining professional skills like creative problem solving and team work.

Acknowledgments. This paper is a continuation of a group project done for the course Industrial Design and the Faculty of Engineering, University of Kragujevac. We would like to thank the Centre for Testing and Calculation of Machine Elements and Systems "Prof. dr Vera Nikolić Stanojević" – CIPMES for the support in 3D printing.

9th International Scientific Conference
Research and Development of Mechanical Elements and Systems
Kragujevac, Serbia, September 5-7 2019

- STUDENT SECTION -

RECONSTRUCTION OF CUTTER FOR TEXTILE USING PRINCIPLES OF REVERSE ENGINEERING AND RAPID PROTOTYPING

Kristijan Micic[1], Srdjan Samardzic[1]

[1]University of East Sarajevo, Faculty of Mechanical Engineering, Vuka Karadzica 30, 71123 Lukavica, BiH, micickristijan@gmail.com

Key words: reverse engineering, rapid prototyping, reconstruction**.**

In this paper is present Reconstruction of cutter for textile using principles of Reverse engineering and Rapid Prototyping. Reverse engineering is the process of exploring the technological principles of a product, object or system by analysing its structure, function and running. In this case, process of reconstructing consist from six steps (Figure 1).

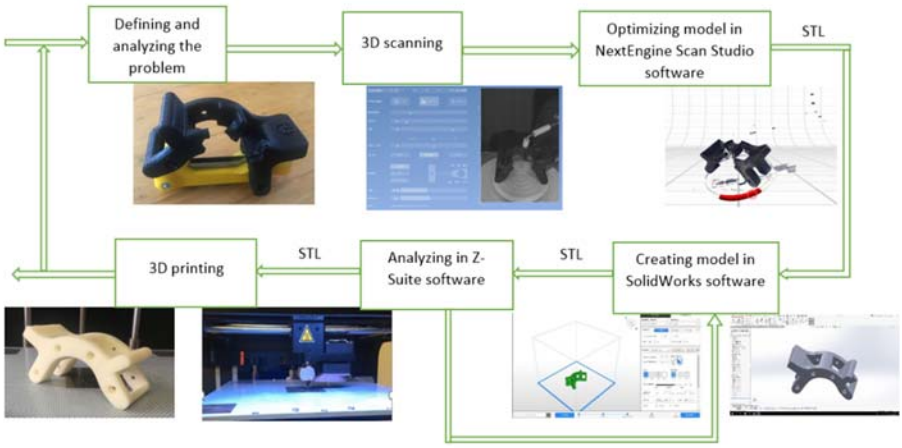

Figure 1. Steps of reconstruction

First step was defining and analysing the problem. The starting point was broken part (carrier) for which was not provided technical documentation, so it was necessary to apply process of reverse engineering. Second step was 3D scanning. Scanning was made using two scans at NextEngine 3D scanner with MultiDrive module. Basics parameters of scanning are presented at Table 1. Next step was optimizing model in NextEngine Scan Studio software. It was necessary to remove some parts using trim tool and to improve quality of scan using

fuse and polish tool. Fourth step was creating model in SolidWorks. It is important to accent that model was imported in SolidWorks as STL format. Model based on the scan was created after that.

Table 1. Basics parameters of scanning

	Positioning	**Start**	**Tilt**	**Division**	**Points/IN^2**
Scan A	360	0	0	5	16k
Scan B	Bracket	-176	31	5	7k

Next step was model analysing in Z-Suite software. At this step, problem was incorrectly of some model parts so it was important to go back to SolidWorks model and correct it. The parameters for production from Table 2 were set after that.

Table 2. Basics parameters for production

Material	**Z-ULTRAT**
Nozzle diameter	0,4 mm
Layer	0,19 mm
Quality	Normal
Infill	70%

Last step was production of final part using FDM (Fused Deposition Modelling) technology at Zortrax M200 device. FDM technology present type of RP technology that uses a continuous filament of a thermoplastic material. Filament is fed from a large coil through a moving, heated printer extruder head, and is deposited on the growing work.

Table 3. Times spent on every step

Step	**Time**
Defining and analysing the problem	60 min
3D scanning	30 min
Optimizing model in NextEngine Scan Studio software	60 min
Creating model in SolidWorks software	300 min
Analyzing model in Z-Suite software	30 min
3D printing	200 min
Total	680 min = 11h 20 min

In this paper has been proved that it is possible to reconstruct product without using CAD tool but it takes a lot more time (Table 3). A reconstructed product has been manufactured, tested and ready for commercial serial production at the end of this process.

Acknowledgments. Thanksgiving to prof. dr Biljana Markovic and Aleksija Djuric for major contribution to creating of this paper.

IRMES KRAGUJEVAC 2019

9th International Scientific Conference
Research and Development of Mechanical Elements and Systems
Kragujevac, Serbia, September 5-7 2019

- STUDENT SECTION -

IMPROVEMENT OF IC ENGINE CRANK MECHANISM KINEMATICS USING NON-CIRCULAR GEARS

Dijana Čavić[1], Jovan Dorić[1], Milan Kostić[1], Nebojša Nikolić[1]

[1]University of Novi Sad, Faculty of Technical Sciences, Trg Dositeja Obradovića 6, 21000 Novi Sad, Serbia, dijana.cavic@uns.ac.rs

Abstract: Increasing the efficiency of IC engines is a frequently discussed topic and one of the approaches taken is to modify the thermodynamic work cycle of the engine so that it resembles the ideal cycle more closely. This paper attempts to achieve that by altering the kinematics of the piston-crank mechanism by introducing a pair of non-circular gears between the crank and the flywheel. The addition of the gears alters the work cycle by introducing a state of pseudo-dwell during key points of the cycle. Possible gear shape solutions were calculated using a known, periodical function to express the gear transmission ratio. These gear shapes were then analyzed in regard to their effect on the work cycle and their technological viability. The final result was a pair of non-circular gears with a shape that has a noticeable effect on the kinematics of the piston-crank mechanism while still being possible to manufacture.

Key words: piston-crank mechanism, non-circular gears, kinematics, IC engine.

1. INTRODUCTION

The chain of thermodynamic reactions occurring in the piston chamber of an IC engine is known as the work cycle. Due to the complexity of these reactions, the work cycle is analyzed through different mathematical models. In theory, the most efficient thermodynamic cycle for IC engines is the Otto cycle, which consists of isentropic compression and expansion processes and isochoric heat addition and expulsion processes [1,2].
The traditional design of IC engines with a simple slider-crank mechanism doesn't allow enough time for isochoric combustion which significantly reduces the cycle efficiency. The ideal scenario is to initiate and complete the combustion event while the piston remains at the TDC position. This provides the maximum thermal potential and eliminates the negative work due to early ignition which is well into the compression stroke with conventional engine strategies. One practical method of achieving this optimization is to significantly reduce the piston velocity at the TDC position to provide extra time for completing the

combustion [3]. Modifications to the motion of the piston made in order to improve the efficiency of the IC engine have been studied by many researchers [3-5].
This paper explores the possibility of increasing the efficiency of IC motors by modifying the piston-crank mechanism with the addition of a pair of non-circular gears, thus changing the law of motion of the piston and forcing a period of pseudo-dwell which in turn would bring the thermodynamic work cycle of the engine closer to the ideal work cycle.
The goal of this paper is to offer a viable solution for the problem of increasing IC engine efficiency in the form of a pair of non-circular gears and analyzing their effect on the whole mechanism and their overall viability.
The paper is structured as follows. Section 1 introduces the topic of this paper and explains the motivation for writing it. Section 2 presents the conventional piston-crank mechanism and its laws of motion as well as its proposed modification, the inclusion of a pair of non-circular gears. The results are presented in Section 3 and include the kinematics of the modified mechanism, the shape of the gears and commentary on the viability and effectiveness of the modifications. Section 4 offers a summation of the paper and outlines possible future works.

2. PISTON-CRANK MECHANISM

2.1. The conventional piston-crank mechanism

The conventional piston-crank mechanism (figure 1) used in IC engines consists of a piston (Figure 1 – link 4), a connecting rod (Figure 1 – link 3) and a crankshaft (Figure 1 – link2). While the piston is technically the driving element in this case, the mechanism is powered by the crankshaft for three out of the four strokes, by way of the kinetic energy accumulated in the flywheel. Due to this, the crankshaft will be regarded as the driving (input) link further in this paper.

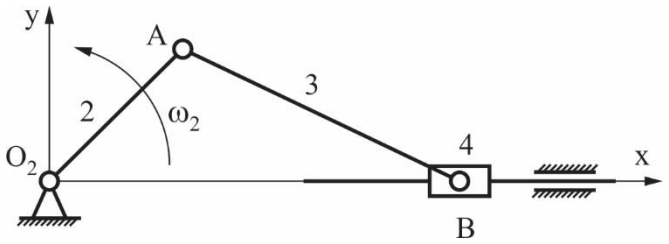

Figure 1. Scheme of the piston-crank mechanism

After conducting the kinematic analysis [6], the following laws of motion are obtained (Figure 2). For graphing purposes, the following parameters were adopted as such (the kinematic parameter of most IC engines being $\lambda = \frac{r_2}{r_3} = 0.25 \div 0.3$):

$$\omega_2 = 100\pi\left[\frac{1}{s}\right]$$

$$r_2 = 0.06[m]$$

$$r_3 = 0.2[m]$$

The parameters ω_2, r_2, r_3 being the velocity of the crankshaft, the radius of the crankshaft and the length of the connecting rod, respectively.

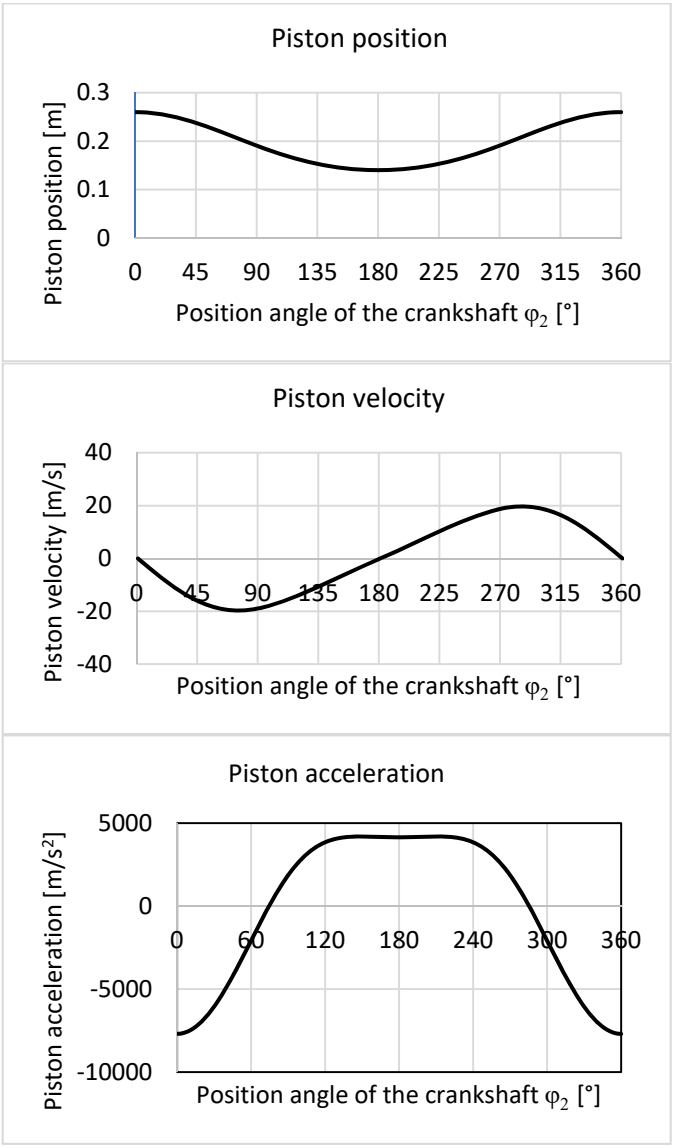

Figure 2. The position (top), velocity (middle) and acceleration (bottom) of the piston

2.2. The proposed modification of the crank piston mechanism and

As is evident in the graphs, the velocity of the piston is equal to zero only in the moments when it passes through the top and bottom dead centers. The graph in figure 3 shows the difference between the law of motion of the conventional mechanism and the law of motion the piston would need to follow to achieve an ideal work cycle.

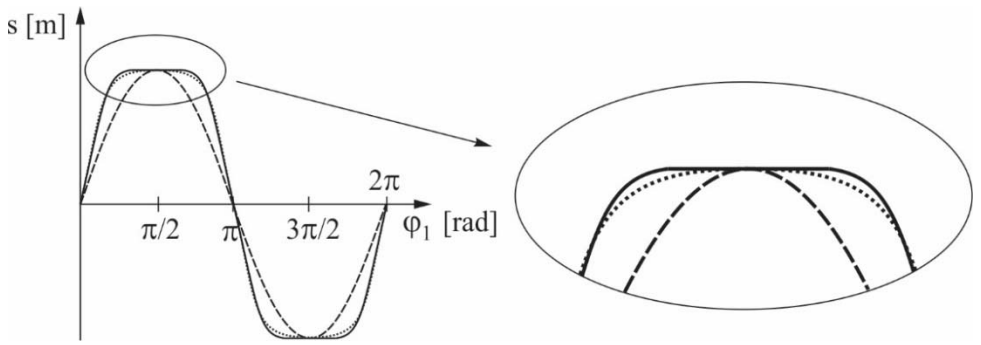

Figure 3. Law of motion of the piston - ideal cycle (solid line), modified mechanism (dotted line), conventional mechanism (dashed line)

The conventional piston-crank mechanism operates on the assumption that the input velocity supplied by the crankshaft is approximately constant due to the flywheel. By changing this velocity from constant to the variable, it becomes possible to influence the law of motion of the piston. However, since the crank piston mechanism is only one part of the more complicated IC engine, which is again only a part of the power train of a vehicle, certain other requirements need to be taken into consideration.

Therefore, the modified mechanism needs to fulfil the following requirements:

1. Supply the variable input speed of the crankshaft needed to achieve the prescribed law of motion of the piston
2. Avoid unnecessary complications of the construction
3. Avoid stopping the latter parts of the vehicle power train (the flywheel, the gearbox elements, etc.)

One possible solution that would fulfil these requirements is a pair of non-circular gears inserted between the flywheel and the crankshaft. The gear connected to the flywheel would be considered the input gear and would have a constant velocity. The gear connected to the crankshaft would have a variable velocity which is dictated by the shape of the gears, therefore theoretically offering the possibility of defining the motion of the crankshaft with an arbitrary function, and consequently, the motion of the piston as well. A scheme of the proposed solution is shown in Figure 4.

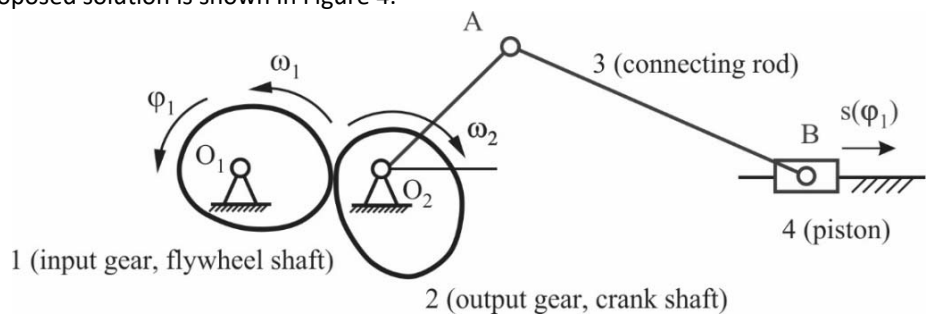

Figure 4. Scheme of the modified piston-crank mechanism

2.3. The introduction of non-circular gears to the piston mechanism

The centrode of non-circular gears is defined by expressing the relation between the radius and the polar angle of each gear [7]. To achieve this, a function must be prescribed that determines the variation of the output velocity.

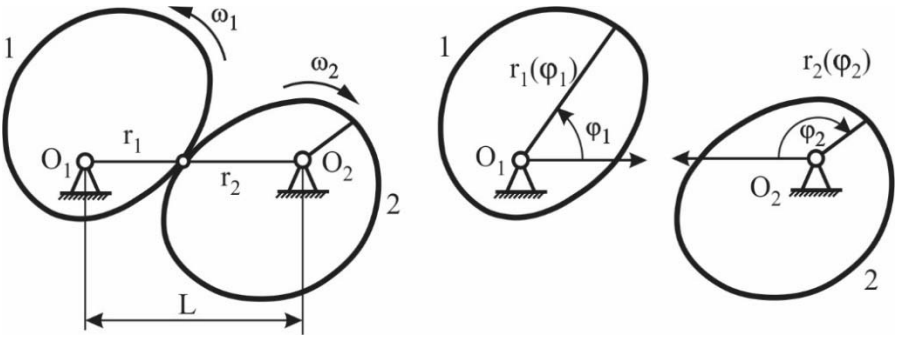

Figure 5. Kinematic parameters of non-circular gears

The parameters (Figure 5) needed to define the shape of non-circular gears are:

1. The transmission ratio:

$$i_{12}(\phi_1) = \frac{r_2(\phi_1)}{r_1(\phi_1)} \tag{1}$$

2. The axial distance:

$$L = r_1(\phi_1) + r_2(\phi_1) = \text{const} \tag{2}$$

3. The centroid radii:

$$r_1(\phi_1) = \frac{L}{1 + i_{12}(\phi_1)} \tag{3}$$

$$r_2(\phi_1) = \frac{L}{1 + i_{12}(\phi_1)} \cdot i_{23}(\phi_1) \tag{4}$$

4. The polar angle of the output gear $\phi_2(\phi_1)$:

$$i_{12}=\frac{\omega_1}{\omega_2}=\frac{d\phi_1}{d\phi_2} \quad \Rightarrow \quad d\phi_2=i_{21}\cdot d\phi_1 \quad \Rightarrow \quad \phi_2(\phi_1)=\int_0^{\phi_2} i_{21}d\phi_1=\int_0^{\phi_2}\frac{1}{i_{12}}d\phi_1 \quad (5)$$

The shape of the input gear is determined by: $r_1(\phi_1)\,\text{and}\,\phi_1$.

The shape of the output gear is determined by: $r_2(\phi_2)\,\text{and}\,\phi_2$.

Since the input velocity is constant, the output velocity can be indirectly expressed using the transmission ratio, which is the approach taken in this paper.

The function used is a member of the following function family:

$$i_{12}(\phi_1)=\begin{cases}\frac{1}{2}\cdot(a+b)-\frac{1}{2}\cdot(b-a)\cdot\cos(\pi\frac{\phi_1}{\phi_0}),\phi_1\in[0,\phi_0)\\ \frac{1}{2}\cdot(a+b)+\frac{1}{2}\cdot(b-a)\cdot\cos(\pi\frac{\phi_1-\phi_0}{2\pi-\phi_0}),\phi_1\in(\phi_0,2\pi]\end{cases} \quad (6)$$

The parameters a,b,ϕ_0 being the minimum of the function, the maximum of the function and the point in time (the angle) where the function achieves the maximum value, respectively. A visual representation of these parameters is shown in Figure 6.

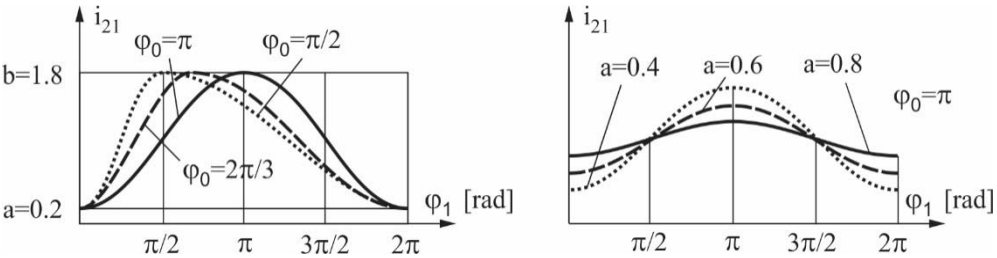

Figure 6. Transmission ratio function with different values of ϕ_0 (left) and *a* (right)

To ensure that the gears rotate continuously and are possible to manufacture, two additional requirements must be fulfilled:

1. The centroids of the gears need to be closed. For this to be the case, the following expression must be true:

$$\frac{T_1}{n_1}=\frac{T_2}{n_2}=T \quad (7)$$

   Where T_1,T_2 are the periods of the input and output gears centrode, n_1,n_2 are arbitrary integers and T is the period of the transmission ration function.

2. The average transmission ratio must be equal to 1, meaning that for each revolution of the input gear, the output gear completes one revolution as well. If this is the case, then the periods of both gears are equal and the following equation can be written.

$$\phi_2(2\pi)=\int_0^{2\pi} i_{21}(\phi_1)d\phi_1=2\pi \quad (8)$$

By solving equation (8), the following expression is established:

$$a + b = 2 \tag{9}$$

Based on equation (9), the parameters are adopted as such:

$$\phi_0 = \pi$$
$$a = 0.1$$
$$b = 2 - a = 1.9$$

After including these parameters in the general function, the specific transmission ratio in the case of this mechanism is defined as such (figure 7):

$$i_{12}(\phi_1) = \begin{cases} 1 - 0.9 \cdot \cos\phi_1, \phi_1 \in [0, \pi) \\ 1 + 0.9 \cdot \cos(\phi_1 - \pi), \phi_1 \in (\pi, 2\pi] \end{cases} \tag{10}$$

Now it becomes trivial to express the variable velocity of the output gear:

$$\omega_2(\phi_1) = i_{21} \cdot \omega_1 . \tag{11}$$

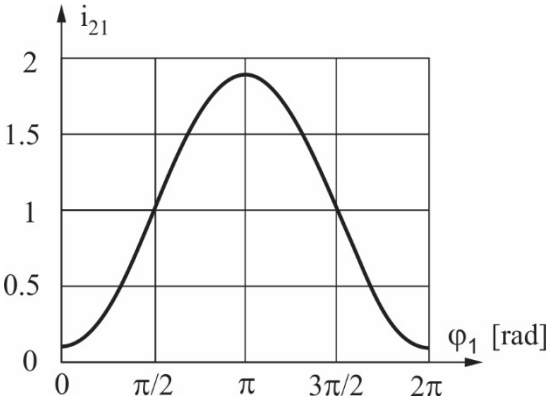

Figure 7. Adopted transmission ratio i_{21}

3. RESULTS

3.1. Kinematics of the modified mechanism

After conducting the kinematic analysis of this newly modified crank piston mechanism, the law of motion of the piston is obtained. Figure 8 shows the modified law of motion, and allows the comparison of the modified and conventional laws of motion.

For graphing purposes, the bottom and top dead center positions and the piston stroke are adopted based on existing IC engines, respectively:

$$s_{BDC} = 140[mm]$$
$$s_{TDC} = 260[mm]$$
$$h = s_{TDC} - s_{BDC} = 120[mm]$$

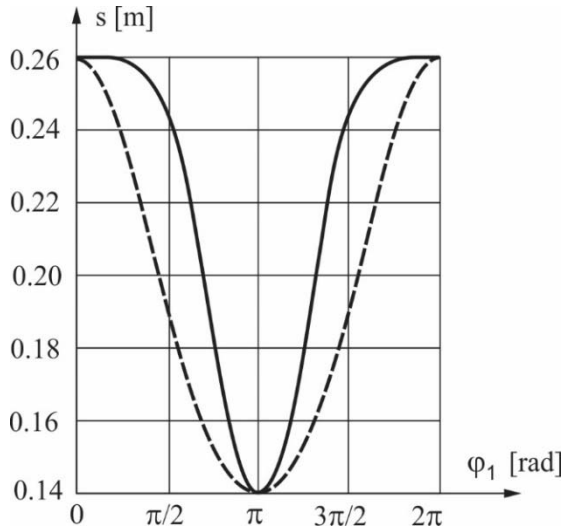

Figure 8. Modified (solid line) and conventional (dash line) mechanism – piston position

The piston of the modified mechanism changes its position very slowly when near the top dead center – in the interval of 0 to 30 degrees of the crankshaft revolution, the piston position changes from 260mm to 259.8mm. The difference between the laws of motion is evident. The modified law of motion describing the velocity is shown in Figure 9.

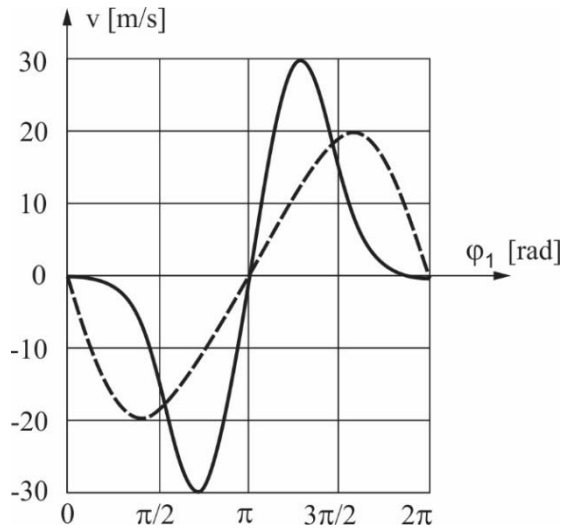

Figure 9. Modified (solid line) and conventional (dash line) mechanism - piston velocity

It is evident that the piston velocity of the modified mechanism is close to zero - during the crankshaft interval of 0 to 30 degrees the velocity changes from 0 to -1.16 m/s, meaning that

a period of pseudo-dwell has been achieved. The difference between the piston velocities of the conventional and modified mechanisms can also be seen in Figure 9.
Due to the fact the input velocity is now variable instead of constant, the law of motion describing piston acceleration of the modified mechanism is different from the piston acceleration of the conventional mechanism. Both piston accelerations can be seen in Figure 10.

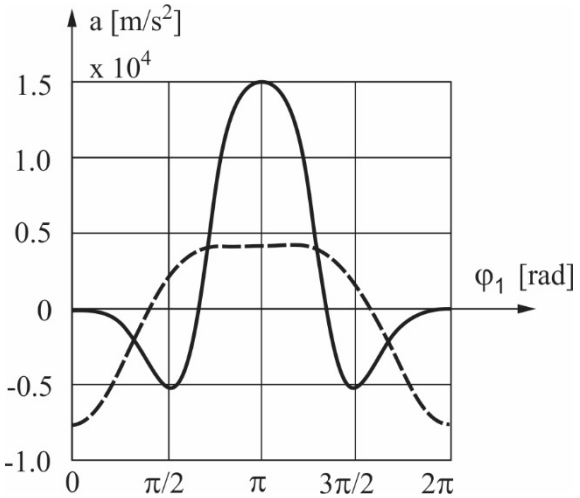

Figure 10. Modified (solid line) and conventional (dash line) mechanism - piston acceleration

The modified piston acceleration is a smooth function with no sudden extreme changes in value, which is favourable. However, it is evident that, when compared to the piston acceleration of the conventional mechanism, the acceleration magnitude of the modified mechanism is much higher. This implies the existence of higher inertial loads, which could be problematic, but this line of inquiry will not be pursued in this paper.

3.2. The shape of the non-circular gears

For graphing purposes, the axial distance between the gears is adopted as L=100 [mm]. Using the adopted axial distance and the output gear velocity $\omega_2(\phi_1)$, the shapes of the non-circular gears are obtained.
The gear shapes are shown in Figure 11.

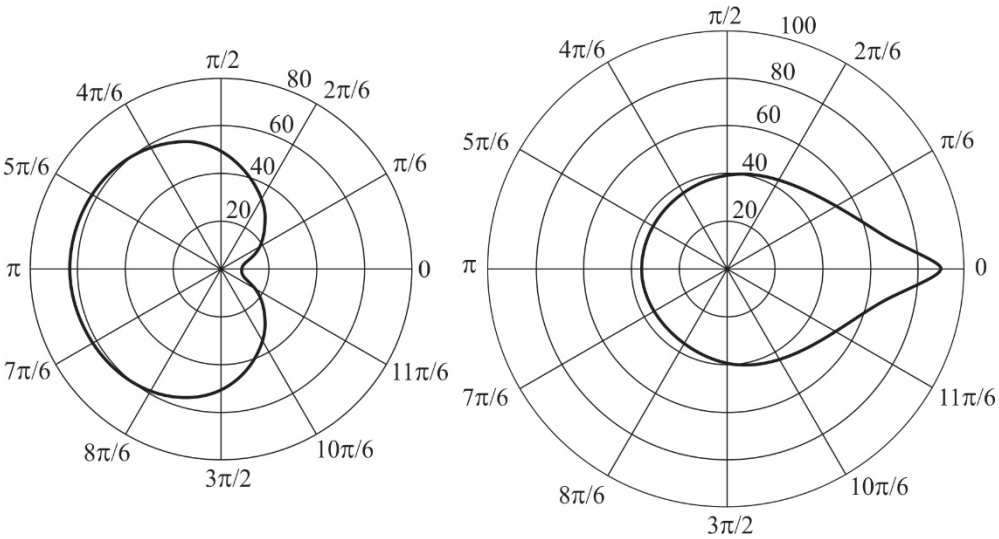

Figure 11. The input (left) and output (right) non-circular gears

A relevant parameter of non-circular gears is the curvature radius. Parts of the gear profile with small curvature radii could have trouble meshing properly, and can make manufacturing the gear teeth difficult or even imposible. Also relevant are inflexion points since they are the points where the curvature changes from concave to convex and vice versa. Both of these parameters are shown in Figure 12 and Figure 13 for the input and output gear, respectively.

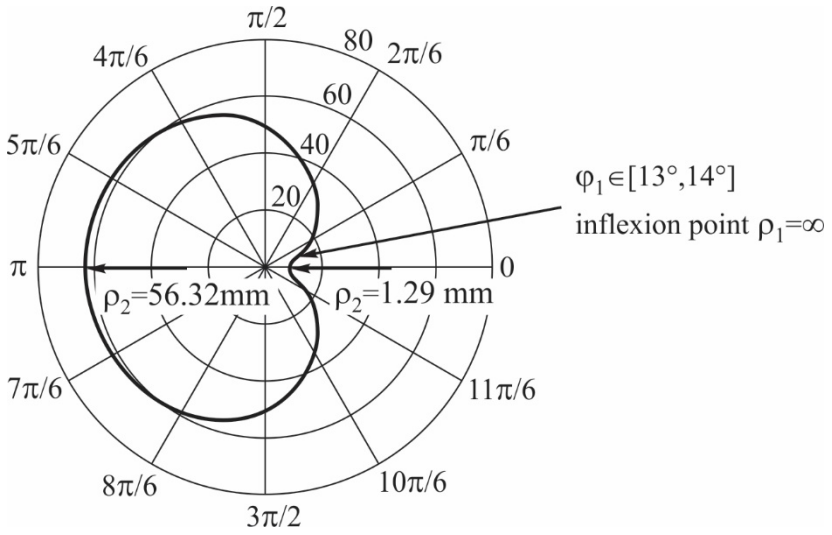

Figure 12. Critical points of the input gear

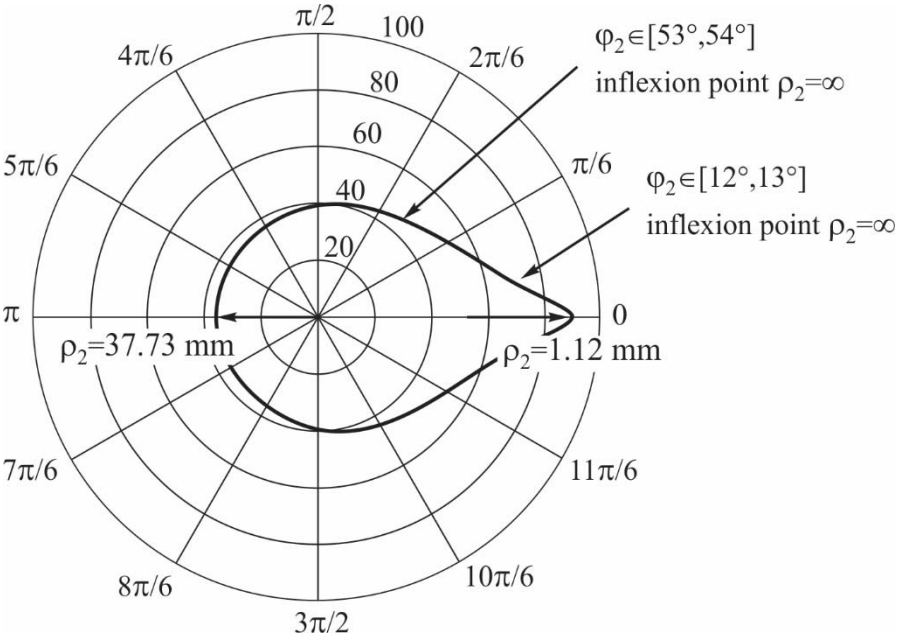

Figure 13. Critical points of the output gear

While a more detailed analysis is needed to determine if these gears can be manufactured, there are no extremes present (ie. Points where the radius equals to zero or forms a cusp). Variations of the gear shape are possible by varying parameter a. The effect of different values of this parameter on the law of motion of the piston is shown in Table 1 and Figure 14. For ease of comparison, the begining and end of the pseudo-dwell is defined as $s_{TDC} \pm 0.2 = 259.8[mm]$.

Table 1. The effect of different values of parameter a on the length of the pseudo-dwell

a	Line type (*Figure 14, Figure 15*)	Crankshaft angle interval during pseudo-dwell ϕ_1 [deg]	Piston position at the beginning and end of pseudo-dwell s [mm]
0.1	Dotted line	$-30^{\circ}...+30^{\circ}$	259.8
0.2	Solid line	$-20^{\circ}...+20^{\circ}$	259.8
0.3	Dash line	$-11^{\circ}...+11^{\circ}$	259.8

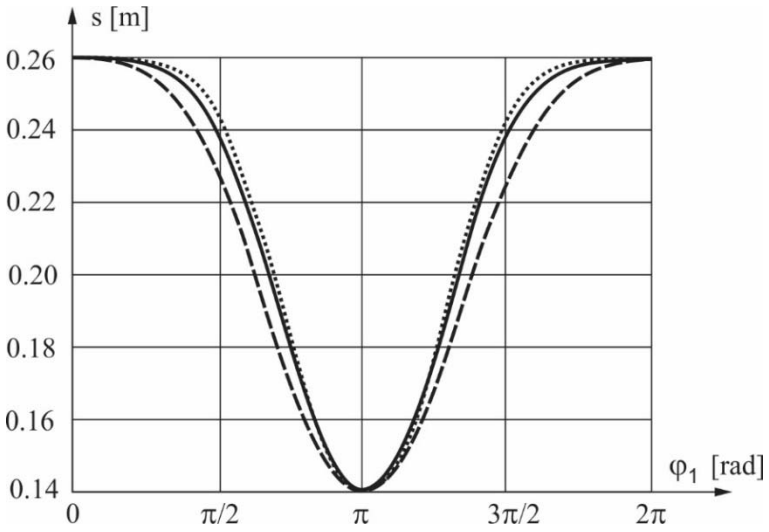

Figure 14. The effect of parameter a on the length of the pseudo-dwell

It is evident that by decreasing the value of a, the length of the pseudo-dwell increases. The effect of different values of parameter a on the gear shape is shown in Figure 15.

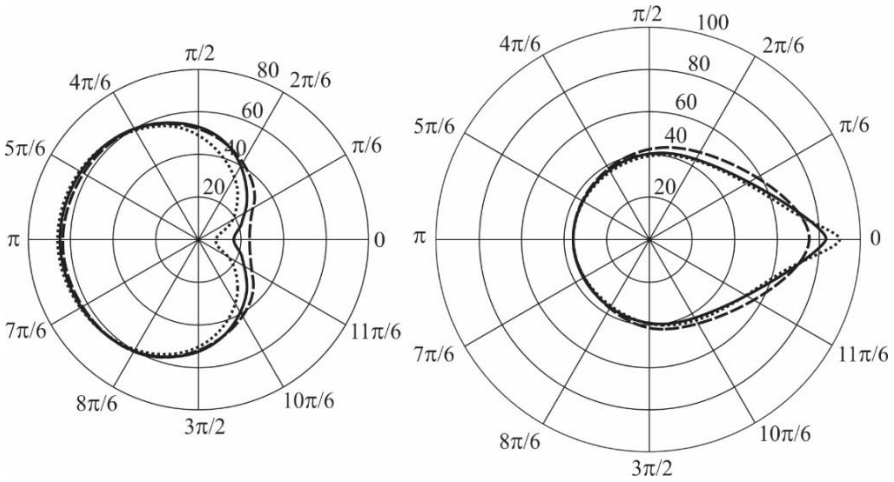

Figure 15. The effect of parameter a on the shape of the input (left) and output (right) gears

It is evident that by decreasing the value of parameter a, the shape of the gears becomes more extreme, making both meshing and manufacturing more difficult. Since a decrease of parameter a provides a more effective modification of the piston motion but also decreases the viability, the solution would need to be a compromise found using a method of optimization, a topic for future study.

3.3. The effect of the modified mechanism on the work cycle

The pV diagram shown in Figure 16 is a visual representation of the influence of parameter a, and consequently the varying gear shapes, on the work cycle. The most efficient cycle, the one with the largest surface area of the upper part, is the ideal work cycle. As the diagram shows, the smaller the value of a, the closer the modified work cycle is to the ideal cycle.

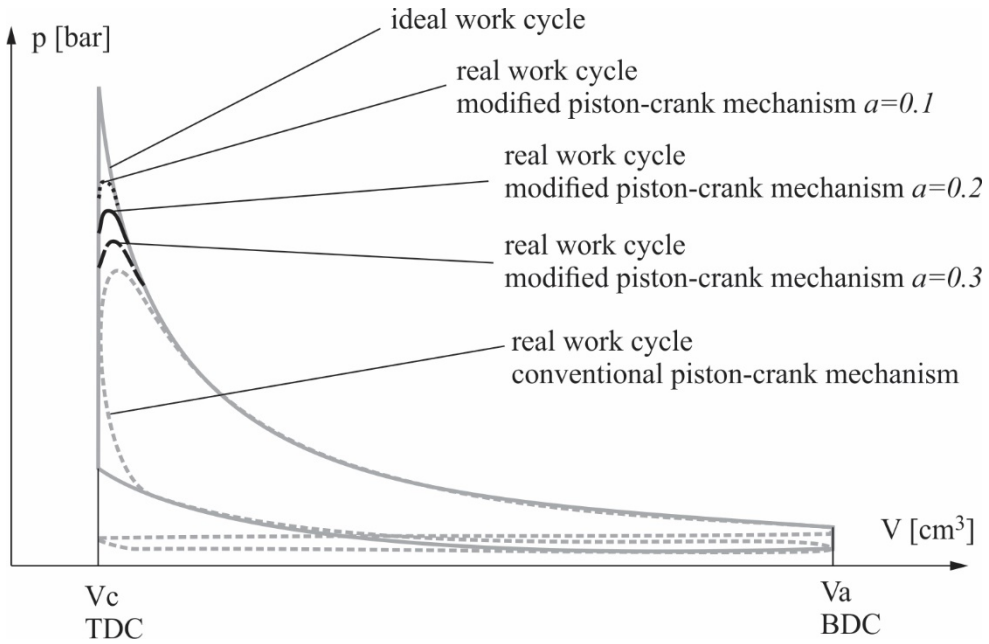

Figure 16. The effect of parameter a on the work cycle

As was stated previously, a lower value of the parameter means a gear pair that is more difficult to manufacture and mesh correctly. However, even the work cycle of the mechanism with the most conservative gear pair shown in this diagram shows an increase in efficiency when compared to the conventional crank piston mechanism.

4. CONCLUSION

This paper explored the possibility of increasing the efficiency of IC engines by modifying the kinematics of the piston-crank mechanism, through the use of non-circular gears. By defining the transmission ration of the gears with a known periodic function (defined by parameter a), possible solutions were obtained.

The results show that there are indeed possible gear shapes that could be used to modify the kinematics of the mechanism, to force the piston into a period of pseudo-dwell while near the top and bottom dead centers. By further analysing the effect of parameter a (and the gear shape), it was made clear that the more pronounced the pseudo-dwell became, the manufacturing difficulty increased.

Apart from the need to compromise between effectiveness and viability, several other downsides were found, notably the drastically faster acceleration of the piston. High acceleration values imply the possibility of high inertial loads, but a full dynamic analysis would need to be conducted to confirm.

The most notable downside, however, would be the fact that this type of mechanism only offers the possibility of pseudo-dwell. To bring the work cycle as close to the ideal cycle as possible, a mechanism that offers true dwell is required. A possible solution for this problem would be non-circular epicyclic gears. A secondary upside to using epicyclic gears is that they keep the construction coaxial, which isn't the case with conventional non-circular gears. Of course, further study is needed to ascertain whether their use would fulfil the requirements listed in this paper, and if so, whether they are possible to manufacture.

REFERENCES

[1] Dorić J 2015 *Teorija motora SUS*, FTN Publishing, Novi Sad

[2] Klinar I 2013 *Motori sa unutrašnjim sagorevanjem*, FTN Publishing, Novi Sad

[3] Dorić J , Klinar I 2014 Efficiency of a New IC Engine Concept with Variable Piston Motion, Thermal Science **18**(1)

[4] Dorić J, Klinar I 2013 Efficiency Characteristics of a New Quasi-Constant Volume Combustion Spark Ignition Engine, Thermal Science **17**(1)

[5] Dorić J, Nikolić, N 2016 Double Acting Piston Engine, *Machine Design* **8**(3) 107-110

[6] Zlokolica M, Čavić M, Kostić M 2013 *Mehanika mašina*, FTN Publishing, Novi Sad

[7] Čavić M, Kostić M, Zlokolica M 2014 *Prenos snage i kretanja*, FTN Publishing, Novi Sad

9th International Scientific Conference
Research and Development of Mechanical Elements and Systems
Kragujevac, Serbia, September 5-7 2019

- STUDENT SECTION -

STRUCTURAL ANALYSIS OF CARDAN CROSS

Tomica Mutavdžić[1], Sandra Veličković[1]

[1]University of Kragujevac, Faculty of Engineering, Sestre Janjić 6,
34000 Kragujevac, Serbia, tmutavdzic@hotmail.com

Abstract. In this paper is shown analysis of the influence of input rotation angle and operation angle on stresses in a cardan cross. The aim of this paper was to perform analysis of cardan cross using two different methods, analytical method and finite element method. Analytical method does not include real geometry in a calculation. Finite element method was performed by using Computer Aided Design software SolidWorks 2017. Based on obtained results it can be concluded that resulting stresses have maximal values in shape transition zone between branches and central section of cardan cross. Optimal range of operation angle, based on this paper, is $\alpha = 0° \div 20°$. Relative stress variation between finite element method and analytical method is about 67%. Resulting stresses, obtained by analytical and numerical methods, have same trendline behaviour as functions of rotation angle of input shaft.

Key words: cardan cross, stress, finite element method, analytical method.

1. INTRODUCTION

Fast development of cardan mechanisms and their wider usage begins by development of transport and agricultural mechanical engineering [1]. The cardan mechanism transmits torque and rotational movement between shafts which axes are under certain angle or by time variable angle [2]. Because of nature of cardan mechanisms, the position of cardan shaft can be variable in exploitation by changing of terrain. It is very important to make correct assembly of these mechanisms as well as manufacturing their parts, because by time of exploitation due to overload, various destructions and fractures can be identified on elements of cardan mechanisms. The most common failure sections are at basis of the cardan yoke and the cardan cross [1,2].

Before any part of the cardan mechanism find its way to exploitation it's important to perform adequate analysis of every part. The problem is in stress concentration at basis of the branches of the cardan cross, aim is to determine that stress and reduce its concentration. The structural analysis in this paper is based on calculation of maximal stresses on bending and shear of a cardan cross, with variation of the position of output

shaft relative to input shaft, which directly impacts stresses that appear on a cardan cross. Causes of failures of the cardan mechanism and its design was analysed by many researches. *Avrigean* et al. performed comparison of results obtained by analytical method, finite element method (FEM) and experiment on a real model. They've concluded that results obtained by finite element method is more relevant than analytical method, as well that results obtained by finite element method and experiment on a real model have difference about 9% [3].While in some papers that observed the influence of operation angle on stresses in a cardan cross, with already known optimisation, relative variations between analytical and numerical method can be about 34% [4].

Stamenić et al. have concluded that with use of numerical method is possible to make optimization of geometrical dimensions from aspect of evenly spreading loads through loaded sections of cardan cross. Main reason of this research was the distribution of loads on loaded sections of cardan cross have big impact on capacity and life of whole cardan mechanism [5]. In order to increase life of cardan mechanism and to decrease oscillations *Vesali* et al. had accomplished better power transmission by increasing degrees of freedom and using finite element method [6]. Many scientists were involved with design and analysis of cardan shaft or its subassemblies, which were based on variation of only loads or only materials at static load. Some of more important conclusions were that maximal stresses are usually at sections with sharp edges of cardan cross, then that results obtained by finite element method are similar to real life experiment and beside that saves a lot of time. Likewise, they've concluded that grey cast iron is desirable choice among tested materials, because of better toleration at loads [7-9]. *Ivanović* et al. were reduced loads on input yoke of cardan shaft by 30% and for cardan cross even to 40%, only with modification of shape and fillet. Optimization was done by adding fillets at basis of yoke and at basis of branches on a cardan cross. Likewise, they've accomplished optimization with small design modifications in sections of yoke where load is negligible compared to the rest of element [10].

After literature review it was noticed that scientists are focusing on using software in order to very easy, faster and reliable obtain convenient conclusions of considered elements. The aim of this paper was to perform structural analysis of cardan cross using two different methods to establish which method provides more accurate results. One of methods used was analytical calculation with help of corresponding equations, while other is standard finite element method. Because of complexity of the problem in this paper analysis of a cardan cross is shown.

2. EXPERIMENT

Need for bigger reliability of cardan mechanisms is getting bigger, because of the more difficult work conditions to which elements of these mechanisms are exposed. Based on the cardan cross geometry and its position in cardan joint assembly, during exploitation it's exposed to loads on twisting, bending, surface pressure and shear [2]. Main characteristic of asynchronous cardan mechanism, like it's cardan joint (figure 1), is to frequently change difference between angles of rotation as well as difference between angular velocities of input and output shafts. This value is even bigger if operation angle α between shafts is bigger, which can lead to unevenly power transmission [2].

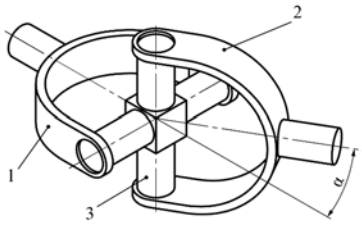

Figure 1. Cardan joint

In figure 1 is simplified presentation of cardan joint, with positions of input and output yokes (1) and (2) which are connected to a cardan cross (3).

2.1. Analytical calculation of resulting stresses

Calculation of resulting stresses was done on model of the cardan cross that is shown in figure 2. Dimensions of considered model are limited by design requirements. Main characteristics which cardan cross needs to fulfill are power: $P = 5\ \mathrm{kW}$, number of revolutions: $n = 1400\ \mathrm{min}^{-1}$, distance between top of branche and critical section A-A: $h_1 = 10.5\ \mathrm{mm}$, length of bearing zone: $h = 9\ \mathrm{mm}$, distance between two top sides of opposite branches: $H = 40\ \mathrm{mm}$, diameter of branches: $d_1 = 11.5\ \mathrm{mm}$, diameter of branche at critical section: $D_1 = 13\ \mathrm{mm}$, diameter of hole for supply of lubricant: $d_p = 3\ \mathrm{mm}$, arm of force from center of cardan cross: $R = 15.5\ \mathrm{mm}$ and operation angle: $\alpha = (0 \div 30°)$. Model of this cardan cross was result of cardan shaft calculation within bachelor thesis [11].

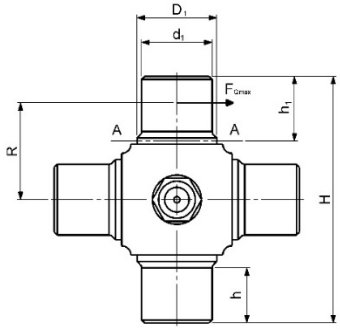

Figure 2. Dimensions of a cardan cross

If losses are neglected, based on virtual moving, equation of balance for cardan mechanism have form as in equation (1) [2]:

$$T_1 \cdot d\varphi_1 = T_2 \cdot d\varphi_2, \tag{1}$$

or like:

$$T_2 = T_1 \cdot \frac{sin^2\,\varphi_1 + cos^2\,\varphi_1 \cdot cos^2\,\alpha}{cos\,\alpha}. \tag{2}$$

where φ_1 and φ_2 are angles of rotation of input and output shafts.
Maximal value of force F_{Qmax} can be presented as in equation (3):

$$F_{Qmax} = \frac{T_{2max}}{2 \cdot R}. \quad (3)$$

Maximal value of bending stress in critical section A-A:

$$\sigma_s = \frac{F_{Qmax} \cdot l}{W}, \quad (4)$$

where l is arm of force F_{Qmax} and W is resistant moment of cardan cross. In this paper cross section on branches of cardan cross is in circle shape, so W can be presented as in equation (5):

$$W = \frac{\pi \cdot D_1^3}{32}. \quad (5)$$

Because of load on shear of cardan cross, shear stress can be calculated as in equation (6):

$$\tau = \frac{4 \cdot F_{Qmax}}{\pi \cdot D_1^2}. \quad (6)$$

So from previous two equations for stresses (4) and (6), it is possible to calculate resulting stress as in equation (7):

$$\sigma = \sqrt{\sigma_s^2 + 3 \cdot \tau^2}. \quad (7)$$

More detailed calculation of previous equations is presented in reference [2].
Based on previous researches like *Rakić* et al. and *Vesali* et al., expectations were that resulting stress reaches its critical value at angles of rotation $\varphi_1 = 0°$and $\varphi_1 = 90°$ [4,6]. Beside analytical calculation it's needed to perform numerical analysis of cardan cross because of conformity of obtained results.

2.2. Numerical calculation of resulting stresses using finite element method

The data accuracy obtained by analytical method is not promising, from simple reason because for calculation it's used simplified model. Numerical method like finite element method is based on calculation of mathematical model with real geometry. Structural analysis using finite element method is more precise relative to analytical method. Finite element method gives opportunity to make fast and repeatable calculations if modification of elements is needed. Within this paper simulation of loads on the cardan cross was done by using Computer Aided Design software SolidWorks 2017. Analysis using finite element method is based on next steps [12,13]:

- creation of geometric model,
- definition of material,
- discretization by finite elements (creation of mesh),
- definition of boundary conditions,
- definition of loads,
- numerical calculation and
- graphic interpretation of results.

Geometrical model of cardan cross in this paper was based on real life model, with recommendations from references [10] and [14]. After a few variations an optimal model came out and it's shown in figure 3. The material used for this particular cardan cross is 16MnCr5. This material is low carbon casted steel and it's recommended by most

manufactures. Main characteristics of 16MnCr5 material are elastic modulus $E = 2.1 \cdot 10^5 \text{MPa}$ and Poisson's ratio $\nu = 0.28$.

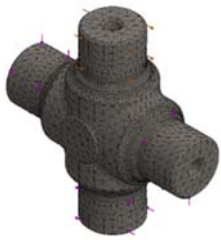

Figure 3. Discretization of model with loads

In figure 3 created mesh and defined loads can be seen. Because of the assumption and on the basis of previous researches, that on shape transition zone between branches and central section will be maximal stress, creation of mesh was done in way to be very fine in shape transition zone. The reason is that with finer mesh stresses can be easier and more precisely localized. Boundary conditions were defined using theoretical basis of cardan cross. Central section was fixed and all branches were loaded with forces in range from 1.1 kN to 1.27 kN. Cardan cross is element that is symmetrical between two axes and have four branches that are creating the angle of 90° by them. Every branches loaded with same forces that are coming from yoke over roller bearings. In reference [10] finite element method was done on quarter of the cardan cross because of symmetry, it was loaded with one force, while in this paper whole cardan cross was loaded.

For whole process to be relevant it was needed to repeat numerical calculation for every value of operation angle α. It was also needed to perform analysis for different positions of input shaft that are defined by angle of rotation φ_1 which can be moving in range from $\varphi_1 = 0°$ to $\varphi_1 = 180°$, but because of symmetry of results experiment was performed until half of rotation. Distribution of von Mises stresses in the cardan cross for different values of operation angle α and angle of rotation φ_1, with graphic chart of stress level is presented in figures 4 and 5.

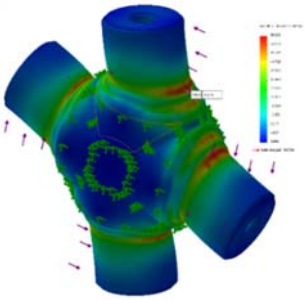

Figure 4. Von Mises stress distribution in the cardan cross at $\alpha = 10°$ and $\varphi_1 = 0°$ ($\sigma = 55.606$ MPa)

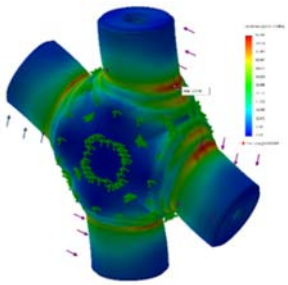

Figure 5. Von Mises stress distribution in the cardan cross at $\alpha = 30°$ and $\varphi_1 = 90°$ ($\sigma = 65.208$ MPa)

2.3. Discussion and analysis of the results

Based on calculation using analytical method values of resulting stresses of cardan cross were obtained. Values of resulting stresses as functions of operation angle are shown in table 1.

Table 1. Values of resulting stresses as functions of operation angle

α (°)	T_2 (Nm)		F_{Qmax} (kN)		σ_s (MPa)		τ (MPa)		σ (MPa)	
	$\varphi_1 = 0°$	$\varphi_1 = 90°$	$\varphi_1 = 0°$	$\varphi_1 = 90°$	$\varphi_1 = 0°$	$\varphi_1 = 90°$	$\varphi_1 = 0°$	$\varphi_1 = 90°$	$\varphi_1 = 0°$	$\varphi_1 = 90°$
0	34.1071	34.1071	1.10023	1.10023	30.6059	30.6059	8.28909	8.28909	33.806	33.806
5	33.9774	34.2374	1.09604	1.10443	30.4894	30.7228	8.25755	8.32076	33.6774	33.9352
10	33.589	34.6333	1.08352	1.1172	30.1409	31.078	8.16316	8.41697	33.2924	34.3275
15	32.945	35.3103	1.06274	1.13904	29.563	31.6855	8.00665	8.5815	32.6541	34.9986
20	32.0502	36.2961	1.03388	1.17084	28.7601	32.5701	7.7892	8.82107	31.7673	35.9756
25	30.9116	37.6331	0.99715	1.21397	27.7384	33.7699	7.51247	9.146	30.6387	37.3008
30	29.5377	39.3835	0.95283	1.27044	26.5055	35.3406	7.17857	9.57142	29.2769	39.0358

The reason why calculation of resulting stresses was not performed for operation angles over 30° is that the majority of manufactures claims that with increase of operation angle oscillations increases as well. Operation angle over 20° is not recommended for use within agricultural machines [15]. After all collected data it was possible to perform comparison of resulting stresses obtained by analytical method and finite element method on example of cardan cross, which is shown in figure 6.

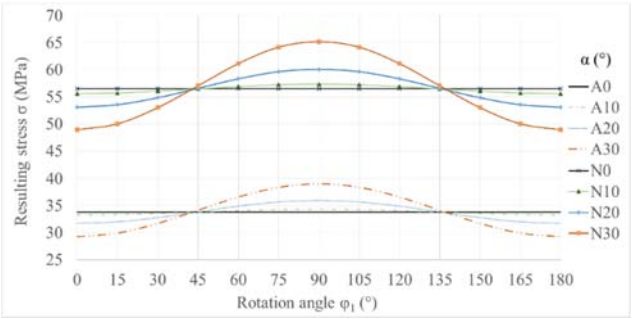

Figure 6. Values of stresses as functions ofoperation angle α and rotation angle φ_1 (A-analytical method, N-numerical method)

It is clearly visible difference in values obtained by analytical and numerical methods. Based on that histogram with presentation of relative resulting stress variation expressed in percentages was made, all of that with help of equation (8) [4]:

$$\Delta\sigma = \frac{|\sigma - \sigma^*|}{\sigma^*} \cdot 100\ (\%) \tag{8}$$

Where $\Delta\sigma$ is relative variation of corresponding value, σ is value of stress obtained by numerical method and $\sigma^*$is value of stress obtained by analytical method. Relative

stress variation for values is shown in figure 7. In order to make results clearer every value of operation angle was divided by corresponding value that was obtained for rotation angle $\varphi_1 = 0°$.

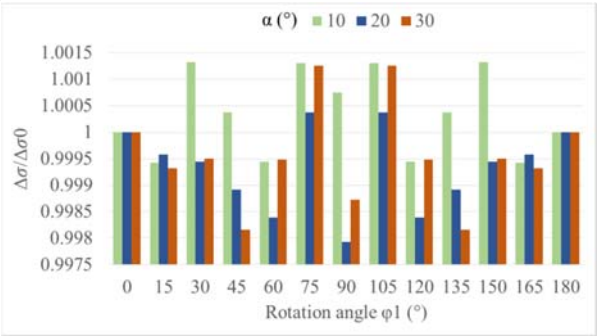

Figure 7. Relative stresses variation

Middle value of relative variation is $\Delta\sigma_{sr} \approx 67\%$, which indicates that value read from histogram in figure 7 is needed to multiply by 67 and in that way to get approximate value for relative stress variation expressed in percentages. In figure 6 it is possible to notice that with increase of operation angle increases resulting stress as well, which is followed along with increase of resulting stress variation range. If resulting stress variation range as a function of rotation angle φ_1 is big, it does not work well for parts of cardan mechanism. That is one of main reasons why manufactures are recommending small values of operation angles. In scope of this paper the biggest variation range of resulting stress is at operation angle of $\alpha = 30°$.

3. CONCLUSİON

Structural analysis of cardan cross was performed using two different methods. One of methods used was analytical calculation with help of corresponding equations, while other is standard finite element method. Finite element method was performed using newer software for an increase of conformity of obtained results. Based on obtained results the following significant conclusions can be distinguished. Diagram of resulting stresses, obtained by analytical and numerical methods, have same trendline behavior of stresses as functions of rotation angle of input shaft. Shape transition zone between branches and central section is not included in analytical calculation because of complexity of real model geometry. However difference between values, obtained by analytical and numerical methods, is huge for today standards and without computer aided analysis it's unimaginable to perform this kind of experiment. The reason behind that is need to determine exact location of maximal stress and based on that to perform future optimization if it's possible. Relative stress variation between finite element method and analytical method was about 67%, the assumption is that these values of variations are big because of particular geometry of cardan cross in this paper. Optimal range of operation angle, based on this paper, is $\alpha = 0° \div 20°$, because of small resulting stress variation as a function of rotation angle φ_1.The theory that resulting stresses have maximal values in shape transition zone between branches and central section has been proven [8,9]. Although experiment was performed

using newer software, for the evaluation of the obtained results, it is recommended to try different relevant software. The further research would be based on structural analysis of remaining parts of cardan shaft and later their optimization.

REFERENCES

[1] Ašonja A and Mikić D 2012 *Development of Cardan Shafts Through History*, Technics and Informatics in Education – TIO, Čačak, Serbia, June 1 – June 3, pp. 824-832

[2] Stojanović B and Blagojević M 2015 *Mechanical Drives*, Faculty of Engineering University of Kragujevac

[3] Avrigean E, Marius P A and Stefan O V 2015 Study of the Cardan Cross using the Experimental and Analytical Method, *Procedia Engineering* **100**(1) 499-504

[4] Rakić B, Ivanović I, Josifović D, Stojanović B and Ilić A 2013 The Influence of Variation in Position of Output Shaft to Load on the Cardan Joint Cross Shaft, *International Journal for Vehicle Mechanics , Engines and Transportation Systems* **39**(1) 53-64

[5] Stamenić Z, Ristivojević M, Tasić M and Mitrović R 2012 Influence of the Geometry Parameters of Cardan Joint Rolling Parts on the Load Distribution, *FME Transactions* **40**(1) 135-143

[6] Vesali F, Rezvani M A and Kashfi M 2012 Dynamics of Universal Joints, its Failures and some Propositions for Practically Improving its Performance and Life Expectancy, *Journal of Mechanical Science and Technology* **26**(8) 2439-2449

[7] Kolekar D, Kalje A and Kulkarni S 2015 Design, Development and Structural Analysis of Universal Joint, *International Journal of Advanced Engineering Research and Studies* **4**(4) 9-12

[8] Sunil R M and Raghunatha R C 2016 Design and Analysis of Universal Coupling Joint, *International Journal of Engineering Science and Computing* **6**(12) 3808-3813

[9] Poorya R S and Azarafza R 2014 Investigate of Mechanical Fuse in Cardan Shaft using FEM, *Review of Information Engineering and Applications* **1**(1) 1-10

[10] Ivanović I, Josifović D, Ilić A, Stojanović B and Živković K 2014 *Optimization of Cardan Joint Design from Load Capacity Aspect*, International Congress Motor Vehicles & Motors, Kragujevac, Serbia, Oct. 9 - Oct. 10, pp. 396-404

[11] Mutavdžić T 2018 *Kinematics of Double Cardan Shaft*, Faculty of Engineering University of Kragujevac, Serbia, Bachelor Thesis

[12] Bi Z 2018 *Overview of Finite Element Analysis*, In book: Finite Element Analysis Applications, Academic Press

[13] Kojić M, Slavković R, Živković M and Grujović N 1998 *Finite Element Method I: Linear Analysis*, Faculty of Mechanical Engineering University of Kragujevac

[14] Ivanović I, Josifović D, Rakić B, Stojanović B and Ilić A 2012 *Shape Variations Influence on Load Capacity of Cardan Joint Cross Shaft*, Proceedings — The 7th International Symposium KOD 2012: Machine and Industrial Design in Mechanical Engineering, Balatonfüred, Hungary, May 24 – May 26, pp. 205-210

[15] Desnica E, Ašonja A, Mikić A and Stojanović B 2015 Reliability Model of Bearing Assembly on an Agricultural Cardan Shaft, *Journal of the Balkan Tribological Association* **21**(1) 38-48

IRMES KRAGUJEVAC 2019

9th International Scientific Conference
Research and Development of Mechanical Elements and Systems
Kragujevac, Serbia, September 5-7 2019

- STUDENT SECTION -

THE HEATING OF PLAIN BEARING LINING OF VARIOUS MATERIALS

Hristina Stojadinović[1], Miloš Radenković[1], Sandra Veličković[1]

[1]University of Kragujevac, Faculty of Engineering, Sestre Janjić 6,
34000 Kragujevac, Serbia, hristojadinovic@gmail.com

Abstract. This paper presents the results of testing the heating of plain bearings from bronze, aluminium and polymers whose plane bearing linings are produced by the same processing technology. Tribological tests of these plain bearings were carried out under the same working conditions, with lubrication and the temperature rise of each bearing was measured by a thermometer in a time interval of 15 minutes. For the lubrication, for all bearings was used Hidrol-46 oil. A three-phase electric motor with a speed of 1500 rpm, was used to start up the plain bearing shaft. The plain bearings worked in conditions without load. By heating the plain bearings during work, the wear debris from each of these materials was clearly visible. By analyzing the results of all the tested materials of the plain bearings, it is noticeable that the temperature increases with operating time. The obtained results indicate that the polymer is the least heated, followed by a bronze and an aluminum bearing.

Key words: plain bearing, temperature, bronze, aluminium, polymer.

1. INTRODUCTION

The plain bearing is the simplest type of bearing that apply where the rolling bearings are not possible to use. It is known that bearings are mechanical elements whose basic function consists in providing conditions for the relative movement of rotational parts, as well as for transferring loads from moving parts to those who are stationary or vice versa. The use of plain bearings is at places where the level of vibration and noise is undesirable, as well as at extremely high rotational speeds. The plain bearing consists of two relatively moving surfaces that are in contact, or are at a close proximity. Load transfer is accomplished by sliding, more precisely, when the moving surface - the journal slides over the immobil surface of the bearing - the plain bearing lining. Some of the advantages of plain bearings are lasting a long time, hit absorption and impact loads by the presence of a layer of lubricant between the journal and the bearing lining, simple constructions, etc. However, in addition to a series of good qualities, certain improvement of the plain bearings in terms of application of new materials, new lubricating systems as well as oils for the purpose of increasing the

application area [1,2]. Materials that are mainly used for making bearing lining are steel, bronze alloys, including aluminum nickel, phosphorus, silicon, and similar. These are materials that can meet the various requirements imposed by the industry in terms of lubrication and elasticity of the elements [3].

The most commonly used bearing lining material is bronze, which is characterized by very good characteristics. Therefore, the bronze bearings are very solid, as opposed to aluminum, which are softer and therefore more easily deformed. For this reason, they last longer and are more resistant to wear. The bronze according to its characteristics corresponds to the largest number of the bearing linings and is most often made from one piece of bronze, while in practice it also occurs in the form of a coating of several millimeters thick on the inner surface of the steel bearing lining [4]. Among the most important properties of the material is behavior at higher temperature, as well as the temperature conduction velocity. In general, the complex function of the bearings imposed the need for the application of special technologies, new materials, as well as new construction solutions for their production. In addition to the aforementioned materials, aluminum and plastic can be used, but only in cases where they can serve the needs of a particular mechanism. One of the new inventions of the materials used for plain bearings is a polymer layer containing solid particles of lubricant and metal oxide particles. The polymer layer consists of a polyamide resin, a molybdenum disulfate and a graphite. To further strengthen this layer, particles of solid material such as ceramic particles [5], are added. Some bearings are made by metal casting technology in the opening of the steel ring of the bearing lining. For the working layer, Cu, Cr and Zr or non-metals such as polytetrafluoroethylene are used, while the outer ring is made of steel or metal alloys. The combination of metal and non-metal elements in contact, a props journal and bearing lining, improves the characteristics and at the same time affects the reduction in the price of the plain bearing [4]. Application of polymer plain bearings is possible in conditions of high moisture, dust, dustiness, low velocity, no lubrication or when it's difficult to lubricate, due to the need for a cheaper and more efficient solution. In recent years, growth in the use of aluminum for the production of bearing lining has been observed, primarily due to its low price. Also, the use of aluminum is avoided by the use of lead, which represents the ecological concern of the manufacturer. The most common application of an aluminum bearing lining is in the automotive, marine, air and electrical industries, as well as in the main internal combustion chambers, due to their low weight and corrosion resistance. Aluminum alloys provide a good combination of strength and corrosion resistance compared to low cost [6].

Cuiet al. have tested the wearing intensity of plain bearings from various materials exposed to sea water. Bronze and aluminum were used as materials of the bearing lining of the plain bearing. It has been found that the aluminum bearing lining has a much higher wearing intensity than a bronze bearing lining, so the bronze is in most cases more convenient. However, aluminum has its pedancy in terms of optimizing the mass, increasing corrosion resistance, or in case of minor overloads [7].

Ünlüet al. conducted the experiment by testing the wear of the plain bearing lining for non-puncture polymeric materials, as well as polymeric materials with graphite and composite fillers. Reinforced ductile polymers have very good characteristics and high resistance to wear. They are often used in machines and mechanisms due to the low friction coefficient in the limiting conditions of the lubrication. Some of the polymeric materials in their composition contain material fillers that have the role of reducing friction in the contact of

the bearing lining and the journal, it can be graphite or composite materials. The investigation concluded that the biggest wear was due to polymeric material without filler [8]. Based on the literature review, it is concluded that the choice of bearing materials depends on the type of bearing, the type of lubrication and the conditions of the environment. In general, the bearing lining must be sufficiently solid and rigid to allow the load to be transmitted, and on the other hand, it is sufficiently soft to make a high-quality sliding pair with the journal. The aim of this paper is to examine plain bearings from various materials under the influence of temperature over time. The materials used in this study for the production of bearing linings are bronze, aluminum and polymer. It is important to note that all three plain bearings were made with the same processing technology and made in the same dimensions, so that the influence of temperature at a certain time interval could be analyzed.

2. EXPERIMENT

It is known that the main part of the plain bearing is the plain bearing lining that can be in the form of a one-piece, with or without a crochet. Based on the above, this paper examines the plain bearing linings of various materials by monitoring the temperature of the heating in a time interval of 15 minutes. The materials used for plain bearing lining (Figure 1) in this study are bronze (CuZn14), aluminum (AlCuMgPb) and polyoxymethylene copolymer (POM-C) and the journal from steel (C45).

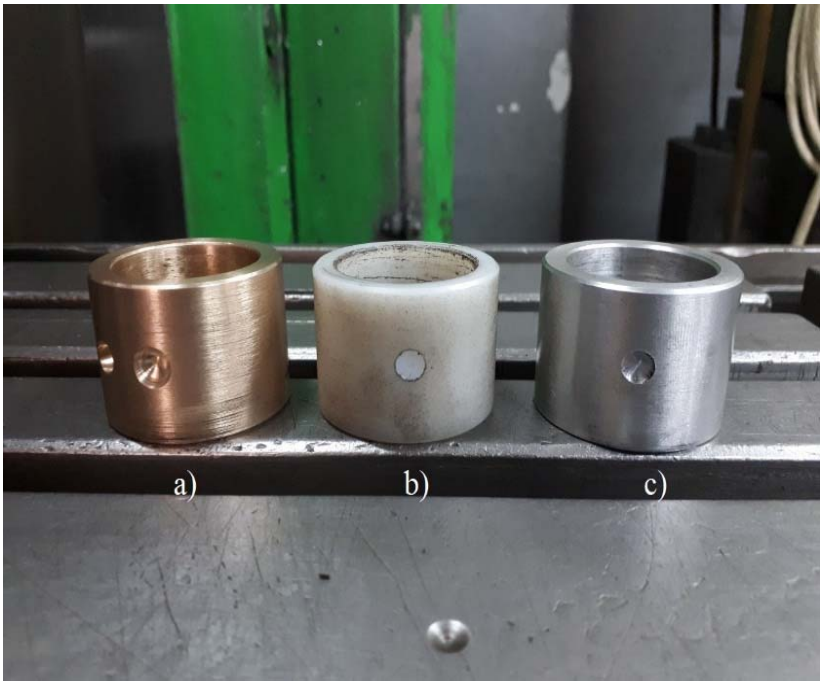

Figure 1. Plain bearing lining from a) bronze, b) polymer and c) aluminium

Experiment for testing the behavior of the plain bearing lining material on the temperature consists of an electric motor of 1 kW with a speed of 1500 rpm. On the shaft of the electric motor there is thejournal that rotates inside the plain bearing lining. The outer diameter of the journal is 30 mm, while the length of the journal is also 30 mm. Prior to the experiment itself, it was preceded by checking the equipment, as well as placing a measuring device on the test table.In this case, due to the very good surface condition, also due to the channel for the wedges on it, a working table of 600 mm length was used. The electric motor is placed on the test table and then attached to the fixture, as shown in Figure 3. Due to the easy and quiet operating conditions, without load, hard hits and vibrations, as well as the calm operation of the electric motor, it was sufficient to fasten it with only one fixture. A plate of textolite is placed between the fixture and the aluminum body of the electric motor so that the fixture pressure is evenly distributed on the entire surface of the plate. This clamping method avoids direct contact between the fixture and the housing of the electric motor, and in this way there is no deformation of the aluminum ribs on the electric motor. The electric motor is placed in the center of the test table so that the temperature and time measuring instruments are positioned one next to each other, enabling a comparative reading of the values. For the front surface of the electric motor, there is a companion flange in which the plain bearing is located. The material used to make the flange is steel (C45). After the preparation was cut out on band-saw, the flange production was further continued with a scraping technique, on a universal lathe, type Potisje Morando PA-22. The processing of all internal diameters was performed in only one clamp due to the retaining of the axis of symmetry of the pieces. After processing on lathe, four holes were made for bonding with the front surface of the electric motor by screw with an imbus head (Figure 2).

Figure 2. Installation elements

Figure 3. The method of clamping an electric motor

The clamping flange on it has two holes, where one connects the probe of the thermometer with plain bearing lining, and through the second hole the lubrication is carried out. The flange is designed so that the plain bearing lining can be changed without damage.
In this experimental study, hydraulic oil - Hydrol 46 was used. This oil belongs to a group of mineral hydraulic oils that have good oxidation stability, antifouling and anti-corrosion properties. Also, it do not foam and have good de-emulsion properties with quick extraction of air. They are intended for hydraulic systems of small and medium forces, loads, pressures and temperatures. The plain bearing operates under the limit lubrication conditions at the time of switching on and off, until the engine receives the maximum revolutions per minute, then switches to the hydrodynamic lubrication conditions. During the examination it was considered that the clearance between the journal and the plain bearing lining was the same during all tests and it was 0.02 mm. The experiment was carried out under room temperature conditions, with a speed of 1500 rpm, in a time interval of 15 min. During the testing of each sample, a temperature change was measured every 60 seconds, indicating heating of the material after a certain working time. A digital stopwatch was used to measure the time. To measure the temperature, a thermometer type TA-288 with a measuring range ranging from -50 to 300 degrees, was used. It is equipped with a probe for measuring the temperature of 110 mm in length. In order for the thermometer probe to be absolutely in touch only at one point of the plain bearing lining, the flange is fitted with a polymer guide with an asbestos insert.

3. RESULTS AND DISCUSSION

The obtained results from the temperature change of the plain bearing lining made of the bronze, polymer and aluminum in time function are shown in the diagram in Figure 4.

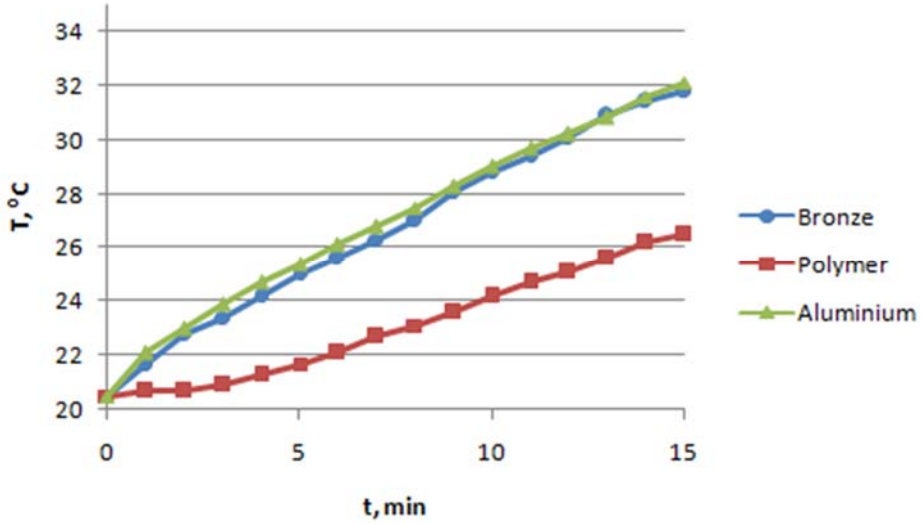

Figure 4. Graphical representation of the change in the temperature of the plain bearing in relation to time

It was found that the aluminum plain bearing lining is heating up the fastest, after the aluminum comes bronze, and last comes the polymer that is much less heated. By comparing the results obtained in this paper and the results published by *Cui* et al. [7], there is a similarity in the character of the wear of the aluminum plain bearing lining. In both papers, it has been proven that aluminum has the worst tribological characteristics, indicating that aluminum has a lower abrasion resistance than bronze. During the experiment bronze had a similar increase in temperature as aluminum, but the wear was more pronounced in aluminum. The placement of the polymeric plain bearing lining, with regard to the least warming, is subject to far less wear, as was shown by *Sadik* et al. [8].

In paper *Ünlü* et al. demonstrates that polymeric materials without fillers behave very similarly to the character of wear and that wear is very low. They concluded that the use of other material in the composition of plain bearing lining reduces the losses in tribological processes and increases the lifetime of the elements in the process [8].

When the materials were tested without filler, the results of the wear of the inner surface of the polymer plain bearing lining had the same look as the plain bearings from this experiment. A similar study was carried out in the field of medicine where the spherical plain bearing was used as an element of an artificial hip. This plain bearing having a sphere of polymeric material rotating around the surgical steel journal has significantly influenced the development of medicine [9]. As this work has experimentally demonstrated the good tribological properties of polymer in terms of wear, it can find its application in any wrist of the human body, the most important is that it does not require lubrication and has good resistance to wear. *Sagbas* et al. carried out a temperature impact test in this spherical articulated plain bearing. For easier comparison, the results were displayed with load and no load. The nave in which the spherical journal is rotated is made of polymeric material, while the journal is made of steel. This is, in particular, a case of friction of metal contact by polymer, which is similar to the case of the tested plain bearing in this scientific work.

The results for the spherical bearing are obtained without loading correspond to the temperatures achieved for the investigated radial bearings with a polymeric plain bearing lining in this paper. The contact between metal and polymer proved to be very reliable for bearings where it is impossible to carry out lubrication. This applies mostly to mechanisms and devices in the food industry. The temperature rise of the spherical bearing corresponds to 3 degrees Celsius within 450 seconds of constant operation [9].

In this paper, in addition to temperature measurement, the filtration of oil passing through the plain bearing occures wearing debris. In the abovementioned papers, it was said that the biggest wear is in the aluminum plain bearing lining, and this was proved in the experiment in this paper, where most microfibers were in the oil that lubricated the aluminum plain bearing lining, the bronze bearing lining had a wearing product in the form of bronze contours, while the polymer did not have clearly visible wearing debris.

4. CONCLUSION

Conducting this experiment, results have been achieved which are undoubtedly characterize the thermal behavior of bronze, polymeric material and aluminum in the role of a plain bearing lining. Also, the velocity of the temperature conduction through the plain bearing lining is observed as a result of friction of the surfaces in the plain bearing. On the basis of

the obtained results it is noted that in the mode of operation without load, at the speed of 1500 rpm, the least heating has a polymeric material. Theoretical assumptions have been proven true in practice, because polymeric materials have a self-degrading property, a very good subjugation and absorb surface working temperatures caused by friction. The bronze, which is most commonly used as a material of a plain bearing, has shown slightly poorer characteristics in the form of increased heat, but the results of the heating do not relate to critical values but to those that are normal in the sliding blades with a bronze plain bearing lining. Bronze is not intended for plain bearings with high speeds, but for smaller numbers or mechanisms with short periods of periodic operation, otherwise there must be a source of lubrication under pressure. Aluminum, as a material that is characterized by good conductivity of the temperature, has the worst characteristics and is used exclusively in special cases, for example, when high corrosion resistance is required and when the speed of the electric motor is small, as with smaller loads. Due to its weight, aluminum has the advantage of some devices where it is essential to maximally optimize the design, but depending on the working conditions. In addition to temperature measurement, the filtration of oil passing through the plain bearing indicates wearing debris. The result of wear debris can be analyzed in the future research using a microscope, in order to precisely define the behavior of materials at different temperatures. This paper included testing and comparison of the temperature of the plain bearings of different materials. The experiment is from a structural point of view, as well as tribological very complex and opens up new fields that could be examined in this experiment, one of the things that is interesting for testing are definitely wear products for the same working conditions. The wearing debris are very important parameters because they can be determined and even predicted in what period of wear and tear will occur, testing of wear debris would have a bigger significance in the process of maintaining plain bearings in different fields of industry.

REFERENCES

[1] Nikolić V 2004*Machine elements,* Faculty of Mechanical Engineering in Kragujevac, Center for testing and calculation of mechanical elements and mechanical systems "CIPMES" Kragujevac

[2] Ognjanović M 2016*Machine elements*, Faculty of Mechanical Engineering in Begrade, Belgrade

[3] THOMAS, *Types of Plain Bearings (Bushings)2019* https://www.thomasnet.com/articles/machinery-tools-supplies/types-of-bushings/ (accessed on July 2019)

[4] C Hentschke, B Pinnekamp and A Unger 2019 Plain Bearing And Method For Producing The Same, *U.S. Patent Application* **No.** 16/115,075

[5] G Leonardelli 2019 *U.S. Patent Application* **No.** 10/184,521

[6] T Rameshkumar, I Rajendran and A D Latha 2010 Investigation on the mechanical and tribological properties of aluminium-tin based plain bearing material, *Tribology in Industry* **32**(2) 3-10

[7] G Cui, Q Bi, S Zhu, L Fu, JYang, ZQiao andW Liu 2013 Synergistic effect of alumina and graphite on bronze matrix composites: Tribological behaviors in sea water, *Wear* **303**(1-

2) 216–224
[8] B S Ünlü, M Uzkut and E Atik 2010 Tribological Behaviors of Polymer-based Particle-reinforced PTFE Composite Bearings, *Journal of reinforces plastics and composites* **29**(9)1353-1358
[9] S B Sagbas, M N Durakbasa, M Sagbas and A Koyun 2014 Measurement and theoretical determination of frictional temperature rise between sliding surfaces of artificial hip joints, *Measurement* **51** 411-419

9th International Scientific Conference
Research and Development of Mechanical Elements and Systems
Kragujevac, Serbia, September 5-7 2019

- STUDENT SECTION -

MONITORING THE HARDNESS OF THE STEEL DEPENDING ON THE HARDENING PARAMETERS

Slobodan Živanović[1], Sandra Veličković[1]

[1]University of Kragujevac, Faculty of Engineering, Sestre Janjić 6,
34000 Kragujevac, Serbia, slobodan95zivanovic@gmail.com

Abstract. Thermal treatment is a procedure for the operation of temperature on the material in order to change the microstructure of the material and therefore its properties. The aim of this paper is to monitor the behaviour of three types of steel by applying the method of heat treatment of hardening at different hardening temperatures and different hardening agents. Tested materials are steel: C45, 42CrMo4 and 51CrV4 with the temperatures of hardening: 860°C, 850°C, 840°C, 830°C and 820°C. Obtained results have shown that steel 42CrMo4 and 51CrV4 have better mechanical characteristics when they were hardened in oil agent.

Key words: thermal treatment, steel, hardness, temperature.

1. INTORDUCTION

Thermal treatment as a branch of metallurgy represents the process of temperature operation on the material in order to change the microstructure of the material and therefore its properties or thermal treatment is a technological process consisting of heating metal to a certain temperature, holding it at that temperature and cooling to room temperature [1]. The aim of the thermal treatment of metals and alloys is to change some of their mechanical and physical-chemical properties, primarily phase and structural changes in solid state, and the changes are mainly in function of the temperature, time and environment in which processing is performed. Types of thermal treatment of steel are:

- Annealing,
- Hardering,
- Releaseing.

Hardening of steel is a thermal treatment that is carried out by heating the workpiece above the temperature Ac_3, for sub-eutectoids and $Ac_{1.3}$ for nad-eutectoid steel, heating at that temperature and cooling at a rate higher than critical [1]. By hardening the steel, the

diffusion change of the austenite to below the Ms temperature is prevented in order to further transform the austenite into the martensite further by the sliding mechanism. As a result of hardening, a deformed iron-martensite grid is obtained which exhibits high hardness and high resistance properties [2]. There are a lot of scientific papers that have dealt with similar topics in recent times. *Frunza* et al. have concluded for the purpose of their research that hardness of C45 steel is about 250 HB and that is similar to the hardness of the steel obtained in other papers. Also *Melat* et al. for the needs of studies which deal with influence of the hardening and annealing thermal treatments applied on two types of steels used for rolling stock got the value of hardness about 53 HRC.
The aim of this paper is to monitor the behavior of three types of steel by applying the method of heat treatment of hardening at different hardening temperatures and different hardening agents.

2. EXPERIMENT

The experiment needed for this work was done in the economic entity S.Z.R. TRGOPRODUKT, Kragujevac. The business entity has a special purpose plant for heat treatment with two chamber furnaces for thermal treatment of steel in an unprotected atmosphere of a temperature range from 0°C to 1200°C. As an integral part of the equipment, there is Rockwell hardness tester. Rockwell Hardness Measurement is a procedure for determining the hardness of the material, where a special impeller is imprinted on the surface of the test material without measuring the surface of the print (as in the case of the Brinell and Vickers hardness test, but its depth). The imager is a diamond needle with an inner angle of 120° (with a curvature half at a top of 0.2 mm), or a guttered steel ball of 1.5875 mm (1/16 inch) or 3.175 mm (1/8 inch) diameter [3]. The hardness measuring tester is a HR-hardness measuring instrument, scale C, manufactured by LIENERT-Zuirch with a force on the impeller of 1471.0 N with conical type of impeller with diamond needle on top. The smallest segment is 1 HR. Etalonated 03/18/2015, the name of the standard: Measurement standard for hardness according to HRC hardness 23.6 HRC, 44.2 HRC and 61.5 HRC. The device is standardized according to SRPS ISO 716 standard. The experimental part of the research is based on the monitoring of the hardness of the steel depending on the drop in tempering temperature in two cooling agents (water and oil) and the comparison of the hardness depending on the type of cooling agent.

2.1. Materials

The materials used in the experiment are C45 (High quality non-alloy carbon steel for improved carbon content), C45 steel is defined as a medium carbon steel offering tensile strengths in the modest range. The material can be maneuverer with hardening by means of quenching and tempering on focused and restricted areas. C45 can also be instigated with induction hardening up to the hardness level of HRC 55 [4], 42CrMo4 (Cr-Mo steel for improvement) this grade is the special high steel grade which can be quenched and tempered. It offers a robust amalgamation of strength and toughness in the state of being quenched and tempered. Different European standards cover the specification of this steel in different forms and processing conditions. The steel can be subjected to induce hardening. This steel grade is usually available in a mix of microstructure i.e. martensite and austenite. The special grade of this steel is subjected to M-treatment to offer good machinability

properties [4] and 51CrV4 (Cr-Mn-V steel for improvement), alloyed heat treatable steel with a typical tensile strength of 900 - 1200 N/mm². For automotive and mechanical engineering components as gear parts, pinions, shafts [5]. Chemical composition of steels used for the experiment can be seen in Tables 1, 2 and 3.

Table 1. Chemical composition of C45 steel

Steel grade, %	C	Si	Mn	S	P	Cr	Mo	Ni	Al	Cu
C45	0.45	0.25	0.65	0.025	0.008	0.4	0.1	0.4	0.01	0.17

Table 2. Chemical composition of 42CrMo4

Steel grade, %	C	Si	Mn	S	P	Cr	Mo
42CrMo4	0.38-0.45	0.40	0.60-0.90	0.035	0.025	0.90-1.20	0.15-0.30

Table 3. Chemical composition of 51CrV4

Steel grade, %	C	Si	Mn	P	Cr	S	Mo	V	Ni	Ti	Sn	Ca	N
51CrV4	0.52	0.33	0.93	0.01	0.005	0.93	0.04	0.16	0.14	0.15	0.012	0.0004	0.013

2.2. Discussion and analysis of the results

Based on carried out experiment in table 4 are given obtained values of hardness for steel C45 depending on temperature and hardening agent, and for better display and comparison of the obtained values for the hardness of the steel in Figure 1 are presented results. The temperatures on which the steel is heated are 860°C, 850°C, 840°C, 830°C and 820°C.

Table 4. Hardness and temperature of hardening for steel C45

C45	**Oil**	**Water**
860°C	29 HRC	61 HRC
850°C	26 HRC	60 HRC
840°C	16 HRC	58 HRC
830°C	25 HRC	57 HRC
820°C	23 HRC	55 HRC

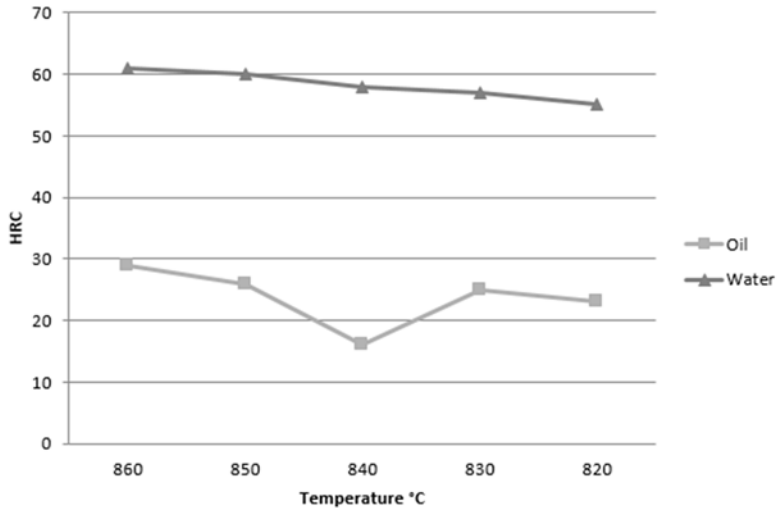

Figure 1. Graphic of dependence of hardness on temperature hardening and agent for steel C45

Based on the graphics, Figure 2 can be seen that the hardness of the tube drops with a decrease in the tempering temperature. Just as it is expected that the hardness produced by hardening in water is considerably greater than the hardness of the hardening in oil. In the steel-graphic article C45 oil hardening, a drop in hardness from 26 HRC at 16 HRC at a temperature of 840oC and then a resumption of 25 HRC is seen, this irregularity does not indicate any special characteristic of the material, but on an error in tempering, namely the great influence on the hardening technology itself is also the skill of worker. The experiment results of hardness, for steel C45 are similar to the results.

Examination of steel 42CrMo4 gave interesting conclusions. Namely steel 42CrMo4 as well as 51CrV4 are not intended for hardening in water, due to the danger of cracks, however, for testing purposes, the tubes of both steels are tempered both in water and in oil, what is interesting is that the hardness differences seen on figure 2 and table 5 for hardening in oil and for hardening in water are not large and do not exceed 5 to 10 HRC.

Table 5. Hardness and temperature of hardening for steel 42CrMo4

42CrMo4	Oil	Water
860°C	56 HRC	64 HRC
850°C	54 HRC	63 HRC
840°C	52 HRC	67 HRC
830°C	52 HRC	61 HRC
820°C	51 HRC	60 HRC

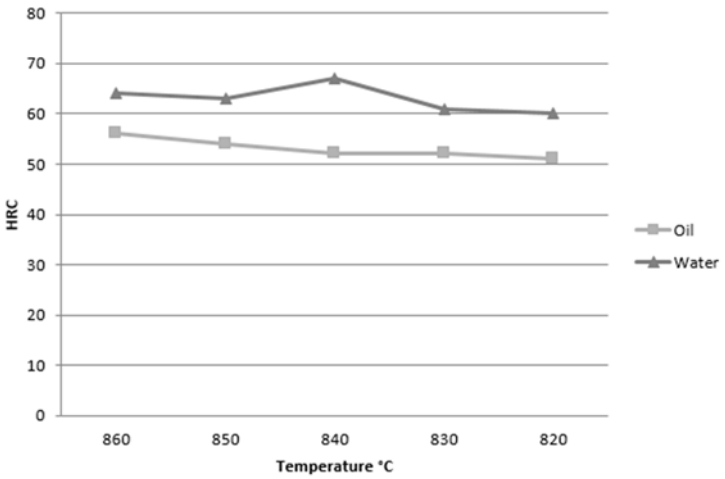

Figure 2. Graphic of dependence of hardness on temperature hardening and agent for steel 42CrMo4

Due to the hardness in water and oil in the oil for 42CrMo4 similar, there is no need to risk and quench that steel in water. Another interesting thing about the hardening of this steel in water is that it is common for hardening in water to break up pieces or the appearance of smaller fissures, which in this case did not happen, which owes gratitude to the extremely small dimensions of the preparation, i.e., the tube was not there many residual voltages remaining after this type of thermal treatment. Although in recommendations for steel 42CrMo4 that it is sensitive to quenching in water and that it is necessary to apply hardening in oil to complicated pieces, while for steel 51CrV4 it is said that it must not explicitly be hardened in water, claims confirmed by these experiments. The results of hardeners fore 42CrMo4 steel are similar to the results shown by the *Melat* et al. [7] where hardness is 53 HRC and also are similar with paper of *Cvetovski* el al. [8] where the hardness of 56 HRC was obtained.

As mentioned above, the characteristics of steel 42CrMo4 are similar to the characteristics of steel 51CrV4, both of which are not intended for hardening in water, but also the steel 51CrV4 is tempered in both hardening agents. As was also noted for the previous steel, and in this steel, the differences between oil and water inlays are small, which can be seen both in the table 6 and on the Figure 3.

Table 6. Hardness and temperature of hardening for steel 51CrV4

51CrV4	Oil	Water
860°C	59 HRC	64 HRC
850°C	58 HRC	63 HRC
840°C	57 HRC	61 HRC
830°C	55 HRC	60 HRC
820°C	54 HRC	60 HRC

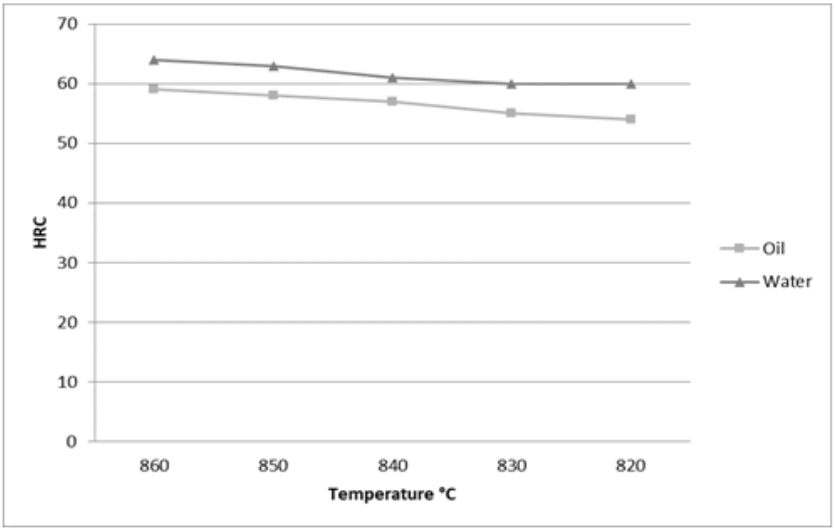

Figure 3. Graphic of dependence of hardness on temperature hardening and agent for steel 51CrV4

On the Figure 3 can be seen the drop in hardness for steel 51CrV4 in two agent, water and oil. In the paper of *Solic* at al [9], there are claims that after hardening of 51CrV4 steel she obtained hardness of about 58 HRC during hardening in oil, and in the research carried out for this paper it can be seen that the hardness obtained is similar to the hardness in the work of *Solic* at al. [9].

Another interesting comparison is made in the hardness of all three steels, but especially for hardening in water, and especially for hardening in oil, which can be seen in Figures 4 and 5.

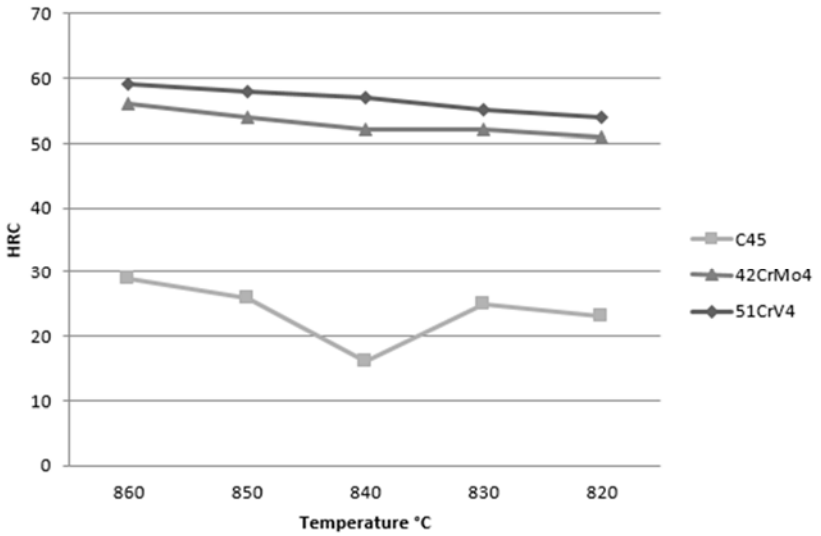

Figure 4. Comparison of hardness for all three oil hardening

From the attached table it can be seen that the steels of 42CrMo4 and 51CrV4, otherwise, the steels of higher hardness in oil hardening achieved a much higher hardness than softer steel C45 whose hardness ranged from 23 HRC to 29 HRC. Also the similarities of these two alloy steels are also seen.

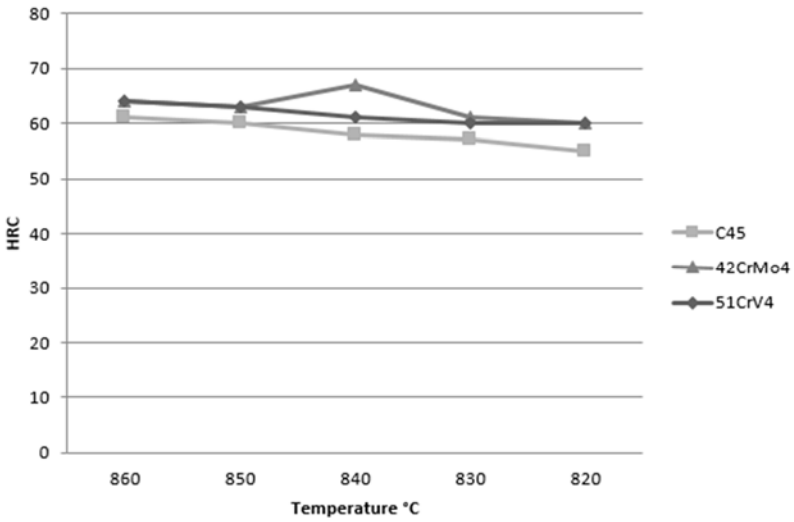

Figure 5. Comparison of hardness for all three water hardening

It is interesting that in many of these tests the dependence of the hardness of the steel on the temperature does not play such a role as a cooling agent, because the hardness is often obtained in an interval of difference from 0 to 6 HRC. But it any case, the hardness still falls.

3. CONCLUSION

The experimental part of the study was based on the monitoring of the hardness of the steel depending on the hardening temperature and the hardening agents. For the experiment purposes, the steels that was used are C45, 42CrMo4 and 51CrV4 and the temperatures of hardening are 860°C, 850°C, 840°C, 830°C and 820°C. Analyzing the accompanying charts, research results, there are several conclusions. The steels listed in the literature as steel that is hardening in oil agent, 42CrMo4 and 51CrV4 definitely have better characteristics when they are hardened in this hardening agent, namely, although the hardening of these steels in the water may result in slightly higher hardness than in the case of hardening in oil, these elements that are hardened in water show themselves as a lot of brittle. Another conclusion that can be made is that the entire research coincides with the other research and testing of steel of this type.

REFERENCES

[1] Jovanovic M, Lazic V, Adamovic D, Ratkovic N 2003 *Mašinski materijali* Faculty of Engineering University of Kragujevac

[2] Jovanovic M, Lazic V, Arsic D 2017 *Nauka o materijalima* Faculty of Engineering University of Kragujevac
[3] Kraut B 1987 *Strojarski priručnik* Tehnička knjiga Zagreb
[4] C45 Medium Carbon Steel grade, https://www.materialgrades.com/c45-medium-carbon-steel-grade-2082.html, (accessed on Jun. 2019)
[5] Material specification sheet, https://www.saarstahl.com/sag/downloads/download/11561, (accessed on Jun. 2019)
[6] Sas-Boca I M, Tintelecan M, Iluțiu-Varvara D A, Pop M, Frunza D and Popa F 2019 Research on the mechanical properties of C45/S235JR multilayer steel systems, *Procedia Manufacturing* **32** pp. 8-14
[7] Melat B and Mihăiță C 2018 Studies Concerning the Microstructure and Hardness Obtained After the Heat Treatment Applied to Steels Used for Components of Rolling Stock *In Journal of Physics: Conference Series- IOP Publishing* **1122**(1) pp. 012005
[8] Cvetkovski S and Nacevski G 2015 Metallographic investigation of induction hardened part two-side lever *Faculty of Technology and Metallurgy*, Ss. Cyril and Methodius University, Skopje, Macedonia
[9] Šolić S, Senčič B and Leskovšek V 2013 Difference between mechanical properties of 51CrV4 high strength spring steel modeled by hardenability software and obtained properties by heat treatment, *INFOTEH-JAHORINA* **12** pp. 504-508

Sponsored by:

PIP-IX INŽENJERING CONSALTING

BERDIZ CONSULTING

FEROHAL

WOODLAND ORANICA

ema HOTEL&SPA

КРАГУЈЕВАЦ

obi

euro heat

FLORES

ГРАДСКА ТУРИСТИЧКА ОРГАНИЗАЦИЈА КРАГУЈЕВАЦ

GRAFOSTIL

PUBLIK

MIND GROUP

SCGM

POLITEK KAMIONSKE NADOGRADNJE

INNOVATIVE ACRYLICS

AMM MANUFACTURING

Hellas Centar

FMO EKONOM

SYSTEM

ALFA TECHNICS

Advanced Machine Design & Manufacturing

Skladišni centar bb, 34000 Kragujevac, Srbija

With the support of:

ADEKO Association for Design, Elements and Constructions

IFToMM

Република Србија

Министарство просвете, науке и технолошког развоја

DOWNLOAD PDF